The role of intracellular Ca^{2+} in the arrhythmogenic activity of pulmonary vein cardiomyocytes

A thesis presented by

Alasdair Henry

In fulfilment of the requirement for the degree of

Doctor of Philosophy

2016

Strathclyde Institute of Pharmacy and Biomedical Sciences

University of Strathclyde

Copyright Statement

Signed:

Date:

Acknowledgements

First and foremost, I would like to thank my supervisors Dr Robert Drummond and Dr Eddie Rowan for their extensive guidance and support throughout my PhD. I would especially like to thank Robert for allowing me the freedom to pursue my ideas and for providing valuable feedback and criticism over the course of my studies. I would also like to thank my clinical collaborator Professor Andrew Rankin for helping me to understand how basic research translates into clinical practice. Finally, I would like to thank Dr Niall MacQuaide and Dr Francis Burton for their help with the analysis software.

During my PhD I made numerous friends which I will keep for life. I would especially like to thank Laura Hutchison, not only for her help as a colleague, but also for her support as a friend. In SIPBS I developed an extensive support network and while there are too many people to name individually, I would especially like to acknowledge Tommy Harwood, Martin Werno, Mark MacAskill, Leon Williamson, Paul Farrell, Sam White, Claire McCluskey, Serge Moudio, Scott Parker, Mark Barbour, David Glass, Cinta Díaz, Joana Faustino and Emma Torrance. I would also like to thank my bandmates Iain, Grant, Tony, Ross and Rory for allowing me to pursue my passion outside science. In addition, I would like to thank my undergraduate friends Laura Shand, Issy Patience and Ian Ruffell; without whom I wouldn't be who I am today. Last but not least I would like to acknowledge by best friends Jack Howells and Richard Lees. I would also like to extend my gratitude to everyone in SIPBS for their help during my PhD and also for making me feel at home. As a late edition, I would like to mention Mandy MacLean's lab at the University of Glasgow, who supported me at the final stretch; Lynn, Mags, Craig, Dawid, Sinéad, Nina, Katie, Gerry and Teja. Finally, I would like to acknowledge Maria who was there with me at the end.

I would also like to acknowledge my family. Not least my brother Andrew for not only being a brother and a great friend, but also for putting up with living with me when I

was writing my thesis. Importantly, I would like to thank my mum and dad for inspiring me to work hard and for providing their love and support along the way. I would also like to thank both my grannies, Henry and McGarrity for being unconditionally proud of me. Sadly my granny McGarrity passed away during the course of my studies. This thesis is dedicated in her memory.

Abstracts

Henry, A.D., Rankin, A.M., Rowan, E.G., Drummond R.M. Effect of electrical field stimulation on spontaneous Ca^{2+} transients in rat pulmonary vein cardiomyocytes. Poster presentation. April 2014. Experimental Biology 2014, San Diego, CA, USA. The FASEB Journal vol. 28 no. 1, 864.4.

Henry, A.D., Rankin, A.M., Rowan, E.G., Drummond, R.M. Spontaneous Ca^{2+} transients in the rat pulmonary vein following electrical field stimulation. Scottish Cardiovascular Forum 2014, Robert Gordon University, Aberdeen, UK. Poster presentation.

Henry, A.D., Rankin, A.M., Rowan, E.G., Drummond, R.M. Spontaneous Ca^{2+} transients in the rat pulmonary vein cardiomyocytes following electrical field stimulation. Scottish Cardiovascular Forum 2013. University of Strathclyde, Glasgow, UK. Poster presentation.

Henry, A.D., Rankin, A.M., Rowan, E.G., Drummond, R.M. Spontaneous Ca^{2+} transients in the rat pulmonary vein cardiomyocytes following electrical field stimulation. SIPBS Annual Research Symposium 2013. University of Strathclyde, Glasgow, UK. Poster flash and presentation.

Henry, A.D., Rankin, A.M., Rowan, E.G., Drummond, R.M. Spontaneous Ca^{2+} transients in the rat pulmonary vein cardiomyocytes following electrical field stimulation. Cardiovascular, Neuroscience and Cell Biology Research Day 2013. University of Strathclyde, Glasgow, UK. Poster presentation.

Henry, A.D., Hutchison, L., Rankin, A.M., Drummond, R.M., Rowan, E.G. Organisation of cardiomyocytes in the rat pulmonary vein. Cardiovascular and Respiratory Physiology Themed Meeting 2012, Manchester, UK. Poster presentation.

Henry, A.D., Rankin, A.M., Drummond, R.M., Rowan, E.G. The role of intracellular Ca^{2+} in the arrhythmogenic activity of pulmonary vein cardiomyocytes. SIPBS Annual Research Symposium 2012, University of Strathclyde, Glasgow, UK. Poster flash and presentation.

Henry, A.D., Rankin, A.M., Drummond, R.M., Rowan, E.G. The role of intracellular Ca^{2+} in the arrhythmogenic activity of pulmonary vein cardiomyocytes. Cardiovascular, Neuroscience and Cell Biology Research Day 2012. University of Strathclyde, Glasgow, UK. Oral presentation.

Table of Contents

Chapter 1. General Introduction

Chapter 2. The arrangement of cardiomyocytes in the rat pulmonary vein and the distribution of proteins involved in excitation-contraction coupling

Chapter 3. Intracellular Ca^{2+} signalling in rat pulmonary vein cardiomyocytes

Chapter 4. The effect of noradrenaline on the contractility of the rat pulmonary vein and the potential for automaticity

Chapter 5. General Discussion

Chapter 6. References

List of figures

Chapter 1

Chapter 2

Chapter 3

Chapter 4

List of tables

Chapter 1

List of Abbreviations

$[Ca^{2+}]_i$	Intracellular Ca^{2+}concentration
$[Ca^{2+}]_o$	External Ca^{2+} concentration
µl	Micro litre
µm	Micro meter
µM	Micro molar
2-APB	2- -Aminoethoxydiphenyl borate
AIP	Autocamtide-2 related inhibitory peptide
AM	Acetoxymethyl ester
ANOVA	Analysis of variance
ATP	Adenosine-5´-triphosphate
BAPTA	1,2-bis*(*o-aminophenoxy*)*ethane-N,N,N′,N'-tetraacetic acid
BP	Band pass
BSA	Bovine serum albumin
Ca^{2+}	Calcium ions
CaMKII	Calcium/calmodulin dependent protein kinase II
cAMP	Cyclic adenosine 3´,5´ -monophosphate
CBX	Carbenoxolone
CICR	Calcium-induced calcium release

CPA	Cycopiazonic acid
Cs^+	Caesium ions
Cx	Connexin
DAPI	4',6-diamidino-2-phenylindole
Di-4 ANEPPS	Pyridinium, 4-(2-(6-(dibutylamino)-2-naphthalenyl)ethenyl)-1-(3-sulfopropyl)-, hydroxide, inner salt 90134-00-2
DMSO	Dimethyl sulfoxide
DNA	Deoxyribonucleic acid
ECG	Electrocardiogram
EGTA	Ethylene glycol-bis(2-aminoethylether)-N,N,N′,N′-tetraacetic acid
FFR	Force-frequency relationship
FPS	Frames per second
g	Grams
HCN	Hyperpolarisation-activated cyclic nucleotide-gated
HEPES	4-(2-Hydroxyethyl_piperazine-1-ethanesulfonic acid, N-(2-Hydroxyethyl)piperazine-N´-(2-ethanesulfonic acid)
HNK-1	Human Natural Killer-1
Hr	Hour
Hz	Hertz
I_{CaL}	L-type Ca^{2+} current

I_f	Funny current
I_{K1}	Inward rectifier potassium current
I_{NCX}	Na^+/Ca^{2+} exchange current
IgG (H + L)	Immunoglobulin G heavy and light chains
IP_3	Inositol 1,4,5-trisphosphate
IP_3R2	Type 2 IP_3 receptor
IU	International units
K^+	Potassium ions
KB	Kraft Brühe
KB-R7943	2-[2-[4-(4-nitrobenzyloxy)phenyl]ethyl]isothiourea methane sulfonate
KCl	Potassium chloride
KHz	Kilohertz
KN-93	N-[2-[N-(4-Chlorocinnamyl)-N-methylaminomethyl]phenyl]-N-(2-hydroxyethyl)-4-methoxybenzenesulfonamide phosphate salt, N-[2-[[[3-(4′-Chlorophenyl)-2-propenyl]methylamino]methyl]phenyl]-N-(2-hydroxyethyl)-4′-methoxybenzenesulfonamide phosphate salt
Kg	Kilogram
Li^+	Lithium ions
L-NAME	L-N^G-Nitroarginine methyl ester

LP	Long pass
LTCC	L-type Ca^{2+} channel
mg	Milligram
Min	Minute
ml	Millilitre
mm	Millimetre
mM	Millimolar
ms	Millisecond
mV	Millivolts
nm	Nanometre
MRI	Magnetic resonance imaging
mRNA	Messenger ribonucleic acid
Na^{+}	Sodium ions
NCX	Na^{+}/Ca^{2+} exchanger
Ni^{2+}	Nickel ions
nm	Nanometre
nM	Nanomolar
ORM-10103	2-[(3,4-Dihydro-2-phenyl-2H-1-benzopyran-6-yl)oxy]-5-nitro-pyridine
PACAP	pituitary adenylate cyclase-activating polypeptide

PBS	Phosphate buffered saline
PKA	Protein kinase A
PKC	Protein kinase C
RH37	*N*-(4-Sulfobutyl)-4-(6-(4-(Dibutylamino)phenyl)hexatrienyl)Pyridinium, Inner Salt
ROI	Region of interest
RyR	Ryanodine receptor
s	Seconds
SA node	Sino-atrial node
SEA0400	2-[4-[(2,5-difluorophenyl) methoxy] phen-oxy]-5-ethoxyaniline
s.e.m.	Standard error of the mean
SERCA	Sarcoplasmic reticulum ATPase
SR	Sarcoplasmic reticulum
SOICR	Store overload-induced Ca^{2+} release
TMRE	Tetramethylrhodamine ethyl ester perchlorate
T-tubule	Transverse tubule
TTX	Tetrodotoxin
U46619	(*Z*)-7-[(1*S*,4*R*,5*R*,6*S*)-5-[(*E*,3*S*)-3-hydroxyoct-1-enyl]-3-oxabicyclo[2.2.1]heptan-6-yl]hept-5-enoic acid
V	Volts

Abstract

The pulmonary veins are widely recognised as a source of ectopic electrical activity that can cause atrial fibrillation. While the ectopic activity likely originates in the cardiomyocytes that form an external sleeve around the veins, the underlying mechanisms are unknown. Changes in intracellular Ca^{2+} signalling have been proposed to play an important role in the arrhythmogenic properties of the pulmonary vein. Therefore, the aim of this thesis was to study factors that might influence Ca^{2+} signalling in the cardiomyocytes. This involved determining the localisation of Ca^{2+} handling proteins in the cardiomyocytes, examining interventions that might alter the characteristics of intracellular Ca^{2+} signalling, as well as looking at the arrhythmogenic effect of adrenergic stimulation.

In the rat pulmonary vein, the cardiomyocytes displayed spontaneous Ca^{2+} transients that were usually manifest as waves, and were asynchronous in neighbouring cardiomyocytes. The frequency of spontaneous Ca^{2+} transients was increased following a brief period of electrical stimulation at 3 Hz or greater, and this effect was enhanced in the presence of isoprenaline, or when the external Ca^{2+} concentration was raised. Noradrenaline also increased the frequency of the spontaneous Ca^{2+} transients; however, synchronous Ca^{2+} transients, like those that could be evoked by electrical field stimulation, were not observed.

As spontaneous Ca^{2+} transients are due to Ca^{2+} released from the sarcoplasmic reticulum through the ryanodine receptors, immunocytochemistry was used to determine their distribution. The ryanodine receptors were arranged in a striated pattern with some distribution at the periphery of the cells, which was similar to myocytes from the atria. When the sarcolemma of the pulmonary vein cardiomyocytes was labelled with Di-4 ANEPPS, they were shown to possess transverse (T)-tubules, which are involved in co-ordinating the intracellular Ca^{2+} transient in response to depolarisation. This differed from atrial myocytes where a T-tubule system was not observed. Furthermore, the L-type Ca^{2+} channels and Na^{+}/Ca^{2+} exchanger (NCX),

which are involved in Ca^{2+} influx and removal during excitation-contraction coupling, were arranged in a more striated manner in the pulmonary vein cardiomyocytes, compared to those of the atria. This could have important consequences for the contractile activity of the cardiomyocytes, as well as their ability to generate abnormal electrical activity, as the NCX is known to cause depolarisation in response to an increase in intracellular Ca^{2+}.

The contractile properties of the pulmonary vein were studied *in vitro* using myography techniques, where it was shown to display a negative force-frequency relationship, whereby increasing the frequency of electrical stimulation reduced the contractile amplitude. In the presence of noradrenaline, the amplitude of the electrically evoked contractions was increased and the negative force-frequency relationship was only evident at the higher stimulation frequencies (5 to 7 Hz). Noradrenaline also induced periodic bursts of contractions that occurred independently of electrical stimulation, suggesting that it had an arrhythmogenic effect. Such activity was partially inhibited by blocking the NCX with ORM-10103. This suggests a potential target for future research into selective pharmacological intervention for catecholamine based arrhythmias.

Chapter 1

General Introduction

1.1. Atrial fibrillation

Atrial fibrillation is the most prevalent cardiac arrhythmia encountered clinically and is associated with substantial morbidity and mortality (Benjamin *et al.*, 1998). The prevalence of atrial fibrillation in the general population of the United Kingdom and United States of America is approximately 1%, with the number of reported cases increasing considerably with advancing age in the patient cohort (Kannel & Benjamin, 2009; Kannel *et al.*, 1998; Murphy *et al.*, 2007). Given its growing prevalence (Go *et al.*, 2001; Tsang *et al.*, 2003), and an increasingly ageing western population (Butler, 1997), atrial fibrillation incurs substantial costs for healthcare and treatment. In the United Kingdom, atrial fibrillation alone accounts for 1% of the National Health Service's annual budget (Stewart *et al.*, 2004), and in the year 2008 the direct cost of atrial fibrillation was estimated as being £429 million (cit. in Kassianos *et al.*, 2014).

Atrial fibrillation occurs when the rhythm of the atria is no longer under the physiological control of the sino-atrial node, due to overriding pacemaker electrical activity occurring outside this region (Khan, 2004; Nattel, 2002). It is characterised on an electrocardiogram (ECG) by the absence of a prominent P-wave, which normally represents atrial depolarisation, and is instead replaced by a rapid oscillatory and fibrillatory waveform (Bennett & Pentecost, 1970; Fuster *et al.*, 2006). The consequence of this is deterioration in the mechanical function of the atria, resulting in ineffective transport of blood to the ventricles. An irregular ventricular rhythm also results, as it is no longer determined by the sino-atrial node, but by the ability of the atrioventricular node to filter the rapid electrical signals from the atria (Khan, 2004; Nattel, 2002). Impaired contraction of the atria can also lead to pooling of the blood, causing clot formation and thromboemboli that can propagate to the brain, obstructing blood flow and causing infarction (Goldman *et al.*, 1999). Thus, atrial fibrillation is associated with a five-fold increase in the incidence of ischaemic stroke (Wolf *et al.*, 1991). The risk of stroke can be reduced using anticoagulant drugs such as warfarin, but this intervention can lead to bleeding complications, such as haemorrhaging (Goldman *et al.*, 1999).

There are three main clinical classifications describing the different types of atrial fibrillation, namely: paroxysmal, persistent and permanent atrial fibrillation. Paroxysmal atrial fibrillation is a recurrent arrhythmia that self-terminates in less than 7 days. Persistent atrial fibrillation lasts longer than 7 days and requires cardioversion by electrical or pharmacological intervention to restore the heart to sinus rhythm. Finally, permanent atrial fibrillation is the term used when the sinus rhythm cannot been restored by cardioversion (Fuster *et al.*, 2006; Lévy *et al.*, 2003).

It is clear from epidemiological data that atrial fibrillation is a growing problem in western society (Allessie *et al.*, 2001; Go *et al.*, 2001; Murphy *et al.*, 2007), and therefore a better understanding of the underlying causes and cellular mechanisms is required in order to develop new treatments for the condition. In 1998, it was first discovered that atrial fibrillation could be triggered by ectopic foci (areas of pacemaker electrical activity occurring outside of the sino-atrial node) in the pulmonary veins (Haïssaguerre *et al.*, 1998). The evidence suggesting that the pulmonary veins are an important foci for atrial fibrillation stems from a study conducted in patients who were diagnosed with paroxysmal atrial fibrillation and were refractory to drug treatment. It was discovered that in 94% of cases, the electrical activity that initiated the arrhythmia originated in the pulmonary veins (Figure 1.1), and was marked by a discharge of spontaneous activity that propagated into the left atrium (Haïssaguerre *et al.*, 1998). This seminal study led to a whole new line of research whereby the pulmonary veins were considered to be important for determining the causes of atrial fibrillation. Several investigations have corroborated the initial findings that, in most cases of atrial fibrillation, the ectopic focus was in the pulmonary veins (Chen *et al.*, 1999a; Hsieh *et al.*, 1999; Pappone *et al.*, 2000). Ectopic electrical activity has also been reported in non-nodal atrial tissue (Chen *et al.*, 1999b; Polain de Waroux *et al.*, 2009 for review; Shah *et al.*, 2003), the ligament of Marshall (Doshi *et al.*, 1999; Hirose & Laurita, 2007; Katritsis *et al.*, 2001), and the superior vena cava (MacLeod & Hunter, 1967; Shah *et al.*, 2003; Tsai *et al.*, 2000); however, the present thesis will focus on the pulmonary veins, as they are the most common site of ectopic electrical activity leading to atrial fibrillation (Haïssaguerre *et al.*, 1998; Shah *et al.*, 2003).

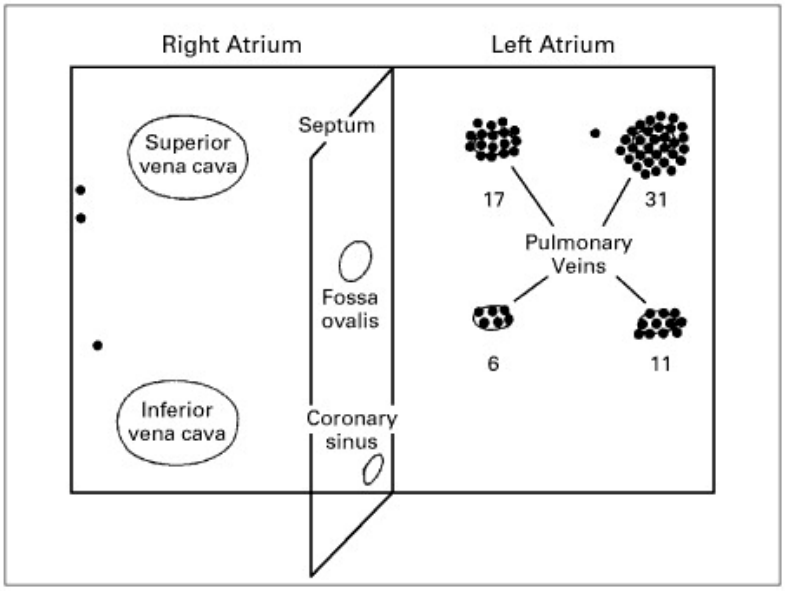

Figure 1.1. Schematic diagram (reproduced from Haïssaguerre *et al.*, 1998) illustrating the sites of 69 ectopic foci that triggered atrial fibrillation in 45 patients. The black circles display the sites of ectopic electrical activity and the numbers represent the distribution of ectopic foci between the different pulmonary veins. The top two veins are the left and right superior pulmonary veins and the bottom two the left and right inferior pulmonary veins.

1.2. Treatment of atrial fibrillation

Currently, the first line of treatment for atrial fibrillation is rhythm control through the use of antiarrhythmic drugs (Polain de Waroux *et al.*, 2009; Savelieva & Camm, 2008; Wyse *et al.*, 2002). Amiodarone, which mainly acts by blocking K^+ channels to prolong the cardiac action potential, thus slowing the heart rate (Kodama *et al.*, 1997), has been found to be the most effective drug for treating atrial fibrillation (Roy *et al.*, 2000; Singh *et al.*, 2005). However, a large clinical trial in Canada revealed that 35% of patients experienced reoccurrence of their arrhythmia. Moreover, 18% of patients eventually had to discontinue amiodarone use due to adverse effects, such as heart failure and severe bradyarrhythmias. Non-cardiac effects such as insomnia and pulmonary toxicity were also reported (Roy *et al.*, 2000). Moreover, as antiarrhythmic drugs do not specifically target the atria, they can be paradoxically proarrhythmic in the ventricular myocardium (Nattel, 1998).

The discovery that atrial fibrillation can be caused by ectopic electrical activity originating in the pulmonary veins lead to the development of focal ablation therapy. Intracardiac catheters were used to map the patient's cardiac conduction to detect rhythm disturbances, and the sites of ectopic electrical activity were thermally ablated using radiofrequency energy (Chen *et al.*, 1999a; Haïssaguerre *et al.*, 1998; Haïssaguerre *et al.*, 2000b). However, this method is limited as it relies on arrhythmias being present during the surgery. The ablation procedure is also associated with the reoccurrence of arrhythmia as, during a follow-up period of 8 ± 6 months, atrial fibrillation had reoccurred in 38% of patients (Haïssaguerre *et al.*, 1998). Therefore, the technique was modified and multiple lesions were performed at the junction of the left atrium and the pulmonary vein, known as the ostia (Haïssaguerre *et al.*, 2000a; Haïssaguerre *et al.*, 2000b). An alternative method of pulmonary vein ablation was developed by a different group where a single lesion was made around the whole circumference of the ostia (Pappone *et al.*, 2001; Pappone *et al.*, 2000). This process generates scar tissue that acts as an insulator to prevent the conduction of electrical signals from the pulmonary vein into the atria (Figure 1.2) (Shapira, 2009 for review).

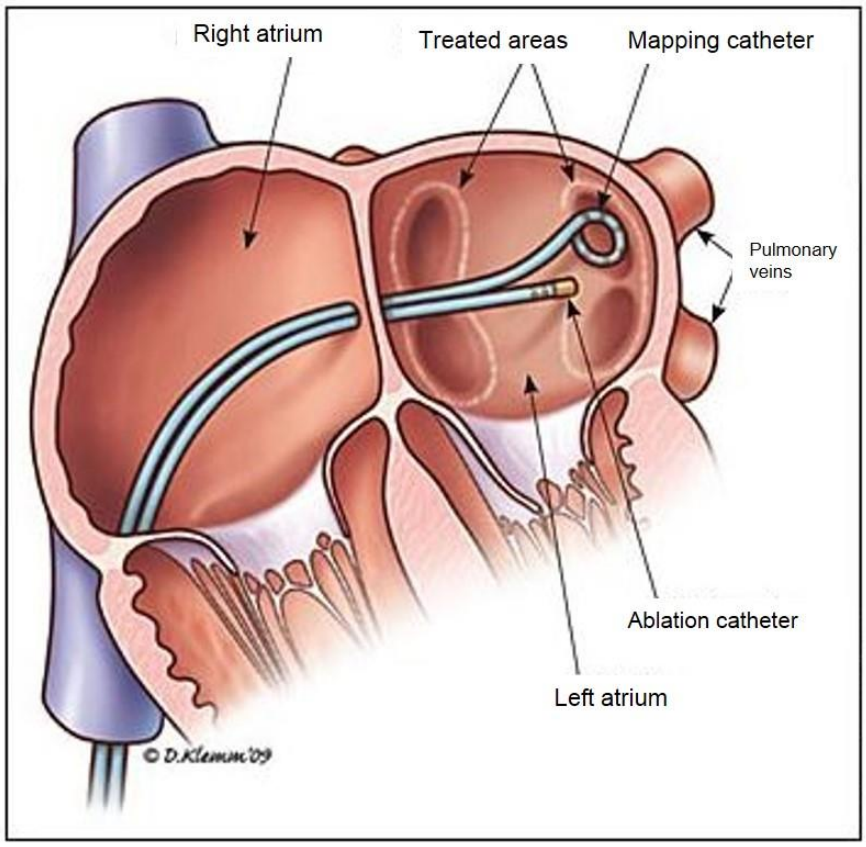

Figure 1.2. Illustration (reproduced from Shapira, 2009) showing the pulmonary vein ablation procedure. Catheters are passed into the left atrium and used to map the cardiac conduction pathways and detect arrhythmias. The sites at the ostia that are responsible for the conduction of electrical activity from the pulmonary veins to the left atrium are then thermally ablated with radiofrequency energy .

There has been a growing shift from traditional pharmacological therapy towards radiofrequency ablation as large meta-analyses have shown that radiofrequency ablation is more successful than antiarrhythmic drugs for maintaining sinus rhythm in patients with atrial fibrillation (Al-Khatib *et al.*, 2014; Nault *et al.*, 2010; Terasawa *et al.*, 2009). However, the surgical procedure is complex and invasive (Wellens, 2000), with a worldwide survey reporting a 6% incidence of severe complications following surgery (Cappato *et al.*, 2005). The most common complication is stenosis of the pulmonary veins (Robbins *et al.*, 1998; Saad *et al.*, 2003; Yu *et al.*, 2001), which in rare cases can lead to severe pulmonary hypertension (Saad *et al.*, 2003; Yu *et al.*, 2001). Despite modifications to the procedure, radiofrequency ablation therapy is still associated with the reoccurrence of atrial fibrillation, and often requires follow-up procedures. A clinical study of patients during a follow-up period after a single ablation procedure showed that 51% had freedom from asymptomatic or symptomatic atrial fibrillation after one year, with this figure decreasing to 23% after 6 years (Sorgente *et al.*, 2012).

1.3. The pulmonary veins

1.3.1. Anatomy of the pulmonary veins

Although research into the arrythmogenic propensity of the pulmonary veins has only been conducted in the last 20 years, studies into its anatomy date as far back as the mid 19th century. The first known record is in a histological text, where Edmond Randolf Peaslee described the large veins entering the human heart (pulmonary veins and vena cava) as containing "a layer of striated muscle fibres, like those of the heart itself" (Peaslee, 1857). Amost 20 years later, Brunton and Frayer found that when they injected cobra venom into the jugular vein of a rabbit, the pulmonary veins continued to independently pulsate, even after the beating of the heart had ceased. They conducted further experiments to eliminate the possibility that this was a result of the venom, and also reported a similar phenomenon in the cat (Brunton & Frayer, 1876). In 1910, Favaro coined the term "pulmonary vein myocardium", demonstrating in the human that the pulmonary vein has a sleeve of cardiomyocytes that extends from the left atrium (Favaro, 1910). In the last 50 years, modern approaches have been employed to gain a better understanding of the pulmonary vein myocardial sleeve.

Early histological studies on pulmonary veins isolated from the rat reported that the external media contained cross striated muscle fibres with an internal circular layer and an external longitudinal layer. The smaller venules, deep within the lungs, possessed muscular bundles that were arranged in an irregular pattern (Klavins, 1963). Ultrastructural investigations using electron microscopy, have reinforced the histological observations that the rat pulmonary veins contain an external sleeve of cardiomyocytes that is continuous with the left atrium and is formed from longitudinal fibres in a mesh like structure, which often display abrupt changes in direction (Hashizume *et al.*, 1998; Ludatscher, 1968; Paes de Almeida *et al.*, 1975) (Figure 1.3). The thickness of the cardiomyocyte layer is variable, within and between species, but in general it is relative to the width of the vessel, becoming thinner and more discontinuous as the vein extends and branches into the lung parenchyma. Fibrous tissue, which is embedded between the muscle fibres, also becomes more abundant as

the veins extend distally to the left atrium (Bronquard *et al.*, 2007; Karrer, 1959; Klavins, 1963; Ludatscher, 1968; Masani, 1986; Mueller-Hoecker *et al.*, 2008). Beneath the cardiomyocyte sleeve, and separated by connective tissue, is a layer composed of smooth muscle cells, arranged in a circular manner, and irregularly distributed along the length of the vein. Elastic lamellae and collagen fibrils are present between the smooth muscle cells, and are also interposed between the smooth muscle layer and an endothelial layer, which encircles the lumen of the vessel (Hashizume *et al.*, 1998; Klavins, 1963; Masani, 1986; Paes de Almeida *et al.*, 1975; Takahara *et al.*, 2011).

In humans, cardiomyocytes are only present in the extrapulmonary veins extending approximately 1-2 cm from the left atrium, and are more prominent in the superior compared to the inferior pulmonary veins (Ho *et al.*, 2001; Mueller-Hoecker *et al.*, 2008; Nathan & Eliakim, 1966; Steiner *et al.*, 2006). Similar observations have been made in the pulmonary veins of the canine (Verheule *et al.*, 2002) and rabbit (Seol *et al.*, 2008). On the other hand, in rodents excluding the guinea pig (Cheung, 1981a; Tasaki, 1969), the cardiomyocyte sleeve extends beyond the hilus of the lungs and into the intrapulmonary veins (Bronquard *et al.*, 2007; Hashizume *et al.*, 1998; Karrer, 1959; Klavins, 1963; Kramer & Marks 1965; Mueller-Hoecker *et al.*, 2008; Nathan & Gloobe, 1970; Paes de Almeida *et al.*, 1975).

The function of the myocardial sleeve has been postulated to be that of a throttle valve, regulating unidirectional blood flow into the left atrium and preventing back-flow into the lungs (Hashizume *et al.*, 1998; Klavins, 1963; Nathan & Eliakim, 1966; Paes de Almeida *et al.*, 1975; Tasaki, 1969). Magnetic resonance imaging (MRI) in the human has revealed that the pulmonary veins contract in synchrony with the atria (Bowman & Kovács, 2005; Lickfett *et al.*, 2005). In addition, the pulmonary vein ablation procedure has been demonstrated to abolish contraction of the vein (Atwater *et al.*, 2011). However, the physiological function of the cardiomyocytes in the pulmonary vein remains to be fully elucidated.

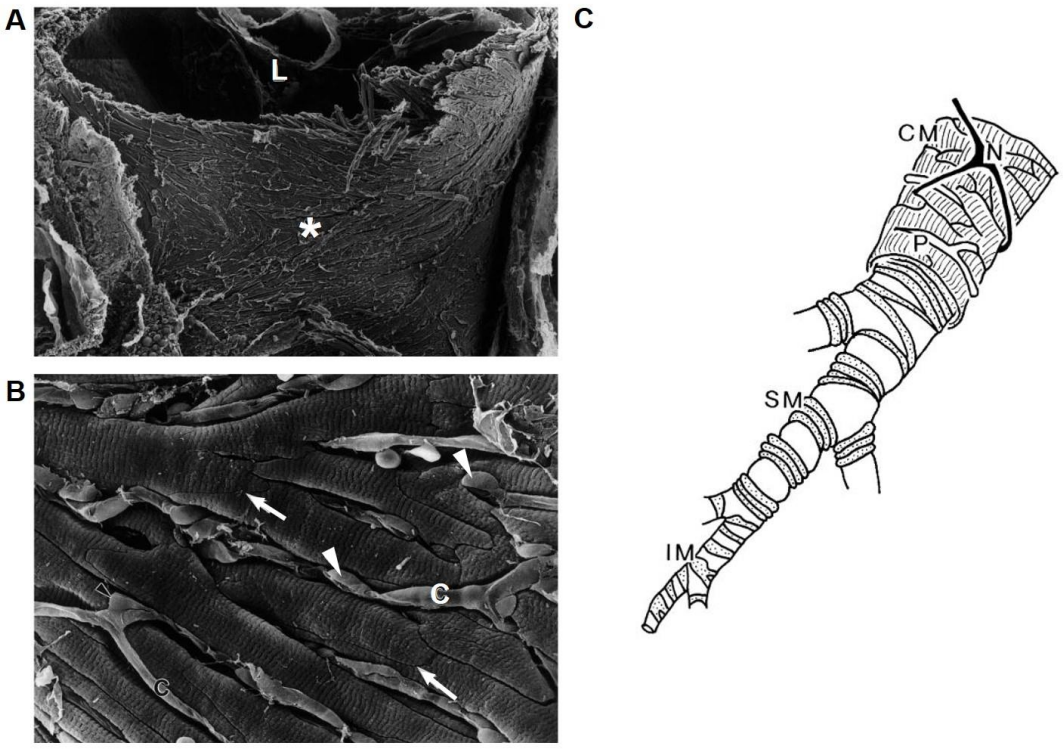

Figure 1.3. Three-dimensional scanning electron micrograph of the rat pulmonary vein (reproduced from Hashizume *et al*., 1998). A. Large pulmonary vein at the hilus (area at the root of the lung where the vein enters the lung) imaged at 70x maginification. The external layer is composed of cardiomyocytes (*) (L = lumen) **B.** Myocardial sleeve at 1000x magnification. Capillaries (C) with pericytes (contractile cells that attach to capillaries – arrow heads) run between the cardiomyocytes. Adjactent cardiomyocytes are connected at the intercalated discs (arrows). **C.** Schematic diagram of the rat pulmonary vein and venule. Note that the vein contains a sleeve of cardiomyocytes (CM), with capillaries (P) and nerve fibres (N) running along it. The venule has circularly arranged bundles of smooth muscle (SM) cells and periendothelial cells (IM), which are an intermediate cell-type between SM cells and pericytes

1.3.2. Arrhythmogenic substrate in the pulmonary vein myocardium

In patients with atrial fibrillation, the pulmonary veins have been shown to be more dilated (Lin *et al.*, 2000; Takase *et al.*, 2004) and possess a thicker myocardium (Guerra *et al.*, 2003). Moreover, the ectopic focal point that initiated the arrhythmia was in these thickened areas (Guerra *et al.*, 2003). Ectopic foci have also been shown to be more likely to occur in the veins with the longest cardiomyocyte sleeves (Haïssaguerre *et al.*, 1998; Ho *et al.*, 2001), and the length of the cardiomyocyte sleeve has been found to be longer in patients with atrial fibrillation than those in sinus rhythm (Hassink *et al.*, 2003; Kholová & Kautzner, 2003). This suggests that there is a correlation between the length and thickness of the cardiomyocyte sleeve and the propensity towards ectopic electrical activity. It should be noted though, that there is conflicting evidence suggesting that no such relationship exists (Saito *et al.*, 2000).

The orientation of muscle fibres in the pulmonary vein myocardial sleeve is complex (Ho *et al.*, 2001; Hocini *et al.*, 2002), and there is often a 90º change in fibre orientation at the junction of the pulmonary vein and left atrium (Chou *et al.*, 2005; Tan *et al.*, 2006). Moreover, patients with ectopic foci in the pulmonary veins have been shown to display a larger degree of scarring and fibrosis compared to those without (Hassink *et al.*, 2003; Steiner *et al.*, 2006; Tagawa *et al.*, 2001). These conditions can lead to slowed conduction of electrical impulses, which can facilitate arrhythmic re-entry circuits (Hassink *et al.*, 2003). Overall, the studies described in this section suggest that structural remodelling of the myocardial sleeve can provide a substrate for the initiation and maintenance of atrial fibrillation (Chard & Tabrizchi, 2009 for review).

1.3.3. Pulmonary vein cardiomyocytes

Cardiomyocytes in the pulmonary vein have been described as typical cardiac rod shaped cells, approximately 50-150 µm long and 10-20 µm wide, with one or two centrally located nuclei and abundant contractile filaments (Hashizume *et al.*, 1998; Klavins, 1963; Masani, 1986). It is the cardiomyocyes that are believed to be responsible for the arrhythmogenic properties of the pulmonary veins (Chen *et al.*,

2000; Haïssaguerre *et al.*, 1998). In previous reports, pulmonary vein cardiomyocytes have been described as being structurally similar to atrial myocytes (Chen *et al.*, 2002b; Karrer, 1959; Klavins, 1963; Masani, 1986; Paes de Almeida *et al.*, 1975; Verheule *et al.*, 2002). Therefore, in the present thesis, where relevant literature on the pulmonary vein is absent, studies on the atria will be initially referred to. Also, the term pulmonary vein cardiomyocytes will be used to describe the cells of the myocardial sleeve. Atrial and ventricular cells will be termed myocytes preceded by their location in the heart.

1.3.4. Embryonic origin of pulmonary vein cardiomyocytes

Genetic profiling has yielded two main hypotheses to explain the developmental origin of the pulmonary vein myocardial sleeve (Chard & Tabrizchi, 2009 for review). The first is that the cardiomyocytes initially develop as atrial myocytes, which then migrate along the pulmonary vein (Jones *et al.*, 1994; Millino *et al.*, 2000). The second hypothesis is that the cardiomyocytes develop by differentiation from an innate pulmonary vein cell line (van den Hoff *et al.*, 2004). Most recently a biphasic mechanism was proposed, whereby a cardiomyocyte population develops at the ostia of the left atrium and pulmonary vein, which then proliferates and expands along the pulmonary vein forming an external sleeve (Mommersteeg *et al.*, 2007).

1.4. Possible mechanisms of atrial fibrillation

1.4.1. Automaticity

The sino-atrial node, which is located in the right atrium, is physiologically the fastest pacemaker, controlling the rate and rhythm of the heart (Boyett & Dobrzynski, 2007; Unudurthi *et al.*, 2014). In the context of the myocyte, the electrical potential is determined by the flux of different ions across the cell membrane (sarcolemma). During an action potential, the rapid influx of Na^+ results in depolarisation, making the membrane potential more positive (Brown *et al.*, 1981; Sakakibara *et al.*, 1992). During repolarisation, the membrane potential gradually becomes more negative due

to the efflux of K^+ (Firek & Giles, 1995; Wang *et al.*, 1994). In a spontaneously depolarising myocyte, there is a progressive depolarisation during the diastolic (resting) phase of the action potential, due to a shift towards the inward movement of positive ions, namely Na^+ (DiFrancesco, 1991) and Ca^{2+} (Lakatta *et al.*, 2003). Once this depolarisation reaches a threshold potential, it will elicit an action potential. Thus, the rate of depolarisation during diastole governs the rate of action potential firing. If diastolic depolarisation is accelerated in a spontaneously depolarising myocyte outside of the sino-atrial node, then there will be a discharge of action potentials at a rate that overrides the sinus rhythm. This forms the basis for automaticity (Figure 1.4A) (Nattel, 2002 for review).

1.4.2. Triggered activity

Abnormal electrical activity in cardiac myocytes can also be caused by an abnormal increase in intracellular Ca^{2+} concentration during the systolic (depolarised) phase of the action potential. During the diastolic phase, excess Ca^{2+} is removed from the myocyte by the Na^+/Ca^{2+} exchanger (NCX), which carries an inward depolarising current due to the stoichiometry of 3 Na^+ ions being exchanged for every Ca^{2+} ion (Mechmann & Pott, 1986). This transient inward current (I_{ti}) generates what have been termed after-depolarisations, which if above the threshold, will elicit premature action potentials. The result is an increased rate of action potential firing (Figure 1.4B) (Ferrier *et al.*, 1973; Kass *et al.*, 1978; Nattel, 2002 for review; Schlotthauer & Bers, 2000). The mechanisms underlying Ca^{2+} induced changes in membrane potential will be covered in more detail later in the chapter; however, it is important at this stage to note that, for triggered activity to occur, it must be preceded by an action potential.

1.4.3. Re-entry

A re-entry circuit is a wave of electrical activty that circulates in a region of tissue due to different tissue zones continually re-exciting one another (Allessie *et al.*, 1976). A schematic example of a re-entry circuit between two tissue zones (I and II) is presented

and described in Figure 1.4C. During an action potential there is a refractory period, whereby a subsequent action potential cannot be elicited until the zone of tissue fully repolarises again. An approaching action potential will initially fail to excite the zone of tissue; however, it can travel via an alternate route around a conduction block to reactivate the tissue zone when is excitable again. If the time for the action potential to return to its orgin is sufficiently long, it will elicit a further action potential, and the re-entrant impulse will circulate indefinitely (Figure 1.4C) (Nattel, 2002 for review).

Conditions that favour the induction and maintenance of re-entry circuits include shorter refractory periods and slower conduction velocities. The pathological result is irregular conduction within the atria, which in turn leads to irregular atrial contraction, having a downstream effect on ventricular filling (Jalife *et al.*, 2002; Khan, 2004; Workman *et al.*, 2011). There are several properties of the pulmonary vein myocardial sleeve that provide a favourable substrate for the generation and maintenace of re-entry circuits. The action potentials recorded in the pulmonary vein have been shown to be of shorter duration compared to those in atrial myocytes (Arora *et al.*, 2003; Ehrlich *et al.*, 2003; Hocini *et al.*, 2002; Kuz'min & Rozenshtraukh, 2012; Malécot *et al.*, 2015; Tasaki, 1969). Moreover, the conduction velocity in the guinea pig pulmonary vein has been found to be half that in the atria (Takahara *et al.*, 2012). The conduction velocity was also found to be more likely to be slower in the pulmonary veins of patients with atrial fibrillation than those in sinus rhythm (Jaïs *et al.*, 2002).

Both shortened refractory periods and slower conduction velocities mean that circulating impulses are more likely to re-excite previously refractory tissue regions. Re-entry circuits have been directly observed in canine pulmonary veins using high resolution optical mapping (Arora *et al.*, 2003; Po *et al.*, 2005). However, re-entry is usually associated with cases of persistent atrial fibrillation. Ectopic foci that can cause paroxysmal atrial fibrillation are thought to be initiated by abnormal automaticity and triggered actvity (Chen *et al.*, 1999a).

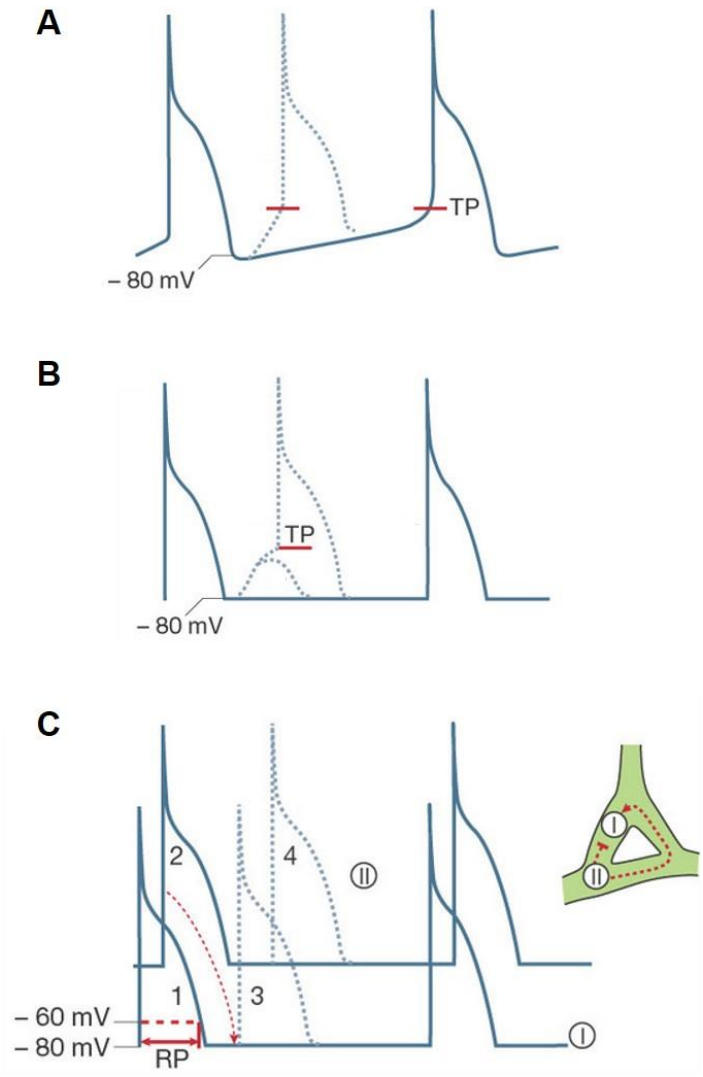

Figure 1.4. Schematic diagrams (reproduced from Nattel, 2002) illustrating the cellular mechanisms of atrial fibrillation. A. Automaticity occurs when accelerated depolarisation during the diastolic phase of the action potential results in the membrane potential reaching the threshold potential (TP) earlier. This results in an increased firing rate, and the additional action potential is indicated by the dotted line. **B.** Triggered activity, when an afterdepolarisation, if above the TP, leads to a premature action potential (3). **C.** Re-entry between tissue zones I and II. A premature action potential in zone II (2) fails to initiate another in zone I as it is still in the refractory period. However, the electrical impulse is conducted back (dotted line) at a time when zone I is excitable resulting in the firing of an action potential (3) that propagates to initiate another (4) in zone II .

1.4.4. Conduction of electrical impulses through gap junctions

Electron microscopy has shown that adjacent cardiomyocytes in the pulmonary vein are connected at the transverse axis by intercalated discs (Hashizume *et al.*, 1998; Karrer, 1960; Ludatscher, 1968; Mueller-Hoecker *et al.*, 2008). In cardiac tissue, gap junctions are present at the intercalated discs and allow for the conduction of electrical current by permitting the movement of ions between cells (Barr *et al.*, 1965; Saffitz *et al.*, 1994). Gap junctions are formed by two connexons, which are each composed of six protein subunits called connexins, denoted by the abbreviation Cx and then their molecular weight in kilodaltons (Yeager, 1998). Three main connexin proteins; Cx40, Cx43 and Cx45 have been identified in cardiac myocytes (Kanter *et al.*, 1992), and the expression of these different connexins determines the conduction properties of the channel by governing the intercellular resistance to current (Davis *et al.*, 1994; 1995).

In the canine, conduction was found to be slower in regions of the pulmonary veins that were distal to the left atrium, compared to the left atrium itself (Arora *et al.*, 2003), which suggests that the connexin expression might be different between the different tissues. The connexins Cx40 and Cx43 are highly expressed in atrial myocytes (Davis *et al.*, 1994; van der Velden *et al.*, 1998; Verheule *et al.*, 2002), whereas in cardiomyocytes of the canine pulmonary vein, Cx40 levels were found to be significantly lower (Verheule *et al.*, 2002). This was similar to what has been reported in myocytes in the rabbit sino-atrial node (Verheule *et al.*, 2001), which may predispose the cardiomyocytes to abnormal automaticity.

Atrial remodelling, specifically atrial dilation, is often present in patients with atrial fibrillation (Sanfilippo *et al.*, 1990; Takahashi *et al.*, 1982). In an experimental canine model, where the mitral valve was ruptured in order to induce regurgitation of blood from the ventricles and atrial dilation, the expression of Cx40 was found to be significantly reduced in pulmonary vein cardiomyocytes, but not in left atrial myocytes (Sun *et al.*, 2008). Moreover, in mice where the gene encoding Cx40 was knocked out, the conduction velocity in the atrial myocardium was slowed and the mice were more

succeptable to atrial tachycardias arising from ectopic foci (Bagwe *et al.*, 2005; Kirchhoff *et al.*, 1998). The expression of Cx40 has also been reported to be altered in patients with chronic atrial fibrillation; however, there has been some debate as to whether the expression is increased (Polontchouk *et al.*, 2001; Wetzel *et al.*, 2005), or decreased (Nao *et al.*, 2003; Nattel *et al.*, 2007 for review; Wilhelm *et al.*, 2006). Overall, the investigations described above signify that Cx40 is the main connexin that determines the conduction properties of electrical impulses in the atria and pulmonary veins, and the expression of Cx40 is altered in atrial fibrillation (Chaldoupi *et al.*, 2009 for review).

1.5. Electrical activity in the pulmonary vein

In 1967, Macleod and Hunter isolated the pulmonary veins from the rat and the mechanical and electrical activity of individual segments was studied using myography and glass microelectrodes respectively. When electrically field stimulated, the tissue responded with contractions and electrical activity in the form of action potentials. The action potentials evoked in the pulmonary vein were described as having similar characteristics to those recorded in the atria and ventricle (MacLeod & Hunter, 1967).

When the pulmonary veins were removed from the guinea pig with the atria still attached, action potentials, which originated in the sino-atrial node, were conducted along the pulmonary vein (Tasaki, 1969). Action potentials could also be directly evoked in the pulmonary vein by electrical field stimulation. The characterstics of the action potentials recorded in the pulmonary vein varied depending on the distance from the left atrium. Those recorded distal to the left atrium had a less negative resting membrane potential and slower upstroke velocity, compared to those recorded in a proximal region. Moreover, the action potentials recorded in the pulmonary vein were of shorter duration than those in the atria (Tasaki, 1969). The ability of the pulmonary veins to conduct electrical activity from the left atrium was later confirmed in the mouse (Challice *et al.*, 1974), rat (Paes de Almeida *et al.*, 1975), canine and human

(Spach *et al.*, 1972). These early studies show that pulmonary vein cardiomyocytes are electrically excitable, and the pulmonary veins are electrically coupled to the left atrium. This suggests that *in situ*, during atrial depolarisation, electrical activity is conducted from the atria into the pulmonary veins resulting in the vein contracting in accordance to the sinus rhythm. This supports the hypothesis that the role of the cardiomyocyte sleeve is to prevent retrograde blood flow into the lungs during the cardiac cycle (Hashizume *et al.*, 1998; Klavins, 1963; Nathan & Eliakim, 1966; Paes de Almeida *et al.*, 1975; Tasaki, 1969).

Electrical activity was first shown to occur spontaneously in the isolated pulmonary vein in 1981, in a study on the guinea pig. Glass microelectrode recordings revealed that the pulmonary vein had a less negative resting membrane potential compared to the atria, and spontaneous action potentials were observed in 41% of the preperations studied (Cheung, 1981a). Similar to the conducted action potentials recorded by Tasaki (1969), the action potential characteristics were different, depending on the location on the vein where the electrical activity was recorded. When recordings were made from areas distal to the left atrium, the membrane potential was less negative and the repolarisation phase was shorter compared to recordings made at the proximal end, where the action potentials more closely resembled those recorded in the atria (Cheung, 1981a). The observation that pulmonary vein cardiomyocytes have a less negative resting membrane potential and shorter action potential durations than atrial myocytes has since been made in the rat (Doisne *et al.*, 2009; Kuz'min & Rozenshtraukh, 2012; Malécot *et al.*, 2015) and canine (Arora *et al.*, 2003; Ehrlich *et al.*, 2003; Hocini *et al.*, 2002).

Since the discovery by Cheung (1981a), spontaneous electrical activity has been recorded under control (unstimulated) conditions in the pulmonary veins of the canine (Chen *et al.*, 2000; Chen *et al.*, 2001), rabbit (Chen *et al.*, 2002a; Honjo *et al.*, 2003a; Seol *et al.*, 2008; Wongcharoen *et al.*, 2006), guinea pig (Namekata *et al.*, 2009), rat (Namekata *et al.*, 2010) and mouse (Tsuneoka *et al.*, 2012). However, whether or not the pulmonary vein displays spontaneous electrical activity without any prior

intervention has been the subject of much debate, and the reported incidence varies considerably within and between species (Table 1.1). Contradictory reports that no spontaneous electrical activity is observed under control conditions have been made in the canine (Arora *et al.*, 2003; Ehrlich *et al.*, 2003; Hirose & Laurita, 2007; Hocini *et al.*, 2002; Wang *et al.*, 2003), rabbit (Luk *et al.*, 2008), guinea pig (Tasaki, 1969), rat (Doisne *et al.*, 2009; MacLeod & Hunter, 1967; Miyauchi *et al.*, 2005; Paes de Almeida *et al.*, 1975) and mouse (Challice *et al.*, 1974).

It is unclear why spontaneous activity is observed in some studies and not in others. The archetypal example of this are the studies on the canine pulmonary vein where one group consistently reports automaticity (Chen *et al.*, 2000), whereas an independent group does not observe any automaticity (Wang *et al.*, 2003). In these studies there are clearly differences in the composition of the external solution that the groups use; specifically Chen *et al*., (2000) use 2.7 mM $CaCl_2$ whereas Wang *et al*., (2003) use 1.8 mM $CaCl_2$, and there are also some other minor differences in composition as well. Thus, unless identical recording conditions are used then these studies don't represent direct comparisons, and this may underlie the discrepancies observed. An additional factor that has been shown to affect the incidence of spontaneous activity is the degree of stretch applied to the tissue. For instance, mechanical stretch has been shown to increase the incidence of spontaneous action potentials in the rabbit pulmonary vein (Chang *et al.*, 2007), and increase the frequency of spontaneous activity in the guinea pig pulmonary vein (Hamaguchi *et al.*, 2016). Therefore, the amount of stretch applied to the tissue during recording could also be an explanation for the presence or absence of spontaneous activity observed in different studies.

Throughout the present thesis, spontaneous activity will be used to describe action potentials, Ca^{2+} transients or contractions that are present under unstimulated conditions, where there has been no prior intervention. Activity that has been induced using a drug or reagent will be termed automaticity.

1.5.1. Electrical activity in the smooth muscle cells

Intracellular recordings in smooth muscle cells in the guinea pig pulmonary vein revealed that they had a stable membrane potential and did not depolarise in response to individual electrical pulses. In addition, action potentials which were evoked in the cardiomyocytes, did not propagate into the smooth muscle cells (Cheung, 1981a). Thus, it would appear that the smooth muscle cells are unlikely to affect the excitabilty of the pulmonary vein myocardial sleeve.

1.5.2. Does the pulmonary vein have specialised pacemaker cells?

An investigation into the ultrastructure of the rat pulmonary vein, using electron microscopy, revealed the presence of small populations of what were termed, clear muscle cells, which were different to typical cardiomyocytes (Masani, 1986). These cells were characterised by their sparse myofilaments and small oval shaped mitochondria, and were described as being structurally similar to sino-atrial node cells (Taylor, 1980). If the ultrastuctural similarity to sino-atrial node cells is also reflected in their electrical activity then these cells may have a role in pacemaker electrical activity.

In patients with a history of atrial fibrillation, pacemaker (P) cells, and also Purkinje cells, have been indentified in the pulmonary vein myocardial sleeve (Perez-Lugones *et al.*, 2003). Interstitial cells of Cajal, which are normally associated with pacemaker electrical activity in the gastrointestinal system (Sanders & Ward, 2006), have also been reported in the pulmonary veins of patients with atrial fribillation (Morel *et al.*, 2008), as well as in the pulmonary veins of canines with persistant atrial fibrillation (He *et al.*, 2012). This would suggest that specialised pacemaker cells in the pulmonary vein may be a cause of ectopic electrical activity leading to atrial fibrillation.

Periodic acid-schiff staining of the canine pulmonary veins revealed large pale cells that were positive for glycogen, which is known to be abundant in Purkinje cells.

Interestingly, these cells were located in regions where focal electrical activity could be induced in the pulmonary veins by rapid pacing of the atria. Other cardiomyocytes in the same tissue were negative for glycogen (Chou *et al.*, 2005; Tan *et al.*, 2008). Periodic acid-schiff positive cells have since been reported to be present in human pulmonary veins (Nguyen *et al.*, 2009). Purkinje-like cells have been shown to be highly expressed in areas of the canine pulmonary vein where ectopic electrical activity could be induced by stimulation of the sympathetic ganglion, which is located near the ostia (Tan *et al.*, 2008). This provides further evidence that these cells may have a role in generating abnormal electrical activity. Despite these findings, there are several studies that have reported the absence of specialised pacemaker cells in the pulmonary vein (Kholová & Kautzner, 2003; Mueller-Hoecker *et al.*, 2008; Steiner *et al.*, 2006; Verheule *et al.*, 2002; Yeh *et al.*, 2003). Thus, the presence of specialised conduction cells in the pulmonary vein remains subject to debate and if these cells are present, their physiological function and pathological role in the generation of ectopic electrical activity remains unresolved.

Species	Reference	Preparation	Incidence of spontaneous activity (%)
Canine	Chen *et al*., 2000b	Tissue	71
	Chen *et al*., 2001	Cells	40
	Hocini *et al*., 2002	Tissue	0
	Arora *et al*., 2003	Tissue	0
	Ehrlich *et al*., 2003	Cells	0
	Wang *et al*., 2003	Tissue	0
	Hirose & Laurita 2007	Tissue	0
Rabbit	Chen *et al*., 2002a	Cells	76
	Chen *et al*., 2002b	Cells	51
	Honjo *et al*., 2003	Tissue	5
	Wongcharoen *et al*., 2006	Tissue	52
	Seol *et al*., 2008	Cells	76
	Luk *et al*., 2008	Tissue	0
Guinea Pig	Namekata *et al*., 2009	Tissue	18
	Tasaki, 1969	Tissue	0
Rat	MacLeod & Hunter 1967	Tissue	0
	Paes de Almeida *et al*., 1976	Tissue	0
	Miyauchi *et al*., 2005	Cells	0
	Doisne *et al*., 2009	Tissue	0
	Namekata *et al*., 2010	Tissue	4
	Okamoto *et al*., 2012	Cells	2
Mouse	Challice *et al*., 1974	Tissue	0
	Tsuneoka et al., 2012	Tissue	45

Table 1.1. Reported incidence of spontaneous action potentials in the intact tissue or isolated cardiomyocytes from the pulmonary veins of different species.

1.6. Intracellular Ca^{2+} signalling in pulmonary vein cardiomyocytes

1.6.1. Calcium and cardiac contraction

The fundamental role of Ca^{2+} in the contraction of the heart was first demonstrated over a century and a half ago in London, UK by Sidney Ringer. When the heart was isolated from the frog, beating could only be maintained when the heart was perfused with solution containing small amounts of Ca^{2+} (Ringer, 1883). It was not until decades later that it was shown that the injection of Ca^{2+} saline into the cut ends of frog muscle fibres could induce contraction, thus determining that Ca^{2+} acts intracellularly to promote muscle contractions (Heilbrunn & Wiercinski, 1947). In the last 70 years, extensive research has gone into characterising the process, which is termed excitation-contraction coupling (Sandow, 1952), whereby electrical signals are converted into mechanical activity in contractile cells. It is now well established that excitation-contraction coupling in cardiac myocytes is mediated by intracellular Ca^{2+} signalling (Allen & Blinks, 1978; Bers, 2002 for review; O'Rourke *et al.*, 1990; Stern, 1992).

1.6.2. Excitation-contraction coupling

Depolarisation of the cardiac myocyte activates voltage-gated L-type Ca^{2+} channels (LTCCs) (also known as dihydropyridine receptors) on the sarcolemma, leading to Ca^{2+} influx (Bean, 1985; Reuter, 1974; Wang *et al.*, 2001). Entry of Ca^{2+} also occurs to a lesser extent through the Na^{+}/Ca^{2+} exchanger (NCX), which is dependent on the electrochemical gradient of Na^{+} (Kimura *et al.*, 1987). This rise in intracellular Ca^{2+} activates ryanodine receptors (RyRs) on the sarcoplasmic reticulum (SR) to induce the local release of stored Ca^{2+}, and this elementary Ca^{2+} release event is termed a Ca^{2+} spark (Cannell *et al.*, 1994; Cheng *et al.*, 1993). The release of Ca^{2+} from the SR triggers further Ca^{2+} release through adjacent RyRs during a process known as Ca^{2+}-induced Ca^{2+} release (CICR) (Fabiato, 1983; Fabiato & Fabiato, 1975). The spatial and temporal summation of several Ca^{2+} release events results in a global rise in intracellular Ca^{2+} throughout the cytosol during systole (Cannell *et al.*, 1994; Cheng *et al.*, 1993).

The contractile process is activated by the binding of Ca^{2+} to the tropomyosin/troponin complex, which is attached to the actin filament (Huxley, 1961). Troponin consists of three subunits; troponin C, the Ca^{2+} binding unit; troponin I, an inhibitory unit that binds to actin to prevent contraction in the absence of Ca^{2+}; and troponin T, which anchors troponin to tropomyosin (Ebashi *et al.*, 1967). The binding of Ca^{2+} to troponin C induces a conformational change in troponin, which moves the position of tropomyosin to reveal the binding sites on actin for the attachment of myosin (Kress *et al.*, 1986; Lehman *et al.*, 2001; Solaro & Rarick, 1998; Takeda, 2005). When myosin binds to actin, the myofilament is pulled toward the center of the sarcomere, which results in the shortening of the sarcomere and thus, muscle contraction (Metzger & Westfall, 2004 for review; Parmacek & Solaro, 2004 for review).

During relaxation, the majority of cytosolic Ca^{2+} is either removed from the myocyte through the NCX, or actively sequestered into the SR by the sarcoplasmic reticulum Ca^{2+} ATPase (SERCA) (Ebashi & Ebashi, 1962). The rate of Ca^{2+} uptake into the SR is regulated by phospholamban which, when in its unphosphorylated state, inhibits SERCA (James *et al.*, 1990; Koss & Kranias, 1996; Mundiña de Weilenmann *et al.*, 1987; Tada *et al.*, 1974).

Cardiac mitochondria also accumulate Ca^{2+} during elevations in cytosolic Ca^{2+}; however, there is continuing debate as to the kinetics of this process and whether mitochondria sequester Ca^{2+} on a beat-to-beat basis in cardiac cells (Dedkova & Blatter, 2013 for review). One of the earliest studies on living cardiac myocytes, as opposed to electron probe X-ray microanalysis on fixed cells, used the Ca^{2+} sensitive fluorescent indicator indo-1 to monitor mitochondrial Ca^{2+} in ventricular myocytes. It was found that mitochondrial Ca^{2+} did not increase in response to a single electrical stimulus; but it did increase slowly during electrical stimulation at 4 Hz or in the presence of noradrenaline (Miyata *et al.*, 1991). In contrast, using the Ca^{2+} sensitive fluorescent indicator rhod-2, which preferentially localises in mitochondria, it was shown that when guinea pig ventricular myocytes were electrically stimulated at 2 Hz, the mitochondrial Ca^{2+} increased and then rapidly decreased to baseline (Trollinger *et*

al., 1997). Over the subsequent years there have been a number of studies both for and against beat-to-beat changes in mitochondrial Ca^{2+}. The identification of the gene encoding the mitochondrial Ca^{2+} uniporter (MCU) (Baughman *et al.*, 2011; De Stefani *et al.*, 2011) has enabled the generation of MCU knockout mice (Pan *et al*. 2013), and the role of mitochondrial Ca^{2+} uptake in cardiac myocytes is likely to be studied more extensively in years to come. Mice in which the pore forming subunit of the MCU was knocked out have been shown to be viable, suggesting that the MCU is not essential for survival. However, when ventricular contractility was measured in MCU knockout mice, the positive inotropic effect of β-adrenergic stimulation was not observed, suggesting that the MCU might be more important during acute stress (Luongo *et al.*, 2015). In addition to the aforementioned mechanisms, cytosolic Ca^{2+} is also actively removed from the myocyte through the plasma membrane Ca^{2+} ATPase (Carafoli, 1991; Schatzmann, 1966), and contractile force decreases along with the intracellular Ca^{2+} concentration (Bers, 2002 for review) (Figure 1.5).

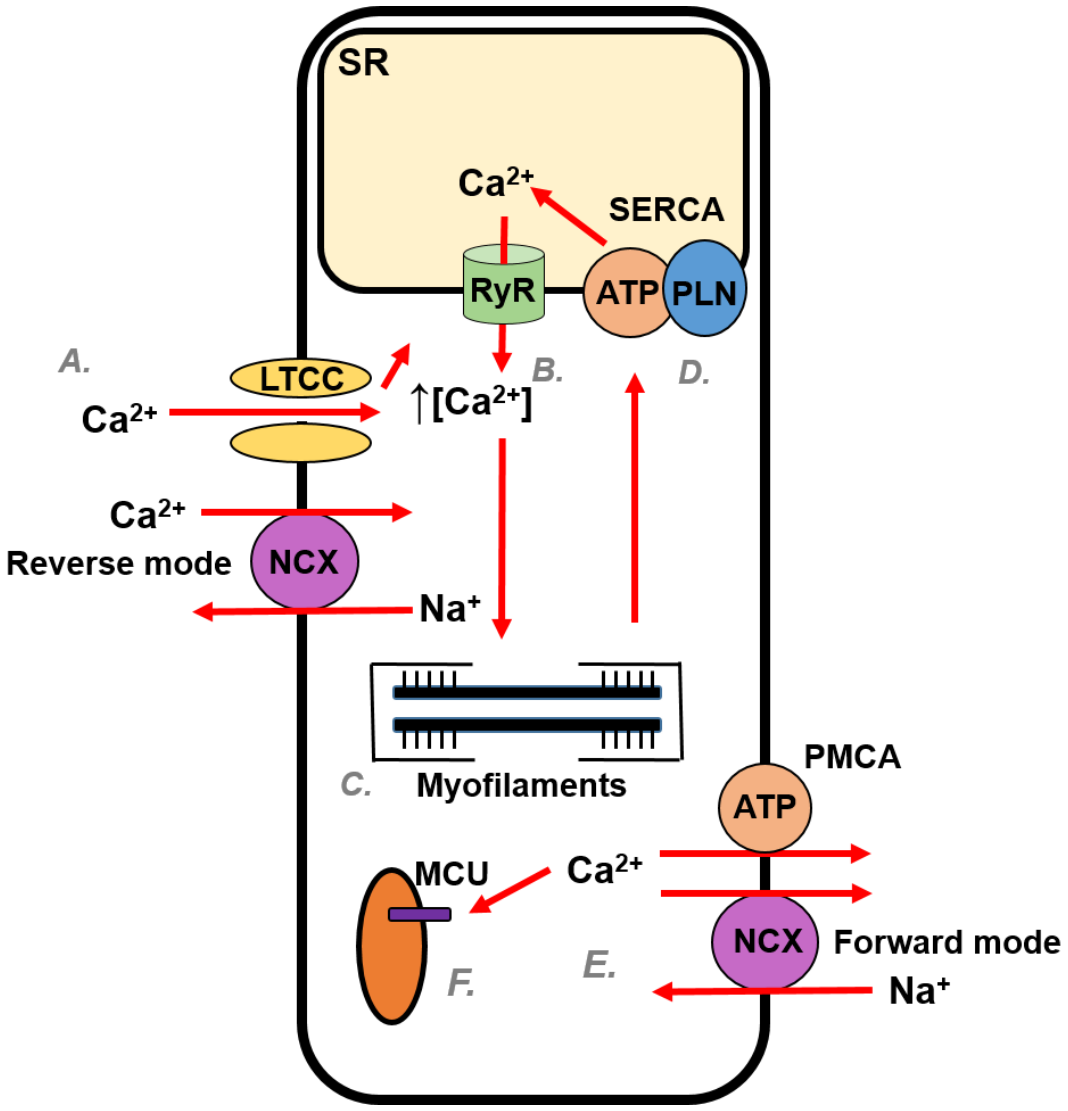

Figure 1.5. Schematic diagram of normal excitation-contraction coupling in a cardiac myocyte. A. Depolarisation of the myocyte allows Ca^{2+} influx through voltage gated L-type Ca^{2+} channels (LTCC). A smaller amount of Ca^{2+} entry can also occur through the reverse mode of the Na^{+}/Ca^{2+} exchanger (NCX). **B.** The increase in intracellular Ca^{2+} triggers the release of Ca^{2+} from the sarcoplasmic reticulum (SR) through ryanodine receptors (RyR). This process of Ca^{2+} -induced Ca^{2+} release results in a large global rise in the intracellular Ca^{2+} concentration. **C.** Activation of the contractile process occurs upon binding of Ca^{2+} to the tropomyosin/troponin complex on the myofilaments. During relaxation, Ca^{2+} is; **D.** sequestered into the SR through the sarcoplasmic reticulum Ca^{2+} ATPase (SERCA); **E.** extruded from the myocyte through the forward mode NCX and plasma membrane Ca^{2+} ATPase (PMCA) or; **F.** taken up by the mitochondria through the mitochondrial Ca^{2+} uniporter (MCU).

1.6.3. Spontaneous Ca^{2+} release from the sarcoplasmic reticulum

In addition to SR Ca^{2+} release regulating normal excitation-contraction coupling, spontaneous diastolic Ca^{2+} release can occur, ranging from highly localised Ca^{2+} sparks arising from a cluster of RyRs to "waves" of regenerative Ca^{2+} release that travel along the length of the myocyte (Cheng *et al.*, 1996; Wier *et al.*, 1987). It has been established in ventricular myocytes that spontaneous Ca^{2+} transients occur when the Ca^{2+} concentration in the SR is above a critical threshold (Jiang *et al.*, 2004; Overend *et al.*, 1997; Trafford *et al.*, 2000; Venetucci *et al.*, 2007 for review).

Caffeine binds to the RyR on the SR, increasing the number of open channels and the duration in which the channels are open (Rousseau & Meissner, 1989). When applied at low concentrations, caffeine has been shown to increase the frequency and decrease the amplitude of spontaneous Ca^{2+} waves, and this was accompanied by a decrease in the SR Ca^{2+} load. It was therefore concluded that sensitising the RyRs enabled spontaneous Ca^{2+} release to occur at lower SR Ca^{2+} concentrations than normal. Thus, caffeine lowered the threshold SR Ca^{2+} concentration required for the appearance of Ca^{2+} waves (Kong *et al.*, 2008; Trafford *et al.*, 2000). Tetracaine, which reduces the opening of the RyRs (Györke *et al.*, 1997), had the opposite effect; decreasing the frequency, and increasing the amplitude of the spontaneous Ca^{2+} waves. Thus, tetracaine increased the threshold SR Ca^{2+} load required for waves to occur (Overend *et al.*, 1997). This suggests that alterations that have an effect on the opening of the RyRs can influence spontaneous SR Ca^{2+} release at a given SR Ca^{2+} load (Venetucci *et al.*, 2008 for review).

1.6.4. Inositol 1,4,5-trisphosphate receptors

As well as the RyRs, the SR also contains inositol 1,4,5-trisphosphate (IP_3) receptors that release Ca^{2+} in response to binding of IP_3 (Berridge & Irvine, 1989; Moschella & Marks, 1993). Studies using atrial myocytes from mice where the gene encoding the cardiac isoform for the IP_3 receptor (IP3R2) was knocked out, showed that there was

no difference in the intracellular Ca^{2+} signalling (Li *et al.*, 2005). Thus, it would appear that IP_3 receptors are not essential for the normal function of the heart. Instead it is believed that IP_3 modulates the Ca^{2+} activity in myocytes through different signalling pathways in response to hormones and neurotransmitters (Vervloessem *et al.*, 2014 for review). For example, the positive inotropic effect of endothelin-1 in the mouse atria, was absent in IP3R2 knockout mice (Li *et al.*, 2005). In addition, the function of IP_3 receptors is also modulated by the intracellular Ca^{2+} concentration (Ramos-Franco *et al.*, 1998; Tu *et al.*, 2005).

The exact role of IP_3 receptors in excitation-contraction coupling is still unclear (ter Keurs & Boyden, 2007 for review), although their expression has been found to be greater in atrial and Purkinje cells compared to ventricular myocytes, which perhaps suggests a role in the cardiac conduction system (Gorza *et al.*, 1993; Lipp *et al.*, 2000; Mackenzie *et al.*, 2002). A recent study has proposed a role for IP_3 receptors in normal Ca^{2+} signalling in sino-atrial node myocytes, as the rate of normal Ca^{2+} transient automaticity was increased by stimulating IP_3 production with the α-adrenoreceptor agonist phenylephrine, and decreased by inhibiting the IP_3 receptors with 2-aminoethoxydiphenyl borate (2-APB) (Kapoor *et al.*, 2015). Immunocytochemistry has revealed that IP_3 receptors are abundantly expressed in rat pulmonary vein cardiomyocytes (Okamoto *et al.*, 2012). Furthermore, 2-APB has been shown to decrease the frequency and amplitude of spontaneous Ca^{2+} transients in the rat pulmonary vein (Logantha *et al.*, 2010).

1.6.5. Cardiac glycosides and abnormal automaticity

The Na^+/K^+ ATPase, which is located on the sarcolemma, is involved in the regulation of the membrane potential in cardiac myocytes by removing 3 Na^+ in exchange for 2 K^+ (Gadsby, 1980; Rakowski *et al.*, 1989). The cardiac glycoside ouabain inhibits the Na^+/K^+ ATPase, which causes an accumulation of intracellular Na^+. This reduces the concentration gradient for Na^+ influx through the NCX, which in turn leads to an incresed intracullar Ca^{2+} concentration by reducing the removal of diastolic Ca^{2+} (Levi

et al., 1994; Wasserstrom & Aistrup, 2005 for review). Ouabain has been shown to induce the firing of action potentials in otherwise electrically quiescent pulmonary veins from the rabbit (Wongcharoen *et al.*, 2006) and guinea pig (Cheung, 1981b; Namekata *et al.*, 2009), which suggests that the action potentials were caused by an increase in the intracellular Ca^{2+} concentration.

1.6.6. The role of intracellular Ca^{2+} in automaticity and triggered activity in the pulmonary vein

In the rabbit pulmonary vein, treatment with a low concentration of ryanodine (0.5 to 2 μM) during electrical stimulation at 2 Hz, resulted in the development of a gradual depolarisation between the evoked action potentials, and also a prolongation of the repolarisation phase. Following a 1 min rest period, a train of electrical stimuli at 3.3 Hz triggered a burst of action potentials that eventually self-terminated (Honjo *et al.*, 2003a). The pulmonary veins were later isolated with both atria still attached and an extracellular electrode array was used to map the propagation of electrical activity. Following the application of 2 μM ryanodine, the leading pacemaker shifted from the sino-atrial node to an ectopic focus in the right superior pulmonary vein. These observations suggest that abnormal Ca^{2+} homeostasis may play a role in ectopic electrical activity in the pulmonary veins (Honjo *et al.*, 2003a). On the other hand, in the guinea pig pulmonary vein, ryanodine (0.1 μM) has been shown to supress pacing induced triggered action potentials (Takahara *et al.*, 2011). This highlights the difficulty in using animal models, as similar experiments can yield conflicting outcomes in tissue obtained from different species. It should be noted, however, that ryanodine can have a dual effect on SR Ca^{2+} release due to the conductance state of the channel. When ryanodine is present at low concentrations (0.1-2 μM) the ryanodine channel typically enters a subconductance state whereby the open probability is increased. This leads to increased Ca^{2+} leak from the SR, which increases the gain for Ca^{2+} -induced Ca^{2+} release. On the other hand, when applied at high concentrations (>10 μM), ryanodine blocks the channel, inhibiting SR Ca^{2+} release (Rousseau *et al.*, 1987; Zucchi & Ronca-Testoni, 1997).

A role for intracellular Ca^{2+} signalling in arrhythmogenesis has also been reported in in the canine pulmonary vein. Very brief pulses (<0.1 ms), which would normally be too short to evoke action potentials, were applied to the pulmonary vein at a high frequency (100 Hz) in order to stimulate neurotransmitter release from the autonomic nerves. This induced action potentials, and such activity could be prevented by the application of a high concentration of ryanodine (10 μM) (Patterson *et al.*, 2005). Also in the canine pulmonary vein, optical techniques were employed to simultaneously monitor the membrane potential and Ca^{2+} signalling using voltage and Ca^{2+} sensitive fluorescent dyes. When the atria were still attached, rapid pacing of the atria, in combination with a low concentration of ryanodine (0.5 μM), triggered action potentials in the pulmonary vein, which were preceded by a rise in intracellular Ca^{2+} (Chou *et al.*, 2005). As the RyR is the main Ca^{2+} release channel in cardiac myocytes (Schlotthauer & Bers, 2000), the investigations described above support the hypothesis that automaticity and triggered activity can occur due to increased Ca^{2+} release from the SR during diastole.

1.6.7. Differences in Ca^{2+} signalling between the pulmonary vein and atria

From the investigations described in the previous section, it would appear that automaticity and triggered activity in the pulmonary veins can be caused by changes in intracellular Ca^{2+}. However, the reasons why the pulmonary veins are more likely to display ectopic electrical activity, compared to the atria (Haïssaguerre *et al.*, 1998; Shah *et al.*, 2003) are unclear. Comparative studies have been performed in isolated cells from the pulmonary vein and left atrium to examine any notable differences in intracellular Ca^{2+} signalling. Cardiomyocytes that were isolated from the different tissue regions in the canine (Coutu *et al.*, 2006) and rabbit (Chang *et al.*, 2008) displayed no significant differences in the characteristics (amplitude and stimulus to half-decay time) of electrically evoked Ca^{2+} transients. This is somewhat suprising since electrically evoked action potentials have been shown to be of smaller magnitude and duration in the pulmonary vein (Arora *et al.*, 2003; Cheung, 1981a; Doisne *et al.*, 2009; Ehrlich *et al.*, 2003; Hocini *et al.*, 2002; Kuz'min & Rozenshtraukh, 2012).

However, in rabbit pulmonary vein cardiomyocytes that displayed spontaneous Ca^{2+} activity, the electrically evoked Ca^{2+} transients were greater in amplitude and had a longer time to peak than in left atrial myocytes (Chang *et al.*, 2008). In a separate study, rabbit pulmonary vein cardiomycoytes were demonstrated to have higher diastolic Ca^{2+} levels compared to atrial myocytes when paced at 3 to 5 Hz (Jones *et al.*, 2008). Caffeine, when added at high concentrations (>20 mM), results in emptying of the intracellular store and can therefore be used as an index of the SR Ca^{2+} content (Rousseau *et al.*, 1988). Using caffeine, it was also demonstrated that the SR Ca^{2+} content was greater in rabbit pulmonary vein cardiomyocytes that displayed spontaneous Ca^{2+} transients, compared to left atrial myocytes (Chang *et al.*, 2008).

1.6.8. The Na^+/Ca^{2+} exchanger and electrical activity in the pulmonary vein

The direction of transport of the NCX is dependent on the electrochemical gradient of Na^+, and the reversal potential of the exchanger is -30 mV (Ehara *et al.*, 1989; Kimura *et al.*, 1987). This means that when the membrane potential is less negative than -30 mV it acts in its 'so called' reverse mode bringing Ca^{2+} into the myocyte. In its forward mode, the NCX removes Ca^{2+} from the cytosol and is generally accepted to exchange 3 Na^+ ions for every Ca^{2+} ion (Ehara *et al.*, 1989; Kang & Hilgemann, 2004; Reeves & Hale, 1984), although it has been reported that the stoichiometry is closer to 4:1 (Fujioka *et al.*, 2000). Nethertheless, this results is depolarisation of the cardiac myocyte due to the net accumlation of positive charge, thus making the NCX electrogenic. The NCX has been implicated in arrhythmogenesis, as its forward mode is believed to be activated by conditions that cause an increase in the intracellular Ca^{2+} concentration, carrying a transient inward current (I_{ti}) during Ca^{2+} removal (Egdell & MacLeod, 2000; Kass *et al.*, 1978; Mechmann & Pott, 1986; Schlotthauer & Bers, 2000). There are numerous studies that have proposed a role for the NCX in the generation of automaticity and triggered activity in the pulmonary veins (Chang *et al.*, 2011; Honjo *et al.*, 2003a; Namekata *et al.*, 2009; Patterson *et al.*, 2006; Wongcharoen *et al.*, 2006).

Pharmacological inhibition of the NCX with KB-R7943 has been shown to reduce the rate of spontaneous action potentials in the rabbit pulmonary vein (Wongcharoen *et al.*, 2006). Moreover, SEA0400, which is a different inhibitor, completely abolished spontaneous action potentials in the guinea pig pulmonary vein (Namekata *et al.*, 2009). When the individual ion currents were measured in isolated cardiomyocytes using the whole-cell patch clamp method, the Ni^{2+} sensitive NCX current (I_{NCX}), which represents the forward mode, was completely inhibibited by KB-R7943 (Wongcharoen *et al.*, 2006). In the canine pulmonary vein, inhibition of the forward mode NCX by transiently increasing the external Ca^{2+} concentration from 1.35 to 5 mM, supressed action potentials that were induced by stimulating the autonomic nervous system using a high frequency burst of brief electrical pulses (Patterson *et al.*, 2006). Furthermore, triggered activity in the rabbit pulmonary vein, which was induced by electrical pacing in combination with a low concentration of ryanodine (0.5-2 μM), was prevented by replacing the Na^{+} in the bath solution with Ni^{2+}, which inhibits the forward mode of the NCX (Honjo *et al.*, 2003a). From the studies described herein it would appear that automaticity and triggered activity in the pulmonary vein is driven by the forward mode NCX.

In the guinea pig pulmonary vein, where 87% of the tissues were quiescent under unstimulated conditions, treatment with ouabain induced action potentials. These action potentials were inhibited by SEA0400 in a concentration dependent manner, reducing the incidence of automaticity to 48% at 1 μM and 18% at 10 μM. Complete inhibition occurred following further treatment with ryanodine. When the cardiomyocytes were enzymatically isolated and loaded with the Ca^{2+} sensitive fluorescent indicator fluo-4, ouabain was shown to induce an increase in the cytosolic Ca^{2+} concentration, followed by automatic Ca^{2+} transients, which were completely inhibited by SEA0400 (Namekata *et al.*, 2009). This suggests that the forward mode NCX current is activated in conditions where there is an increase in intracellular Ca^{2+}, which can generate action potentials.

1.6.9. The role of Ca^{2+} in normal pacemaker automaticity

The rate of pacemaker automaticity in the sino-atrial node is driven by two "clocks"; the Ca^{2+} clock and the membrane clock, although the relative contribution of these different mechanisms is the subject to much controversy (Lakatta & DiFrancesco, 2009).

The hypothesis of the Ca^{2+} clock is that the periodic release of Ca^{2+} from the SR, which is mediated by the RyR, activates the forward mode NCX current (I_{NCX}) causing a gradual depolarisation during diastole (Lakatta *et al.*, 2003; Lipsius *et al.*, 2001; Vinogradova *et al.*, 2004). There are several studies that support this hypothesis. The application of ryanodine (1 µM) to pacemaker myocytes from the right atrium of the cat, reduced the I_{NCX}, in turn causing a reduction in the slope of diastolic depolarisation, and an increased cycle length between action potentials (Zhou & Lipsius, 1993). Similarly, in the guinea pig atria, the rate of spontaneous action potentials recorded in the SA node was significantly reduced by the application of ryanodine (2 µM) or the SERCA inhibitor cyclopiazonic acid (CPA) (100 µM) (Rigg & Terrar, 1996). Ryanodine has also been shown to reduce the rate of action potential firing in rabbit sino-atrial node cells in a concentration dependent manner. Furthermore, inhibition of the forward mode NCX by rapidly replacing the Na^+ in the bath solution with Li^+ supressed firing completely (Bogdanov *et al.*, 2001). However, another study on rabbit sino-atrial node myocytes concluded that SR Ca^{2+} release is not the dominant factor for pacemaker activity, as ryanodine (30 µM) only reduced the rate of automaticity by 19% (Honjo *et al.*, 2003b). It has been proposed however, that this discrepancy can be explained by the heterogenous expression of RyRs between myocytes located in different regions in the sino-atrial node (Lakatta *et al.*, 2003).

According to the membrane clock hypothesis, diastolic depolarisation is driven by the hyperpolarisation-activated cyclic nucleotide-gated potassium current (I_f) that occurs through HCN4 channels. The I_f, or "funny" current as it is termed due its unique conductance properties, was first described as contributing towards pacemaker activity

in rabbit SA node myocytes (DiFrancesco, 1991). The mRNA expression of HCN4 channels has since been confirmed by polymerase chain reaction (PCR) in non-nodal atrial and ventricular myocytes (Gaborit *et al.*, 2007; Han *et al.*, 2002; Ludwig *et al.*, 1999). The presence of HCN4 channels and I_f has been reported in canine pulmonary vein cardiomyocytes (Li *et al.*, 2012), and selective inhibition of I_f with ivabradine has been shown to reduce the rate of spontaneous action potentials in isolated cardiomyocytes (Li *et al.*, 2012). However, there have been contradictory reports that HCN4 channels are not present in canine pulmonary vein cardiomyocytes (Tan *et al.*, 2008). The expression of HCN4 channels has also been reported in the rabbit, but not rat pulmonary vein (Yamamoto *et al.*, 2006). However, despite this, triggered activity in the rabbit pulmonary vein, which was induced by a period of electrical pacing and a low concentration of ryanodine, was not inhibited by blocking I_f with Cs^+ (Yamamoto *et al.*, 2006).

1.6.10. Spontaneous Ca^{2+} transients in pulmonary vein cardiomyocytes

Fluorescence imaging of the rat pulmonary vein using the Ca^{2+} indicator fluo-4 revealed that, under resting (unstimulated) conditions, the cardiomyocytes displayed spontaneous Ca^{2+} transients, usually in the form of waves that propagated along the longitudinal axis of the cells (Logantha *et al.*, 2010). The Ca^{2+} transients were asynchronous in nature, often propagating in opposite directions between adjacent cells and there was no consistent pattern of activity. When Ca^{2+} was removed from the external solution there was a small, but significant decrease in the amplitude and frequency of the spontaneous Ca^{2+} transients. Together with the observation that the spontaneous Ca^{2+} transients were unaffected in the presence of the LTCC inhibitor verapamil, it was suggested that Ca^{2+} influx from the extracellular space is not a requirement for spontaneous Ca^{2+} transients to occur. The addition of ryanodine (20 μM) or the IP_3 receptor blocker 2-APB (20 μM) abolished spontaneous Ca^{2+} transients in 67% and 47% of cardiomyocytes respectively, and the frequency and amplitude was significantly reduced in the remaining spontaneously active cells. Therefore, the source of Ca^{2+} is presumably the SR (Logantha *et al.*, 2010).

Spontaneous Ca^{2+} transients have also been observed in mouse lung slices, where a relatively low concentration of caffeine (1 mM), sufficient to promote SR Ca^{2+} release but not empty the store, increased the frequency of spontaneous Ca^{2+} transients (Rietdorf *et al.*, 2014). However, in the case of the mouse pulmonary vein, perfusion of the preparation with a Ca^{2+} free medium completely supressed spontanteous Ca^{2+} activity in 58% of lung slices, and the LTCC nifedipine also reduced the frequency of the Ca^{2+} transients. Moreover, inhibiton of IP_3 receptors with 2-APB had no effect on the intracellular Ca^{2+} signalling (Rietdorf *et al.*, 2014). In both species, depolarising the tissue by applying KCl caused a transient increase in the frequency of spontaneous Ca^{2+} transients, which suggets that inducing Ca^{2+} influx can affect the properties of spontaneous Ca^{2+} signalling (Logantha *et al.*, 2010; Rietdorf *et al.*, 2014). As well as in the intact pulmonary vein, spontaneous Ca^{2+} transients or sparks have also been reported in isolated cardiomyocytes from the canine (Coutu *et al.*, 2006) and rabbit (Chang *et al.*, 2008; Jones *et al.*, 2008).

1.6.11. Electrically evoked Ca^{2+} transients in the pulmonary vein

Electrical field stimulation of the rat or mouse pulmonary vein has been shown to evoke a synchronous rise in intracellular Ca^{2+} in neighbouring cardiomyocytes (Logantha *et al.*, 2010; Rietdorf *et al.*, 2014). The magnitude of the electrically evoked Ca^{2+} transients in the rat pulmonary vein was significantly reduced by inhibiting the voltage gated (L-type) Ca^{2+} channels with either nicardipine or verapamil, and also by removing Ca^{2+} from the extracellular solution. The electrically evoked Ca^{2+} transients were also reduced in amplitude by treatment with a high concentration of ryanodine (Logantha *et al.*, 2010). In the mouse pulmonary vein, if a spontaneous Ca^{2+} transient occurred shortly before the electrical stimulus, it prevented the occurrence of an evoked synchronous Ca^{2+} transient suggesting that there is a refractory period for SR Ca^{2+} release. Moreover, if the frequency of spontaneous Ca^{2+} transients was greater than the rate of stimuli, the tissue was less likely to respond with an electrically evoked Ca^{2+} transient during every stimulus (Rietdorf *et al.*, 2014; Rietdorf *et al.*, 2015). These findings are consistent with the accepted model of excitation-contraction coupling

whereby Ca^{2+} enters the myocyte through voltage-gated Ca^{2+} channels, inducing further Ca^{2+} release from the SR (Bers, 2000a).

1.6.12. Are the spontaneous Ca^{2+} transients capable of generating action potentials?

Most of the studies on the rat pulmonary vein have reported the absence of spontaneous action potentials under control conditions (Doisne *et al.*, 2009; MacLeod & Hunter, 1967; Miyauchi *et al.*, 2005; Paes de Almeida *et al.*, 1975), and in the study that does, they were recorded in only 3.8% of preparations (Namekata *et al.*, 2010). This would suggest that the spontaneous Ca^{2+} transients observed in the rat and mouse pulmonary veins (Logantha *et al.*, 2010; Rietdorf *et al.*, 2014) are unlikely to generate action potentials.

Although the relationship between spontaneous Ca^{2+} transients and the generation of electrical activity in pulmonary vein cardiomyocytes is not fully understood, it has been extensively studied in ventricular myocytes. In isolated myocytes, contraction can be used as a marker for spontaneous SR Ca^{2+} release as, when a Ca^{2+} wave propagates along a myocyte there is an accompanying contractile wave, and such contractile activity can be prevented by inhibiting SR Ca^{2+} release (Kort & Lakatta, 1984). Simultaneous microelectrode recordings in ventricular myocytes determined that spontaneous contractile waves were accompanied by transient depolarisations that were subthreshold to elicit action potentials. However, when the contractile waves occured at multiple foci in the myocytes (i.e. originating at either end and propagating towards the middle), depolarisation was sometimes sufficient to reach the threshold to activate Na^{+} channels (approximately -67 mV), and action potentials were elicited. Moreover, action potentials could be induced by the rapid application of caffeine. However, when caffeine was applied more slowly, the resultant depolarisations were subthreshold, as the SR Ca^{2+} release would have occured over a longer time-scale (Capogrossi *et al.*, 1987). Caffeine induced depolarisation has been shown to be prevented by perfusing ventricular myocytes with Ca^{2+} or Na^{+} free solution, and also

by inhibiting the forward mode of the NCX with Ni^{2+}. When the intracellular Ca^{2+} concentration was monitored, the decline phase of the caffeine induced Ca^{2+} transient, was slowed by the inhibition of the I_{NCX} (Schlotthauer & Bers, 2000). Thus, it can be concluded that SR Ca^{2+} release is capable of inducing depolarisation, due to the forward mode NCX. However, SR Ca^{2+} release must be of sufficient magnitude and occur within a relatively brief time-scale to be above the threshold to elicit action potentials.

In isolated ventricular myocytes from the rat, Ca^{2+} waves could be induced by lowering the external K^+ concentration, which inhibits the Na^+/K^+ ATPase resulting in Na^+ accumulation, which in turn increases the intracellular Ca^{2+} concentration. Moreover, these Ca^{2+} waves preceded a depolarising transient inward (I_{ti}) current (Berlin *et al.*, 1989). In the intact rat heart, Ca^{2+} transients that were asynchronous in neighbouring myocytes could be induced using the same method. However, in the case of the whole tissue, there were no associated depolarisations (Fujiwara *et al.*, 2008). Therefore it is likely that the asynchronous nature of the spontaneous Ca^{2+} transients in the tissue means that when depolarisation is generated by a myocyte (source), the surrounding inactive tissue acts as a current sink, preventing sufficient depolarisation for the induction of action potentials (Spach & Boineau, 1997; Unudurthi *et al.*, 2014; Winslow *et al.*, 1993; Xie *et al.*, 2010).

1.7. The influence of the autonomic nervous system on the electrical activity in the pulmonary veins

1.7.1. Pharmacological studies on pulmonary vein contractility

Contractile studies on the rat pulmonary vein showed that exogenous application of the α and β adrenoreceptor agonist noradrenaline increased the force of electrically evoked contractions (MacLeod & Hunter, 1967; Maupoil *et al.*, 2007; Sweeney *et al.*, 1999). In contrast, activation of muscarinic cholinergic receptors with acetylcholine reduced the contractile amplitude. This suggests that the contractility of the pulmonary

vein myocardial sleeve is regulated by the neurotransmitters of the autonomic nervous sytem (MacLeod & Hunter, 1967; Sweeney *et al.*, 1999).

1.7.2. Innervation of the pulmonary veins

Anatomical investigations of the rat and mouse pulmonary vein, using electron microscopy and histological techniques, reported the presence of unmyelinated nerve terminals, suggesting that the veins are innervated by the autonomic nervous system (Hashizume *et al.*, 1998; Karrer, 1960; Masani, 1986; Paes de Almeida *et al.*, 1975).

In humans, the density of nerve fibres has been shown to be significantly higher at the ostia compared to distal regions of the pulmonary veins (Chevalier *et al.*, 2005). Immunohistochemistry, which can be used to distiguish between the different nerve fibres, determined that 25% of nerve bundles possessed adrenergic and cholinergic nerves. Of the remaining fibres, approximately 60% were adrenergic and 10% were cholinergic. The autonomic ganglion, which is located at the ostia, was found to be rich in both adrenergic and cholinergic nerves (Tan *et al.*, 2006).

In the canine, the injection of acetylcholine into the autonomic ganglion has been shown to induce atrial fibrillation *in vivo* (Po *et al.*, 2006). However, in contrast to the human, the density of nerve bundles in the canine was greater in the distal compared to the proximal regions of the pulmonary vein. Also, 67% of fibres contained adrenergic and cholinergic nerves, while all the remaining fibres were purely cholinergic (Arora *et al.*, 2008). These studies show that the pulmonary veins are highly innervated by the nerves of the automonic nervous system, but they also highlight that there are notable histological differences between species.

1.7.3. Autonomic tone and atrial fibrillation

In patients with paroxysmal atrial fibrillation where the origin of ectopic electrical activity was in the pulmonary veins, electrocardiographic techniques were employed and the heart rate variability was analysed as an indicator of autonomic tone. It was found that there was a primary drive in sympathetic adrenergic activity, followed by an abrupt shift in autonomic tone towards vagal predominance, which occured immediately before the onset of atrial fibrillation (Bettoni & Zimmermann, 2002; Zimmermann & Kalusche, 2001). Moreover, complete vagal denervation during the circumferential pulmonary vein ablation procedure has also been shown to reduce the reoccurrence of atrial fibrillation (Pappone *et al.*, 2004). These clinical studies suggest that variations in autonomic tone can act as a precursor towards pulmonary vein ectopy.

1.7.4. The influence of autonomic tone on automaticity and triggered activity in the pulmonary vein

In vivo experiments have been performed in the canine whereby rapid electrical pacing (200 Hz) with very brief pulses (0.1 ms) was delivered to the pulmonary veins. The objective was to directly stimulate the autonomic nervous system by delivering pulses that were too brief to evoke action potentials, but could still induce local neurotransmitter release. This intervention induced ectopic beats, which led to atrial fibrillation, and this could be prevented with the muscarinic acetylcholine receptor antagonist atropine. Furthermore, when the β-adrenoreceptor blocker propranolol was administered intravenously, the threshold voltage required to induce the activity was significantly increased. This suggests that both sympathetic and parasympathetic nerve stimulation contributed to abnormal electrical activity in the pulmonary veins, which lead to atrial fibrillation (Schauerte *et al.*, 2001).

When the canine pulmonary vein was isolated, the autonomic nervous system was stimulated by delivering a high-frequency electrical stimulus (0.05 to 0.1 ms duration

at 100 Hz), synchronised with a separate stimulus at 2 Hz in a different region on the vein. The result was a shortening of the action potential duration and early afterdepolarisations, which are afterdepolarisations that occur during the repolarisation phase of the action potential. This also lead to triggered activity in 79% of the preparations, which was prevented in 6 out of 8 tissues by pre-treatment with atropine or in 8 out of 8 tissues with the β_1-adrenoreceptor antagonist atenolol. These findings lead to the conclusion that automaticity occurred due to the combined stimulation of the parasympathetic and sympathetic nervous system. It was suggested that, as the duration of action potentials is relatively short in pulmonary vein cardiomyocytes, parasympathetic stimulation further shortens the action potential duration, which combined with sympathetic stimulation, resulted in rapid firing, similar to what is observed in patients with focal atrial fibrillation (Patterson *et al.*, 2005).

In a separate study, triggered action potential firing, which was induced in the pulmonary vein of the canine by high frequency electrical stimulation, was supressed by autonomic denervation through ablating the ganglionic plexi (Lu *et al.*, 2009). In the same species, the heart and pulmonary veins were removed, and pituitary adenylate cyclase-activating polypeptide (PACAP) was injected into the left coronary artery as a surrogate for autonomic imbalance. The electrical activity and Ca^{2+} signalling in the pulmonary vein was then monitored by fluorescence microscopy. Rapid pacing induced action potentials, which were supressed by inhibiting the LTCCs with verapamil. This suggests that an increase in the intracellular Ca^{2+} concentration occurs during autonomic stimulation and this can underlie abnormal automaticity (Hirose & Laurita, 2007).

1.7.5. Noradrenaline induced automaticity in the pulmonary vein

Microelectrode recordings in the guinea pig pulmonary vein showed that treatment with noradrenaline can induce action potentials in otherwise electrically quiescent preparations, and these action potentials originated at the end of the vein that would have been distal to the left atrium. In preparations with the atria still attached,

noradrenaline accelerated the rate of spontaneous action potentials, and the rate of firing in the atria eventually superseded that in the pulmonary vein. Thus, the atria and pulmonary veins became electrically uncoupled as they displayed action potentails at different rates (Cheung, 1981a).

More recently, treatment with noradrenaline induced contractions (Maupoil *et al.*, 2007) and action potentials (Doisne *et al.*, 2009) that occurred independently of electrical stimulation in the rat pulmonary vein (93% of preparations), but not left atrium. Following the application of noradrenaline, there was an approximately 10-15 min latency period, during which there was a gradual hyperpolarisation of the membrane potential, before automaticity occured as periodic bursts of contractions and action potentials. The frequency of automaticity within a burst initially increased before decreasing again, and at the end of each burst there were one or more afterdepolarisations, which were subthreshold to elicit further action potentials (Doisne *et al.*, 2009; Maupoil *et al.*, 2007). Noradrenaline has since been shown to induce repetitive bursts of action potentials in the mouse pulmonary vein (Tsuneoka *et al.*, 2012), and the sustained firing of action potentials in the guniea pig pulmonary vein (Namekata *et al.*, 2010).

In isolated pulmonary vein cardiomyocytes from the rat, noradrenaline also induced action potentials, albeit with a lower incidence than in the tissue, of 27%. As opposed to repetitive bursts, automaticity was manifest as the sustained firing of action potentials, which eventually self-terminated. Simultaneous measurement of the intracellular Ca^{2+} signalling showed that following treatment with noradrenaline, Ca^{2+} oscillations of gradually increasing magnitude were observed, until they were above the threshold to elicit action potentials (Okamoto *et al.*, 2012). Inhibition of the NCX with SEA0400 supressed the noradrenaline induced action potentials, but not the Ca^{2+} transients. However, both were abolished by inhibiting the IP_3 receptors with 2-APB. It was therefore proposed that noradrenaline increased the production of IP_3, thus increasing spontanous SR Ca^{2+} release, and causing a rise in the intracellular Ca^{2+} concentration. This in turn would activate the forward mode NCX causing

depolarisation during Ca^{2+} removal, and the induction of action potentials (Okamoto *et al.*, 2012).

In both the tissue preparation and in isolated cardiomyocytes, noradrenaline induced automaticity could be inhibited with the α_1-adrenoreceptor antagonist prazosin or the β_1-adrenoreceptor antagonist atenolol (Doisne *et al.*, 2009; Maupoil *et al.*, 2007; Okamoto *et al.*, 2012). Moreover, in the tissue, automaticity could only be induced by the simultaneous addition of the α-adrenoreceptor agonists phenylephrine or cirazoline, and the β-adrenoreceptor agonist isoprenaline; but not by their individual application (Doisne *et al.*, 2009; Maupoil *et al.*, 2007). Thus, it was proposed that noradrenaline induced automaticity requires the co-activation of α_1 and β_1-adrenoreceptors (Doisne *et al.*, 2009; Maupoil *et al.*, 2007; Okamoto *et al.*, 2012).

1.8. Aims of the thesis

Based on the research carried out to this date, it would appear that changes in intracellular Ca^{2+} play a key role in pulmonary vein arrhythmogenesis (Chen *et al.*, 2000; Honjo *et al.*, 2003a; Namekata *et al.*, 2010; Patterson *et al.*, 2005). Thus, factors that might influence Ca^{2+} signalling may contribute towards the arrhythmogenic properties of the pulmonary vein.

The initial aim of this thesis was to compare the structural characteristics of the pulmonary vein cardiomyocytes to those of the atria and ventricle. Specifically, these studies focussed on establishing the existence of t-tubules in pulmonary vein cardiomyocytes as well as determining the distribution of the LTCCs, RyRs and the NCX. Knowing the distribution of these ion channels and exchanger are crucial in understanding how Ca^{2+} signalling is regulated in these different myocytes. Since the spontaneous Ca^{2+} transients that have previously been observed in the rat pulmonary vein occur in an asynchronous manner, different experimental manipulations were then used to determine whether these events could be entrained to become more synchronous in neighbouring cardiomyocytes. If the spontaneous Ca^{2+} transients occur

more synchronously, then they will be more likely to be arrhythmogenic. Following on from this, as there is a growing body of evidence to suggest that adrenergic stimulation is involved in arrhythmogenic activity in the pulmonary veins, the effect of adrenergic stimulation on the spontaneous Ca^{2+} transients and contractile activity was studied using isoprenaline and noradrenaline. Finally, the underlying mechanims of noradrenaline induced automaticity were investigated using pharmacological inhibitors. In particular, the role of the NCX was examined, as it is thought be involved in the generation of automaticity and triggered activity in response to an increase in intracellular Ca^{2+} concentration.

Chapter 2

The arrangement of cardiomyocytes in the rat pulmonary vein and the distribution of proteins involved in excitation-contraction coupling

2.1. Introduction

2.1.1. T-tubules in ventricular myocytes

The structure and morphology of the cardiac myocytes of the heart has been extensively studied. It is well established that the surface membrane of ventricular myocytes has narrow invaginations, approximately 200 nm in diameter, known as transverse (T) – tubules that occur along the z-lines and penetrate deep towards the centre of the cells (Ayettey & Navaratnam, 1978; Orchard & Brette, 2008; Soeller & Cannell, 1999; Wagner *et al.*, 2012). It is believed that the function of the T-tubules is to ensure a spatially and temporally homogenous intracellular Ca^{2+} transient during excitation-contraction coupling (Brette *et al.*, 2006; Kawai *et al.*, 2009). This is supported by immunolabelling studies in isolated ventricular myocytes, which showed that voltage-gated L-type Ca^{2+} channels (LTCCs) were concentrated along the T-tubules. Moreover, the majority were found to be adjacent to ryanodine receptors (RyRs) on the sarcoplasmic reticulum (SR) forming functional subunits or couplons (Carl *et al.*, 1995; Franzini-Armstrong *et al.*, 2005; Scriven *et al.*, 2010; Sun *et al.*, 1995). The Na^{+}/Ca^{2+} exchanger (NCX) has also been shown to be distributed along the T-tubules, where they were adjacent to RyRs (Jayasinghe *et al.*, 2009; Scriven *et al.*, 2000; Thomas *et al.*, 2003).

2.1.2. T-tubules in atrial myocytes

Whether T-tubules are present in atrial myocytes has been the subject of much discussion. However, it is widely regarded that in small mammals such as the mouse (Forbes *et al.*, 1984), rat (Ayettey & Navaratnam, 1978; Brette *et al.*, 2002; Kirk *et al.*, 2003), guinea pig (Lipp *et al.*, 1996), rabbit (Kettlewell *et al.*, 2013; Tidball *et al.*, 1991) and cat (Blatter *et al.*, 2003; Hüser *et al.*, 1996), the atrial myocytes lack a well-developed T-tubule system. Thus, the LTCCs and the NCX are primarily located along the periphery and outer surface of the myocytes. On the other hand, RyRs have been shown to be mainly aligned in striations running perpendicular to the longitudinal axis (Carl *et al.*, 1995; Frisk *et al.*, 2014; Schulson *et al.*, 2011). More recently, it has been shown that atrial myocytes from large mammals such as the canine (Wakili *et al.*,

2010), sheep (Dibb *et al.*, 2009), pig (Frisk *et al.*, 2014), horse and human (Richards *et al.*, 2011) possess a more substantial T-tubule network.

2.1.3. T-tubules in pulmonary vein cardiomyocytes

Investigation into the structure and architecture of the pulmonary vein myocardial sleeve has generally focused on the organisation of cardiomyocytes in the intact vein (Klavins, 1963; Kramer & Marks 1965; Ludatscher, 1968; Masani, 1986; Mueller-Hoecker *et al.*, 2008; Paes de Almeida *et al.*, 1975; Verheule *et al.*, 2002). Despite the cardiomyocyte sleeve being anatomically and electrically continuous with the left atrium (Cheung, 1981a), structural differences between cells from the different regions have been reported. Most notably, there are some studies that have reported the presence of T-tubules in pulmonary vein cardiomyocytes (Ludatscher, 1968; Masani, 1986; Melnyk *et al.*, 2005). However, whether or not the cardiomyocytes of the pulmonary vein possess T-tubules, and if so, how their expression compares to atrial and ventricular myocytes is still unclear.

Studies using electron microscopy to image the canine pulmonary vein reported the absence of T-tubules (Verheule *et al.*, 2002). However, in another study where the sarcolemma of isolated cardiomyocytes was stained with wheat germ agglutinin, it was reported that they were present (Melnyk *et al.*, 2005). In the rat pulmonary vein, T-tubules have been observed by electron microscopy (Ludatscher, 1968; Masani, 1986), and when Di-8 ANEPPS was used to stain the sarcolemma of isolated cardiomyocytes it was shown there was a dense T-tubular network. Furthermore, the NCX was abundantly expressed at the T-tubules (Okamoto *et al.*, 2012), and it was believed that this predisposed the cardiomyocytes to automaticity generated by the depolarising transient inward current (I_{ti}) (Schlotthauer & Bers, 2000). In mouse lung slices, T-tubules were not observed by staining with Di-8 ANEPPS; however, RyRs were shown to be expressed in transverse striations (Rietdorf *et al.*, 2014).

2.1.4. Aims

The distribution of the key transporters involved in Ca^{2+} signalling has been well established in atrial and ventricular myocytes (Carl *et al.*, 1995; Schulson *et al.*, 2011; Scriven *et al.*, 2010; Scriven & Moore, 2013 for review). However, the equivalent knowledge on pulmonary vein cardiomyocytes is limited. The aim of the current chapter was therefore to investigate the structure and morphology of the pulmonary vein cardiomyocytes using membrane bound dyes and immunocytochemistry. Initially, the pulmonary vein and isolated cardiomyocytes were imaged using fluorescence dyes that attach to the sarcolemma. The arrangement of the LTCCs, RyRs and the NCX was then investigated by immunocytochemistry. Determining the organisation of these transporters is key towards understanding how Ca^{2+} release is regulated in the cardiomyocytes of the pulmonary vein.

2.2. Materials and Methods

2.2.1. Animals and pulmonary vein isolation

Adult male Sprague-Dawley rats, 8-10 weeks and weighing 250-430 g were sacrificed by cervical dislocation according to the Animals (Scientific Procedures) Act, 1986. After opening the thoracic cavity, the heart and lungs were removed *en bloc* and immediately placed in ice cold physiological salt solution of the following composition (in mM): 119 NaCl, 25 $NaHCO_3$, 4.7 KCl, 1.17 $MgSO_4$, 1.18 KH_2PO_3, 2.5 $CaCl_2$, and 5.5 glucose (pH 7.4 equilibrated with 95% O_2 and 5% CO_2). The heart and lungs were then pinned onto a Sylgard® 184 (Dow Corning Corporation, Midland, MI, USA) coated petri dish where the postcaval right (PCR) lobe was removed. The main pulmonary vein branches to the left (L) and posterior right (PR) lung lobes were then dissected from the lung parenchyma under a light microscope (Nikon SMZ645 stereomicroscope) (Figure 2.1). Once each of the branches, measuring approximately 10-15 mm in length and 2-3 mm outside diameter, were removed from the lungs, the veins were cleaned of any surrounding lung parenchyma.

2.2.2. Imaging cardiomyocytes in the intact pulmonary vein

The ANEP group of dyes fluoresce in response to changes in electrical potential across cell membranes and therefore, due to their binding properties, are a useful tool for imaging live cells (Bub *et al.*, 2010; Fluhler *et al.*, 1985). Isolated segments of the pulmonary vein were loaded in the dark for 10 min, in physiological solution containing 10 µM Di-4 ANEPPS. The tissue was then washed in fresh physiological salt solution and pinned onto a Sylgard® 184 coated tissue chamber containing 4 ml of the same solution. The outer surface of the pulmonary vein was then imaged using an epifluorescence microscope (Zeiss Axioscop 50, Carl Zeiss, Germany). The tissue was excited by light from a 50 W mercury short ARC lamp (Osram, Germany), passed through a 450-490 nm band pass excitation filter. Emission at 515 nm was captured with a Hamamatsu multiformat CCD camera (C4880-80, Hamamatsu Photonics K. K., Japan) using either a 5x, 40x or a 63x objective lens (Achroplan, Carl Zeiss, Germany). Images were acquired using WinFluor V3. 2.19. (Dr John Dempster, University of

Strathclyde) before they were exported as TIFF files into ImageJ 1.49 for presentation and the application of a yellow pseudocolour lookup table.

2.2.3. Arrangement of the mitochondria

The arrangement of the mitochondria in the pulmonary vein cardiomyocytes was assessed using the potentiometric dye, tetramethylrhodamine ethyl ester perchlorate (TMRE) (Scaduto & Grotyohann, 1999). The tissue was loaded with TMRE (1 μM) for 10 min in the dark, and then washed and pinned on a Sylgard® 184 coated tissue chamber containing 4 ml physiological salt solution. Images were acquired by wide-field epifluorescence microscopy as described in 2.2.2. For TMRE, the tissue was excited by light at BP 546 ± 12 nm and emission was captured at LP 590 nm. For the presentation of representative recordings, square ROIs (5 x5 pixels) were employed.

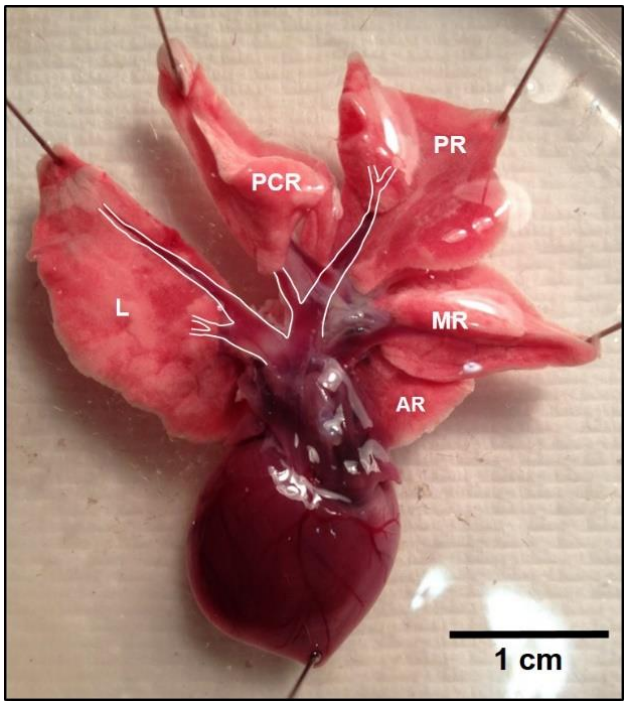

Figure 2.1. Photograph of the heart and lungs showing the sections of the pulmonary veins that were used in the present investigations. Lung lobes are labelled as: L, left; PCR, postcaval right; PR, posterior right; MR, median right; AR, anterior right. The preparation has been pinned out on a Sylgard® 184 coated petri dish and the sections of the pulmonary veins that were dissected and used in the experiments are highlighted in white.

2.2.4. Cardiomyocyte isolation

Cardiomyocytes from the rat ventricles, atria and pulmonary vein were enzymatically isolated using a modified Langendorff retrograde perfusion protocol (Louch *et al.*, 2011). The system was primed with Ca^{2+} free Tyrode's solution of the following composition (in mM); 120 NaCl, 20 HEPES, 5.4 KCl, 0.52 NaH_2PO_4, 3.5 $MgCl_2$, 20 taurine, 10 creatine, 11.1 glucose (pH 7.4 with NaOH). During priming, ethylene glycol-bis(2-aminoethylether)-N,N,N′,N′-tetraacetic acid (EGTA) (1 mM) was added to the Tyrode's solution to chelate any residual Ca^{2+} in the system. The temperature was maintained at 37 °C throughout the entire procedure using a heating coil and thermal chamber connected to a water bath.

Adult male Sprague-Dawley rats (8 to 10 weeks and 250-400 g) were anesthetised by intraperitoneal injection of sodium pentobarbital (Euthanase®) (100 mg/kg), before they were transported to the laboratory in accordance with the regulations of the University of Strathclyde Biological Procedures Unit. The rats were sacrificed by cervical dislocation, and the heart and lungs were removed and placed in Ca^{2+} free Tyrodes solution containing 0.2 ml Heparin (5000 U/ml) (Leo Laboratories Ltd.). This was to prevent coagulation of blood within the chambers of the heart and the surrounding blood vessels. The heart, with the lungs still attached, was cannulated at the ascending aorta and perfused with Ca^{2+} free Tyrode's solution for approximately 6-7 min until blood cleared from the coronary and pulmonary circulation (Figure 2.2A). The heart and lungs were then perfused with 0.66 mg/ml (240 U/ml) collagenase type I (Worthington Biochemical Corporation batch number 43D14199B) and 0.04 mg/ml protease type XIV (Sigma Aldrich) for approximately 11 min until the heart and lungs appeared suitably digested. This was assessed by the level of discolouration and elasticity of the heart, as well the viscosity of the enzyme solution that was collected underneath the heart, which was recycled during the procedure. The preparation was then perfused with Ca^{2+} free Tyrodes solution containing 0.8% w/v bovine serum albumin (BSA) for 7 min to block any further enzymatic activity. The heart and lungs were removed from the cannula, and the left atrium and ventricles were dissected and diced into small chunks in separate dishes containing oxygenated Kraft

Brühe (KB) solution of the following composition (in mM); 70 L-glutamic acid, 25 KCl, 20 taurine, 10 KH_2PO_4, 3 $MgCl_2$, 10 glucose, 10 HEPES, 0.5 EGTA, 0.8 % w/v BSA (pH 7.4 with KOH). The atrial and ventricular chunks were gently triturated with a fire polished glass pipette or plastic Pasteur pipette respectively to release the single myocytes.

The partially digested pulmonary veins were dissected from the lungs under a light microscope in Ca^{2+} free Tyrode's solution containing 0.8% w/v BSA (Figure 2.2.B). The isolated veins were then incubated in collagenase type I (20 mg/ml) and protease type XIV (10 mg/ml) for a further 15-20 min, at 37 °C. The time that the pulmonary veins were exposed to the enzyme solution depended on how digested the heart was after removal from the Langendorff apparatus. The pulmonary veins were then cut into small segments and gently triturated in KB solution using a fire polished glass pipette. Isolated cardiomyocytes were stored for 1 hr at 4 °C before use.

2.2.5. Fluorescence imaging of the isolated cardiomyocytes

A round glass coverslip (22 mm diameter) was sealed with silicone grease to the bottom of a circular petri dish, which was supported in a custom made Perspex chamber. Isolated cardiomyocytes were suspended in KB solution and a drop of the cell suspension (~50 µl) was placed on the cover slip. The cardiomyocytes were then allowed 5 min to settle, before 2 ml physiological salt solution containing Ca^{2+} was carefully applied at the edge on the petri dish, so as not to disturb the cells. The final Ca^{2+} concentration in the solution would be approximately 1 mM. The concentration of Di-4 ANEPPS used was varied between 1-5 µM in order to determine the optimum (1 µM) for cell imaging. Di-4 ANEPPS was added directly into the physiological salt solution and after 10 min exposure, the cells were imaged by wide-field epifluorescence microscopy using a 40x or 63x objective lens as described in 2.2.2. During the recording period, which was within the first 5 min after the incubation period, Di-4 ANEPPS was present in the physiological salt solution.

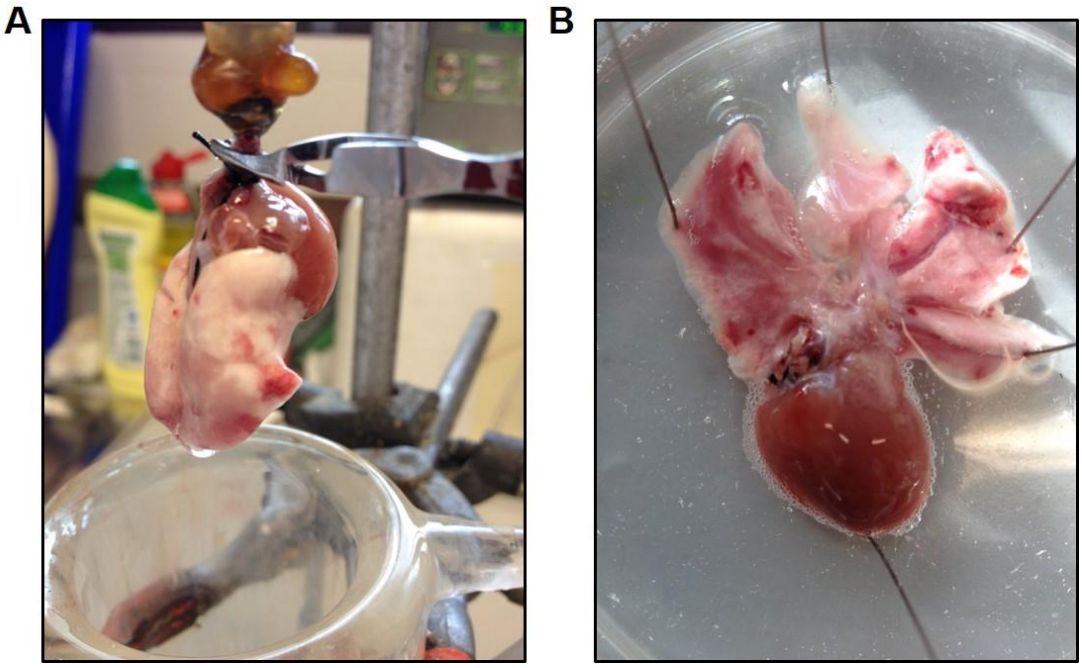

Figure 2.2. Photographs of the cardiomyocyte isolation procedure. A. Photograph of the rat heart and lungs mounted on the Langendorff apparatus and being retrogradely perfused through the ascending aorta. **B.** The heart and lungs post enzymatic digest and pinned onto a Sylgard® 184 coated petri dish. Note the discolouration of the heart, pulmonary vasculature and lungs.

2.2.6. Immunolabelling of the L-type Ca^{2+} channels, ryanodine receptors and the NCX

Glass cover slips (18 x 18 mm square) were cleaned using 100% ethanol and then sterile water, before being allowed to dry in a laboratory oven. They were then coated with 0.01% w/v poly-L-lysine and placed in six well plates before being left to dry for 1 hr in the oven. A drop of cell suspension was applied and the cardiomyocytes were allowed 15 min to adhere to the cover slips, before being fixed with 2.5% w/v formalin (1% paraformaldehyde) for 20 min. The cover slips were then washed twice for 10 min with phosphate buffered saline (PBS) of the following composition (in mM); 10 Na_2HPO_4, 2.7 KCl and 137 NaCl (pH 7.4). The cardiomyocytes were permeabilised with 0.1% w/v Triton-X 100 for 15 min and, following a further two washes in PBS, the cells were exposed to 10% w/v goat serum for 60 min to block non-specific binding sites. After another wash in PBS, the solution was removed from the well and the cover slips were placed face down on parafilm containing 25 µl diluted primary antibody solution and left overnight at 4 ºC. All of the reagents used in the protocol were diluted in PBS. Moist tissue paper was placed on the underside of the lid of the plate to maintain a moist atmosphere and to prevent the cells from drying out.

The next day, the primary antibody solution was removed and the cardiomyocytes were washed for 10 min, three times in PBS. The cells were then incubated for 60 min at room temperature with Alexa Fluor® 488-conjugated secondary antibodies (2 mg/ml, dissolved in PBS at a dilution factor of 1:250) (Invitrogen™, Glasgow, UK). After another three washes of 10 min duration in PBS, the coverslips were mounted face down on glass slides with 25 µl hard-set Vectashield®. In some of the studies, the Vectashield® contained 4',6-diamidino-2-phenylindole (DAPI) for labelling of the nuclei. The coverslips were allowed to set before being sealed with clear nail polish and the glass slides were stored in the dark at 4 ºC prior to imaging.

The LTCCs were labelled with rabbit polyclonal $Ca_v1.2$ (1:100) (Merck Millipore, Billerica, MA, USA), and goat secondary anti-rabbit IgG (H+L) antibodies. RyRs were

probed with mouse (IG1) monoclonal RyR2 (1:50) (Pierce Antibody Products, Thermo Fisher Scientific Inc., Waltham, MA, USA) and goat anti-mouse IgG (H+L) antibodies. Finally the NCX was detected using rabbit polyclonal NCX-1 (1:100) (Alomone Labs Ltd., Jerusalem, Israel), followed by goat anti-rabbit IgG (H+L) antibodies. In order to ensure that the secondary antibodies were detecting the specific primary antibodies targeted, the same procedure was repeated with no primary antibody.

Immunolabelled cardiomyocytes were imaged at 63x using a confocal microscope (Leica TCS SP50, Leica Microsystems, UK). Once a cell was identified, an image stack was obtained every 2.5 µm through the z-axis of the cell using an upright microscope with a DM6000 B lens. Alexa fluor® 488 was excited at 488 nm and the emission was captured at 510 nm. At each frame, DAPI was excited at 360 nm and the emission was captured at 460 nm. Leica image file format (LIF) files were imported into ImageJ using LOCI Bio-Formats Importer software for analysis and presentation.

2.2.7. Measurement of cardiomyocyte dimensions

Data represent mean ± s.e.m. The length and width of the isolated cardiomyocytes was determined in ImageJ from the immunofluorescence images, by measuring the maximum distance between either end of the cells across the longitudinal (length) and the transverse (width) axes. The dimensions of the ventricular, left atrial and pulmonary vein cardiomyocytes were compared via a one-way ANOVA with Tukey's post-test and $P<0.05$ was considered as statistically significant.

2.2.8. Chemicals and drugs

The membrane bound dye; Di-4 ANEPPS (Invitrogen™, Life Technologies, Glasgow, UK) was prepared at a stock concentration of 2 mM in dimethyl sulfoxide (DMSO) (Sigma Aldrich, Gillingham, Dorset, UK). The membrane potential sensitive indicator; TMRE (Invitrogen™) was prepared in DMSO at a stock concentration of 1 mM, and

both dyes were aliquoted and stored at 4 °C. Collagenase type I (Worthington Biochemical Corp., Lakewood, NJ, USA) was stored at 4 °C and protease type XIV (Sigma Aldrich, Gillingham, Dorset, UK) was stored at -20 °C, and both enzyme containing solutions were prepared on the day of experimentation. Bovine serum albumin, creatine, EGTA, formalin, goat serum, HEPES (4-(2-hydroxyethyl)-1-piperazineethanesulfonic acid), L-glutamate, poly-L-lysine, taurine and Triton X-100 were all obtained from Sigma. Heparin was obtained from Leo Laboratories Ltd. (Hurley, Berkshire, UK) and stored at 4 °C. Vectashield® was obtained from Vector Laboratories (Peterborough, Cambridgeshire, UK), and stored in the dark at 4 °C. All other reagents ($CaCl_2$, glucose, KCl, KH_2PO_3, KOH, $MgCl_2$, $MgSO_4$, NaCl, NaHCO3, NaOH, $NaHPO_4$) were obtained from BDH Laboratories (VWR International, Radnor, PA, USA).

2.3. Results

2.3.1. Pulmonary vein cardiomyocytes

In order to assess the organisation of cardiomyocytes in the pulmonary vein, intact segments were labelled with Di-4 ANEPPS, and the vein was imaged by wide-field fluorescence microscopy. Rod shaped cardiomyocytes orientated along the longitudinal axis of the vein are visible in Figure 2.3A, and demarcation of the individual cardiomyocytes can be clearly observed at the higher magnifications (Figure 2.3B and C). The myocardial sleeve extended into the intrapulmonary regions of the veins. While striations are visible in the individual cardiomyocytes, consistently spaced T-tubules like those in skeletal muscle from the rat diaphragm were not observed (Figure 2.3D).

Cardiomyocytes that were enzymatically dissociated from the pulmonary veins were compared to myocytes isolated from the ventricle and left atria. All of the ventricular myocytes that were imaged had a consistent network of evenly spaced T-tubules, 2.08 ± 0.03 μm apart, running perpendicular to the longitudinal axis, towards the centre of the cells (n = 16 myocytes from 3 rats) (Figure 2.4A). On the other hand, in left atrial myocytes, the dye predominantly stained the cell boundaries, suggesting that they do not possess a substantial T-tubule system (Figure 2.4B). T-tubules were observed in 11% of atrial myocytes, but there was a sparse distribution and striations were not observed (n = 18 myocytes from 3 rats). In 92% of pulmonary vein cardiomyocytes, T-tubules were observed at regular intervals along the longitudinal axis of the cell, where there was a mean distance of 1.86 ± 0.03 μm between striations (n = 36 cardiomyocytes from 3 rats) (Figure 2.5). However, the T-tubules were not always transverse and occasionally projected along the longitudinal axis (Figure 2.5A and B). The T-tubules did appear to be more abundant when the pulmonary vein cardiomyocytes were imaged at higher resolution using a confocal microscope (n = 6 cardiomyocytes from 1 rat), where they were visible through the height of the image stack (Figure 2.5C).

2.3.2. Arrangement of mitochondria in the pulmonary vein cardiomyocytes

The pulmonary vein was labelled with TMRE in order to look at the arrangement of the mitochondria in the cardiomyocytes. In Figure 2.6A cardiomyocytes are visible, aligned obliquely in the pulmonary vein. When imaged at higher magnification, small rod shaped structures arranged in consistent rows along the cardiomyocytes are visible (Figure 2.6B and C). These are likely to be individual mitochondria due to their length of 1-2 µm (Hollander *et al.*, 2014; Lukyanenko *et al.*, 2009). In some mitochondria there appeared to be a spontaneous decrease in TMRE fluorescence (Figure 2.6D), which is indicative of a depolarisation in the mitochondrial membrane potential and is commonly referred to as a mitochondrial flicker (Duchen, 1999; Loew *et al.*, 1993). The mitochondria appeared to flicker independently of one another and whilst the imaging period (5 seconds) was too short to allow for a detailed analysis of the time course of these events, the depolarisation was often maintained for the duration of the recording period (Fig 2.6D). Not all mitochondria within a cardiomyocyte flickered during the recording period and whilst not investigated in detail, it appeared that there were some cells where the mitochondria flickered and other cells where no flickers were observed.

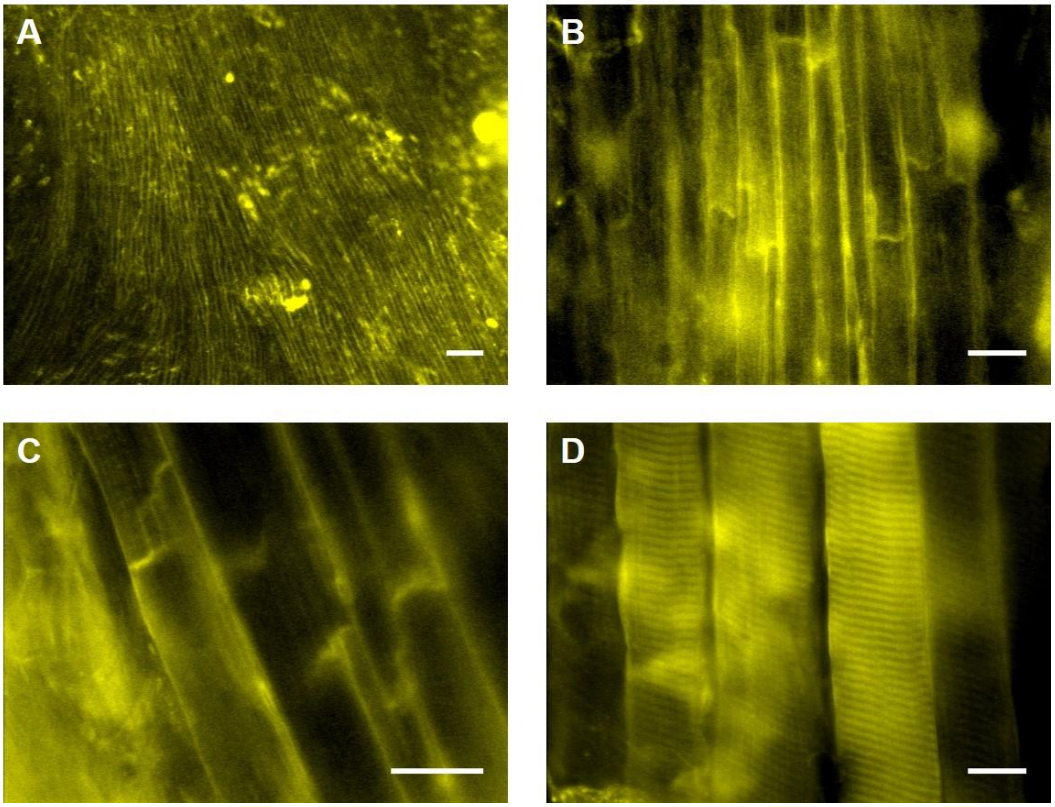

Figure 2.3. Imaging of the rat pulmonary vein and diaphragm with Di-4 ANEPPS. A. The pulmonary vein, which has been labelled with Di-4 ANEPPS (10 µM), and presented in yellow pseudocolour. Imaging was by wide-field epifluorescence microscopy at 5x magnification. The pulmonary vein was also imaged using a 40x **(B)** and 63x **(C)** objective lens. **D.** For comparison with the cardiac tissue, an image of Di-4 ANEPPS fluorescence from the skeletal muscle of the thoracic diaphragm was obtained. Scale bars represent 100 µm for **A**. and 20 µm for **B**, **C** and **D**.

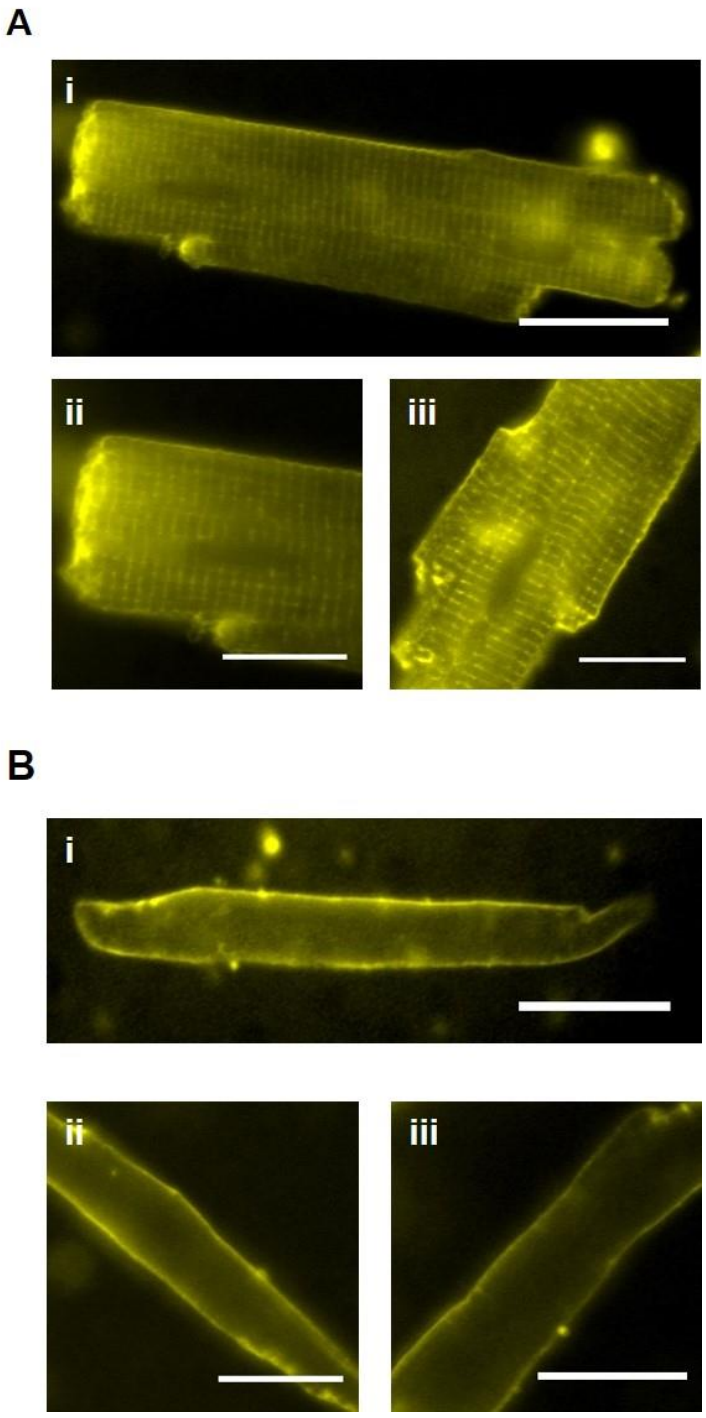

Figure 2.4. Imaging of ventricular and left atrial myocytes with Di-4 ANEPPS. Isolated ventricular **(A)** and left atrial **(B)** myocytes labelled with Di-4 ANEPPS (1-5 µM). Images were obtained by wide-field epifluorescence microscopy with a 40x **(A(i) and B(i))** or 63x **(A(ii and iii) and B(ii and iii))** objective lens. Images are representative of 16 ventricular myocytes and 18 atrial myocytes from 3 separate cell isolations. Scale bars represent 20 µm.

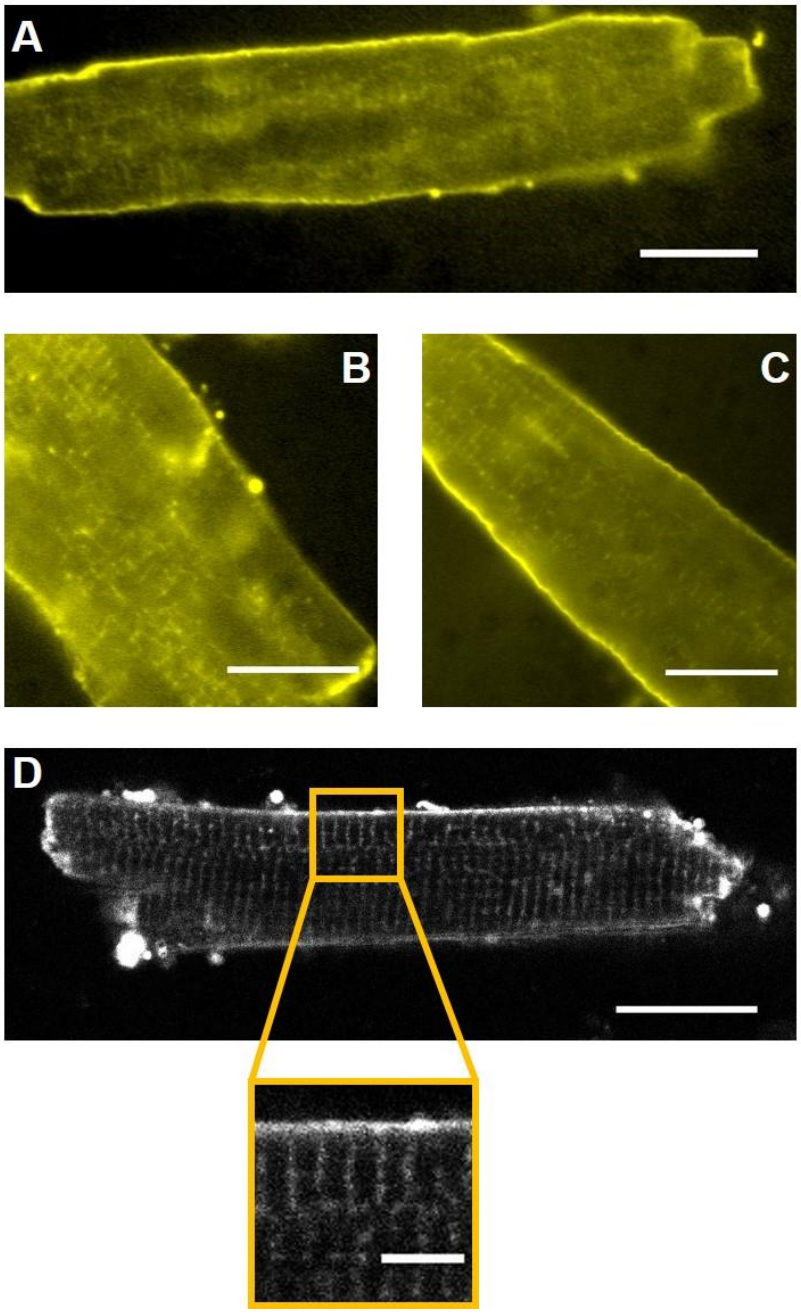

Figure 2.5. Imaging of pulmonary vein cardiomyocytes with Di-4 ANEPPSs. Isolated pulmonary vein cardiomyocytes labelled with Di-4 ANEPPS and imaged by wide-field epifluorescence microscopy at 40x **(A)** and 63x **(B and C)**. Images are representative of 36 cardiomyocytes from 3 separate cell isolations. **D.** Image obtained by confocal microscopy at x63 magnification (representative of 1 cell isolation). Scale bars represent 20 µm. The region in the orange box has been expanded and the scale bar represents 5 µm.

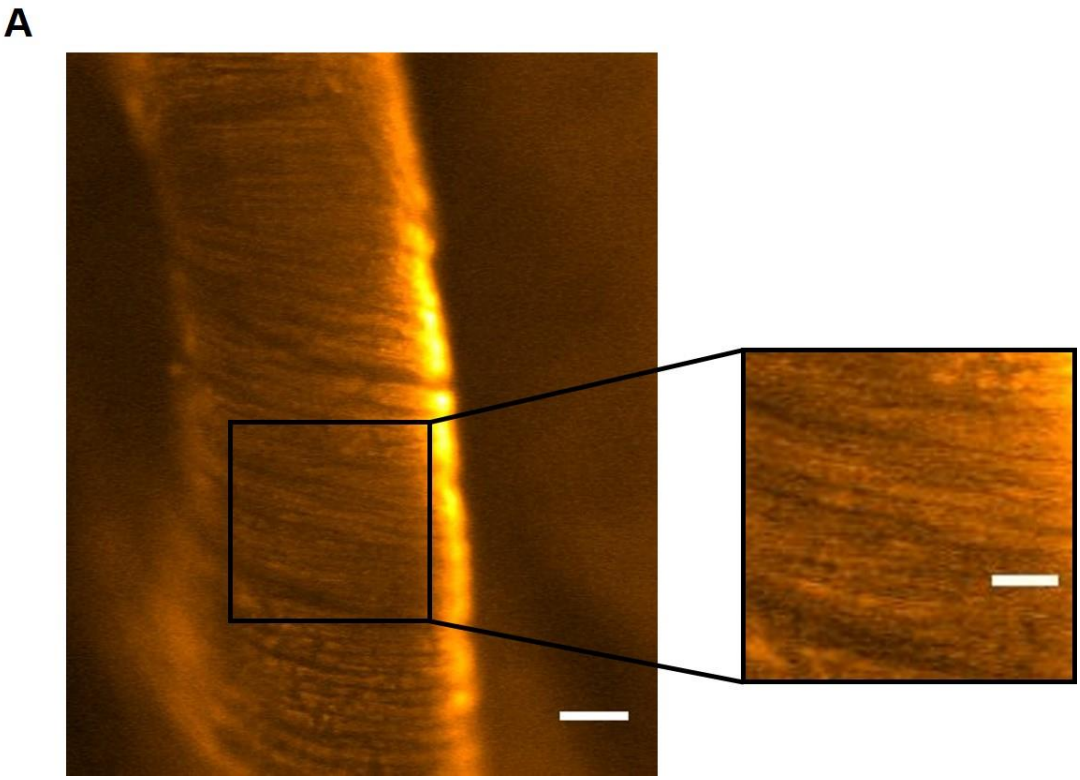

Figure 2.6. Imaging of the mitochondria in the pulmonary vein. A. Image of the pulmonary vein, which has been labelled with TMRE (1 µM) and presented in orange pseudocolour. Imaging was by wide-field epifluorescence microscopy at 5x magnification and the scale bar represents 100 µm. The region in the black box has been expanded and the scale bar represents 10 µm.

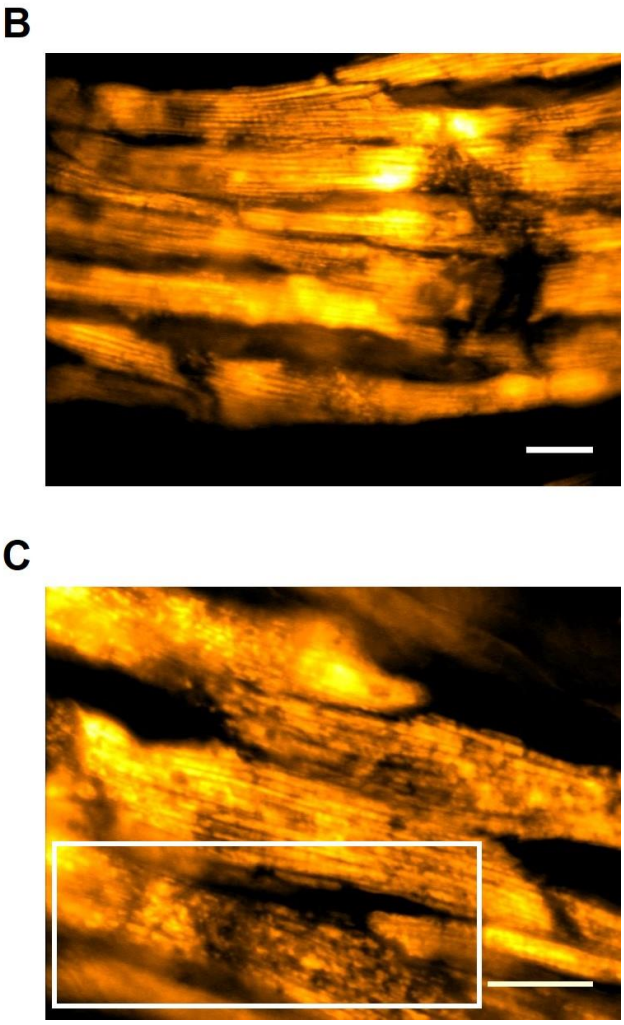

Figure 2.6. (cont.). Pseudocolour images of TMRE (1 µM) fluorescence in the pulmonary vein at 40x **(B)** and 63x **(C)** magnification. Scale bars represent 20 µm.

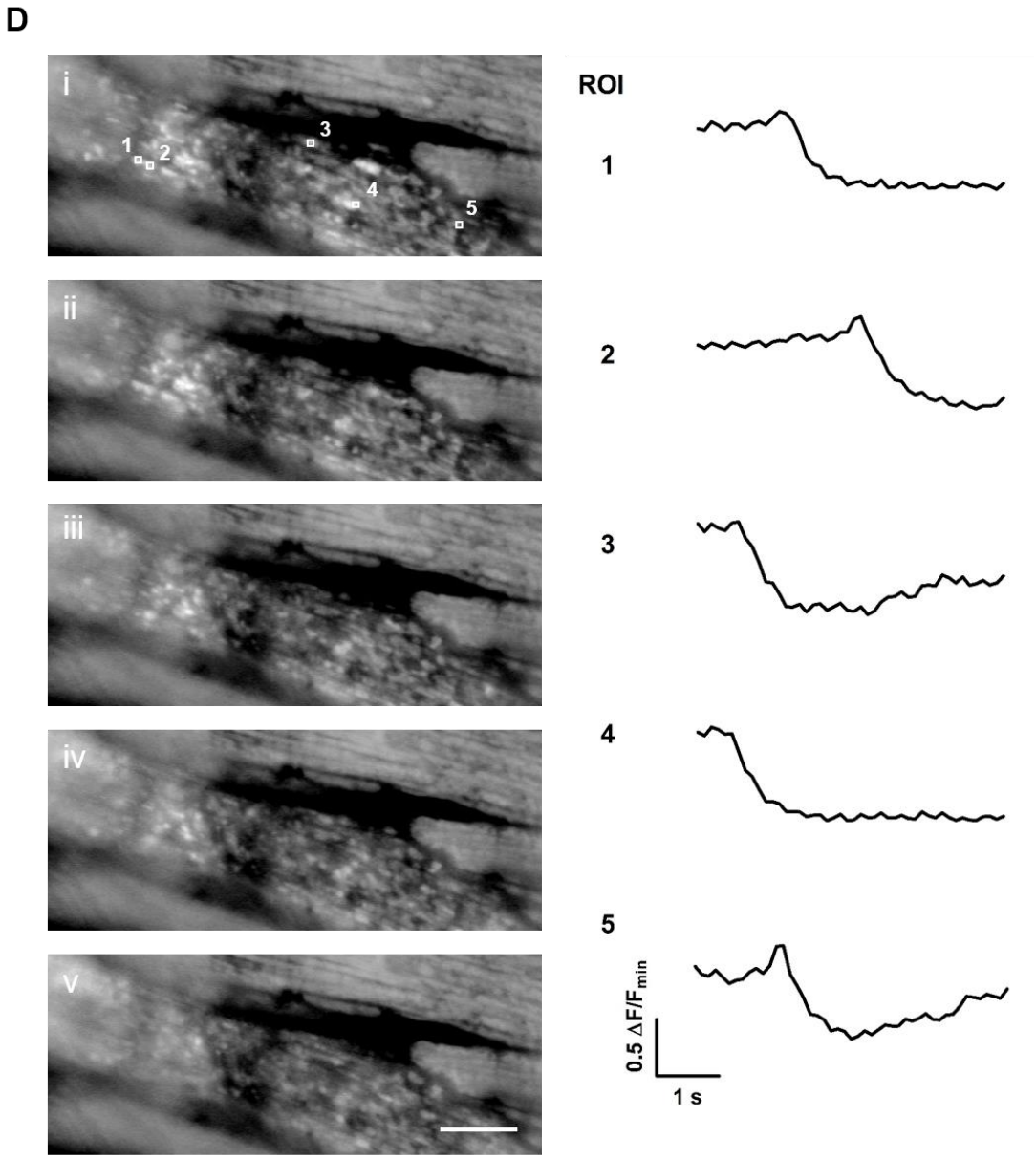

Figure 2.6. (cont.). D. Sequential images (i-v), presented every 1 s, of TMRE fluorescence in the region of tissue indicated by the white box in **(C)**. Scale bar represents 10 µm. The fluorescence intensity in the ROIs (5 x 5 pixels) (1-5) are displayed to the right.

2.3.3. Comparison of cell size

Pulmonary vein cardiomyocytes had a mean length of 135.7 ± 5.06 µm and width of 23.63 ± 1.10 µm (n = 28 cardiomyocytes from 14 cell isolations). Left atrial myocytes were significantly smaller than those from the pulmonary vein, having a length of 99.77 ± 4.54 µm ($P<0.001$) and a width of 17.17 ± 1.25 µm ($P<0.05$; n = 17 myocytes from 14 cell isolations). Ventricular myocytes, being 142.1 ± 5.94 µm long, were not significantly different in length compared to pulmonary vein cardiomyocytes; however, they were significantly wider at 40.6 ± 2.13 µm ($P<0.001$; n = 22 myocytes from 13 cell isolations) (Figure 2.7).

2.3.4. Localisation of the key transporters involved in intracellular Ca^{2+} signalling

2.3.4.1. Control experiments

Control studies suggest that there was no non-specific binding of Alexa fluor® 488 in isolated cells from the ventricles, left atrium and pulmonary veins. Counterstaining DNA with DAPI revealed that ventricular myocytes were binuclear (Figure 2.8), whereas pulmonary vein and left atrial cells were mononuclear (Figures 2.9 and 2.10).

2.3.4.2. The L-Type Ca^{2+} channels

Isolated cells from the ventricles, left atrium and pulmonary veins were labelled with antibodies raised against the $Ca_v1.2$ subunit (Catterall *et al.*, 2005). In 100% of ventricular myocytes, the LTCCs were aligned in regular transverse striations, spaced 1.95 ± 0.05 µm apart, along the length of the cell (n = 10 myocytes from 5 cell isolations) (Figure 2.8). In 75% of left atrial myocytes $Ca_v1.2$ was predominantly expressed in a punctate manner on the cell surface and, as illustrated in the section obtained through the middle of the cell, continued along the periphery. There was also some channel distribution in the cell interior. In the 25% of left atrial myocytes that displayed a striated distribution of $Ca_v1.2$, the distance between the striations was 1.90

± 0.1 µm (n = 8 myocytes from 5 cell isolations) (Figure 2.9). Pulmonary vein cardiomyocytes also displayed a punctate distribution of $Ca_v1.2$ on the cell surface and boundary, as well as in the cell interior. Compared to left atrial myocytes, there was a more regular alignment of LTCCs, and striations were observed in 83% of cardiomyocytes, where they were spaced 1.72 ± 0.11 µm apart (n = 6 cardiomyocytes from 5 cell isolations). However, these striations were not as well-defined as in the ventricular cells (Figure 2.10).

2.3.4.3. Ryanodine receptors

The localisation of RyRs was investigated by immunostaining for the cardiac isoform, RyR2 (Otsu *et al.*, 1990). In 100% of ventricular myocytes, RyR2 was expressed in regular transverse striations, spaced 1.89 ± 0.04 µm apart along the length of the cells. Furthermore, RyR2 did not align along the cell periphery in any of the ventricular myocytes studied (n = 10 myocytes from 5 cell isolations) (Figure 2.11). Cardiomyocytes from the left atria (n = 5 myocytes from 5 isolations) and pulmonary vein (n = 7 cardiomyocytes from 5 isolations) also displayed striations that were spaced 1.85 ± 0.06 µm and 1.70 ± 0.05 µm apart respectively. However, RyR2 was also expressed along the periphery, as can be seen more clearly in the expanded images, and this was observed in every cell studied (Figures 2.12 and 2.13). It is notable that the present investigation is the first to show RyR2 expression along the periphery of pulmonary vein cardiomyocytes. There was also some punctate distribution of RyR2 between the striations in the left atrial and pulmonary vein cardiomyocytes (Figures 2.12 and 2.13).

2.3.4.4. The Na^+/Ca^{2+} exchanger

In order to investigate the expression of the NCX, the cells were labelled with antibodies raised against the cardiac isoform NCX-1 (Philipson *et al.*, 1988; Quednau *et al.*, 1997). In all of the ventricular myocytes studied, NCX-1 was expressed in regularly arranged striations, running perpendicular to the longitudinal axis of the cells

with a mean spacing of 2.02 ± 0.06 µm. However, there was also a punctate distribution between the striations. There was no expression of NCX-1 along the cell periphery; however, there was a dense expression at the intercalated discs (n = 2 myocytes from 1 cell isolation), which was not observed in the pulmonary vein or left atrial myocytes (Figure 2.14). Myocytes isolated from the left atria displayed a heterogonous expression of NCX-1 in the cell population. While there was a largely punctate distribution observed in the interior, and around the periphery of the cells, in 38% of myocytes there was a more striated pattern of NCX-1, where the striations were spaced 1.86 ± 0.06 µm apart (n = 6 myocytes from 4 isolation) (Figure 2.15). Similar observations were made in the pulmonary vein cardiomyocytes; however, in the 67% of cardiomyocytes that showed a striated distribution (n = 3 cardiomyocytes from 3 isolations), the NCX did appear to be more organised than in the left atrial cells. This is shown in Figure 2.16, where the cell on the left displays consistently spaced striations, whereas the cardiomyocyte on the right displays a more punctate distribution of NCX-1. The mean spacing between striations in the pulmonary vein cardiomyocytes was 1.95 ± 0.01 µm (Figure 2.16).

2.3.4.5. Dual labelling of the ryanodine receptors and L-type Ca^{2+} channels

In order to try and establish the co-distribution of the LTCCs and RyRs, the cells were labelled with anti-mouse RyR2 and anti-rabbit $Ca_V1.2$ primary antibodies. The cells were then labelled with anti-mouse Alexa Fluor® 488 and anti-rabbit Alexa Fluor® 594 secondary antibodies (Figure 2.17A). However, control data showed that spectral bleed through from the Alexa Fluor® 488 fluorescence was detected by the emission channel for Alexa Fluor® 594 (Figure 2.17B). In a separate experiment, anti-rabbit Alexa fluor® 594 antibodies were also found to bind to the anti-mouse primary antibodies for RyR2 (Figure 2.17C). Thus, the data was inconclusive. Alexa fluor® 350 was also tested; however, the emission at 442 nm could not be captured using the available settings on the confocal microscope.

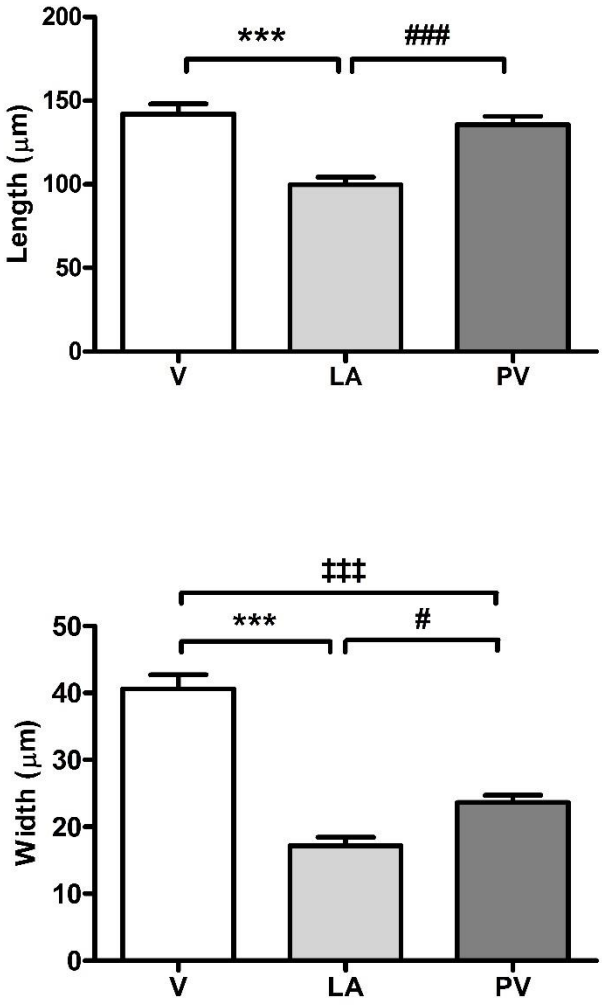

Figure 2.7. Comparison of cardiomyocyte dimensions. Graphs displaying the mean length and width of the ventricular (V) (n = 22 cells), left atrial (LA) (n = 17 cells), and pulmonary vein (PV) (n = 28 cells) cardiomyocytes. Data represent mean ± s.e.m. $^{\#}P<0.05$ LA *vs*. PV, $^{***}P<0.001$ V *vs*. LA, $^{\#\#\#}P<0.001$ LA *vs*. PV and $^{‡‡‡}P<0.001$ V *vs*. PV.

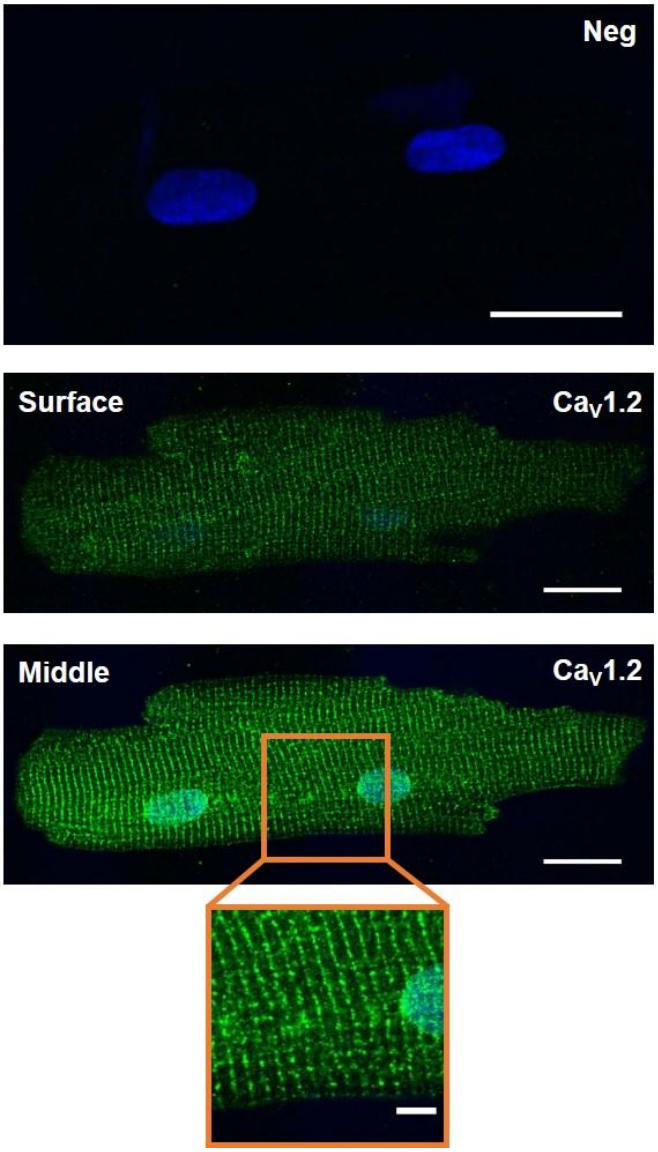

Figure 2.8. Localisation of L-type Ca^{2+} channels in ventricular myocytes. Isolated ventricular myocyte labelled with primary antibodies against $Ca_V1.2$ and Alexa Fluor® 488 secondary antibodies (green), and counterstained with DAPI (blue). Negative control (Neg) where no primary antibody was used. A fluorescence image where the focal plane was at the cell surface and another from the middle. Cell is representative of 10 myocytes from 5 cell isolations. Scale bars represent 20 µm. The region in the orange box has been expanded and the scale bar represents 5 µm.

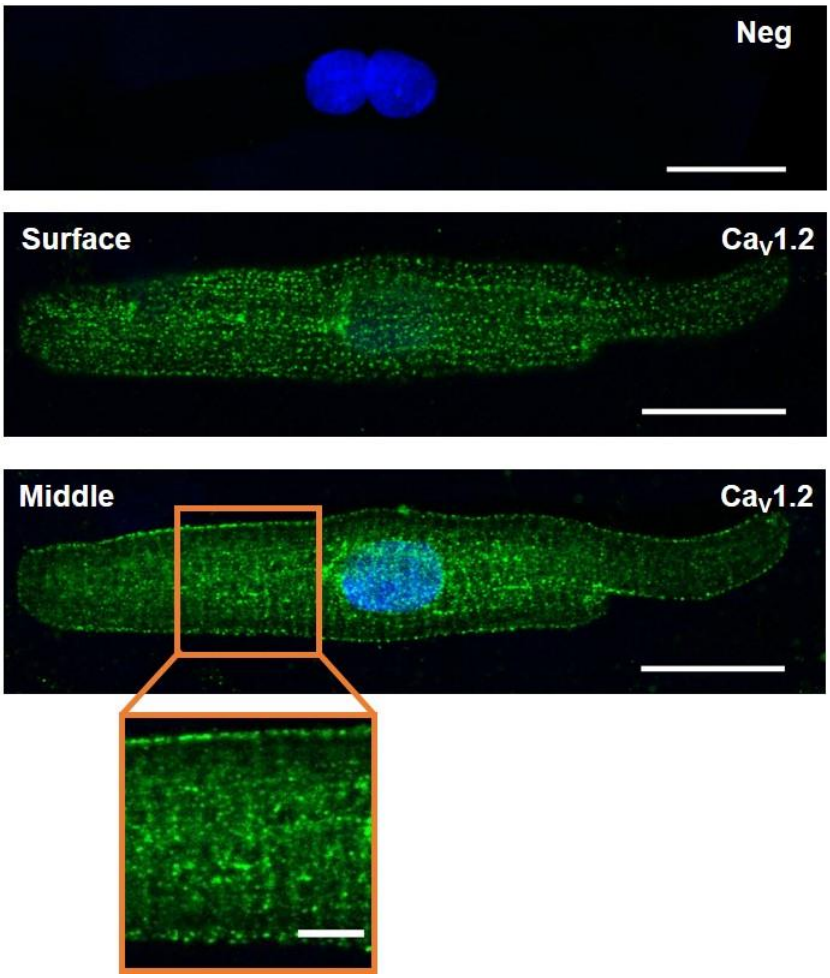

Figure 2.9. Localisation of L-type Ca^{2+} channels in left atrial myocytes. Isolated left atrial myocyte labelled with primary antibodies against $Ca_v1.2$ and Alexa Fluor® 488 secondary antibodies (green), and counterstained with DAPI (blue). Negative control (Neg) where no primary antibody was used. A fluorescence image where the focal plane was at the cell surface and another from the middle. Cell is representative of 8 myocytes from 5 isolations. Scale bars represent 20 µm. The region in the orange box has been expanded and the scale bar represents 5 µm.

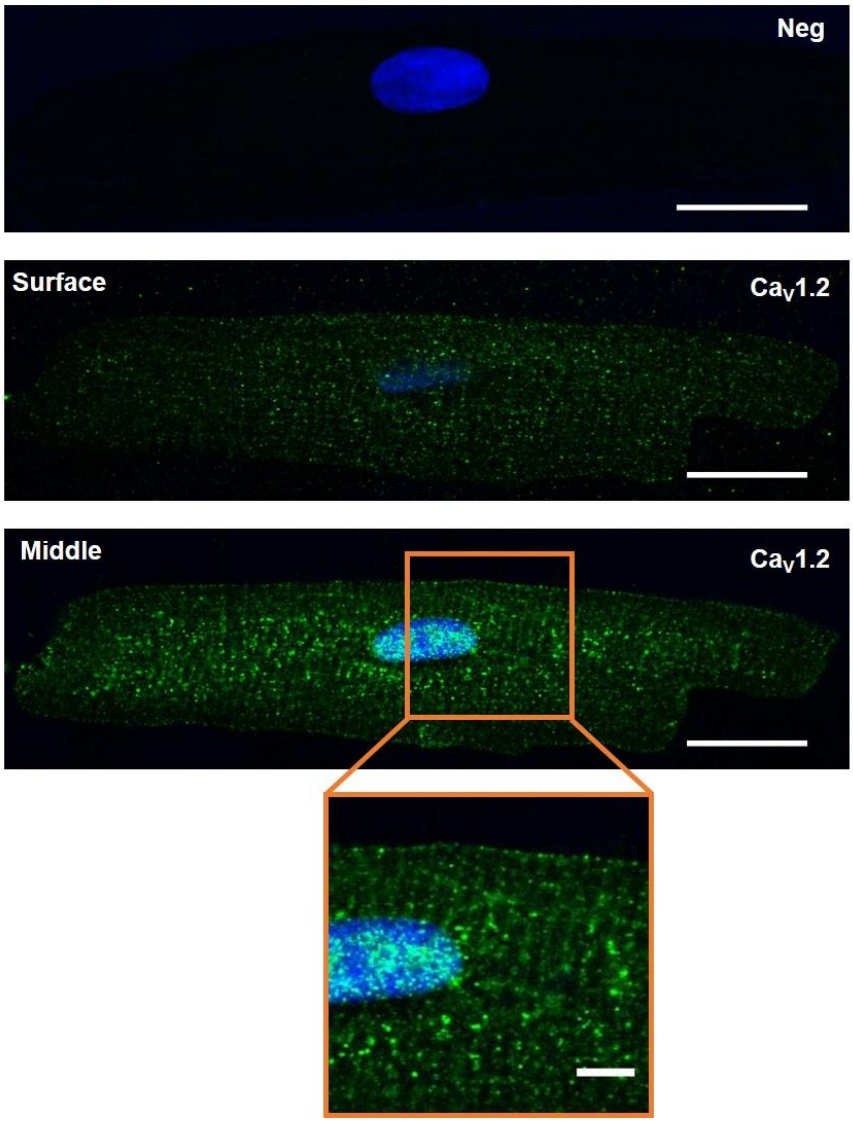

Figure 2.10. Localisation of L-type Ca^{2+} channels in pulmonary vein cardiomyocytes. Isolated pulmonary vein cardiomyocyte labelled with primary antibodies against $Ca_V1.2$ and Alexa Fluor® 488 secondary antibodies (green), and counterstained with DAPI (blue). Negative control (Neg) where no primary antibody was used. A fluorescence image where the focal plane was at the cell surface and another from the middle. Cell is representative of 10 myocytes from 5 isolations. Scale bars represent 20 µm. The region in the orange box has been expanded and the scale bar represents 5 µm.

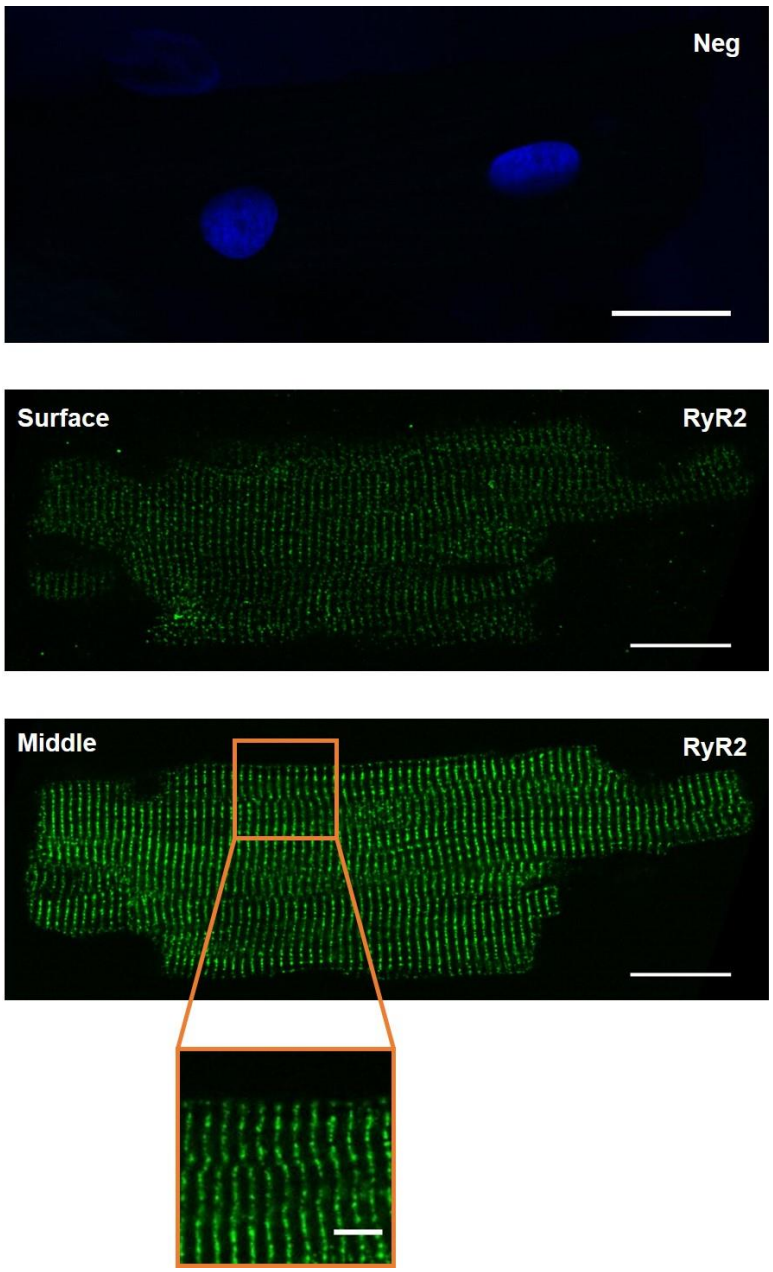

Figure 2.11. Localisation of ryanodine receptors in ventricular myocytes. Negative control (Neg) where no primary antibody was used and the nuclei were labelled with DAPI (blue). Isolated ventricular myocyte labelled with primary antibodies against RyR2 and Alexa Fluor® 488 secondary antibodies (green). A fluorescence image where the focal plane was at the cell surface and another from the middle. Cell is representative of 10 myocytes from 5 cell isolations. Scale bars represent 20 µm. The region in the orange box has been expanded and the scale bar represents 5 µm.

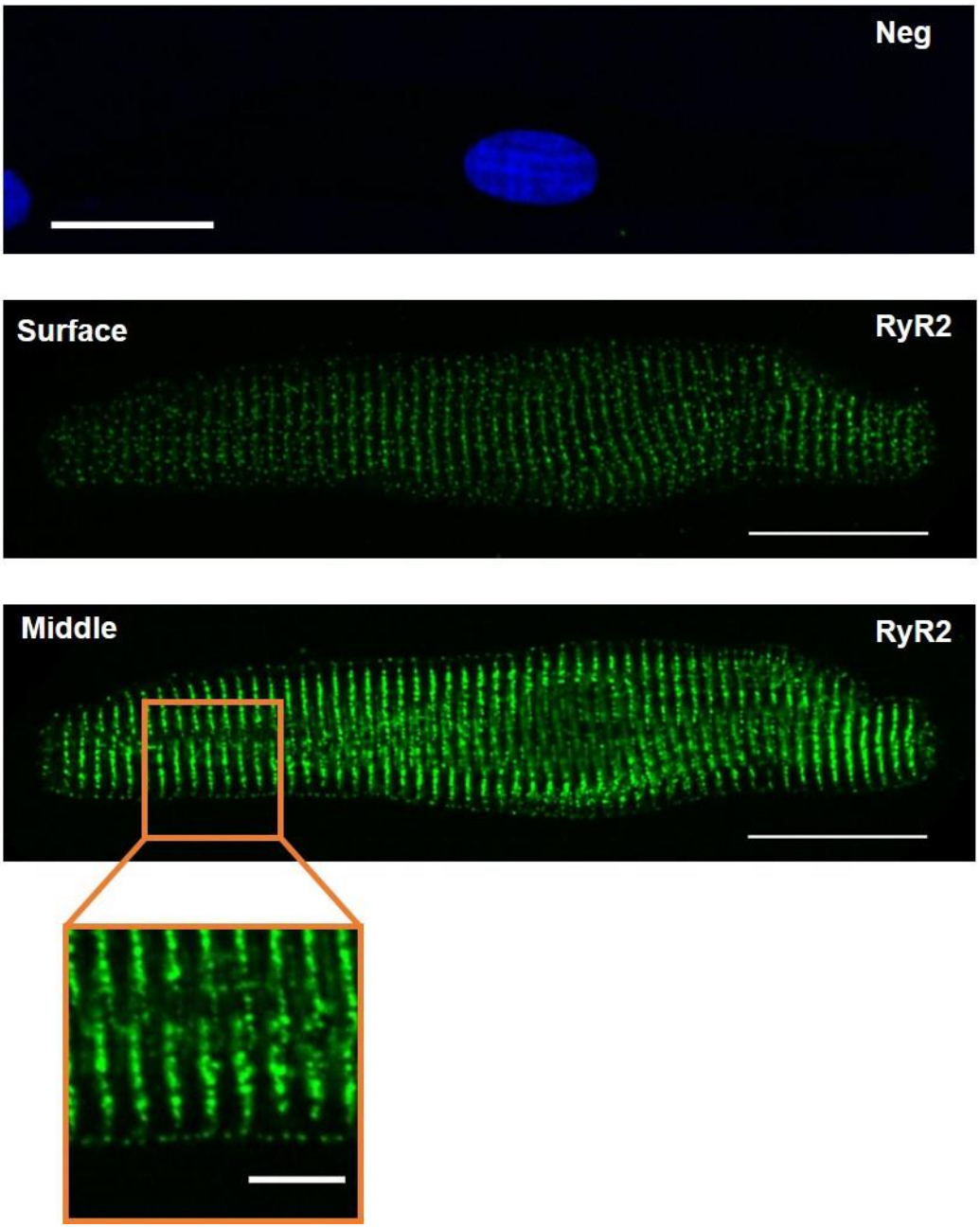

Figure 2.12. Localisation of ryanodine receptors in left atrial myocytes. Negative control (Neg) where no primary antibody was used and the nucleus was labelled with DAPI (blue). Isolated left atrial myocyte labelled with primary antibodies against RyR2 and Alexa Fluor® 488 secondary antibodies (green). A fluorescence image where the focal plane was at the cell surface and another from the middle. Cell is representative of 5 myocytes from 5 cell isolations. Scale bars represent 20 µm. The region in the orange box has been expanded and the scale bar represents 5 µm.

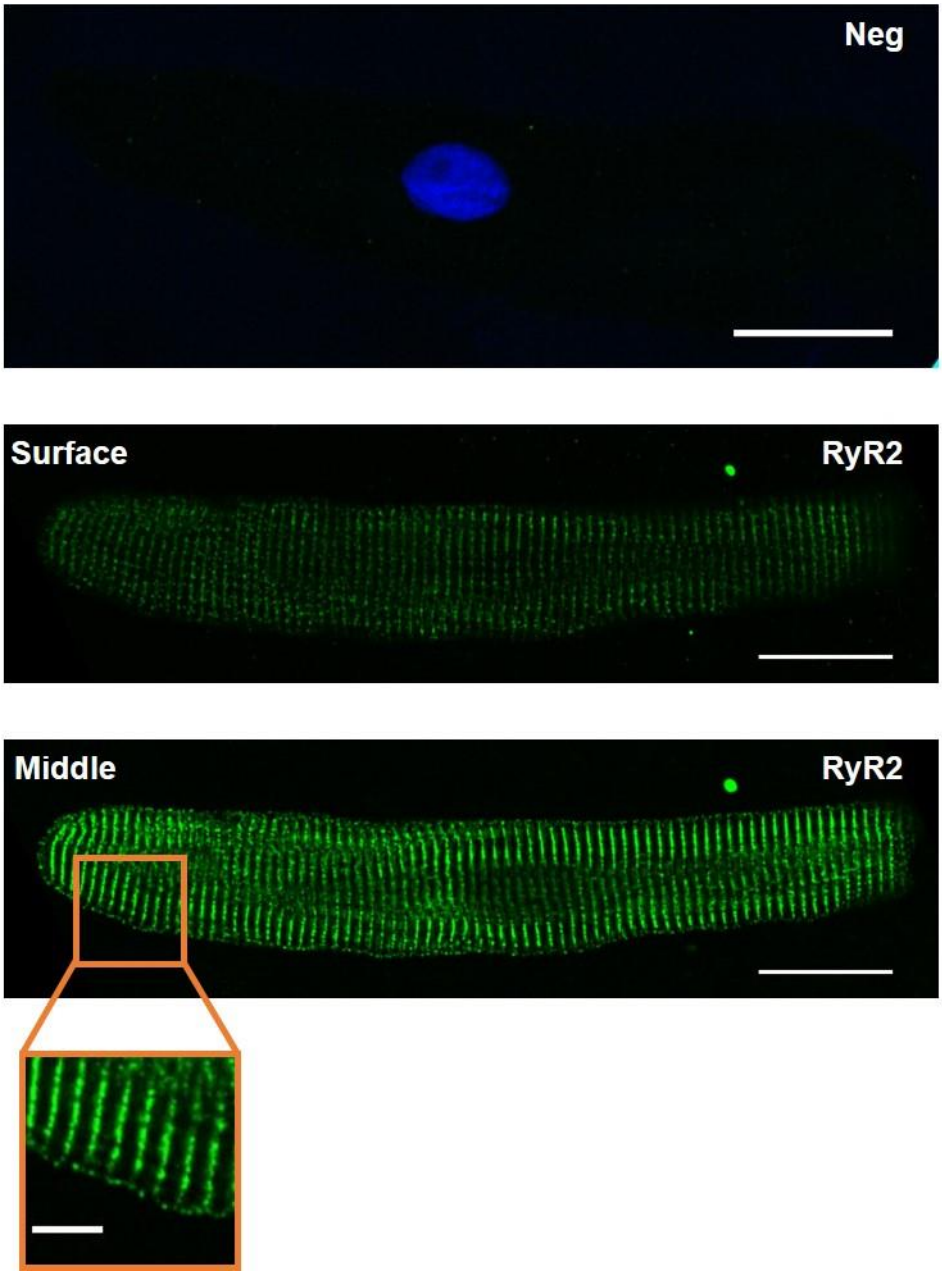

Figure 2.13. Localisation of ryanodine receptors in pulmonary vein cardiomyocytes. Negative control (Neg) where no primary antibody was used and the nucleus was labelled with DAPI (blue). Isolated pulmonary vein cardiomyocyte labelled with primary antibodies against RyR2 and Alexa Fluor® 488 secondary antibodies (green). A fluorescence image where the focal plane was at the cell surface and another from the middle. Cell is representative of 7 myocytes from 5 cell isolations. Scale bars represent 20 µm. The region in the orange box has been expanded and the scale bar represents 5 µm.

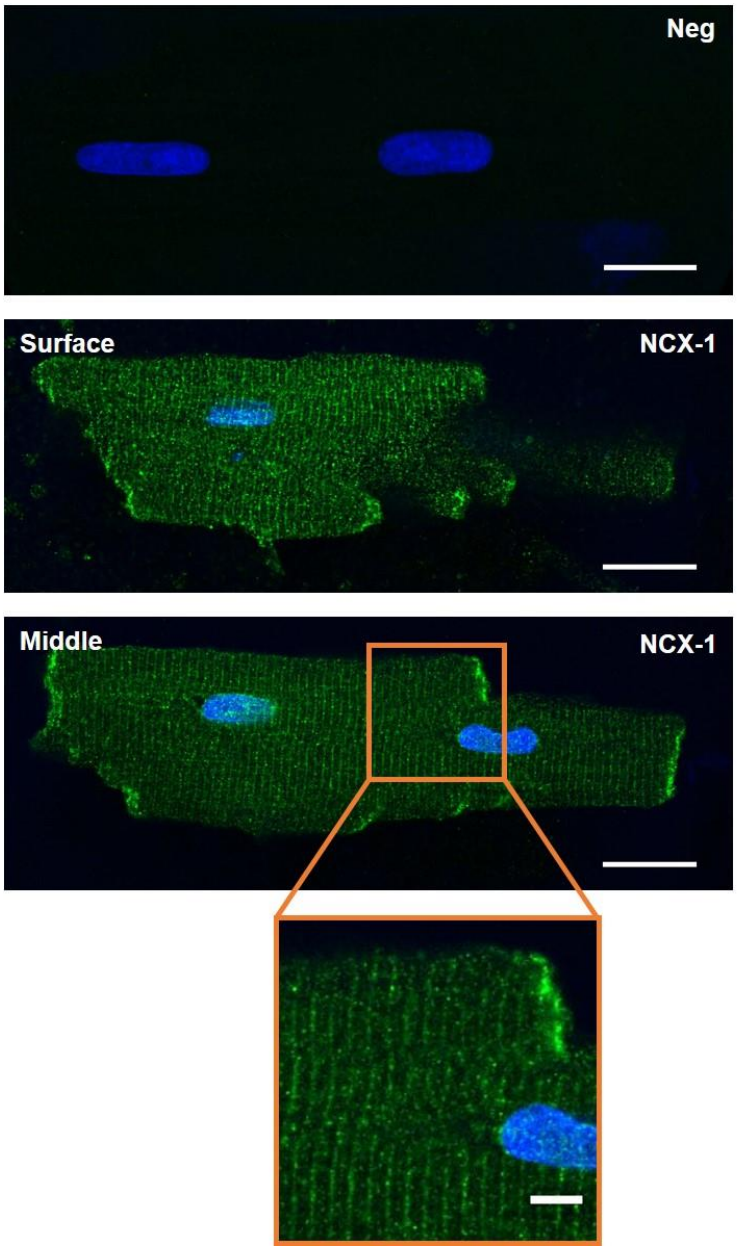

Figure 2.14. Localisation of Na^+/Ca^{2+} exchanger in ventricular myocytes. Isolated ventricular myocyte labelled with primary antibodies against NCX-1 and Alexa Fluor® 488 secondary antibodies (green), and counterstained with DAPI (blue). Negative control (Neg) where no primary antibody was used. A fluorescence image where the focal plane was at the cell surface and another from the middle. Cell is representative of 2 myocytes from 1 cell isolation. Scale bars represent 20 µm. The region in the orange box has been expanded and the scale bar represents 5 µm.

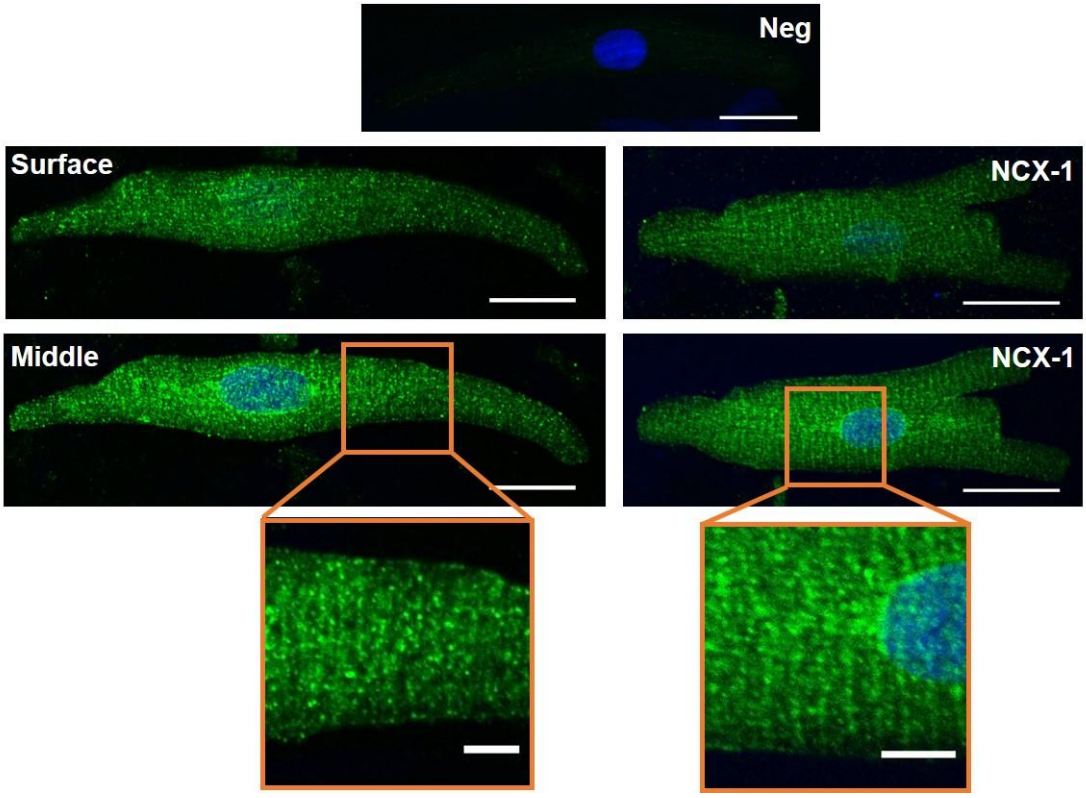

Figure 2.15. Localisation of the Na^+/Ca^{2+} exchanger in left atrial myocytes. Isolated left atrial myocytes labelled with primary antibodies against NCX-1 and Alexa Fluor® 488 secondary antibodies (green), and counterstained with DAPI (blue). Negative control (Neg) where no primary antibody was used. Fluorescence images where the focal plane was at the cell surface and another from the middle. Cells are representative of 6 myocytes from 4 cell isolations. Scale bars represent 20 µm. The regions in the orange boxes have been expanded and the scale bars represent 5 µm.

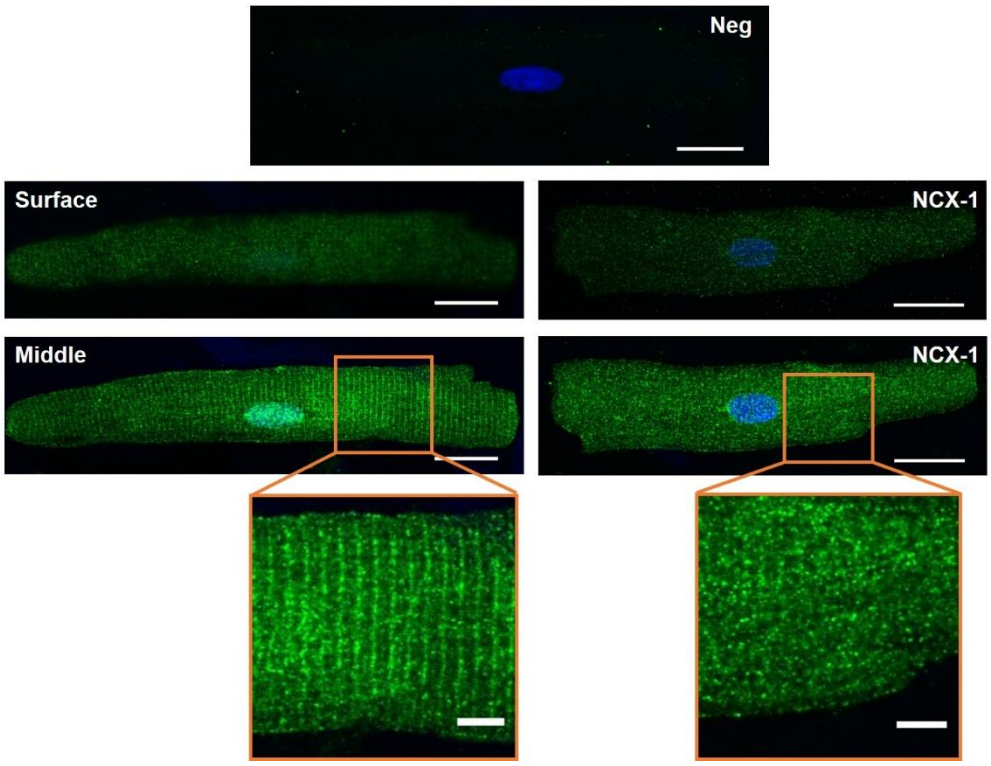

Figure 2.16. Localisation of Na^+/Ca^{2+} exchanger in pulmonary vein cardiomyocytes. Isolated pulmonary vein cardiomyocytes labelled with primary antibodies against NCX-1 and Alexa Fluor® 488 secondary antibodies (green), and counterstained with DAPI (blue). Negative control (Neg) where no primary antibody was used. Fluorescence images where the focal plane was at the cell surface and another from the middle. Scale bars represent 20 µm. Cells are representative of 3 myocytes from 3 cell isolations. The regions in the orange boxes has been expanded and the scale bars represent 5 µm.

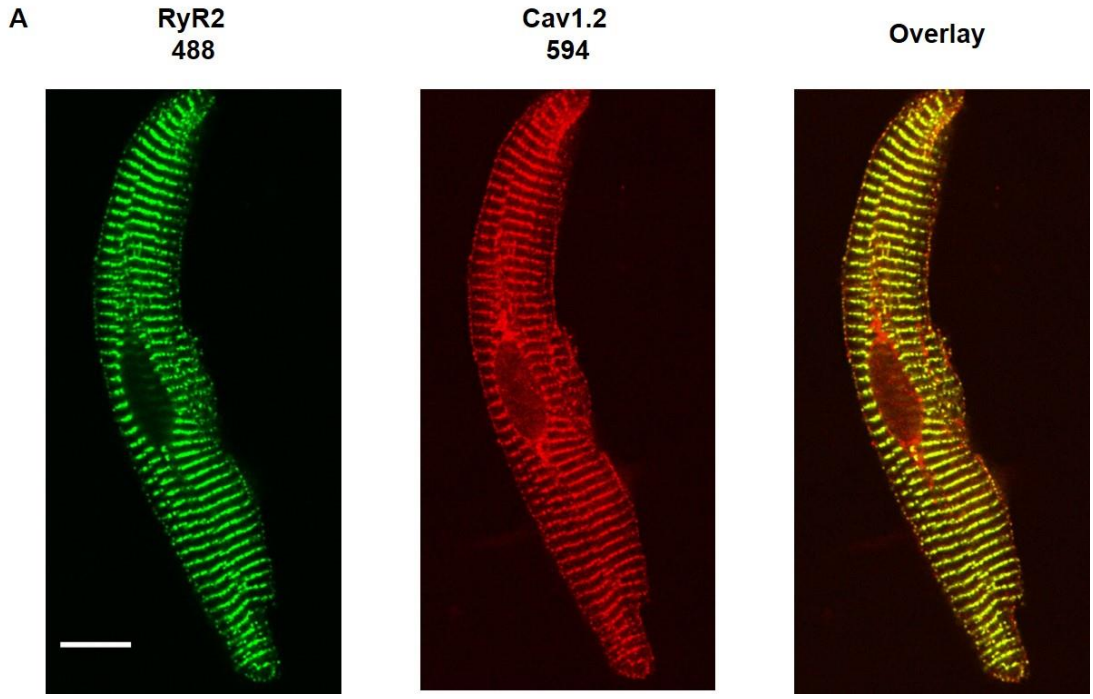

Figure 2.17. Dual labelling in cardiac myocytes A. Left atrial myocyte labelled with primary antibodies raised against RyR2 and $Ca_v1.2$. The images were obtained using the emission channels for Alexa Fluor® 488 and 594. In the overlay, the images from both emission channels have been merged. Scale bar represents 10 µm.

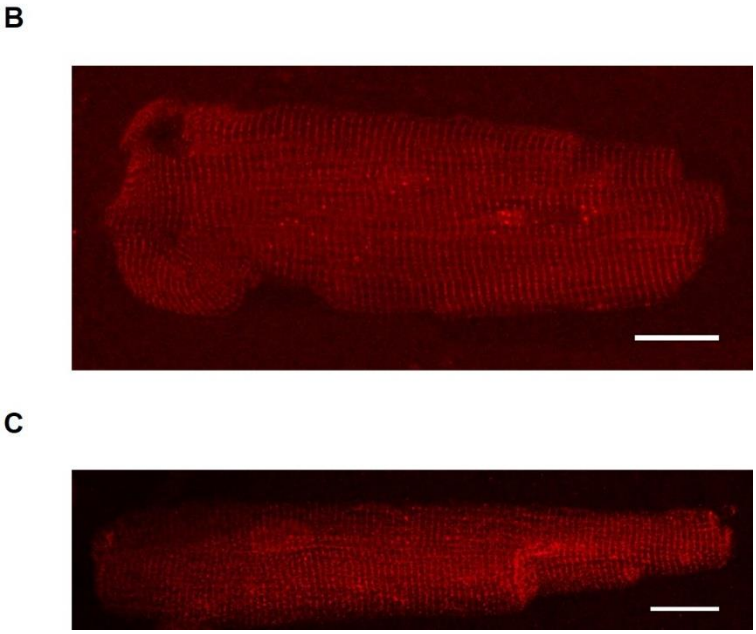

Figure 2.17. (cont.). B. Ventricular myocyte labelled with primary antibodies raised against anti-mouse RyR2 and anti-mouse Alexa Fluor® 488 secondary antibodies. Emission was captured at 617 nm. **C.** Ventricular myocyte labelled with primary antibodies raised against anti-mouse RyR2 and anti-rabbit Alexa Fluor® 594 secondary antibodies**.** Excitation/emission settings were for 594 nm. Scale bars represent 20 µm.

2.4. Discussion

2.4.1. Pulmonary vein cardiomyocytes

When the pulmonary vein was labelled with Di-4 ANEPPS, cardiomyocytes were observed, orientated either longitudinally or obliquely in the vein. This is consistent with earlier reports on the rat pulmonary vein using electron microscopy and histological techniques (Hashizume *et al.*, 1998; Ludatscher, 1968; Paes de Almeida *et al.*, 1975). It was evident when the pulmonary vein cardiomyocytes were isolated that T-tubules were present. However, the T-tubule network was inconsistent and their expression varied between cardiomyocytes. There also appeared to be fewer connections to the surface membrane compared to ventricular myocytes.

The distance between the T-tubules in rat ventricular myocytes was approximately 2 µm, which is very similar to what has been reported previously for these cells (1.8-2 µm) (Asghari *et al.*, 2009; Smyrnias *et al.*, 2010; Soeller & Cannell, 1999; Song *et al.*, 2006). In pulmonary vein cardiomyocytes the T-tubule spacing was slightly less, being approximately 1.8 to 1.9 µm. Okamoto *et al.*, (2012) previously showed, using Di-8 ANEPPS, that rat pulmonary vein cardiomyocytes have T-tubules; however, they did not provide specific details regarding their spacing. Nevertheless, they did report that the NCX and IP_3 receptors were arranged in a striated distribution with a cyclic interval of 1.8 to 1.9 µm and suggested that they may co-localise in the T-tubule microdomain (Okamoto *et al.*, 2012). In contrast, in lung slices from the mouse, Di-8 ANEPPS was shown to predominantly stain the boundary of the pulmonary vein cardiomyocytes (Rietdorf *et al.*, 2014) suggesting an absence of T-tubules in these cells. When atrial myocytes were labelled with Di-4 ANEPPS, staining was typically only observed around the periphery of the cells, suggesting that they possessed few or no T-tubules, an observation that was also made in the earlier study by Okamoto *et al.*, (2012).

2.4.2. Organisation of mitochondria in the pulmonary vein

Mitochondria were organised in a regular manner throughout the length of the cardiomyocytes, which is similar to what has been observed in ventricular (Delcamp *et al.*, 1988; Jang *et al.*, 2007; Kurz *et al.*, 2010) and atrial myocytes (Mackenzie *et al.*, 2004). Early electron microscopy studies also reported abundant mitochondria in pulmonary vein cardiomyocytes (Karrer, 1959; Ludatscher, 1968; Masani, 1986; Paes de Almeida *et al.*, 1975).

Mitochondrial flickers were observed for the first time in pulmonary vein cardiomyocytes, and these events occurred asynchronously within an individual cell. While it wasn't possible to provide detailed information regarding the time course of the mitochondrial flickers; they did appear to be much slower than what was reported in the seminal study showing spontaneous mitochondrial depolarisations in rat ventricular cardiomyocytes (Duchen *et al.*, 1998). In ventricular cardiomyocytes, the mitochondrial depolarisations were transient and the recovery time constant was approximately 0.5 s. However, more recently the duration of spontaneous mitochondrial depolarisations was found to be approximately 60 s in mouse ventricular myocytes (Lu *et al.*, 2016). In both studies, influx of Ca^{2+} into the mitochondrial matrix was found to be important for depolarisation of the mitochondrial membrane potential (Duchen *et al.*, 1998; Lu *et al.*, 2016).

Further studies are clearly necessary to understand the nature of the mitochondrial flickers in pulmonary vein cardiomyocytes. Initially, the tissue would need to be imaged over a much longer time period in order to establish the kinetics of the mitochondrial depolarisations. More detailed information regarding the frequency of these events would also be informative. Whilst Ca^{2+} influx has been shown to play an important role in mitochondrial flickers in ventricular myocytes (Duchen *et al.*, 1998; Lu *et al.*, 2016), there are also reports that reactive oxygen species are responsible (Brady *et al.*, 2004; Zorov *et al.*, 2000; Zorov *et al.*, 2006). Thus, the underlying mechanisms of the mitochondrial flickers merit future investigation.

2.4.3. Localisation of Ca^{2+} handling proteins in pulmonary vein cardiomyocytes compared to left atrial and ventricular myocytes

In ventricular myocytes, the LTCCs, RyRs and the NCX were arranged in consistently spaced (~1.8 to 2 μm) striations orientated transversely to the longitudinal axis of the cells, which is in agreement with the previous reports (Carl *et al.*, 1995; Scriven *et al.*, 2000). RyRs were not distributed along the cell periphery, suggesting that all of the receptors align at the T-tubules (Mackenzie *et al.*, 2001). It has been established that this forms a dyadic cleft where the close coupling of the LTCCs to the RyRs allows for a rapid and homogenous rise in intracellular Ca^{2+} throughout the entire cytosol during systole (Brette *et al.*, 2004; Cannell *et al.*, 1995; Shacklock *et al.*, 1995). In ventricular myocytes that were detubulated by osmotic shock treatment with formamide, a loss of the NCX current (I_{NCX}) has been demonstrated using the whole-cell patch clamp technique (Yang *et al.*, 2002). This suggests that transsarcolemmal Ca^{2+} flux via the NCX also occurs in the domain of the T-tubules in ventricular myocytes.

It was notable that the NCX appeared to be densely expressed at the intercalated discs in ventricular, but not left atrial or pulmonary vein cardiomyocytes. Localisation of the NCX at the intercalated disc region has previously been observed in guinea pig (Kieval *et al.*, 1992) and rat ventricular myocytes (Bootman *et al.*, 2006; Garciarena *et al.*, 2013; Thomas *et al.*, 2003). However, it has been suggested that bright fluorescence at the intercalated discs reflects extensive infolding of the membrane, which encompases a large fraction of the total sarcolemmal surface area (Kieval *et al.*, 1992; Page, 1978). Electon microscopy studies have shown that cardiomyocytes in the rat (Kramer & Marks 1965) and mouse (Kracklauer *et al.*, 2013) pulmonary vein are connected by intercalated discs, so the difference in distribution of the NCX in ventricular and pulmonary vein cardiomyocytes may reflect differences in the functional properties of the exchanger, for example to allow transport of Ca^{2+} between cells. It has been shown in the failing heart that Cx43 is downregulated, whereas NCX is upregulated (Jóhannsson *et al.*, 1997; Wasserstrom *et al.*, 2000), and it has therefore

been suggested that the presence of NCX at the disc region could be to maintain homgenous contraction in viable regions of the myocardium (Thomas *et al.*, 2003).

In left atrial myocytes, RyRs were arranged in regularly arranged transverse striations, approximatly 1.8 to 2 µm apart, as well as along the cell periphery. This has previously been observed in numerous immunolabelling studies (Carl *et al.*, 1995; Mackenzie *et al.*, 2001; Schulson *et al.*, 2011; Smyrnias *et al.*, 2010). The RyRs at the cell periphery have been termed junctional RyRs, as they are located in the subsarcolemmal region. Those located on the striations have been described as being non-junctional since they are distributed in the cell interior (Mackenzie *et al.*, 2001; Mackenzie *et al.*, 2004). In several species such as rat, guinea pig and human, it has been shown that the influx of Ca^{2+} through LTCCs, and the initial Ca^{2+} -induced Ca^{2+} release occuring at the junctional RyRs is localised primarily at the periphery of the cell. The Ca^{2+} signal then propagates towards the interior of the cell, and a variable degree of Ca^{2+}-induced Ca^{2+} release occurs at the non-junctional RyRs depending on the intracellular Ca^{2+} concentration (Berlin, 1995; Hatem *et al.*, 1997; Kockskämper *et al.*, 2001; Mackenzie *et al.*, 2001; Tanaami *et al.*, 2005; Woo *et al.*, 2002).

The distribution of RyRs was similar in pulmonary vein cardiomyocytes, with non-junctional RyRs aligned as transverse striations along the interior of the cells. This is consistent with a previous report where RyR2 was immunolabelled in mouse pulmonary vein cardiomyocytes (Rietdorf *et al.*, 2014). However, this is the first study to show that pulmonary vein cardiomyocytes display junctional RyR aligned along the cell periphery.

In the majority of left atrial myocytes, the LTCCs were primarily located at the periphery, with some punctate distribution in the cell interior; however, there was also slight striated distribution in some of the cells. It is unclear why, despite rat atrial myocytes lacking discernible T-tubules, there was a striated distribution of $Ca_v1.2$ in 25% of cells, particularly since previous studies have shown LTCCs to be primarily

localised around the periphery (Schulson *et al.*, 2011; Smyrnias *et al.*, 2010). However, a detailed study has recently reported a much more variable distribution of LTCCs in rat atrial myocytes, with 10% of cells showing a regular striated appearance of LTCCs and these cells also had an extensive T-tubule system. (Frisk *et al.*, 2014).

In the present study, the atrial cells where a striated distribution was observed displayed quite a high level of fluorescence between the striations. This was very similar to that observed in a separate study investigating the distribution of T-type Ca^{2+} channels in mouse atrial cells (Curran *et al.*, 2015). Clearly, there is some question as to the specificity of the primary antibody used in these studies, and it would be advantageous to perform additional investigations with a primary antibody obtained from a different supplier.

In the pulmonary vein cardiomyocytes, the LTCCs were more likely to form a striated distribution compared to atrial myocytes, which could be a reflection of the T-tubules. It is plausible that transsarcolemmal Ca^{2+} flux through the LTCCs occurs to a larger degree in the cell interior in the pulmonary vein, compared to left atrial cardiomyocytes. Indeed, it has been shown that the L-type Ca^{2+} current was greater in atrial myocytes with T-tubules, compared to those without (Frisk *et al.*, 2014). Consequently, the non-junctional RyRs might also be more likely to play a larger role in the initial SR Ca^{2+} release during excitation-contraction coupling.

Left atrial and pulmonary vein cardiomyocytes had a heterogeneous distribution of NCX-1, with some cells displaying a punctate and others displaying a striated distribution. Overall, the NCX was more likely to be organised in a striated manner in pulmonary vein cardiomyocytes. It was notable that there was a high degree of punctate distribution of NCX-1 compared to what has been reported previously (Schulson *et al.*, 2011) and therefore it is possible that there was some unspecific binding of the primary antibody. An alternative explanation for the striated distribution of NCX in atrial myocytes is that these cells did possess T-tubules and were

preferentially detected due to being more visible in the immunolabelling studies compared to the experiments carried out with Di-4 ANEPPS using the epifluorescence microscope.

To determine if the LTCCs and NCX align at the T-tubules in the pulmonary vein cardiomyocytes that displayed a striated distribution, studies would have to be performed using techniques whereby the T-tubules could be labelled in fixed cells. Antibodies raised against the membrane scaffolding protein dystrophin have been shown to be effective for labelling T-tubules, particularly in tissue (Frank *et al.*, 1994; Frisk *et al.*, 2014; Klietsch *et al.*, 1993; Kostin *et al.*, 1998). Initially dichroic settings would be used to prevent any potential spectral bleed through between the emission channels for Alexa-Fluor® 488 and 594 (Koyama-Honda *et al.*, 2005), and highly cross absorbed secondary antibodies could also be used to minimise unspecific binding to the primary antibodies.

2.4.4. Functional significance of T-tubules in pulmonary vein cardiomyocytes

A possible reason why T-tubules were usually observed in pulmonary vein, but not left atrial cardiomyocytes is because of the larger cell width. In reports that have described atrial myocytes as possessing a rudimentary T-tubule system, it was shown to be more apparent in cells that had a larger width (Kirk *et al.*, 2003; Smyrnias *et al.*, 2010). Furthermore, the density of T-tubules in human atrial myocytes was found to be proportional to cell width (Richards *et al.*, 2011). Detubulation of ventricular myocytes with formamide is associated with the loss of a synchronous Ca^{2+} transient during electrical stimulation, whereas Ca^{2+} signalling in atrial myocytes has been shown to be unaffected following treatment with formamide. (Brette *et al.*, 2002; Kawai *et al.*, 2009). The above observations suggest that cardiomyocytes of a larger width, such as those in the pulmonary vein and ventricle, require a more extensive T-tubule network, to enable a more homogenous intracellular Ca^{2+} transient in the interior of the cell.

2.4.5. Summary

In the present chapter it was shown that pulmonary vein cardiomyocytes have a similar distribution of RyRs to atrial myocytes, whereby junctional RyRs were distributed along the cell periphery in addition to the striations in the interior. However, the expression of LTCCs and the NCX was largely more organised in the pulmonary vein cardiomyocytes, where a striated distrubution was observed in a greater proportion of cells. It was shown that the vast majority of pulmonary vein cardiomyocytes had T-tubules suggesting intrinsic differences in Ca^{2+} handling compared to atrial cells. It is conceivable that these differences could account for the different electrophysiological properties of the pulmonary vein cardiomyocytes (Chen *et al.*, 2002b; Cheung, 1981a; Ehrlich *et al.*, 2003).

Chapter 3

Intracellular Ca^{2+} signalling in rat pulmonary vein cardiomyocytes.

3.1. Introduction

Intracellular Ca^{2+} signalling controls a vast array of cellular processes such as gene transcription, differentiation, neurotransmission and contraction. The temporal and spatial properties of the Ca^{2+} signal are controlled through a diverse range of intracellular transport and buffering processes; therefore the way in which the cell utilises Ca^{2+} can be discretely regulated to control cell function (Bootman *et al.*, 2001 for review). As well as intracellular Ca^{2+} oscillations controlling normal cell function, spontaneous Ca^{2+} release from the intracellular store, or sarcoplasmic reticulum (SR), can occur. These spontaneous Ca^{2+} transients can range from highly localised events, to large Ca^{2+} waves that travel along the length of the cell (Cheng *et al.*, 1996). Spontaneous Ca^{2+} transients have been implicated in arrhythmogenesis in cardiac tissue (ter Keurs & Boyden, 2007 for review).

3.1.1. Spontaneous Ca^{2+} transients in cardiac myocytes

The notion that cardiac myocytes display spontaneous Ca^{2+} transients in the absence of electrical stimulation was first proposed in the early 1980s, from studies on isolated ventricular myocytes. Fluctuations in scattered light were used as a marker for contractility and these fluctuations increased in frequency following manipulations that would increase Ca^{2+} influx, such as increasing the external Ca^{2+} concentration or applying ouabain (Lakatta & Lappé, 1981). Furthermore, the fluctuations in scattered light could be abolished by inhibiting Ca^{2+} influx with verapamil, or by inhibiting SR Ca^{2+} release with ryanodine, confirming that they were caused by changes in intracellular Ca^{2+} (Kort & Lakatta, 1984). Studies using light microscopy later showed that isolated ventricular myocytes displayed mechanical oscillations that propagated longitudinally along the cell as contractile waves. These oscillations could also occur simultaneously at multiple foci, either originating in the centre of the cell before splitting into two waves, or occurring as two waves originating at either end of the cell before colliding in the middle. Spontaneous contractile waves were more likely to occur at multiple foci in the myocytes after increasing the external Ca^{2+} concentration,

or in the presence the β-adrenoreceptor agonist isoprenaline (Capogrossi *et al.*, 1987; Capogrossi & Lakatta, 1985).

Spontaneous increases in intracellular Ca^{2+} were directly recorded for the first time in frog ventricular myocytes using the bioluminescent protein aequorin (Orchard *et al.*, 1983). The advent of Ca^{2+} sensitive fluorescent indicators has since established that spontaneous Ca^{2+} transients are the temporal and spatial summation of the elementary Ca^{2+} sparks that occur when Ca^{2+} is spontaneously released from the SR through the ryanodine receptor (RyR) (Cheng *et al.*, 1996; Wier *et al.*, 1997). It is now widely regarded that spontaneous Ca^{2+} transients in cardiac myocytes are typically manifest as waves of regenerative Ca^{2+} release that propagate along the longitudinal axis of the cell.

In the context of ventricular tissue, where the myocytes are electrically coupled in a large multicellular preparation, Ca^{2+} waves would tend to extinguish when they reached a cell boundary, or upon collision with another Ca^{2+} wave propagating in the opposite direction (Fujiwara *et al.*, 2008; Kaneko *et al.*, 2000; Minamikawa *et al.*, 1997; Wasserstrom *et al.*, 2010). However, approximately 13% of Ca^{2+} waves continued to propagate into myocytes that were adjacent at the transverse axis (Kaneko *et al.*, 2000; Lamont *et al.*, 1998). Spontaneous Ca^{2+} waves have been shown to occur asynchronously in neighbouring ventricular myocytes, meaning that the myocytes displayed spontaneous Ca^{2+} waves at variable frequencies. Simultaneous measurement of the membrane potential determined that any oscillatory depolarisations were subthreshold to elicit action potentials (Fujiwara *et al.*, 2008; Hama *et al.*, 1998; Kaneko *et al.*, 2000; Wasserstrom *et al.*, 2010).

Spontaneous Ca^{2+} sparks and waves have been recorded in isolated pulmonary vein cardiomyocytes from the canine (Coutu *et al.*, 2006), rabbit (Chang *et al.*, 2008; Jones *et al.*, 2008) and rat (Cruickshank & Drummond, 2003). In rat and mouse pulmonary vein tissue, spontaneous Ca^{2+} transients have been shown to occur asynchronously in

neighbouring cells, and were almost completely inhibited by blocking the RyRs (Logantha *et al.*, 2010; Rietdorf *et al.*, 2014). In the rat pulmonary vein, inhibiting the L-type Ca^{2+} channels (LTCCs) with verapamil or preventing Ca^{2+} entry by removing Ca^{2+} from the external solution had no significant effect on the frequency of the spontaneous Ca^{2+} transients. This indicates that the spontaneous Ca^{2+} transients in rat pulmonary vein cardiomyocytes are primarily caused by Ca^{2+} release from the SR (Logantha *et al.*, 2010).

3.1.2. Electrically evoked Ca^{2+} transients in the pulmonary vein

In the rat and mouse pulmonary vein, electrical field stimulation has been shown to evoke a synchronous rise in intracellular Ca^{2+} in neighbouring cardiomyocytes (Logantha *et al.*, 2010; Rietdorf *et al.*, 2014). The Ca^{2+} transient amplitude was significantly reduced by inhibiting the LTCCs with nicardipine or verapamil, or completely abolished by removing Ca^{2+} from the external solution. In addition, the Ca^{2+} transients were mostly abolished by inhibiting the RyRs (Logantha *et al.*, 2010; Rietdorf *et al.*, 2014). Thus, it was determined that both Ca^{2+} entry through the LTCCs and SR Ca^{2+} release through the RyRs are responsible for the electrically evoked Ca^{2+} transients in the pulmonary vein.

3.1.3. The influence of electrical stimulation on the spontaneous Ca^{2+} transients in the pulmonary vein

Depolarisation of the sarcolemma with KCl activates voltage-gated Ca^{2+} channels, leading to Ca^{2+} influx, and this has been shown to increase the frequency of spontaneous Ca^{2+} transients in the rat and mouse pulmonary vein (Logantha *et al.*, 2010; Rietdorf *et al.*, 2014). It has also been shown in the guinea pig pulmonary vein that a brief period of electrical stimulation at 10 Hz induced one or two action potentials after termination of the stimulus. This triggered activity was prevented by verapamil or ryanodine, suggesting that it was caused by intracellular Ca^{2+} signalling (Takahara *et al.*, 2011).

3.1.4. The influence of electrical stimulation on the spontaneous Ca^{2+} transients in the ventricle

The influence of electrical stimulation on spontaneous Ca^{2+} transients has been well established in the ventricle. Following the cessation of a period of electrical stimulation, there is a transient pause, or latency period, before the spontaneous Ca^{2+} transients re-emerge (Kaneko *et al.*, 2000; Shkryl & Blatter, 2013; Wasserstrom *et al.*, 2010). Early contractile studies have inferred that spontaneous Ca^{2+} signalling in ventricular myocytes is influenced by the rate of the prior electrical stimulus. In isolated ventricular myocytes, increasing the stimulation frequency from 0.4 to 1.4 Hz, shortened the latency period between the removal of the electrical stimulus and the re-emergence of spontaneous contractile oscillations. Furthermore, when the spontaneous contractile oscillations reappeared they did so at an increased frequency (Capogrossi & Lakatta, 1985).

More recently, the spontaneous Ca^{2+} transients that immediately followed a period of electrical stimulation were recorded in the rat heart, using the Ca^{2+} sensitive fluorescent indicator fluo-4. The spontaneous Ca^{2+} transients were shown to occur more frequently after a period of electrical stimulation at 1 Hz, compared to with no prior stimulation. It was suggested that the increase in frequency was due to increased Ca^{2+} loading of the cells (Kaneko *et al.*, 2000). In a separate study on the rat heart, when the frequency of electrical stimulation was increased from 2 to 5 Hz, the latency period for the re-emergence of spontaneous Ca^{2+} transients was shortened, and the frequency of the spontaneous Ca^{2+} transients was increased (Wasserstrom *et al.*, 2010). Raising the external Ca^{2+} concentration caused a further reduction in the latency period after a period of electrical stimulation, and also increased the frequency of the subsequent spontaneous Ca^{2+} transients to a greater extent than under control conditions. While the mechanism underlying these changes in latency and frequency of the spontaneous Ca^{2+} transients was not extensively investigated in this study, it was hypothesised that they were due to an increased SR Ca^{2+} load. The electrical activity of the heart was also recorded using an ECG and, following a period of electrical stimulation in conditions of high external Ca^{2+}, extra systoles were observed. Of

particular note, these extra systoles occurred when spontaneous Ca^{2+} transients were present at the same time in all of the myocytes in the field of view (Wasserstrom *et al.*, 2010). While it wasn't possible to determine the site of origin of the extrasystole, the fact that that it coincided with the point when spontaneous Ca^{2+} release occurred, indicated that the site of origin was nearby or that the spontaneous Ca^{2+} release is occurring with fairly uniform timing throughout the heart. Furthermore, this study goes on to use a mathematical model to show that a decrease in the variability in the timing of the spontaneous Ca^{2+} release leads to a higher amplitude delayed afterdepolarisation, and is likely to be pro-arrhythmic.

3.1.5. The effect of adrenergic stimulation on the spontaneous Ca^{2+} transients

Stimulation of β-adrenoreceptors with isoprenaline has also been shown to shorten the latency period between the termination of electrical stimulation to the re-emergence of spontaneous contractile oscillations in isolated ventricular myocytes (Capogrossi & Lakatta, 1985), and the re-emergence of spontaneous Ca^{2+} waves in the fluo-4 loaded rat heart (Fujiwara *et al.*, 2008). Simultaneous measurement of the membrane potential using the fluorescent indicator RH237 revealed that, following termination of a period of electrical stimulation at 2 Hz or higher, the spontaneous Ca^{2+} transients re-emerged as a synchronous burst, and this was accompanied by afterdepolarisations. These afterdepolarisations were abolished with a high concentration of ryanodine or by inhibiting the NCX with SEA0400 (Fujiwara *et al.*, 2008). This suggests that the cause of the afterdepolarisations was increased SR Ca^{2+} release, which activated the forward mode NCX causing depolarisation (Kass *et al.*, 1978; Schlotthauer & Bers, 2000). Thus, it is apparent that transiently increasing the frequency of spontaneous Ca^{2+} transients means that there is a better chance that they will be present in neighbouring cardiomyocytes at the same time, which in turn can influence the electrical activity of the tissue (Fujiwara *et al.*, 2008). Additionally, noradrenaline, which activates α and β adrenoreceptors, has been shown to induce automaticity in the rat pulmonary vein in the form of repetitive bursts of contractions (Maupoil *et al.*,

2007) or action potentials (Doisne *et al.*, 2009). However, the role of intracellular Ca^{2+} signalling in noradrenaline induced automaticity has yet to be determined.

3.1.6. Aims

The hypothesis of the present chapter was that, if a cardiomyocyte in the pulmonary vein depolarises due to spontaneous SR Ca^{2+} release, electrical coupling between quiescent neighbouring cells would act as a current sink, preventing depolarisation (Spach & Boineau, 1997; Winslow *et al.*, 1993; Xie *et al.*, 2010). This would mean that for changes in intracellular Ca^{2+} signalling to be arrhythmogenic, there would need to be synchronisation or entrainment of spontaneous activity. Manipulations that alter the characteristics of the spontaneous Ca^{2+} transients may be capable of increasing their frequency, such that they are more likely to occur in neighbouring cardiomyocytes at the same time. Increasing the frequency of spontaneous Ca^{2+} transients in a number of neighbouring cardiomyocytes would therefore reduce the disparity between frequencies, improving synchronisation and leading to entrainment, as has been demonstrated in mathematical models of action potential firing in cardiac myocytes (Krishnan *et al.*, 2005; Michaels *et al.*, 1987). A more synchronous increase in intracellular Ca^{2+} in neighbouring cardiomyocytes could result in depolarisation due to the transient inward current (I_{ti}) generated by Ca^{2+} removal through the NCX (Capogrossi *et al.*, 1987; Houser, 2000; Schlotthauer & Bers, 2000).

The primary aim of the present chapter was therefore to investigate whether the characteristics of the spontaneous Ca^{2+} transients that have previously been observed in the rat pulmonary vein (Logantha *et al.*, 2010) are altered by interventions that might entrain them to become more synchronous and thus arrhythmogenic. This included subjecting the pulmonary vein to brief periods of electrical stimulation at increasing frequencies, and also increasing the external Ca^{2+} concentration. The effect of isoprenaline and noradrenaline on the characteristics (frequency, amplitude and propagation velocity) of the spontaneous events was also investigated to determine the influence of adrenergic stimulation.

3.2. Materials and methods

3.2.1. Animals and pulmonary vein isolation.

The pulmonary vein was isolated from adult male Sprague-Dawley rats (8-10 weeks) as described in section 2.2.1.

3.2.2. Imaging of the Ca^{2+} signalling in the pulmonary vein

Changes in intracellular Ca^{2+} were monitored using the Ca^{2+} sensitive fluorescent indicator, fluo-4 (Gee *et al.*, 2000). Isolated sections of the pulmonary vein were incubated for 60 min in the dark, at room temperature, in physiological salt solution containing 10 μM fluo-4 AM and the non-ionic solubilising agent cremophor EL (0.03%). The tissue was then washed in fresh solution and pinned onto a Sylgard® 184 coated recording chamber containing 4 ml physiological salt solution of the following composition (in mM): 119 NaCl, 25 $NaHCO_3$, 4.7 KCl, 1.17 $MgSO_4$, 1.18 KH_2PO_3, 2.5 $CaCl_2$ and 5.5 glucose (pH 7.4 with 95% O_2 and 5% CO_2). The preparation was allowed 15 min for equilibration before commencing experimentation.

The tissue was imaged using wide-field epifluorescence microscopy, with a Zeiss Axioscop 50 (Carl Zeiss, Germany) as described in section 2.2.2. Fluo-4 was excited at BP 450-490 nm and emission was captured at LP 515 nm using the CCD camera set up. Images were acquired using WinFluor 2.19 (Dr John Dempster, University of Strathclyde) with an exposure time of 110 ms (~9 frames per second). Unless indicated otherwise, a 128 frame image series was obtained, which approximates a 14 s recording period. This was to provide a suitable time frame by which to analyse the characteristics of the spontaneous Ca^{2+} transients, without overexposing the tissue to light and photobleaching the dye.

3.2.3. Electrical stimulation of the pulmonary vein

The pulmonary vein was electrically stimulated using a pair of platinum or silver wire electrodes positioned either side of the tissue, approximately 1-2 cm apart. A Grass SD9 stimulator was used to provide rectangular pulses, 2 ms in width, at supramaximal

voltage (80-100 V) via a stimulus isolation unit (SIU 5A, Grass Instrument Co., USA). The frequency of electrical stimulation was 1 Hz unless stated otherwise.

3.2.4. Application of caffeine to the pulmonary vein

Caffeine sensitises the RyRs, causing Ca^{2+} to be released from the SR (Rousseau *et al.*, 1987). When rapidly applied at a high concentration, the magnitude of the caffeine induced Ca^{2+} transient can be used as an indicator of the Ca^{2+} load of the SR (Bers, 2000b; Chang *et al.*, 2008; Varro *et al.*, 1993). A region of tissue displaying spontaneous Ca^{2+} transients was located with a 5x objective lens using fluorescence imaging. A glass micropipette (World Precision Instruments, Sarasota, FL, USA) was then fabricated from a borosilicate glass capillary using a vertical micropipette puller (pp-830, Narishige, Japan), and filled with 100 mM caffeine dissolved in physiological salt solution. The tip of the micropipette was broken on a glass coverslip in the tissue chamber, just enough to allow for adequate release of the caffeine solution, but not too much as to result in leak prior to application. During the recording, caffeine (100 mM) was applied onto the surface of the tissue for 5 s using a pressure ejection system (Picospritzer, Parker Hannifin, N.J., USA). A 224 frame image series was obtained, which approximates a 27 s recording period. This was to allow a suitable time frame for the fluo-4 fluorescence to decline following the application of caffeine. The tissue was allowed 15 min to recover before any subsequent application of caffeine.

3.2.5. Analysis of intracellular Ca^{2+} transients

Images were imported into ImageJ in the TIFF format. Spontaneous Ca^{2+} transients were analysed for peak amplitude and frequency using a custom-made plugin written for ImageJ (Dr Francis Burton, University of Glasgow). A region of interest (ROI) (20 x 20 pixels) was drawn in a cardiomyocyte that displayed spontaneous Ca^{2+} transients, and an initial trace of pixel intensity through time was obtained. The plugin then fitted a polynomial 4th order curved baseline to the raw data and divided the pixel intensity value at each time point by the calculated baseline value at each time point. This provided dimensionless data with a baseline level of 1 at points where the original data

was equal to the fitted baseline and >1 when the fluorescence signal had increased (Figure 3.1). This allowed for a direct comparison between tissues obtained from different animals and also corrected for any reduction in fluorescence caused by photobleaching of the dye. For each image series, 2-7 cardiomyocytes were analysed depending on the number of clearly defined cells in the field of view (FOV) that displayed spontaneous Ca^{2+} transients.

The plugin contained an algorithm that distinguished instances where there was an increase or decrease in the fluorescence signal, which accounted for the peaks and troughs. The change in fluorescence for each Ca^{2+} transient was then automatically calculated from the peak fluorescence, providing a value for the amplitude ($\Delta F/F_{min}$). The mean amplitude of the Ca^{2+} transients during the recording period was calculated for each cardiomyocyte. The number of peaks per second was also obtained, which provided a value for the mean frequency of the Ca^{2+} transients in each cardiomyocyte during the recording period.

The settings in the ImageJ plugin could be adjusted to change the way in which the algorithm identified the Ca^{2+} transients. An exclusion threshold was applied so that peaks in the trace that were lower than a specified percentage (approximately 10%) of the maximum peak fluorescence in the recording could be excluded (Figure 3.1, red arrow head). Small peaks occurring within a specified time-scale before and after a Ca^{2+} transient (Figure 3.1, yellow arrow head), and small peaks during the upstroke or downstroke (Figure 3.1, green arrow head) were also excluded from the analysis. Therefore, genuine Ca^{2+} transients could be distinguished from noise in the background fluorescence. The same settings were applied when successive recordings were made using the same ROIs (Figure 3.1).

Sometimes when obtaining successive recordings the tissue moved slightly, either due to contraction, or during the application of a drug or reagent. When this happened the coordinates of an anatomical reference point were used to quantify the shift on a pixel

by pixel basis, and the ROIs were moved accordingly. This was checked visually in successive image series to ensure that the ROIs were in the same cells.

Electrically evoked Ca^{2+} transients were analysed for peak amplitude using the same ImageJ plugin, and the fluo-4 fluorescence was measured in the FOV (40x magnification). All of the electrically evoked Ca^{2+} transients that occurred during the sampling period were used to calculate the mean amplitude. The spontaneous Ca^{2+} transients between those that were evoked were also analysed by placing ROIs in the individual cardiomyocytes. Once fluorescence recordings were obtained in the ROIs, they were compared with a recording from the FOV and the spontaneous Ca^{2+} transients were distinguished from those that were evoked.

To measure the velocity of the spontaneous Ca^{2+} transients that manifested as waves, a line was drawn parallel to the longitudinal axis of the cell, following the trajectory of the waves. A line-scan was then obtained using the "Kymograph" plugin in ImageJ, which creates a 2-dimensional image, in which time is displayed along the y-axis and the Ca^{2+} waves were visible as oblique diagonal lines. The differences in the x and y axes were then used to calculate the change in distance and time respectively, and the wave velocity was calculated as distance/time.

A custom script written in the Python language for the Spyder integrated development environment by Dr Niall MacQuaide (University of Glasgow), was used to determine whether the spontaneous Ca^{2+} transients occurred more synchronously after a specific intervention. This code determined the maximum and minimum intensity of every pixel during an image series. The half maximal pixel intensity was then calculated and a threshold applied so that a binary image series was created, whereby any pixel more intense than this value was white (active) and any pixel less intense than this value was black (inactive). Thus, the spontaneous Ca^{2+} transients were represented as white and inactive tissue as black. A mask was then applied to select the region of tissue that was most in focus and displayed spontaneous Ca^{2+} transients. The code then calculated the percentage of pixels that was active for each frame, in other words calculating the area

of tissue that was displaying spontaneous Ca^{2+} transients at any one time point. This produced a synchronisation index between 0 and 1, whereby a value of 0 represents 0% of the pixels displaying an increase in Ca^{2+} and a value of 1 represents the whole FOV displaying an increase in Ca^{2+} and these values were displayed over time.

3.2.6. Pseudo-linescan images

The spatiotemporal properties of the spontaneous and electrically evoked Ca^{2+} transients were visualised by generating pseudo-linescan images. When a TIFF image was imported into ImageJ, a straight pixel-wide line was applied across the transverse axis of the cardiomyocytes, spanning multiple cells in the FOV. The fluo-4 fluorescence across the line was then displayed over time using the 'reslice' command, which provided a 2-dimensional image where distance was represented horizontally and time vertically (x-t).

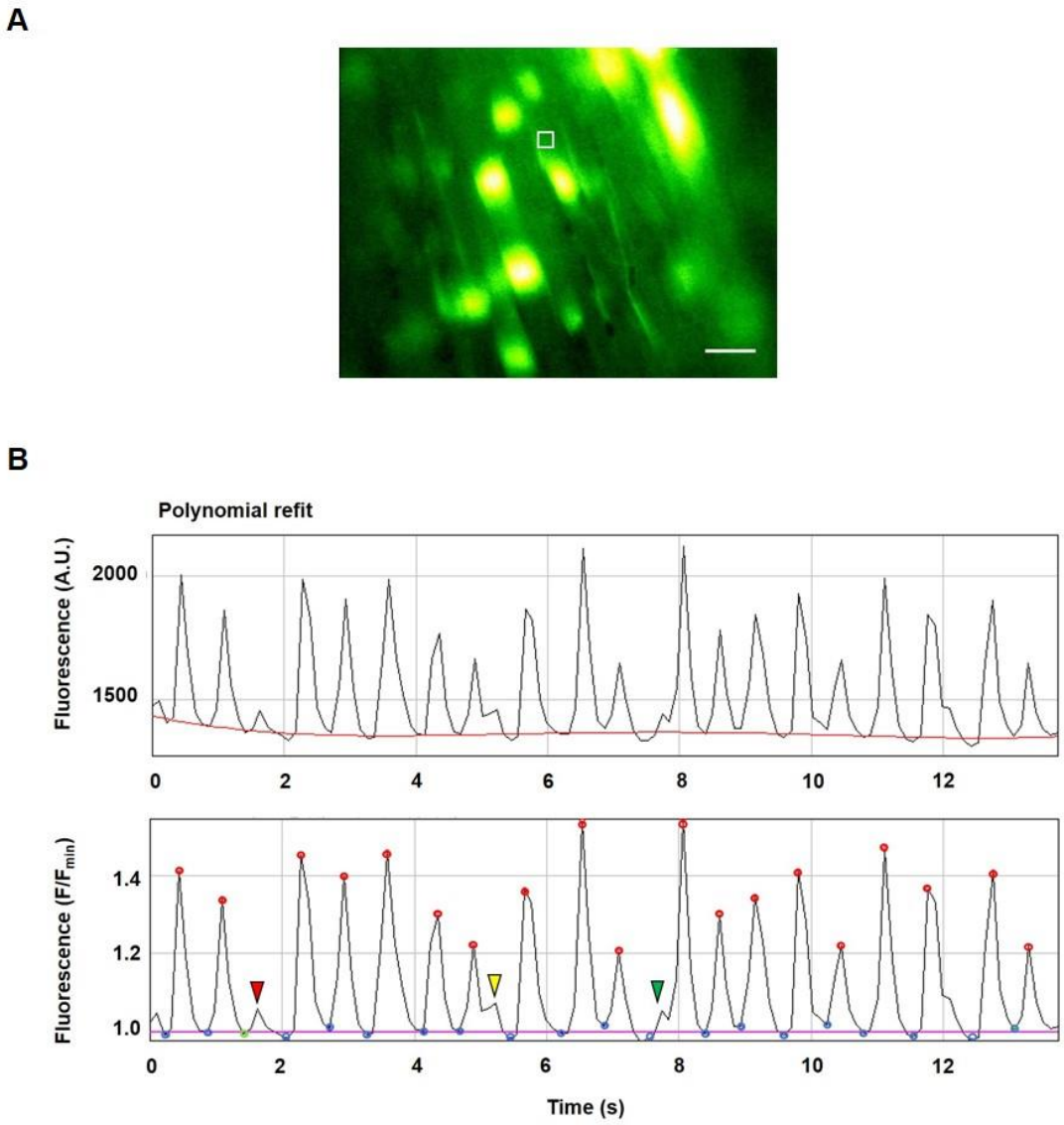

Figure 3.1. ImageJ plugin used to calculate the frequency and amplitude of Ca^{2+} transients in an image series. A. Wide field image of fluo-4 fluorescence, presented in green pseudocolour, in a region of the rat pulmonary vein. The white square is a region of interest (ROI) that was analysed using the custom plugin. Scale bar represents 20 µm. **B.** The raw fluorescence intensity in the ROI, where the red line displays the fitted baseline (upper trace). The lower trace displays the F/F_{min} at each time point. The red circles indicate the peaks and the blue circles indicate troughs in fluorescence, with green circles displaying where the end of a Ca^{2+} transient is different to the beginning of the subsequent one. The pink line displays the baseline normalised to 1. The red arrow head indicates a small Ca^{2+} transient, and the yellow and green arrow heads indicate noise that were excluded from the analysis.

3.2.7. Analysis of the sarcoplasmic reticulum Ca^{2+} content

The magnitude of the caffeine induced Ca^{2+} transient was analysed in ImageJ, where a ROI (20 x 20 pixels; 75 x 75 μm) was placed in the region of tissue where caffeine was initially applied. The minimum fluorescence was quantified as the fluorescence intensity before the application of caffeine, and each fluorescence value was divided by this minimum in order to normalise the data to 1. The peak of the Ca^{2+} transient was identified as the maximum fluorescence value during the recording, and the difference in fluorescence was used to estimate the SR Ca^{2+} content. The rise time of the caffeine induced Ca^{2+} transient was defined as the time from 10 to 90% of the upstroke and was measured using OriginPro (OriginLab Corp., Northampton, Massacheussets). The time to 50% decline in fluorescence was used as a metric to compare the rate of Ca^{2+} removal under the different experimental conditions.

3.2.8. Experimental Protocols

All experiments were performed at room temperature (21-24ºC) unless stated otherwise.

3.2.8.1. Effect of β-adrenergic stimulation on the spontaneous and electrically evoked Ca^{2+} transients

To investigate the effect of β-adrenergic stimulation on the characteristics of the spontaneous Ca^{2+} transients, an initial control recording of fluo-4 fluorescence was obtained in the absence of electrical stimulation. The tissue was then treated with isoprenaline (10 μM) and after a 2 min equilibration period, a second recording was obtained. To investigate the effect of isoprenaline on the electrically evoked Ca^{2+} transients, a control recording was obtained during electrical field stimulation at 1 Hz. The tissue was treated with isoprenaline (10 μM) and following a 2 min equilibration period, during which electrical stimulation was maintained, a subsequent recording was obtained.

3.2.8.2. Effect of increasing the external Ca^{2+} concentration on the spontaneous and electrically evoked Ca^{2+} transients

The same protocol described in 3.2.8.1 was used to examine the effect of increasing the external Ca^{2+} concentration on the spontaneous and electrically evoked Ca^{2+} transients. Between the first and second recordings, the concentration of Ca^{2+} in the physiological salt solution was increased from 2.5 to 4.5 mM. In a separate series of experiments, the protocol was repeated in the presence of both isoprenaline (10 μM) and an increased external Ca^{2+} concentration.

3.2.8.3. Effect of a period of electrical stimulation on the spontaneous Ca^{2+} transients

A region of tissue that both displayed spontaneous Ca^{2+} transients at rest, and also responded to electrical stimulation was located, and a control recording was obtained under unstimulated conditions. The tissue was then electrically stimulated at 1 Hz for 5 s, and the fluo-4 fluorescence was recorded immediately after the cessation of the stimulus. Following a 2 min rest period, the pulmonary vein was electrically stimulated for 5 s at 3 Hz, and a subsequent recording was made in the same region of tissue. The same procedure was repeated after a period of electrical stimulation at 5, 7 and 9 Hz.

The same experiments were repeated in the presence of isoprenaline (10 μM) and/or a high external Ca^{2+} concentration (4.5 mM). The pulmonary vein was treated 2 min prior to the initial recording, which was obtained with no prior electrical stimulation. The characteristics of the spontaneous Ca^{2+} transients (amplitude and frequency) were analysed using ROIs as described in 3.2.5.

3.2.8.4. Estimation of sarcoplasmic reticulum Ca^{2+} content using caffeine

To examine the effect of a period of electrical stimulation on the caffeine induced Ca^{2+} transient, an initial control recording was obtained where caffeine was applied to the pulmonary vein under unstimulated conditions. After a 15 min recovery period, the tissue was stimulated for 5 s at a frequency of 5 Hz, and immediately after termination of the stimulus, caffeine was applied to the same region of tissue.

The effect of increasing the external Ca^{2+} concentration in combination with isoprenaline (10 μM), on the caffeine induced Ca^{2+} transient after a period of electrical stimulation was also investigated. The pulmonary vein was electrically stimulated at 3 Hz for 5 s, and an initial recording was obtained where caffeine was applied immediately after termination of the stimulus. After 13 min, the tissue was treated with isoprenaline (10 μM) and the external Ca^{2+} concentration was increased to 4.5 mM. The preparation was allowed to equilibrate for 2 min, which accounts for a 15 min recovery period from the initial application of caffeine. A subsequent recording was then obtained where caffeine was applied to the same region of tissue after another 5 s period of electrical stimulation at 3 Hz.

3.2.8.5. Effect of noradrenaline on the spontaneous Ca^{2+} transients

The following experiments were conducted at near physiological temperature (37 °C), the reasons for which will be explained in the results section In order to analyse the effect of noradrenaline on the characteristics of the spontaneous Ca^{2+} transients, a control recording of the fluo-4 fluorescence was obtained in the absence of electrical stimulation. The tissue was then treated with noradrenaline (10 μM), and after a 2 min equilibration period, a subsequent recording was obtained

3.2.9. Statistical Analysis

Data are expressed as the mean ± standard error of the mean (s.e.m.), and n refers to the number of cardiomyocytes from the number of pulmonary veins from the number of rats. When performing statistical analyses, the frequency, amplitude and wave velocity data for all the cardiomyocytes (i.e. ROIs) that were analysed were compared. When comparing two groups (i.e. before and after a treatment), Student's paired *t*-test was used. Student's unpaired *t*-tests were also used to compare the properties of the spontaneous Ca^{2+} transients at room temperature and at 37 °C. Comparison of the frequency, amplitude and wave velocity of the spontaneous Ca^{2+} transients following electrical stimulation at increasing frequencies (3.2.8.3) was performed via a repeated-measures analysis of variance (ANOVA) followed by Dunnett's multiple comparison test. The amplitude and frequency of the subsequent spontaneous Ca^{2+} transients after electrical stimulation at 1-9 Hz was compared with the initial (control) recording, which was obtained when the pulmonary vein had been unstimulated for 2 min. Finally, student's paired t-tests were used to compare the Ca^{2+} transient synchronisation between the first and last 2 s of the recordings. Statistical significance was considered when $P<0.05$.

3.2.10. Chemicals and drugs

Fluo-4 AM (Invitrogen™, Glasgow, UK) was prepared at a stock concentrations of 1 mM in DMSO, and stored at -20 °C. Isoprenaline and noradrenaline were obtained from Sigma-Aldrich and prepared at stock concentrations of 1 mM in physiological salt solution on the day of experimentation. Caffeine was also obtained from Sigma and was prepared at a stock concentration of 100 mM in physiological salt solution on the day of experimentation. All other reagents (NaCl, KCl, $MgCl_2$, $CaCl_2$, NaOH, $MgSO_4$, $NaHCO_3$, KH_2PO_4 and glucose) were obtained from BDH Laboratories, and the physiological salt solution was prepared on the morning of the experiments.

3.3. Results

3.3.1. Spontaneous Ca^{2+} transients in pulmonary vein cardiomyocytes

When the pulmonary vein was isolated from the rat and loaded with fluo-4, spontaneous Ca^{2+} transients were observed in the cardiomyocytes in the absence of electrical stimulation. Not every cell in a preparation displayed spontaneous Ca^{2+} transients, though the cells that did were usually widespread throughout the pulmonary vein, including the intrapulmonary regions, and were observed in almost every tissue studied.

Figure 3.2A shows a typical region of the pulmonary vein, displaying spontaneous Ca^{2+} transients apparent as waves propagating along the longitudinal axis of the cells. Analysis of the fluorescence intensity in the 3 ROIs, shows that the frequency of spontaneous Ca^{2+} transients was variable in the individual cardiomyocytes. Furthermore, the pseudo-linescan image shows that the Ca^{2+} transients were asynchronous in neighbouring cardiomyocytes, as the peaks in fluorescence occurred at different time points (Figure 3.2B). The initial figures (3.3-3.8) show the different types of Ca^{2+} transients that were observed in the pulmonary vein. During the analysis, the different types of Ca^{2+} transients were not discriminated.

Overall, there was no consistent pattern in the propagation of the spontaneous Ca^{2+} transients, as waves in cardiomyocytes that were side-to-side propagated in the same (Figure 3.3), or opposite directions (Figure 3.4). Occasionally, a localised rise in intracellular Ca^{2+} occurred in a cardiomyocyte, which would then produce two waves that propagated in opposite directions (Figure 3.5). In other cases, two separate waves propagated towards each other and extinguished upon collision (Figure 3.6). Sometimes there would be a localised rise in Ca^{2+} in a cardiomyocyte that did not propagate (Figure 3.7), and other times a Ca^{2+} wave would propagate in a circular as opposed to linear manner (Figure 3.8). The spontaneous Ca^{2+} transients were associated with slight movement in the cardiomyocytes; however, because this occurred asynchronously, it did not result in co-ordinated contraction of the tissue.

In the time matched control recordings, the mean frequency of spontaneous Ca^{2+} transients in the pulmonary vein was 1.33 ± 0.08 Hz, and this was not significantly different at 1.31 ± 0.09 Hz when a second recording was obtained after a 2 min break in the recording (Figure 3.9A and B). Similarly, the mean amplitude was 0.20 ± 0.02 ($\Delta F/F_{min}$), and after 2 min was 0.19 ± 0.02 ($\Delta F/F_{min}$) (n = 31 cardiomyocytes from 7 PVs from 7 rats, n.s.) (Figure 3.9A and C). The mean velocity of the spontaneous Ca^{2+} waves under control conditions was 118.0 ± 5.57 µm/s and this was not significantly different at 111.8 ± 5.2 µm/s, 2 min later (n = 30 cardiomyocytes from 9 PVs from 7 rats, n.s.) (Figure 3.9A and D).

3.3.2. Electrically evoked Ca^{2+} transients in pulmonary vein cardiomyocytes

Electrical field stimulation evoked a synchronous rise in intracellular Ca^{2+} in neighbouring cardiomyocytes. Notably, the electrically evoked Ca^{2+} transients occurred in discrete regions, surrounded by cardiomyocytes that did not respond to the electrical stimulus. The electrically evoked Ca^{2+} transients ranged in size from a region of 2-5 cardiomyocytes to large regions of tissue approximating 500 x 500 µm (Figure 3.10). It was possible to electrically evoke Ca^{2+} transients in cardiomyocytes that also displayed spontaneous activity, as well as in cells that did not display spontaneous Ca^{2+} transients under resting conditions (Figures 3.10 and 3.11). Figure 3.10 shows the fluo-4 fluorescence in the pulmonary vein, imaged at low magnification, during electrical stimulation. Note that asynchronous spontaneous Ca^{2+} transients are visible before the electrically evoked Ca^{2+} transient. The pseudo-linescan image confirms that the electrically evoked Ca^{2+} transients were synchronous in the region of tissue, as they occurred at the same time in all of the cardiomyocytes across the white line (Figure 3.10).

When imaged at 40x, spontaneous Ca^{2+} transients could be observed in the individual cardiomyocytes. It is clear from the pseudo-linescan image that electrical stimulation evoked a synchronous rise in Ca^{2+} in the neighbouring cardiomyocytes, regardless of

whether or not spontaneous Ca^{2+} transients were present between those that were evoked. This can be seen more clearly when the fluo-4 fluorescence was analysed in the individual cardiomyocytes using ROIs. In ROIs 2 and 3, spontaneous Ca^{2+} transients were present between those that were electrically evoked at 1 Hz. However, the cardiomyocytes still consistently responded with Ca^{2+} transients, albeit of a lower amplitude, according to the rate of electrical stimulation (Figure 3.11).

3.3.3. Caffeine induced Ca^{2+} transient

The rapid application of caffeine (100 mM) induced an increase in Ca^{2+} concentration in the proximity of the glass microelectrode, and the Ca^{2+} concentration continued to increase as the caffeine solution diffused across the tissue (Figure 3.12A). In the time matched control recordings, the amplitude of the caffeine induced Ca^{2+} transient was 0.16 ± 0.03 ($\Delta F/F_{min}$), and was not significantly different at 0.15 ± 0.05 ($\Delta F/F_{min}$) when a subsequent recording was made after a 15 min break in the recording (Figure 3.12B and C). The mean time for the fluo-4 fluorescence to rise to peak was 0.59 ± 0.25 s and was also not significantly different at 0.43 ± 0.11 after 15 min (Figure 3.12B and D). The time for caffeine induced Ca^{2+} transient to decline by 50% from the peak was 6.37 ± 1.16 s in the first recording and was shorter during the second recording, being 5.16 ± 0.62 s; however, this decrease was not statistically significant (n = 3 PVs from 3 rats, n.s.) (Figure 3.12B and E).

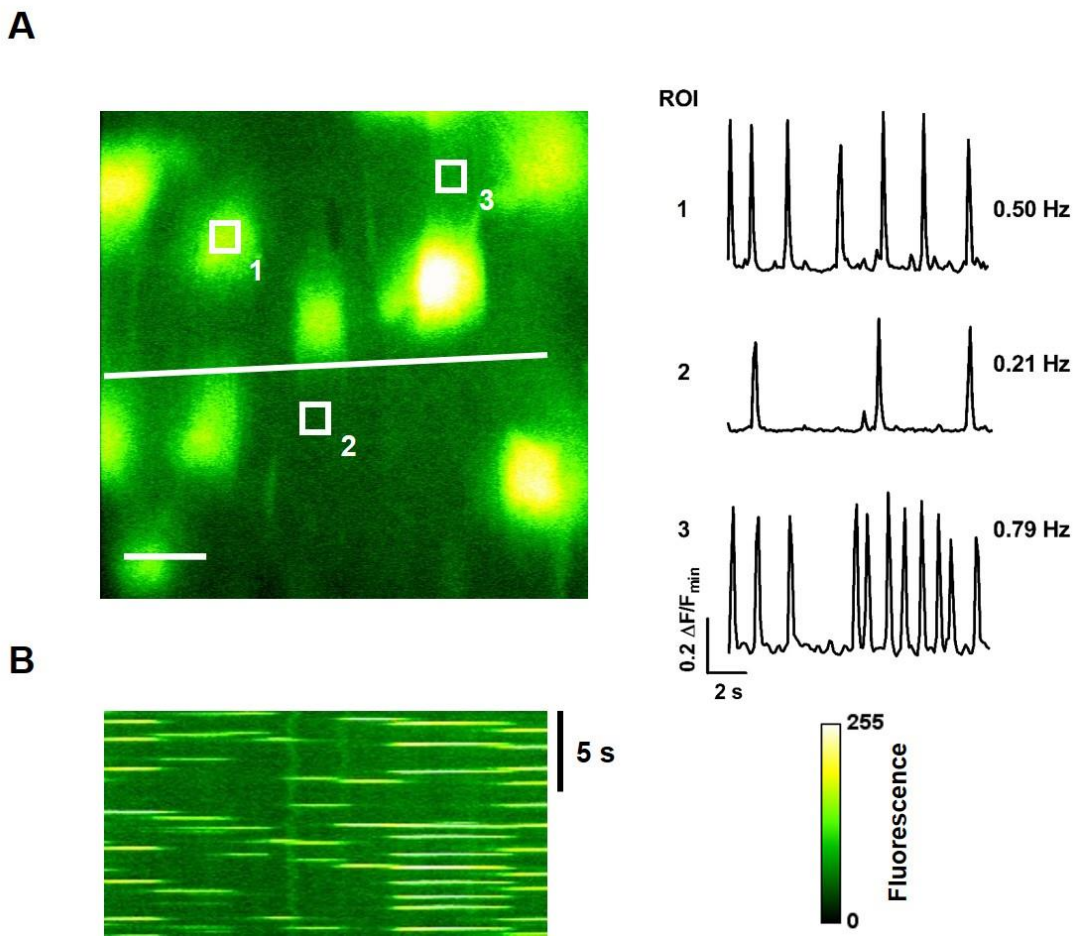

Figure 3.2. Spontaneous Ca^{2+} transients in rat pulmonary vein cardiomyocytes. **A.** Wide field image of fluo-4 fluorescence in the pulmonary vein, which was imaged at 40x magnification and displayed in green pseudocolour. The traces represent the fluorescence intensity in the 3 regions of interest (ROI), depicted by the white boxes. **B.** Pseudo-linescan displaying the fluo-4 fluorescence over time in the section of tissue indicated by the white line in **A.** Scale bar represents 20 µm.

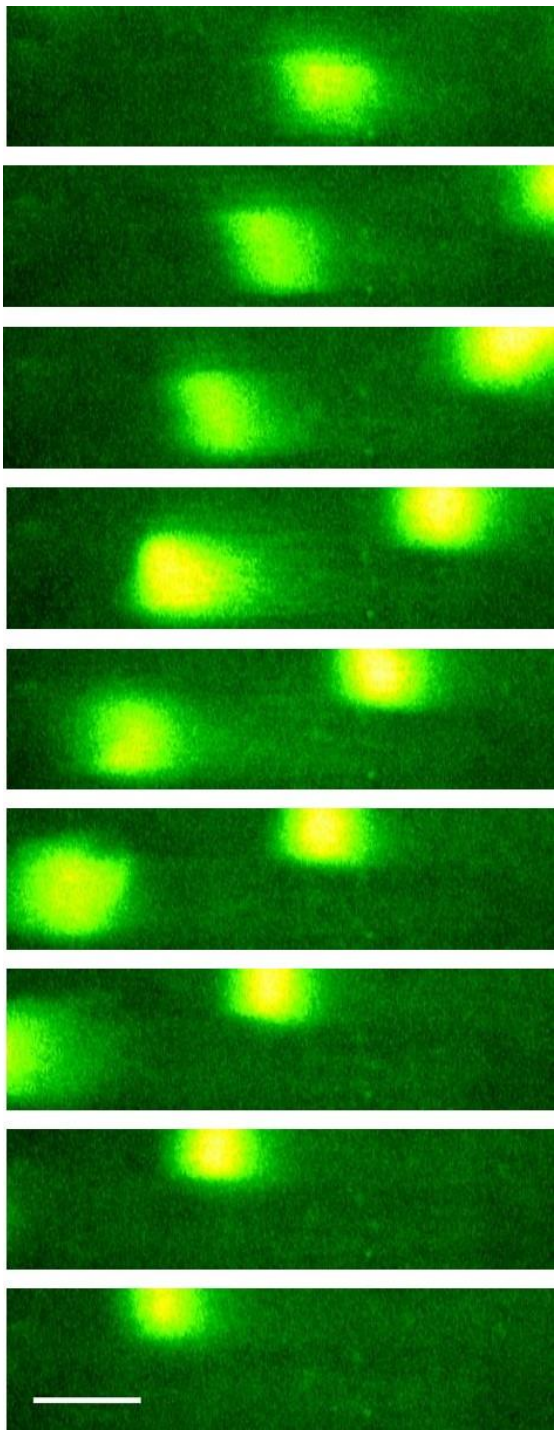

Figure 3.3. Propagation of Ca^{2+} waves in the same direction in adjacent cardiomyocytes. Sequential images, obtained every 109 ms, of fluo-4 fluorescence in the pulmonary vein. Two Ca^{2+} waves in adjacent cardiomyocytes can be observed propagating in the same direction along the longitudinal axis of the cardiomyocytes. Scale bar represents 20 μm.

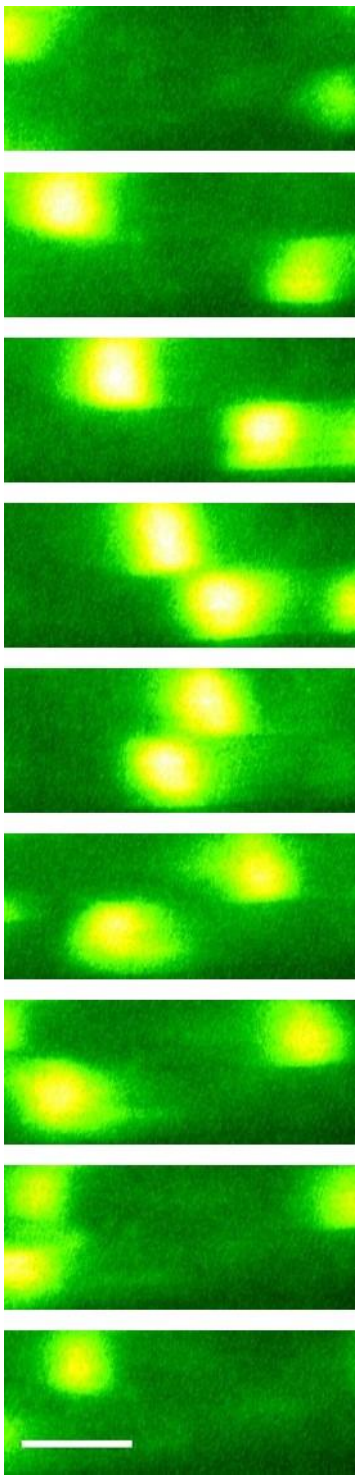

Figure 3.4. Propagation of Ca^{2+} waves in opposite directions in adjacent cardiomyocytes. Sequential images, obtained every 109 ms, of fluo-4 fluorescence in the pulmonary vein. Two Ca^{2+} waves in adjacent cardiomyocytes can be observed propagating in opposite directions along the longitudinal axis of the cardiomyocytes. Scale bar represents 20 µm.

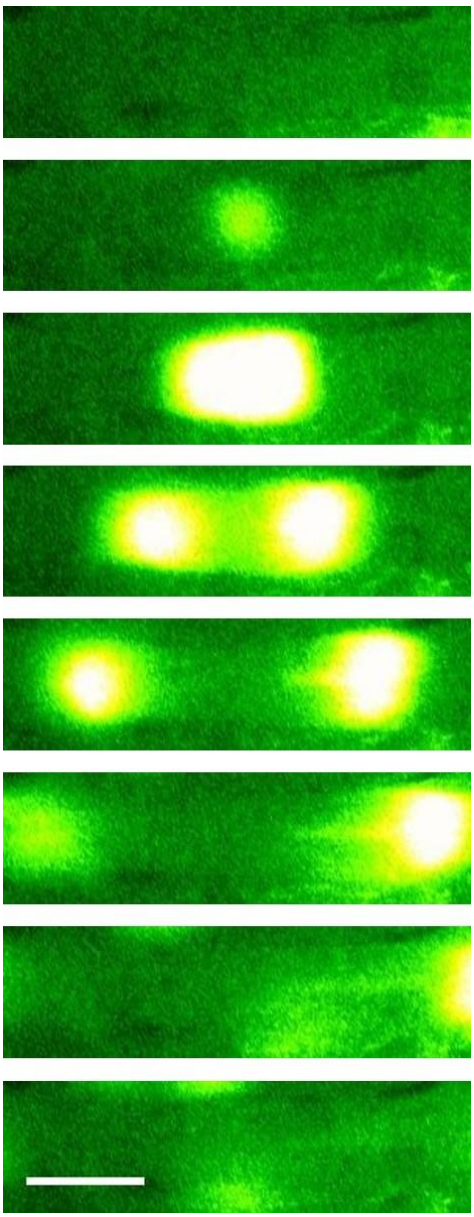

Figure 3.5. Initiation and propagation of Ca^{2+} waves from a single site. Sequential images, obtained every 109 ms, of fluo-4 fluorescence in the pulmonary vein. A localised rise in intracellular Ca^{2+} can be observed before splitting into two Ca^{2+} waves that propagated in opposite directions along the longitudinal axis of the cardiomyocyte. Scale bar represents 20 μm.

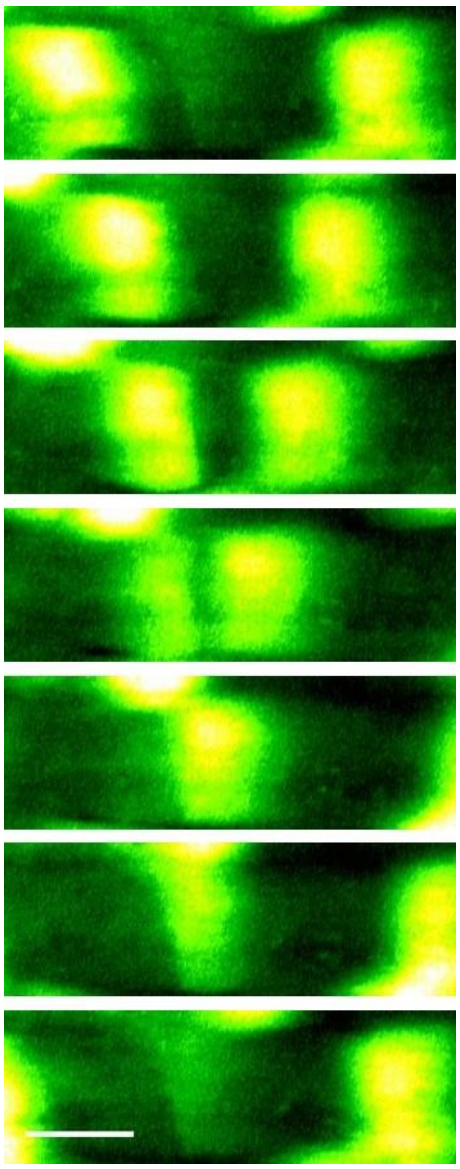

Figure 3.6. Collision of two Ca^{2+} waves propagating in opposite directions. Sequential images, obtained every 109 ms, of fluo-4 fluorescence in the pulmonary vein. Two Ca^{2+} waves can be observed propagating in opposite directions, which extinguish after colliding. Scale bar represents 20 µm.

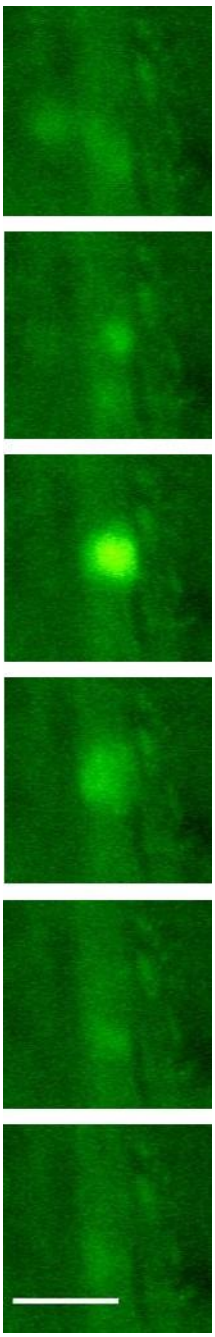

Figure 3.7. Non-propagating Ca^{2+} transient. Sequential images, obtained every 109 ms, of fluo-4 fluorescence in the pulmonary vein. A localised rise in intracellular Ca^{2+} that diminishes without propagating as a wave can be observed. Scale bar represents 20 µm.

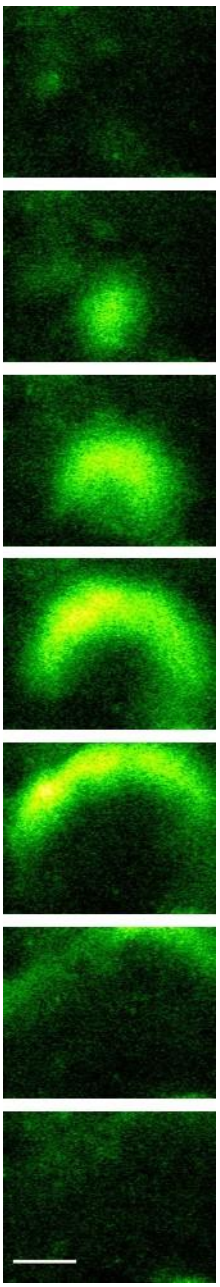

Figure 3.8. Circularly propagating Ca^{2+} wave. Sequential images, obtained every 109 ms, of fluo-4 fluorescence in the pulmonary vein. A rise in intracellular Ca^{2+} which propagates as a wave in a circular manner, as opposed to along the longitudinal axis. Scale bar represents 20 μm.

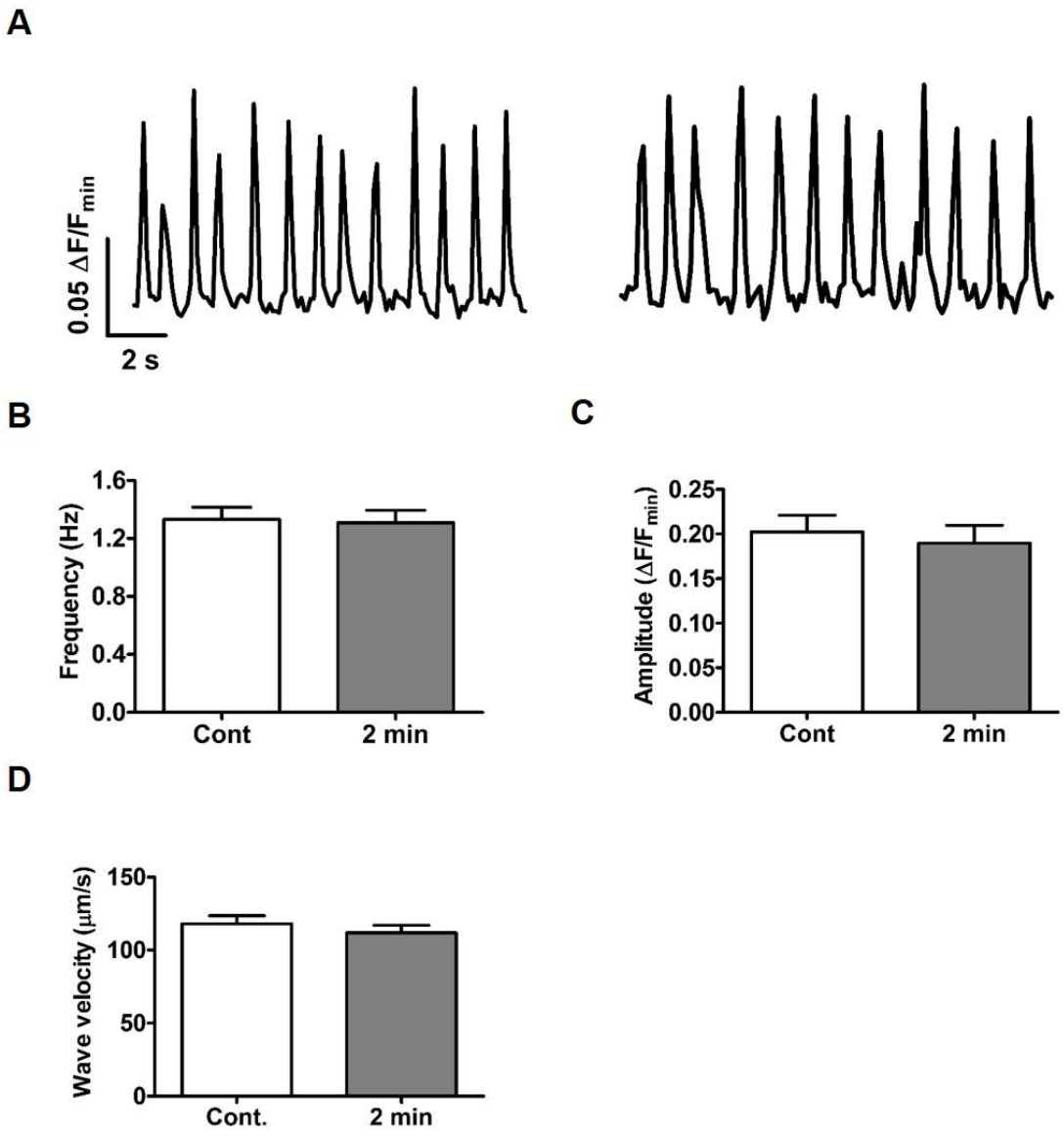

Figure 3.9. Time matched control recordings of spontaneous Ca^{2+} transients in pulmonary vein cardiomyocytes. A. Representative recordings of fluo-4 fluorescence in a cardiomyocyte in the pulmonary vein under control conditions and in the same cell following a 2 min break in the recording. The mean frequency **(B)** and amplitude **(C)** of the spontaneous Ca^{2+} transients and the Ca^{2+} wave velocity **(D)**. For the frequency and amplitude data, n = 31 cardiomyocytes from 7 PVs from 7 rats and for the wave velocity, n = 30 cardiomyocytes from 9 PVs from 7 rats.

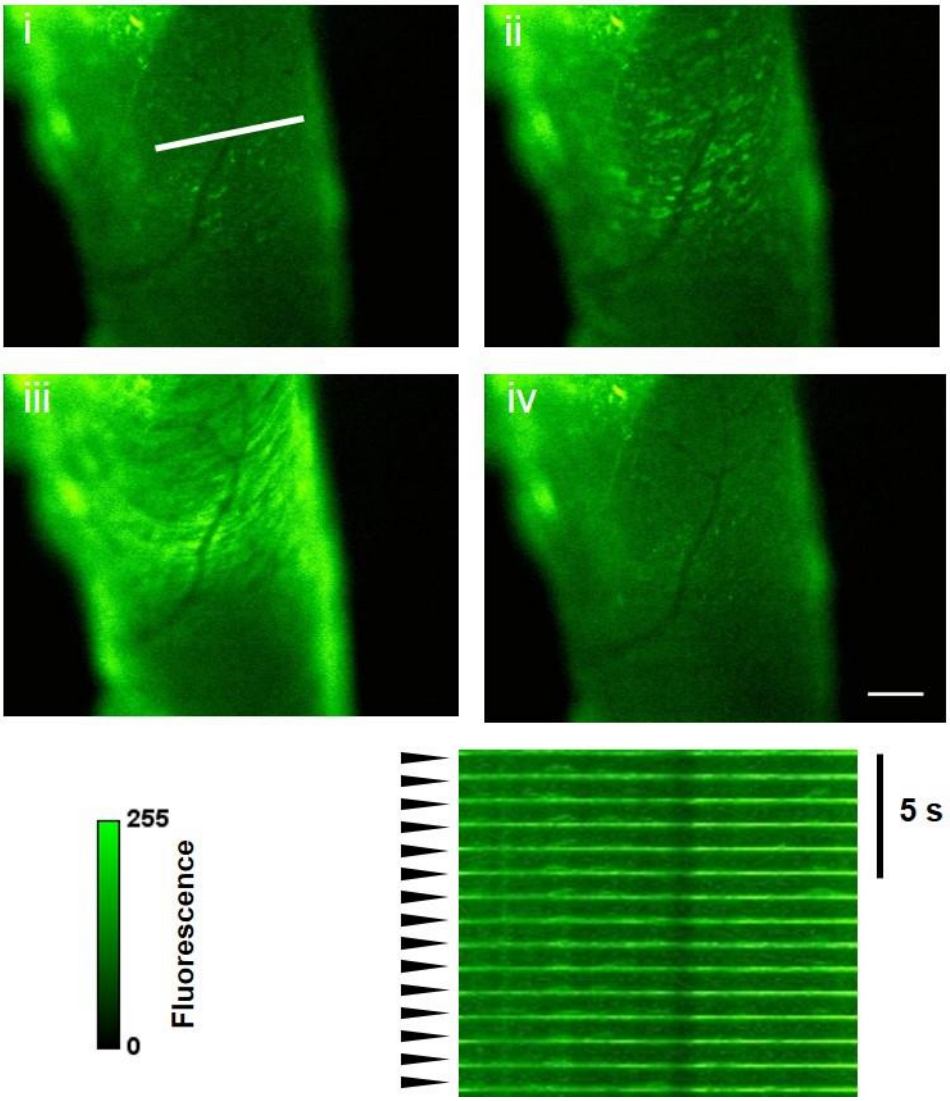

Figure 3.10. Electrically evoked Ca^{2+} transients in the pulmonary vein. A. Images presented every 218 ms (i-iv) of fluo-4 fluorescence in the pulmonary vein at 5x magnification when electrically stimulated. The image appears slightly out of focus in iii due to the contraction of the vein. Scale bar represents 100 µm. The pseudo-linescan image displays the fluo-4 fluorescence over a 14 s period in the section of tissue indicated by the white line in i. The arrow heads indicate the electrical stimulus, applied at 1 Hz.

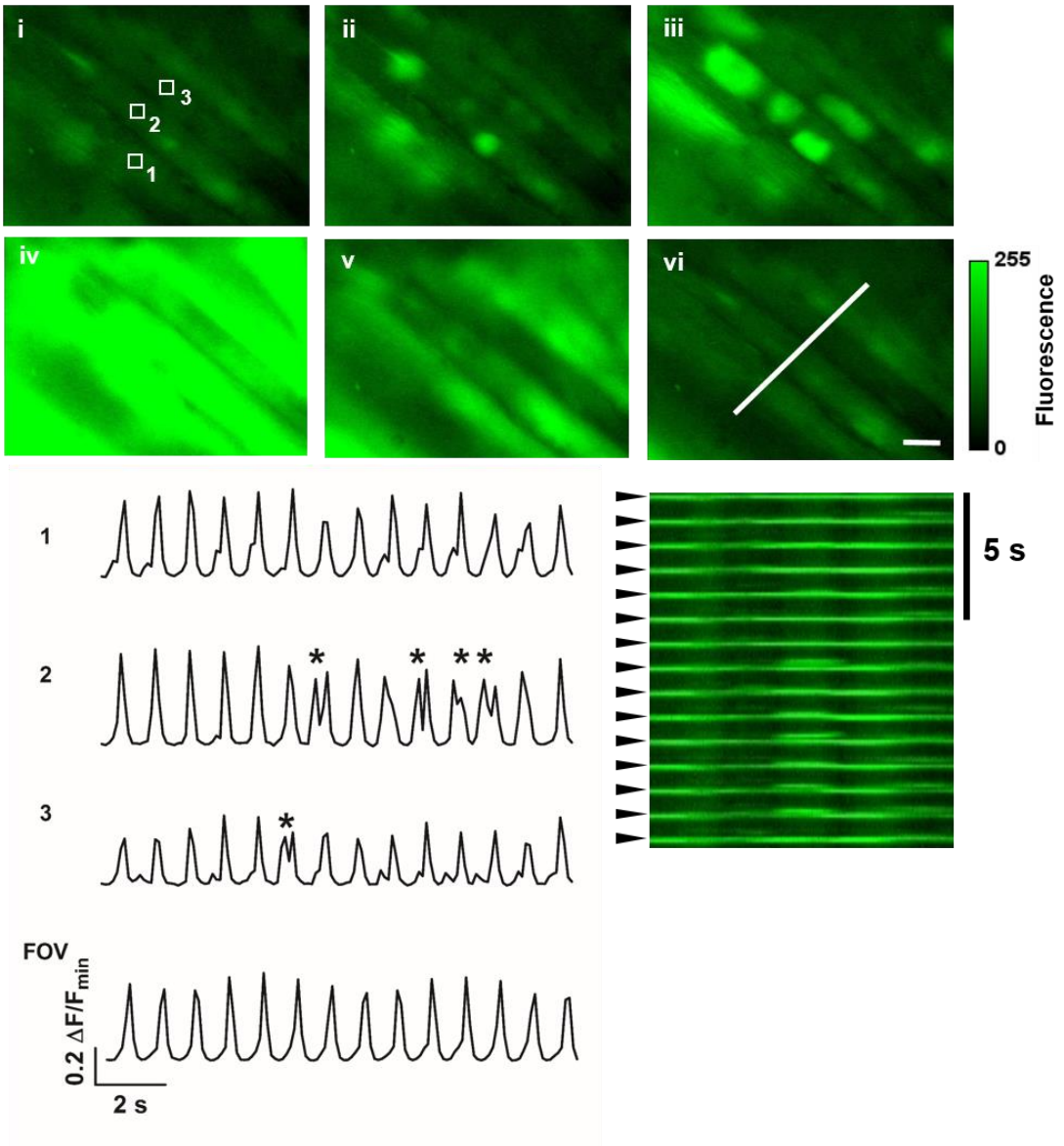

Figure 3.11. Electrically evoked Ca^{2+} transients in the individual pulmonary vein cardiomyocytes. Sequential images (i-vi), obtained every 109 ms, displaying fluo-4 fluorescence in the pulmonary vein at 40x magnification, during electrical stimulation. Images are presented in green pseudocolour. Scale bar represents 20 µm. The fluo-4 fluorescence in the FOV is also displayed. Recordings of the fluo-4 fluorescence in the ROIs indicated in **(i)**. Note the spontaneous Ca^{2+} transients in ROIs 2 and 3, which are indicated by asterisks. The pseudo-linescan displays the fluo-4 fluorescence over a 14 s recording period in the section of tissue indicated by the white line in **(vi)**. The Arrow heads indicate the electrical stimulus applied at 1 Hz.

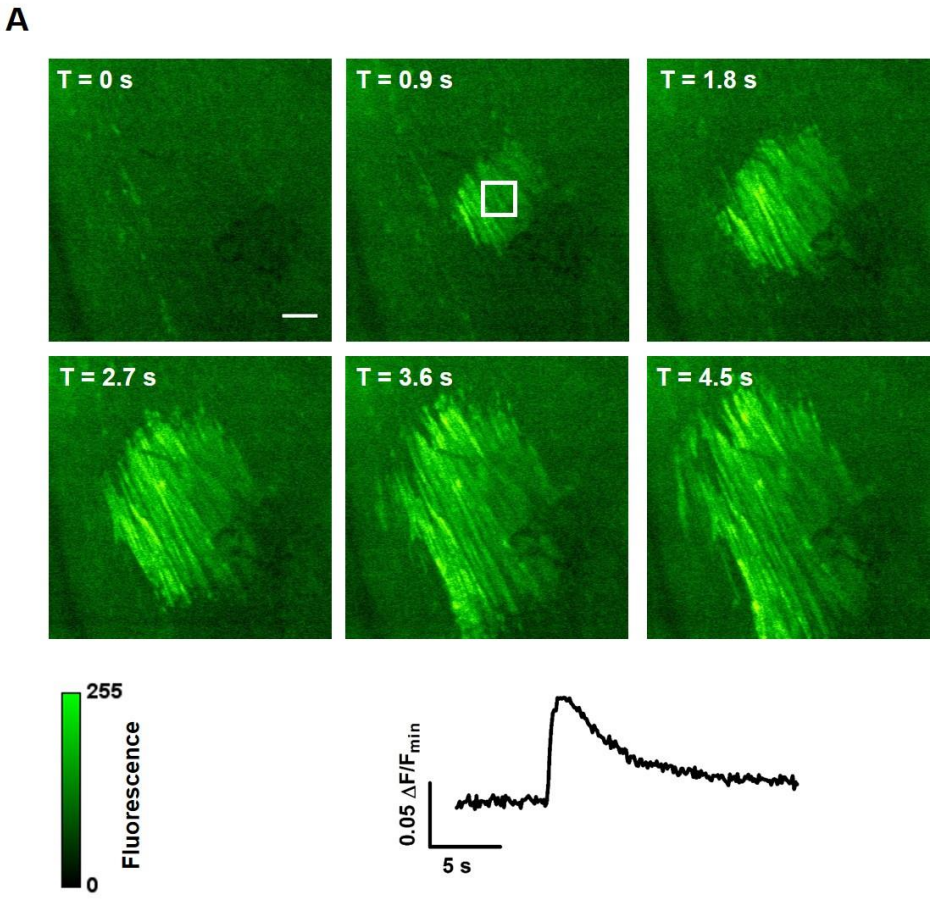

Figure 3.12. Caffeine induced Ca^{2+} transient in the pulmonary vein A. Images of fluo-4 fluorescence in a region of the pulmonary vein during the application of caffeine (100 mM). Images are displayed every 900 ms and are presented in green pseudocolour. Magnification is 5x and the scale bar represents 100 μm. The representative recording displays the fluor-4 fluorescence in the ROI (20 x 20 pixels) indicated by the white box.

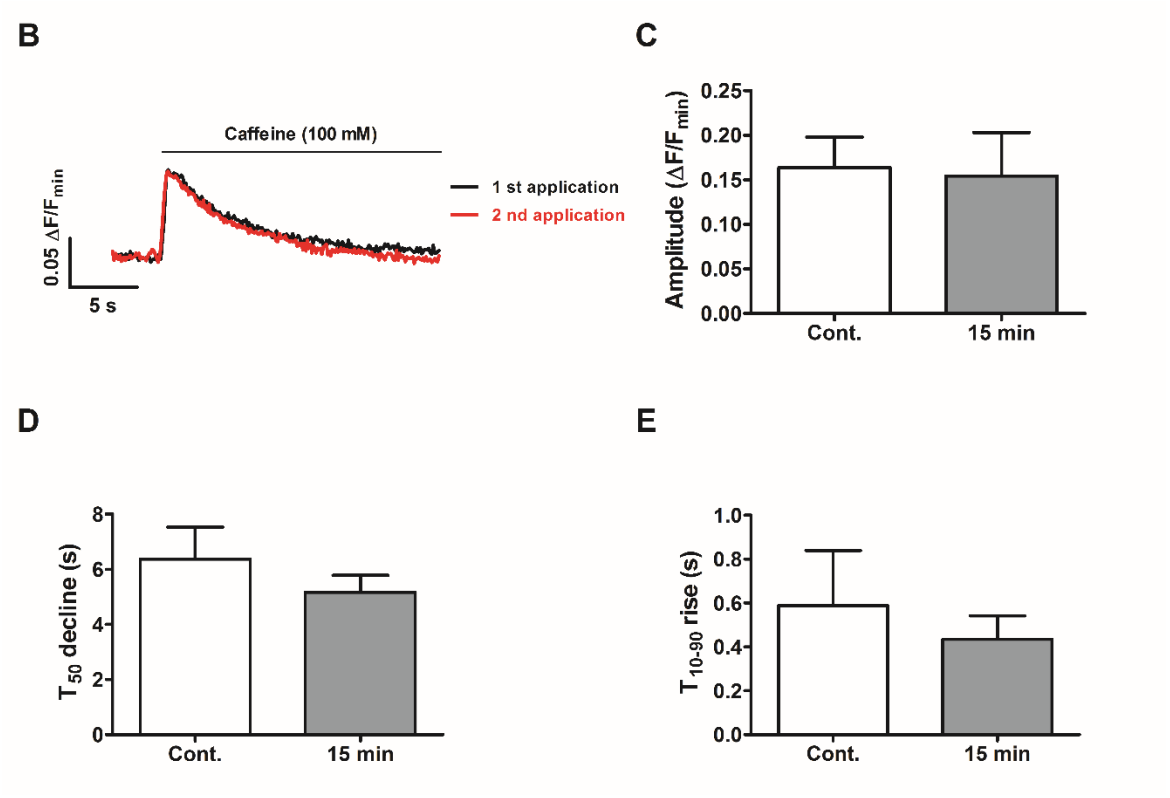

Figure 3.12. (cont.). B. Representative recordings of fluo-4 fluorescence during an initial application of caffeine (100 mM) (black), and during a second application in the same region of tissue after a 15 min recovery period (red). **C.** The mean amplitude of the caffeine induced Ca^{2+} transient during the first and the second application. **D.** The mean rise time (10 to 90%) of the caffeine induced Ca^{2+} transient. **E.** Mean time for the Ca^{2+} transient to decline by 50%. Data represent mean ± s.e.m and n = 3 PVs from 3 rats.

3.3.4. Effect of a period of electrical stimulation on the subsequent spontaneous Ca^{2+} transients

Following a period of electrical stimulation at 3 Hz or greater, it was apparent that the spontaneous Ca^{2+} transients re-emerged at an increased frequency. This can be seen in the pseudo-linescan images and representative recordings, which compare a control tissue with no prior electrical stimulation, to the same region of tissue immediately after a period of stimulation at 1-9 Hz (Figure 3.13A).

This effect was dependent on the rate of prior electrical stimulation, as the frequency of the spontaneous Ca^{2+} transients was greater after a period of electrical stimulation at higher frequencies (5 to 9 Hz). There was a significant increase in the frequency of spontaneous Ca^{2+} transients from 0.45 ± 0.06 Hz in the control, to 0.59 ± 0.05 Hz after electrical stimulation at 3 Hz ($P<0.001$ *vs.* no prior E.S.).The frequency of the spontaneous Ca^{2+} transients was increased to 0.65 ± 0.05 Hz after stimulation at 5 Hz. However, there was no additional increase after electrical stimulation at 7 Hz and 9 Hz, where the frequency of spontaneous Ca^{2+} transients was 0.64 ± 0.05 Hz and 0.65 ± 0.06 Hz respectively (n = 26 cardiomyocytes from 6 PVs from 6 rats) (Figure 3.13B).

Despite causing an increase in the frequency, a period of electrical stimulation had no effect on the amplitude of the subsequent spontaneous Ca^{2+} transients. The mean Ca^{2+} transient amplitude in the control recordings was 0.26 ± 0.02 ($\Delta F/F_{min}$) and was not significantly different after a period of electrical stimulation at 1-9 Hz (n = 26 cardiomyocytes from 6 PVs from 6 rats, n.s.) (Figure. 3.13C).

The mean velocity of the spontaneous Ca^{2+} transients was increased from 95.62 ± 3.87 µm/s under control conditions, to 120.2 ± 13.15 µm/s after electrical stimulation at 1 Hz. After a period of electrical stimulation at 3 Hz, the mean wave velocity was 114.2 ± 9.76 µm/s. However, neither increase was statistically significant. The wave velocity was significantly increased to 127 ± 10.31 µm/s following a period of electrical

stimulation at 5 Hz ($P<0.05$ vs. no prior E.S.). However, after stimulation at 7 and 9 Hz, the wave velocity was 115 ± 8.98 µm/s and 115.6 ± 6.69 µm/s, which was not significantly greater than with no prior electrical stimulation (n = 21 cardiomyocytes from 7 PVs from 7 rats) (Figure 3.13D).

In order to determine if the spontaneous Ca^{2+} transients occurred more synchronously following a period of electrical stimulation, the percentage of active tissue was analysed for every time-frame to provide a synchronisation index between 0 and 1. It was apparent during the analysis that the Ca^{2+} transient synchronisation was increased after a period of electrical stimulation; however this effect was transient with the synchronisation returning to control levels during the time course of the recording (Figure 3.13E). Therefore the data has been presented as the mean synchronisation index during the first and last 2 s of the recordings. In the control recordings with no electrical stimulation the mean synchronisation was 0.13 ± 0.02 in the first 2 s and this was not significantly different in the last 2 s, being 0.11 ± 0.01. After a period of electrical stimulation at 1 Hz, the mean synchronisation was 0.17 ± 0.03 in the first and 0.11 ± 0.02 in the last 2 s; however, this was not a statistically significant difference. Following electrical stimulation at 3 Hz, the mean synchronisation was significantly greater in the first 2 s, being 0.23 ± 0.04 compared to 0.08 ± 0.01 in the last 2 s ($P<0.001$). The mean synchronisation remained significantly greater in the first 2 s after a period of electrical stimulation at 5, 7 and 9 Hz; being, 0.23 ± 0.04, 0.25 ± 0.05, 0.24 ± 0.05 respectively in the first 2 s and 0.09 ± 0.01, 0.09 ± 0.01 0.09 ± 0.02 respectively in the last 2 s (Figure 3.13F).

Caffeine was used to investigate if the increase in the frequency of the spontaneous Ca^{2+} transients was caused by an increased SR Ca^{2+} content. With no prior electrical stimulation, the mean magnitude of the caffeine induced Ca^{2+} transient was 0.12 ± 0.01 ($\Delta F/F_{min}$), and remained the same at 0.12 ± 0.02 ($\Delta F/F_{min}$) immediately following a period of electrical stimulation at 5 Hz (Figure 3.14A and B). The rise time was also not significantly changed, being 0.72 ± 0.18 s during the initial recordings and 0.69 ± 0.21 s after electrical stimulation at 5 Hz (Figure 3.14A and C). Similarly, the time to

50% decline was 6.84 ± 1.9 s in the control recordings and was not significantly changed at 5.92 ± 1.43 s after a period of electrical stimulation at 5 Hz (n = 4 PVs from 4 rats, n.s) (Figure 3.14A and D).

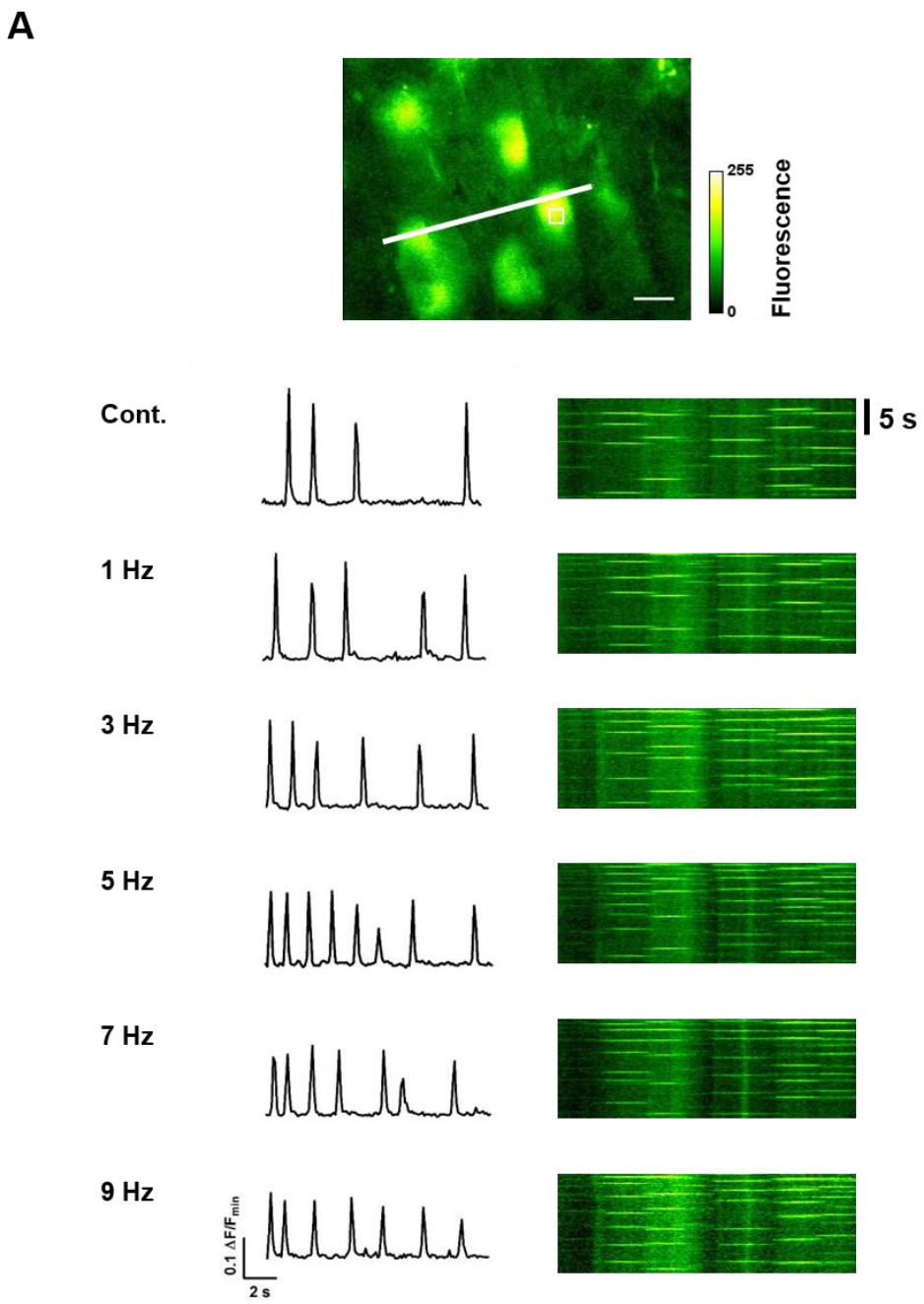

Figure 3.13. The effect of a period of electrical stimulation on the subsequent spontaneous Ca^{2+} transients in the pulmonary vein. A. Wide field image depicting the region of interest that was used to produce the fluorescence vs. time records and the while line used to generate the pseudo-linescans that are shown below. Images were obtained during a control recording with no prior electrical stimulation, and immediately following termination of a period of electrical stimulation at 1-9 Hz. Scale bar represents 20 μm.

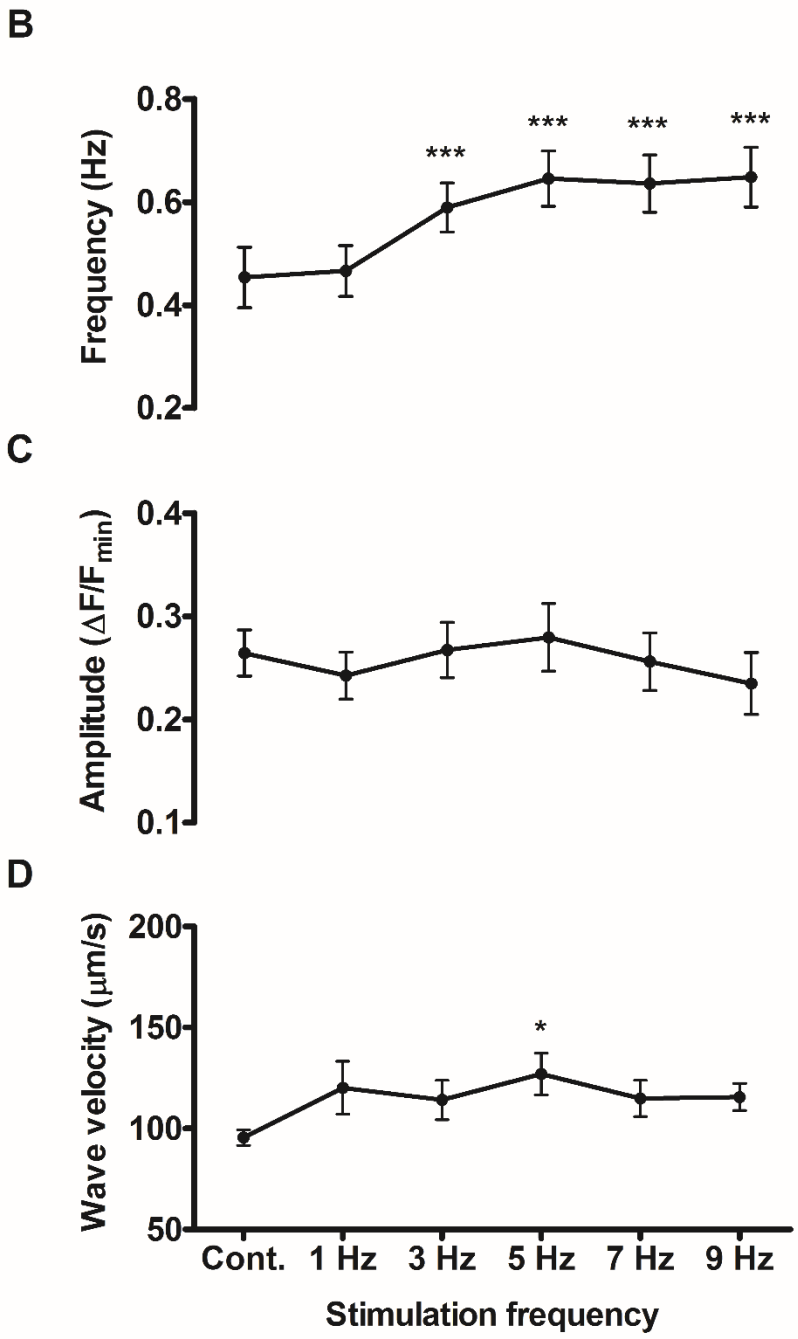

Figure 3.13. (cont.). The mean frequency **(B)** and amplitude **(C)** of the spontaneous Ca^{2+} transients and velocity of Ca^{2+} waves **(D)** in the control recordings and immediately following electrical stimulation at 1-9 Hz. Data represent mean ± s.e.m., $^{*}P<0.05$ *vs*. Cont. $^{***}P<0.001$ *vs*. Cont. n = 26 cardiomyocytes from 6 PVs from 6 rats for the frequency and amplitude and n = 21 cardiomyocytes from 7 PVs from 7 rats for wave velocity.

E

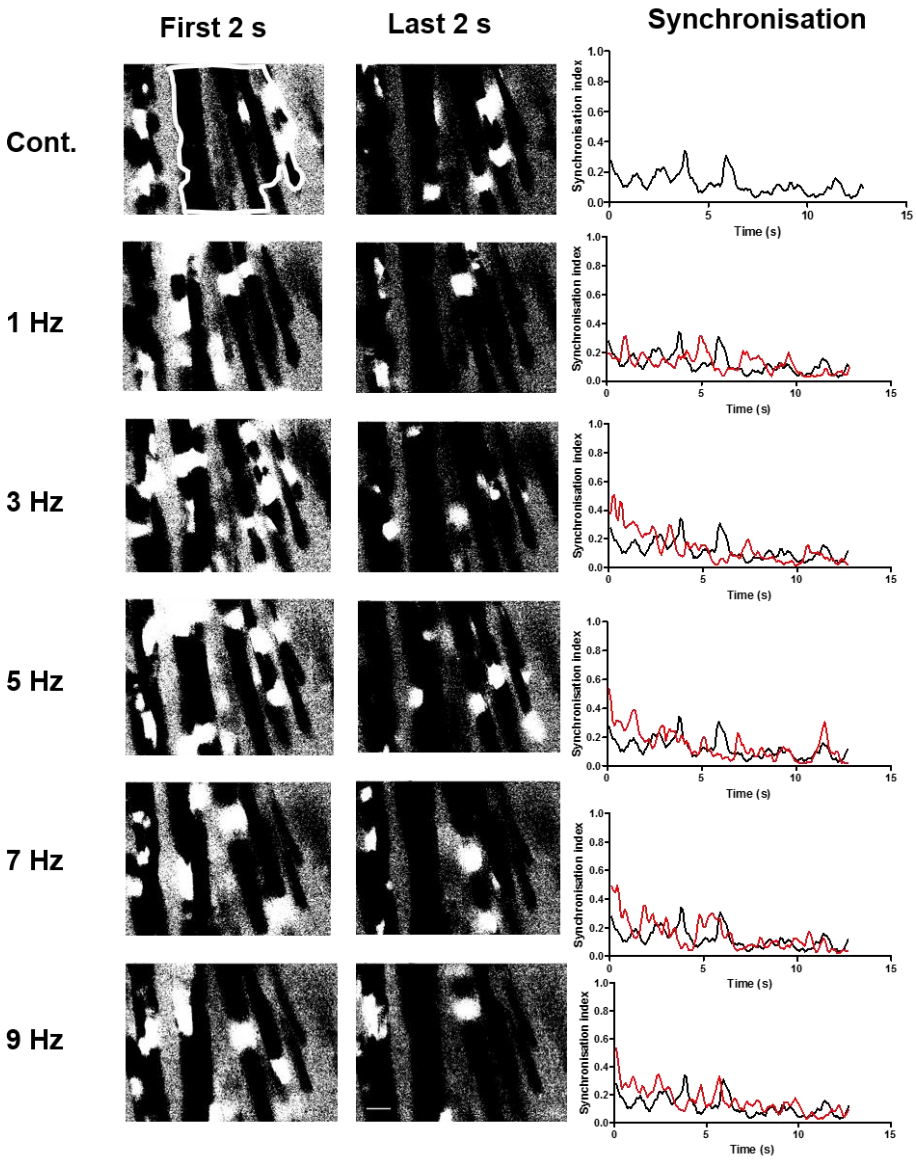

Figure 3.13. (cont.). E. Representative analysis of spontaneous Ca^{2+} transient synchronisation in a control recording with no prior electrical stimulation, and immediately following termination of a period of electrical stimulation at 1-9 Hz. The wide-field images are threshold images displaying pixels that have a greater intensity than half maximum as white. The mask used for the analysis is shown in white in the top left panel. The recordings on the right represent the synchronisation index for each frame over time in the control recording (black) and after a period of E.S. at 1-9 Hz (red). Scale bar represents 10 µm.

F

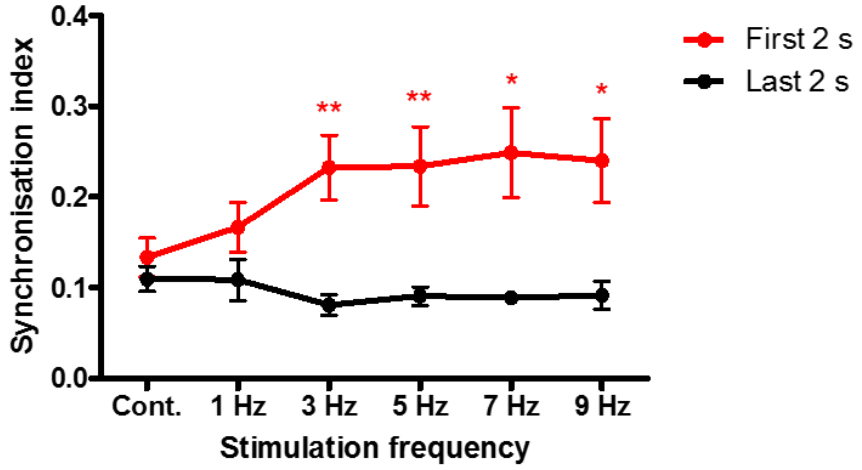

Figure 3.13. (cont.). F. The mean synchronisation during the first 2 s and last 2 s of the recording period in the control recordings with no prior electrical stimulation and immediately following a period of E.S. at 1-9 Hz. Date represent mean ± s.e.m. $^{*}P<0.05$ and $^{**}P<0.01$; first 2 s vs. last 2 s. n = 6 PVs from 6 rats.

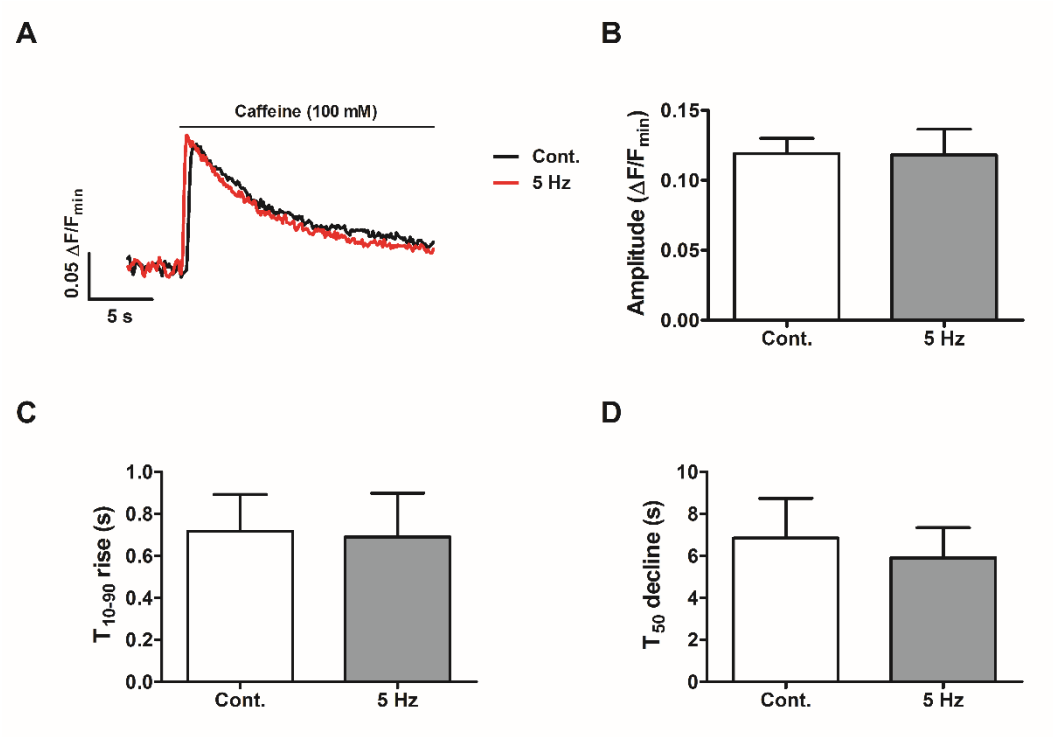

Figure 3.14. The effect a period of electrical stimulation on the caffeine induced Ca^{2+} transient. A. Representative recordings of fluo-4 fluorescence in a region of the pulmonary vein during the application of caffeine (100 mM) in a control recording with no prior electrical stimulation (black), and in the same region immediately after electrical stimulation at 5 Hz (red). **B.** The mean amplitude of the caffeine induced Ca^{2+} transient in the control recordings and immediately following stimulation at 5 Hz. **C.** The mean rise time (10 to 90%) of the caffeine induced Ca^{2+} transient. **D.** The mean time to 50% decline from the peak of the caffeine induced Ca^{2+} transient in the control recordings and after electrical stimulation at 5 Hz. Data represent mean ± s.e.m. n = 4 PVs from 4 rats.

3.3.5. Effect of isoprenaline on the spontaneous and electrically evoked Ca^{2+} transients

Isoprenaline was used to examine the effect of β-adrenergic stimulation on the characteristics of the spontaneous and electrically evoked Ca^{2+} transients. In the presence of isoprenaline (10 μM) there was a small but statistically significant decrease in the frequency of the spontaneous Ca^{2+} transients from 1.2 ± 0.1 Hz to 1.1 ± 0.1 Hz (n = 42 cardiomyocytes from 8 PVs from 8 rats, $P<0.05$) (Figure 3.15A and B). The mean amplitude of the spontaneous Ca^{2+} transients was 0.15 ± 0.01 ($\Delta F/F_{min}$), and was unaffected at 0.15 ± 0.02 ($\Delta F/F_{min}$) (n = 42 cardiomyocytes from 8 PVs from 8 rats, n.s.) (Figure 3.15A and C). Isoprenaline also had no significant effect on the wave velocity. The mean propagation velocity was 123.1 ± 10.53 μm/s before and then 108.6 ± 12.43 μm/s in the presence of isoprenaline (n = 12 cardiomyocytes from 7 PVs from 7 rats, n.s.) (Figure 3.15D).

Surprisingly, as isoprenaline has been shown to increase the Ca^{2+} transient amplitude in ventricular myocytes (Ginsburg & Bers, 2004; Hussain & Orchard, 1997), there was a small, but statistically significant, decrease in the amplitude of the electrically evoked Ca^{2+} transients from 0.22 ± 0.04 ($\Delta F/F_{min}$) to 0.20 ± 0.04 ($\Delta F/F_{min}$) ($P<0.05$, n = 7 PVs from 7 rats) (Figure 3.16). ROIs were placed in the individual cardiomyocytes to determine if the frequency of spontaneous Ca^{2+} transients between those that were evoked by electrical stimulation was changed by isoprenaline. Although variable between preparations, there was no significant difference as the frequency of spontaneous Ca^{2+} transients, which was 0.52 ± 0.22 Hz under control conditions and 0.52 ± 0.16 Hz in the presence of isoprenaline.

3.3.6. Effect of a period of electrical stimulation on the subsequent spontaneous Ca^{2+} transients in the presence of isoprenaline

Similar to the experiments performed under control conditions, a period of electrical stimulation resulted in an increase in the frequency of the subsequent spontaneous Ca^{2+}

transients (Figure 3.17A and B). However, unlike under untreated conditions, this effect was statistically significant after a period of electrical stimulation at 1 Hz, where there was an increase from 0.50 ± 0.07 Hz in the control recordings to 0.59 ± 0.05 Hz after stimulation at 1 Hz ($P<0.05$ *vs.* no prior E.S.). The frequency of the spontaneous Ca^{2+} transients was increased further to 0.73 ± 0.04 Hz after a period of electrical stimulation at 3 Hz ($P<0.001$ *vs.* no prior E.S.). Following electrical stimulation at 5, 7 and 9 Hz, the increase in the frequency of the spontaneous Ca^{2+} transients plateaued, being 0.75 ± 0.05 Hz, 0.79 ± 0.04 Hz and 0.73 ± 0.04 Hz respectively (n = 33 cardiomyocytes from 6 PVs from 6 rats) (Figure 3.17B).

The mean amplitude of the spontaneous Ca^{2+} transients decreased significantly from 0.31 ± 0.03 ($\Delta F/F_{min}$) in the control recordings, to 0.25 ± 0.02 ($\Delta F/F_{min}$) after electrical stimulation at 1 Hz ($P<0.01$ *vs.* no prior E.S.), and remained significantly decreased, after a period of electrical stimulation at 3 to 9 Hz (n = 33 cardiomyocytes from 6 PVs from 6 rats) (Figure 3.17C).

The mean wave velocity was 94.22 ± 6.06 µm/s in the presence of isoprenaline and was not significantly different at 94.82 ± 5.77 µm/s following a period of electrical stimulation at 1 Hz. However, following stimulation at 3 Hz, the Ca^{2+} wave velocity was significantly increased to 115.5 ± 9.9 µm/s ($P<0.05$ *vs.* no prior E.S.). The wave velocity after a period of electrical stimulation at 5 Hz was 119 ± 8.26 µm/s ($P<0.05$ *vs.* control) and continued to steadily increase after electrical stimulation at 7 and 9 Hz, where the wave velocity was 122.4 ± 7.06 µm/s ($P<0.01$ *vs.* no prior E.S.) and 125.2 ± 9.67 µm/s ($P<0.001$ *vs.* no prior E.S.) respectively (n = 26 cardiomyocytes from 7 PVs from 7 rats) (Figure 3.17D).

In the presence of isoprenaline, the mean synchronisation index for the spontaneous Ca^{2+} transients was 0.20 ± 0.02 in the first 2 s and 0.15 ± 0.03 in the last 2 s of the recordings. After a period of electrical stimulation at 1 Hz, the mean synchronisation was increased to 0.24 ± 0.02 in the first 2 s, which was significantly greater than in the

last 2 s, where it was 0.12 ± 0.02 ($P<0.01$). Immediately following a period of electrical stimulation at 3 Hz, there was a much greater increase in synchronisation to 0.35 ± 0.02 in the first 2 s, compared with 0.10 ± 0.03 in the last 2s ($P<0.001$). Increasing the frequency of electrical stimulation to 5, 7 and 9 Hz resulted in no further increase in the synchronisation of spontaneous Ca^{2+} transients. The mean synchronisation index was 0.36 ± 0.02, 0.34 ± 0.02 and 0.34 ± 0.02 in the first 2s after electrical stimulation at 5, 7 and 9 Hz respectively. During the last 2 s of the same recordings, the mean synchronisation index was significantly lower, being 0.12 ± 0.02, 0.11 ± 0.02 and 0.14 ± 0.02 respectively ($P<0.001$) (Figure 3.17E and F).

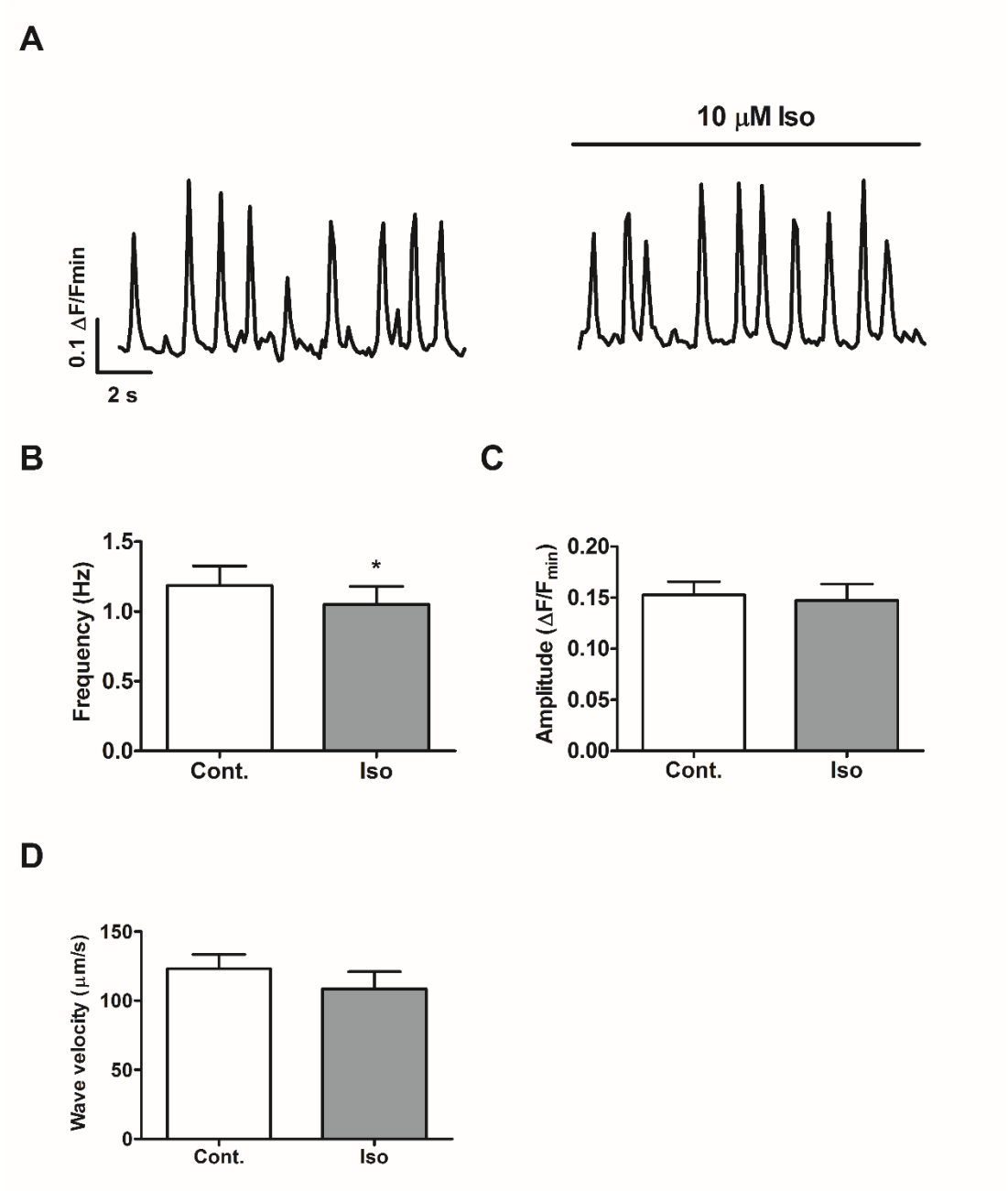

Figure 3.15. The effect of isoprenaline on the spontaneous Ca^{2+} transients in pulmonary vein cardiomyocytes. A. Representative recordings of fluo-4 fluorescence in a cardiomyocyte under control conditions, and in the same cell in the presence of isoprenaline (10 μM). The mean frequency **(B)** and amplitude **(C)** of the spontaneous Ca^{2+} transients, and the Ca^{2+} wave velocity **(D)** under control conditions and in the presence of isoprenaline (10 μM). Data represent mean ± s.e.m., *P<0.05 and n = 42 cardiomyocytes from 8 PVs from 8 rats for frequency and amplitude and n = 12 cardiomyocytes from 7 PVs from 7 rats for wave velocity.

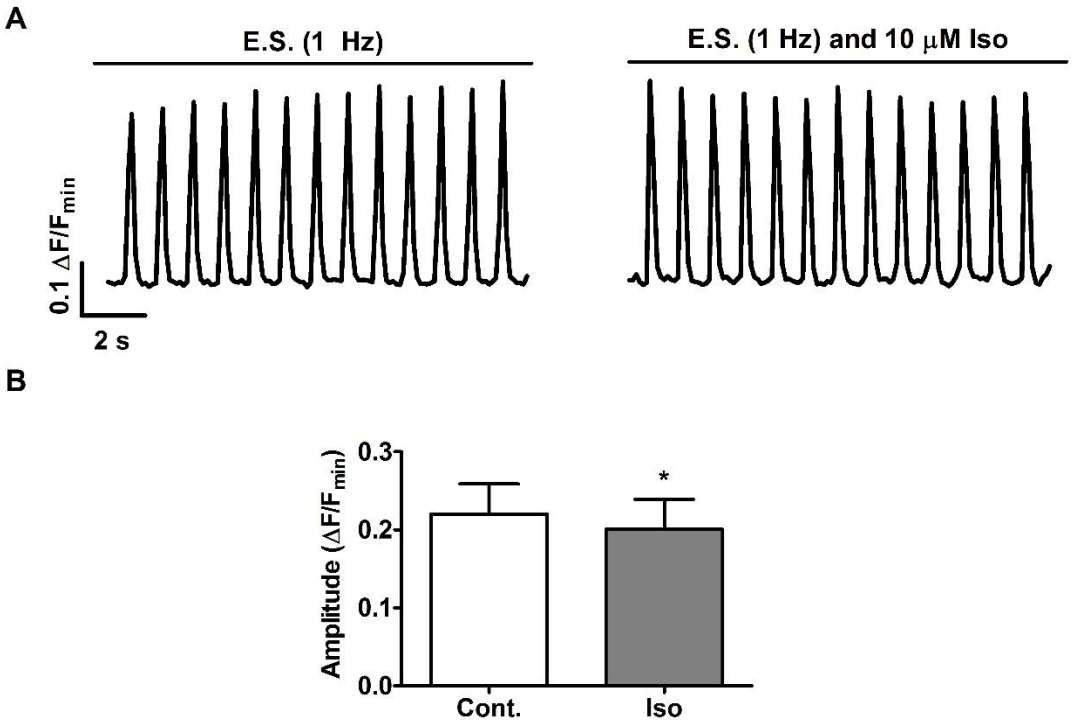

Figure 3.16. The effect of isoprenaline on the electrically evoked Ca^{2+} transients in the pulmonary vein. A. Representative recordings of the fluo-4 fluorescence in the entire FOV during electrical stimulation at 1 Hz, and in the same region in the presence of isoprenaline (10 μM). **B**. The mean amplitude of the electrically evoked Ca^{2+} transients under control conditions and in the presence of isoprenaline (10 μM). Data represent mean ± s.e.m.,*P<0.05 and n = 7 PVs from 7 rats.

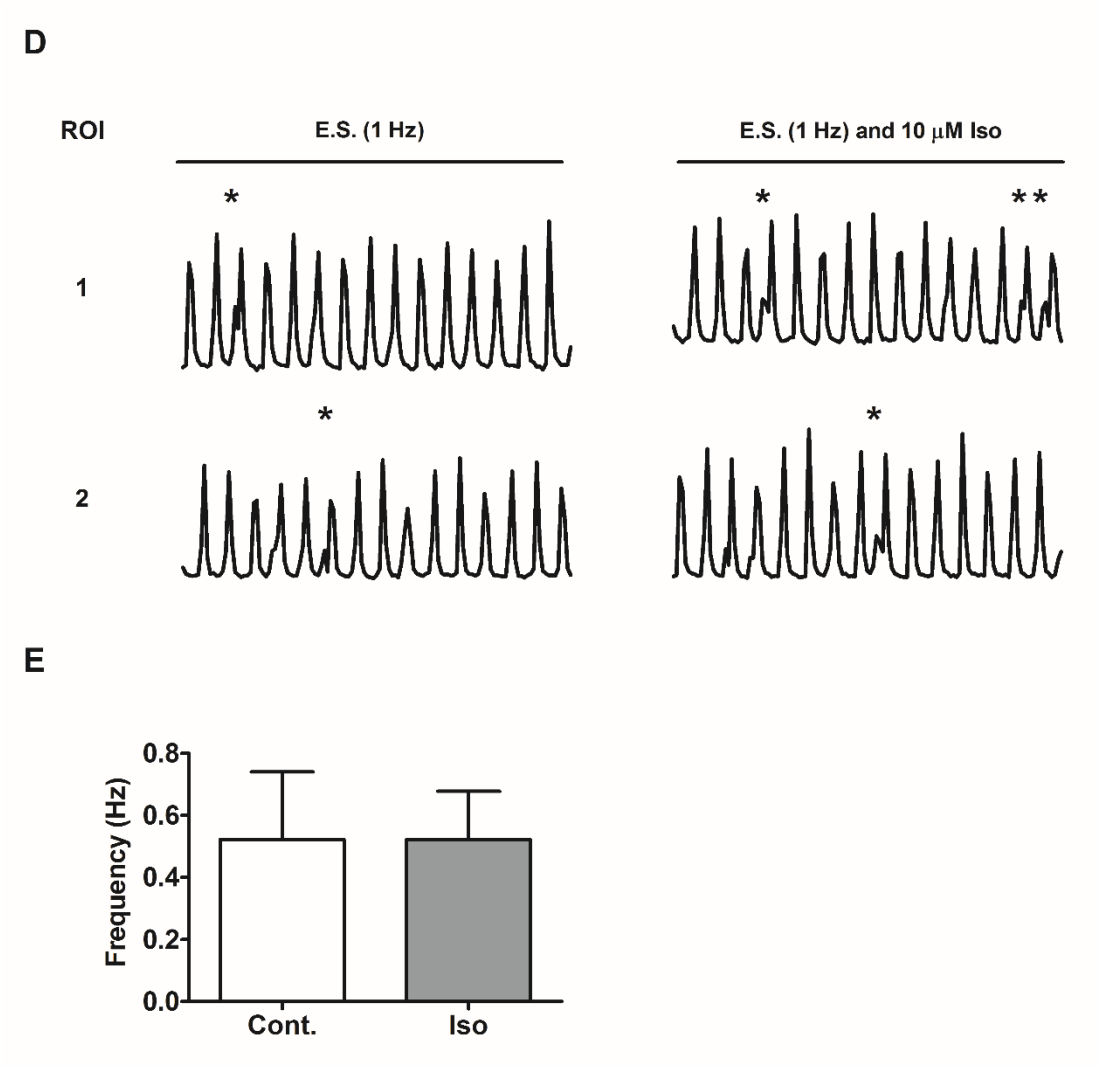

Figure 3.16. (cont.) **D.** Representative recordings displaying fluo-4 fluorescence in individual cardiomyocytes (ROIs) during electrical stimulation at 1 Hz in a control recording and in the presence of isoprenaline (10 μM). Spontaneous Ca^{2+} transients are indicated by the asterisks. **E.** Mean frequency of spontaneous Ca^{2+} during electrical stimulation at 1 Hz in the control recordings and in presence of isoprenaline. Data represent mean ± s.e.m. and n = 10 cardiomyocytes from 5 PVs from 5 rats.

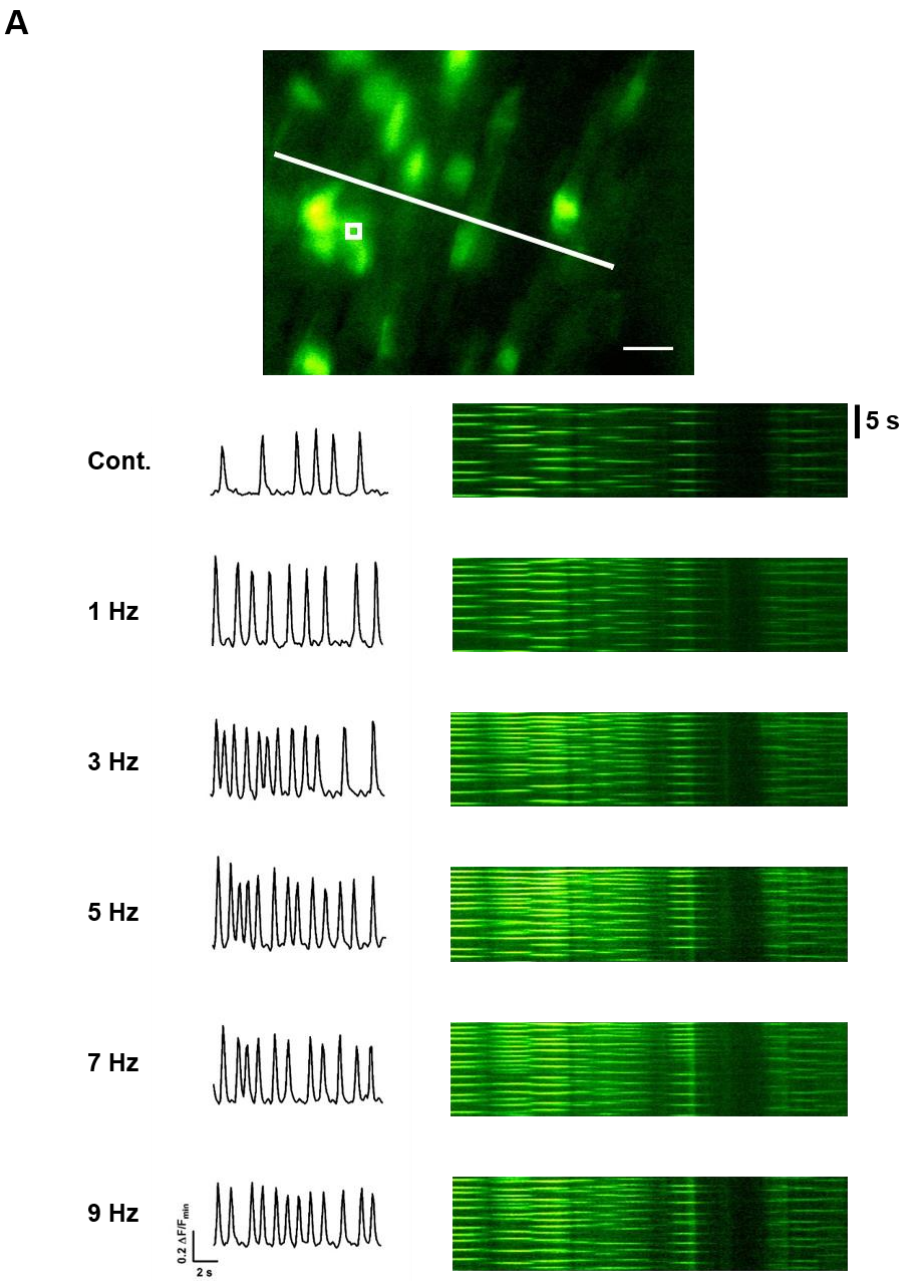

Figure 3.17. The effect of isoprenaline on the subsequent spontaneous Ca^{2+} transients in the pulmonary vein after a period of electrical stimulation. A. Wide field image depicting the region of interest that was used to produce the fluorescence vs. time records and the while line used to generate the pseudo-linescans that are shown below. Images were obtained during a control recording with no prior electrical stimulation, and immediately following termination of a period of electrical stimulation at 1-9 Hz. The pulmonary vein was treated with isoprenaline 2 min prior to commencing the recordings. Scale bar represents 20 μm.

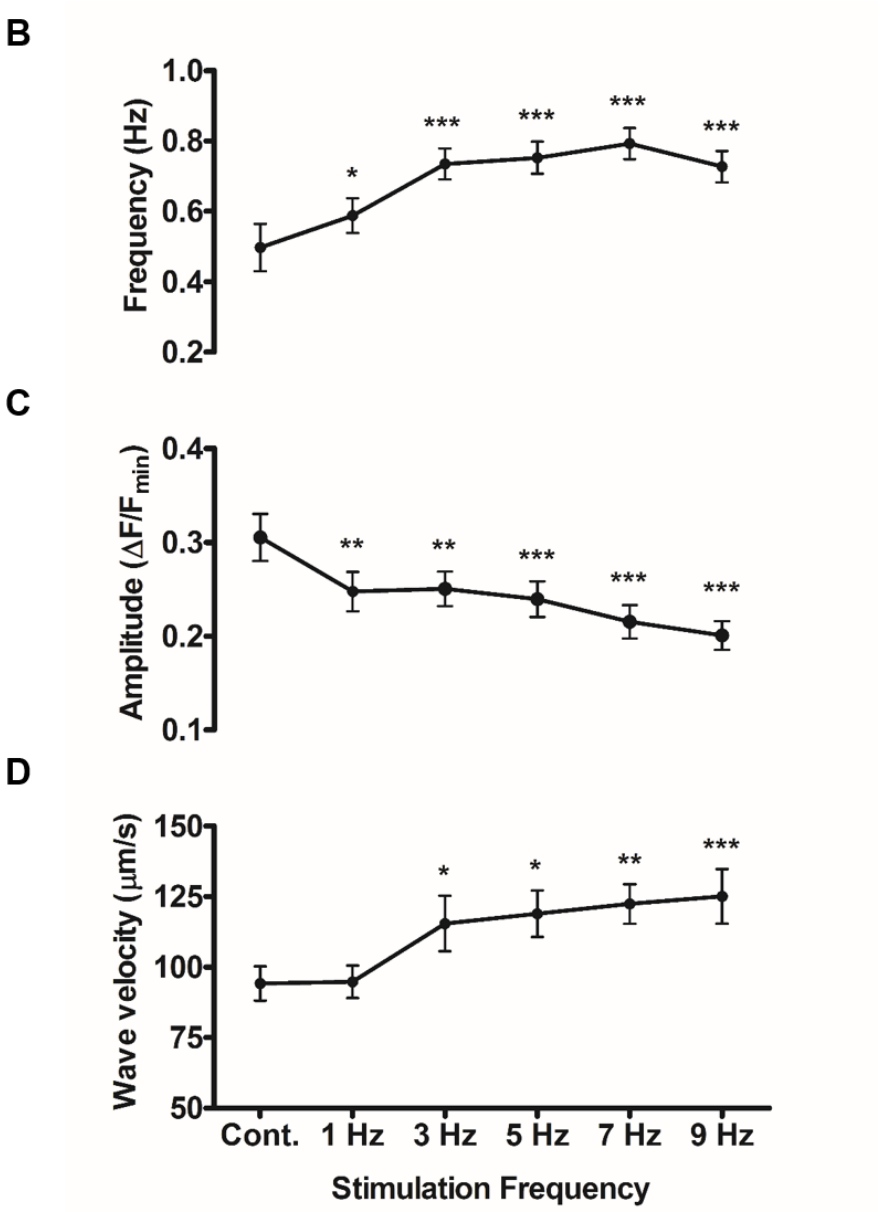

Figure 3.17 (cont.). The mean frequency **(B)** and amplitude **(C)** of the spontaneous Ca^{2+} transients and velocity of Ca^{2+} waves **(D)** in the presence of isoprenaline (10 μM), in the control recordings with no prior electrical stimulation, and immediately following electrical stimulation at 1-9 Hz. Data represent mean ± s.e.m., *P<0.05; **P<0.01; ***P<0.001 *vs*. Cont. n = 33 cardiomyocytes from 6 PVs from 6 rats for amplitude and frequency and 26 cardiomyocytes from 7 PVs from 7 rats for the wave velocity.

E

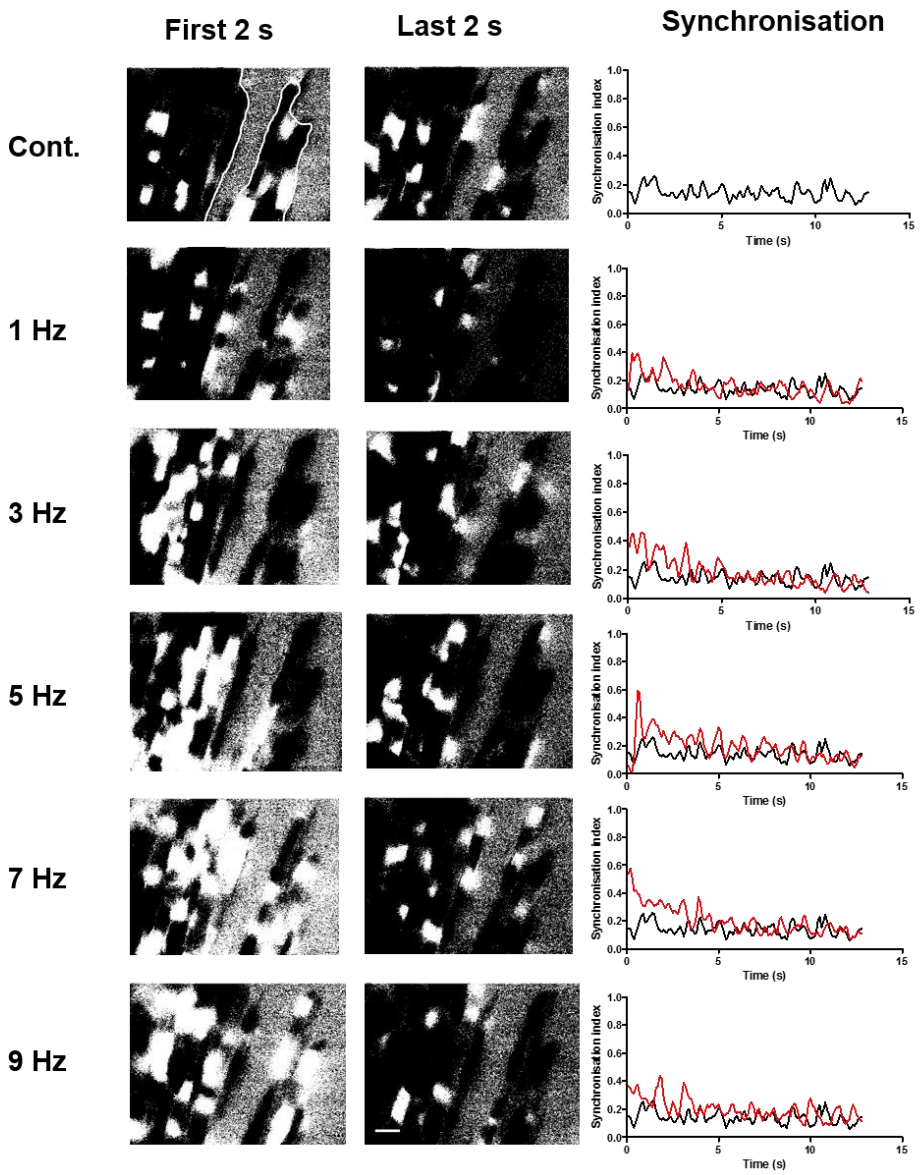

Figure 3.17. (cont.). **E.** Representative analysis of spontaneous Ca^{2+} transient synchronisation in the presence of isoprenaline in a control recording with no prior electrical stimulation, and immediately following termination of a period of electrical stimulation at 1-9 Hz. The wide-field images are threshold images displaying pixels that have a greater intensity than half maximum as white. The mask used for the analysis is shown in white in the top left panel. The recordings on the right represent the synchronisation index for each frame over time in the control recording (black) and after a period of E.S. at 1-9 Hz (red). Scale bar represents 10 µm.

F

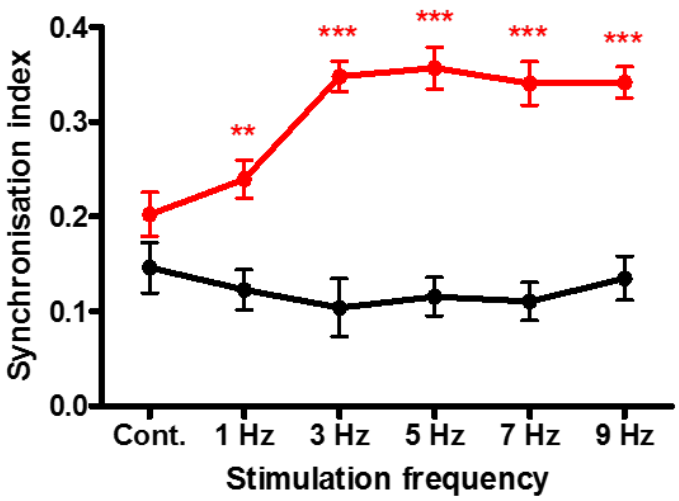

Figure 3.17. (cont.). F. The mean synchronisation during the first 2 s and last 2 s of the recording period in the control recordings with no prior electrical stimulation and immediately following a period of E.S. at 1-9 Hz. Data represent mean ± s.e.m. $^{**}P<0.01$ and $^{***}P<0.001$; first 2 s vs. last 2 s. n = 7 PVs from 7 rats.

3.3.7. Effect of increasing the external Ca^{2+} concentration on the spontaneous and electrically evoked Ca^{2+} transients

The effect of increasing the external Ca^{2+} concentration on the spontaneous and electrically evoked Ca^{2+} transients was next examined. The frequency of spontaneous Ca^{2+} transients was 1.3 ± 0.1 Hz under control conditions and was significantly reduced to 1.1 ± 0.09 Hz after the external Ca^{2+} concentration was increased (n = 52 from 8 cardiomyocytes from 8 rats, $P<0.001$) (Figure 3.18A and B). The mean amplitude of the spontaneous Ca^{2+} transients was 0.22 ± 0.02 ($\Delta F/F_{min}$) under control conditions and was not significantly altered at 0.20 ± 0.01 ($\Delta F/F_{min}$) after increasing the external Ca^{2+} concentration (Figure 3.18A and C) (n = 52 from 8 cardiomyocytes from 8 rats, n.s.). Similarly, the wave velocity was 109.1 ± 11.3 μm/s and this was not significantly different at 100.4 ± 11.29 μm/s after increasing the external Ca^{2+} concentration (28 cardiomyocytes from 12 PVs from 11 rats, n.s.) (Figure 3.18D).

Figure 3.19A and B shows the fluo-4 fluorescence in the FOV from two different preparations in the presence of a high external Ca^{2+} concentration, during electrical stimulation (1 Hz). In the first pulmonary vein, the characteristics of the electrically evoked Ca^{2+} transients resemble those that were evoked under control conditions (Figure 3.19A). However, in 22% of preparations there was a premature rise in the fluorescence signal in the FOV that preceded each electrically evoked Ca^{2+} transient (Figure 3.19B). The mean amplitude of the electrically evoked Ca^{2+} transients was 0.3 ± 0.05 ($\Delta F/F_{min}$) and was not significantly different at 0.27 ± 0.04 ($\Delta F/F_{min}$) when the external Ca^{2+} concentration was increased (n = 7 PVs from 7 rats, n.s.) (Figure 3.19C).

In order to determine if the premature rise in fluorescence observed in 22% of the preparations reflects changes in spontaneous Ca^{2+} signalling, the fluo-4 fluorescence was analysed in individual cardiomyocytes using ROIs. It was found that the frequency of spontaneous Ca^{2+} transients between those that were evoked was significantly increased from 0.11 ± 0.06 Hz to 0.41 ± 0.28 Hz (n = 16 cardiomyocytes from 7 PVs from 6 rats, $P<0.001$), suggesting that an increase in the frequency of spontaneous Ca^{2+}

transients may have been the cause of the rise in fluorescence in the FOV between the electrically evoked Ca^{2+} transients (Figure 3.19D and E).

3.3.8. Effect of electrical stimulation on the subsequent spontaneous Ca^{2+} transients in the presence of high external Ca^{2+}

The effect of increasing the external Ca^{2+} concentration on the spontaneous Ca^{2+} transients after a period of electrical stimulation was also investigated. The pseudo-linescan images demonstrate that, when the pulmonary vein was maintained in physiological salt solution containing a high external Ca^{2+} concentration, there was an increase in the frequency of the spontaneous Ca^{2+} transients immediately following cessation of electrical stimulation (Figure 3.20A). It is also evident in the pseudo-linescan images that the spontaneous Ca^{2+} transients that initially re-appeared after a period of electrical stimulation at 5 Hz or greater were present in all of the cardiomyocytes in the FOV the same time (Figure 3.20A).

The increase in the frequency of spontaneous Ca^{2+} transients that immediately followed a period of electrical stimulation reached statistical significance after electrical stimulation at 3 Hz. The frequency of spontaneous transients was 0.39 ± 0.06 Hz in the control recordings with no prior electrical stimulation, and was 0.75 ± 0.06 Hz immediately after electrical stimulation at 3 Hz ($P<0.001$ *vs.* no prior E.S.). After a period of electrical stimulation at 5 Hz, the frequency of spontaneous transients was increased further to 0.91 ± 0.07 Hz ($P<0.001$ *vs.* no prior E.S.), which was a greater increase compared to the recordings obtained under control conditions. Following a period of electrical stimulation at 7 and 9 Hz, the increase in the frequency of spontaneous Ca^{2+} transients plateaued, being 0.94 ± 0.09 Hz and 0.93 ± 0.1 Hz respectively (n =34 from 6 PVs from 6 rats) (Figure 3.20B).

There was no significant change in the mean amplitude of the spontaneous Ca^{2+} transients after a period of electrical stimulation up to 5 Hz. However, there was a

significant decrease in the amplitude after stimulation at 7 and 9 Hz. The mean amplitude of the spontaneous Ca^{2+} transients was 0.29 ± 0.02 ($\Delta F/F_{min}$) in the control recordings with no prior electrical stimulation, and was 0.25 ± 0.02 ($\Delta F/F_{min}$) and 0.23 ± 0.02 ($\Delta F/F_{min}$) after a period of electrical stimulation at 7 and 9 Hz respectively (n = 34 cardiomyocytes from 6 PVs from 6 rats, P<0.001 *vs.* no prior E.S.) (Figure 3.20C).

Increasing the external Ca^{2+} concentration resulted in an increase in the velocity of the Ca^{2+} waves following a period of electrical stimulation. This effect reached significance after stimulation at 3 Hz, where the wave velocity was increased to 141.7 ± 10.09 µm/s, compared to 103.5 ± 6.27 µm/s under control conditions (n = 32 cardiomyocytes from 6 PVs from 6 rats, P<0.05 vs. no prior E.S.). After a period of electrical stimulation at 5 Hz, the propagation velocity of the subsequent Ca^{2+} waves was increased further to 166.9 ± 14.73 µm/s (n = 32 cardiomyocytes from 6 PVs from 6 rats, P<0.001 vs. no prior E.S.). The wave velocity plateaued after electrical stimulation at 7 and 9 Hz, being 171.5 ± 17.03 µm/s and 170.5 ± 16.17 µm/s respectively (|Figure 3.20D).

When the external Ca^{2+} concentration was increased, a brief period of electrical stimulation at 3 Hz or greater transiently increased the synchronisation of the subsequent spontaneous Ca^{2+} transients. This can be seen in the representative recordings in Figure 3.20E. Under control conditions the mean synchronisation index was 0.11 ± 0.02 in the first 2s and 0.10 ± 0.02 in the last 2 s of the recordings. After a period of electrical stimulation at 1 Hz, the mean synchronisation was not significantly different in the first and last 2 s, being 0.14 ± 0.02 and 0.10 ± 0.01 respectively. The mean synchronisation after a period of electrical stimulation at 3 Hz was 0.26 ±0.04 in the first 2 s, which was significantly greater than in the last 2 s where it was 0.09 ± 0.01 (P<0.01). Similarly, after electrical stimulation at 5, 7 and 9 Hz, the synchronisation was greater in the first 2 s, being 0.28 ± 0.05, 0.29 ± 0.04 and 0.28 ± 0.05, compared to 0.09 ± 0.02, 0.10 ± 0.01 and 0.13 ± 0.00 respectively (Figure 3.20F).

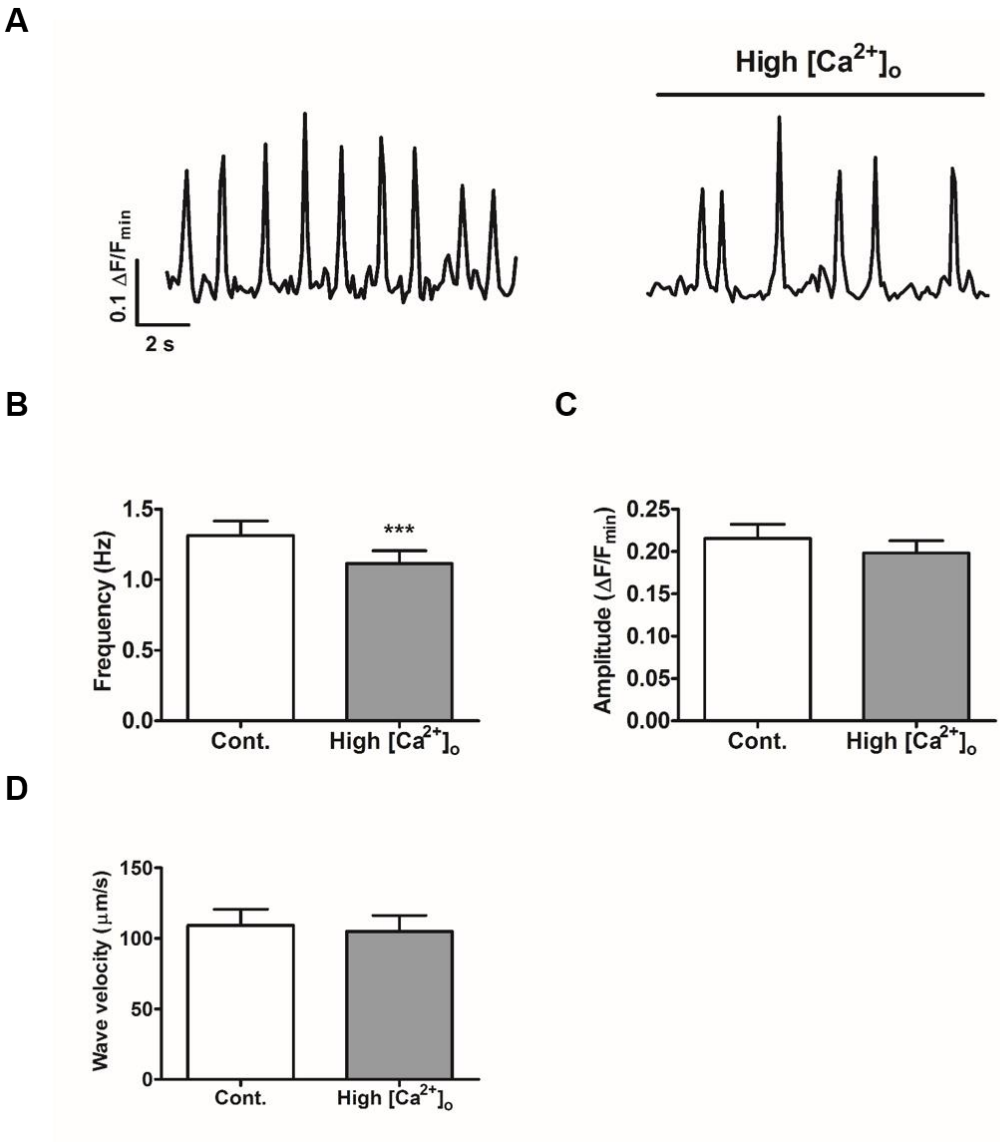

Figure 3.18. The effect of increasing the external Ca^{2+} concentration on spontaneous Ca^{2+} transients in pulmonary vein cardiomyocytes. A. Representative recordings of fluo-4 fluorescence in a cardiomyocyte under control conditions and in the same cell 2 min after the external Ca^{2+} concentration ($[Ca^{2+}]_o$) was increased to 4.5 mM. The mean frequency **(B)** and amplitude **(C)** of spontaneous Ca^{2+} transients, and Ca^{2+} wave velocity **(D)** under control conditions and after the $[Ca^{2+}]_o$ was increased. Data represent mean ± s.e.m., $^{*}P<0.05$ and n = 52 cardiomyocytes from 8 PVs from 8 rats and 28 cardiomyocytes from 12 PVs from 11 rats for wave velocity.

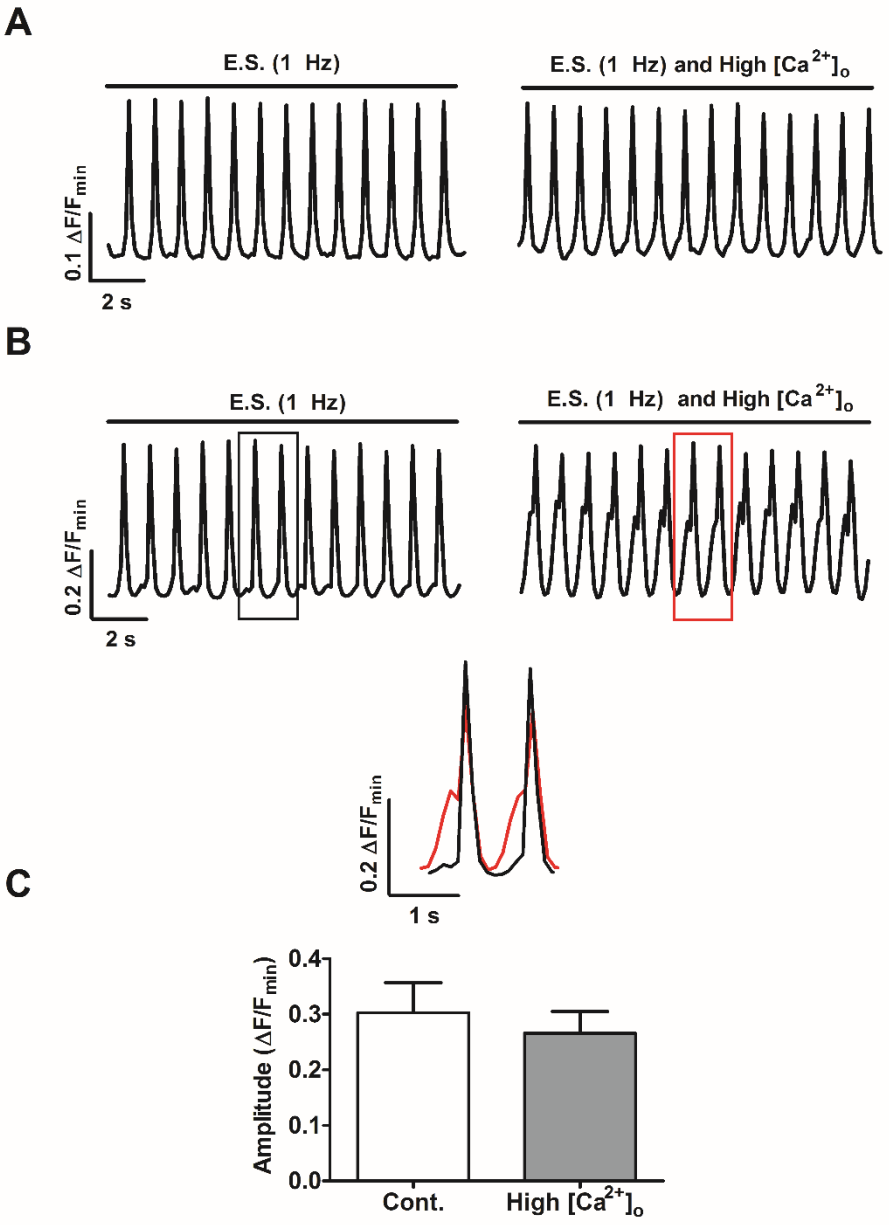

Figure 3.19. The effect of increasing the extracellular Ca^{2+} concentration on the electrically evoked Ca^{2+} transients in the pulmonary vein. A. Representative recordings of fluo-4 fluorescence in the entire FOV during electrical stimulation at 1 Hz in a control recording and in the same region after the external Ca^{2+} concentration ($[Ca^{2+}]_o$) was increased to 4.5 mM. **B.** Representative recordings from a different preparation. A section from each recording, indicated by the black and red boxes, has been merged and presented over an expanded time scale. **C**. The mean amplitude of the electrically evoked Ca^{2+} transients under control conditions and after the $[Ca^{2+}]_o$ was increased. Data represent mean ± s.e.m. and n = 9 PVs from 7 rats.

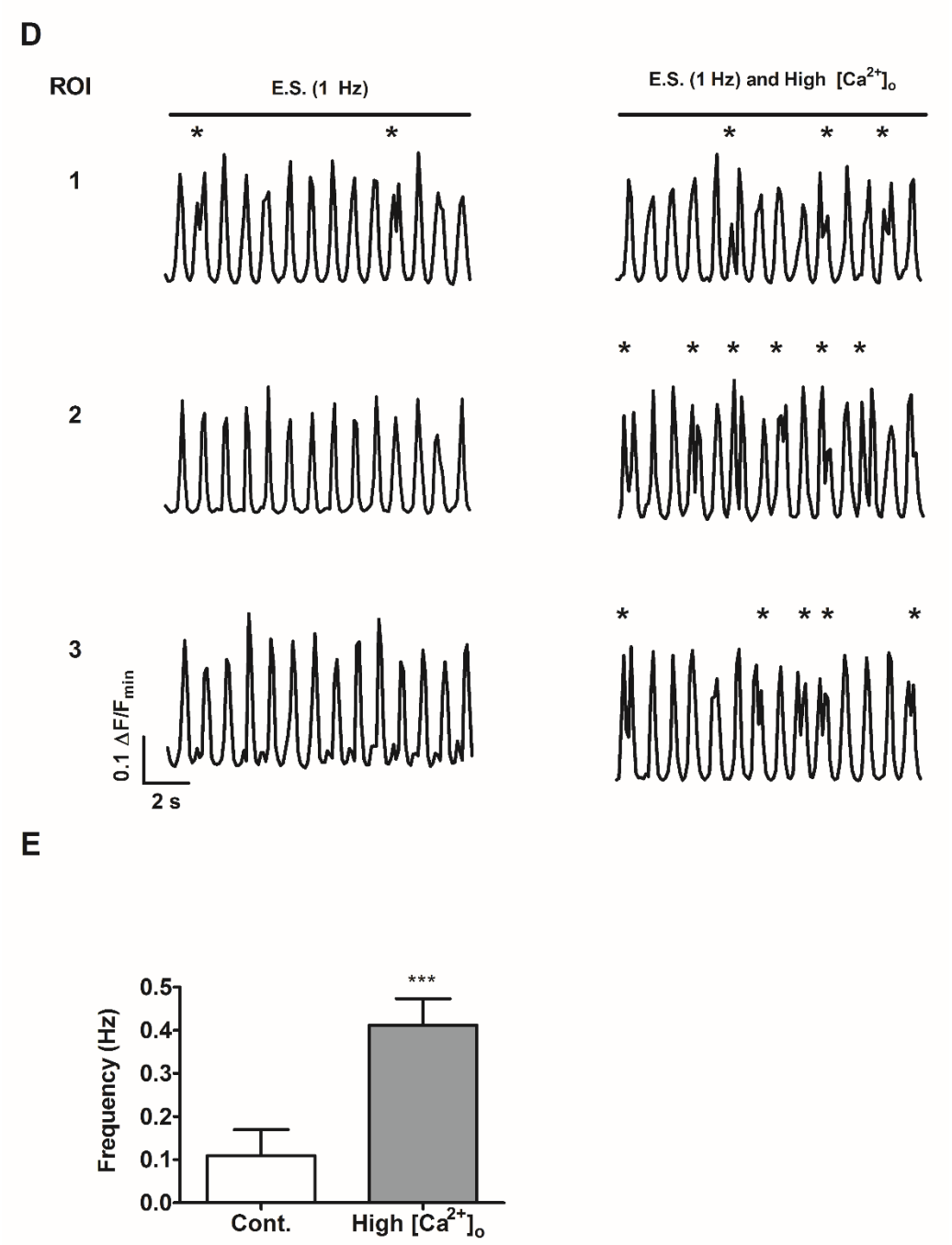

Figure 3.19. (cont.) D. Representative recordings displaying fluo-4 fluorescence in ROIs during electrical stimulation at 1 Hz in a control recording and after the external Ca^{2+} concentration ($[Ca^{2+}]_o$) was increased to 4.5 mM. Spontaneous Ca^{2+} transients are indicated by the asterisks. **E.** Mean frequency of spontaneous Ca^{2+} transients during electrical stimulation at 1 Hz in the control recordings and after the $[Ca^{2+}]_o$ was increased. Data represent mean ± s.e.m. $^{***}P<0.01$ and n = 16 cardiomyocytes from 7 PVs from 6 rats.

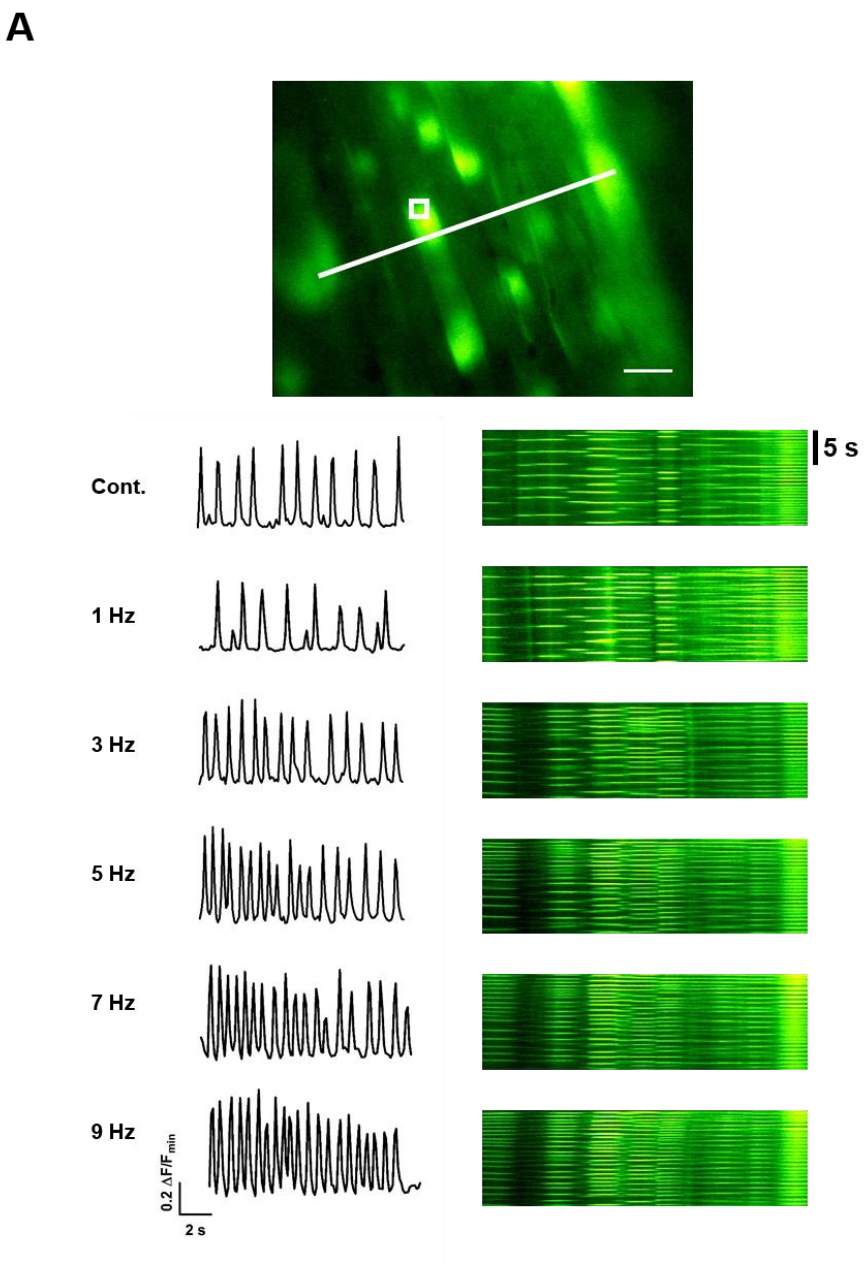

Figure 3.20. The effect of increasing the external Ca^{2+} concentration on the subsequent spontaneous Ca^{2+} transients in the pulmonary vein after a period of electrical stimulation. Wide field image depicting the region of interest that was used to produce the fluorescence vs. time records and the while line used to generate the pseudo-linescans that are shown below. Images were obtained during a control recording with no prior electrical stimulation, and immediately following termination of a period of electrical stimulation at 1-9 Hz. The external concentration of Ca^{2+} was raised from 2.5 to 4.5 mM, 2 min prior to commencing the recordings. Scale bar represents 20 μm.

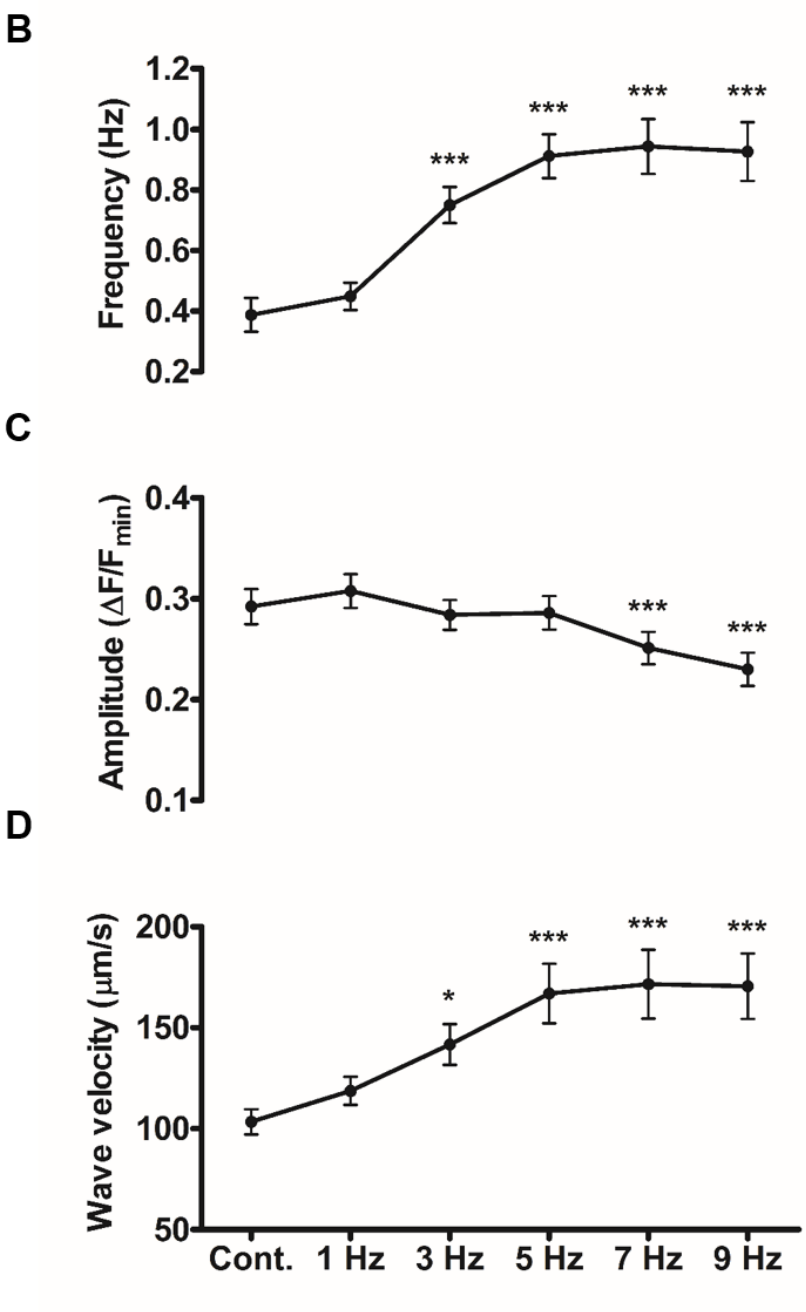

Figure 3.20 (cont.). The mean frequency **(B)** and amplitude **(C)** of the spontaneous Ca^{2+} transients and velocity of Ca^{2+} waves **(D)** in the presence of high $[Ca^{2+}]_o$ in the control recordings with no prior electrical stimulation, and immediately following a period of electrical stimulation (E.S.) at 1-9 Hz. Data represent mean ± s.e.m., $^{*}P<0.05$ vs. Cont., $^{***}P<0.001$ *vs.* Cont. and n = 34 cardiomyocytes from 6 PVs from 6 rats for frequency and amplitude and n = 32 cardiomyocytes from 6 PVs from 6 rats for wave velocity.

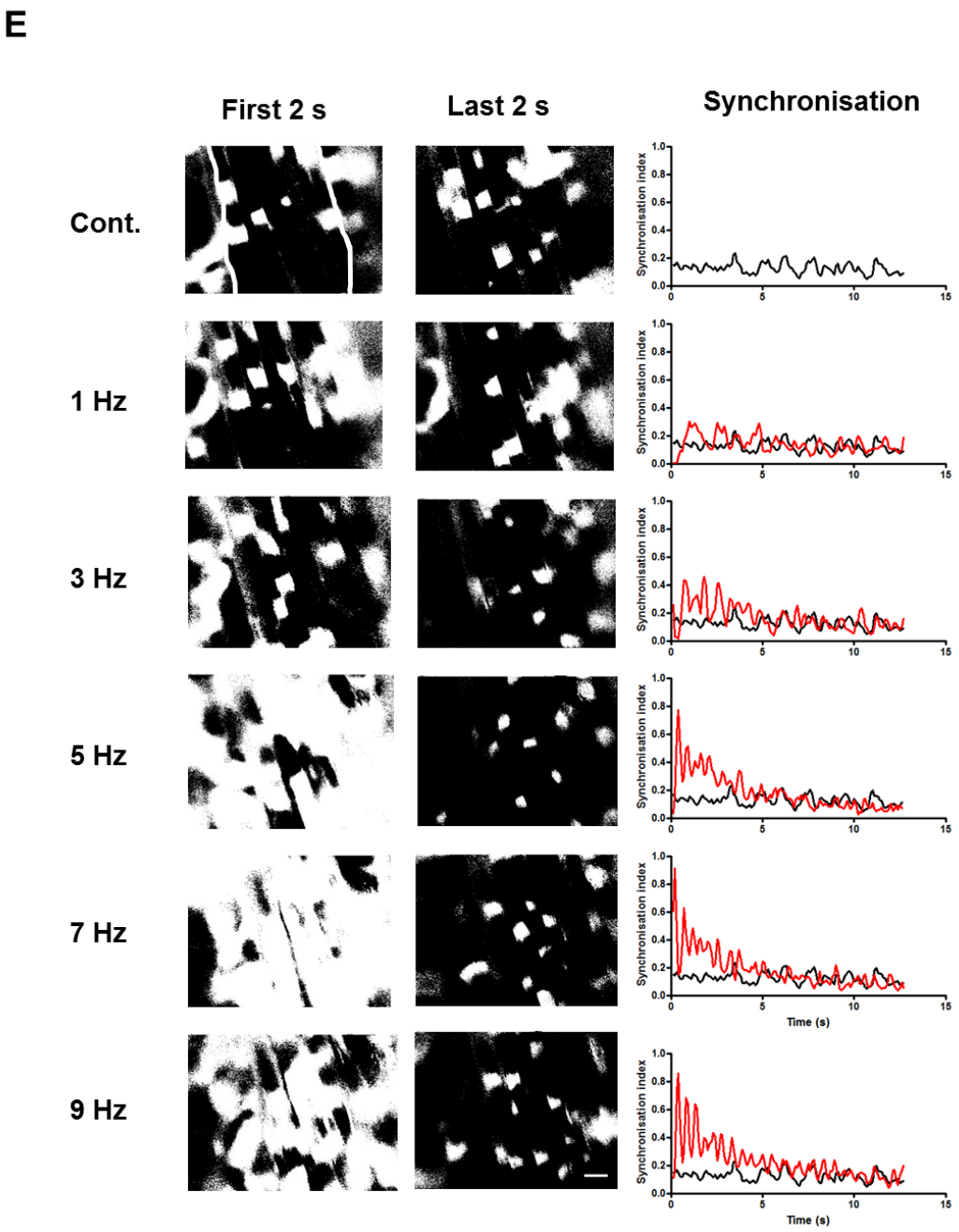

Figure 3.20. (cont.). E. Representative analysis of spontaneous Ca^{2+} transient synchronisation in the presence of high external Ca^{2+} in a control recording with no prior electrical stimulation, and immediately following termination of a period of electrical stimulation at 1-9 Hz. The wide-field images are threshold images displaying pixels that have a greater intensity than half maximum as white. The mask used for the analysis is shown in white in the top left panel. The recordings on the right represent the synchronisation index for each frame over time in the control recording (black) and after a period of E.S. at 1-9 Hz (red). Scale bar represents 20 μm.

F

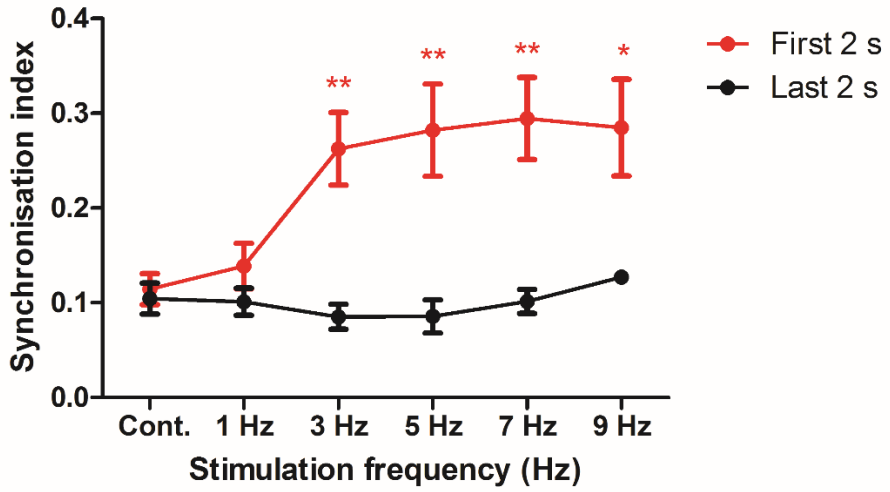

Figure 3.20. (cont.). F. The mean synchronisation during the first 2 s and last 2 s of the recording period in the control recordings with no prior electrical stimulation and immediately following a period of E.S. at 1-9 Hz. Data represent mean ± s.e.m. $^{*}P<0.05$ and $^{**}P<0.01$; first 2 s vs. last 2 s. n = 6 PVs from 6 rats.

3.3.9. Effect of isoprenaline in combination with increasing the external Ca^{2+} concentration on the spontaneous and electrically evoked Ca^{2+} transients

The frequency of the spontaneous Ca^{2+} transients was 0.90 ± 0.13 Hz under control conditions and was not significantly different at 0.94 ± 0.13 Hz in the presence of isoprenaline (10 μM) and high external Ca^{2+} (n = 60 cardiomyocytes from 7 PVs from 7 rats, n.s.) (Figure 3.21A and B). There was, however, a statistically significant decrease in the amplitude of the spontaneous Ca^{2+} transients from 0.23 ± 0.02 ($\Delta F/F_{min}$) to 0.20 ± 0.01 ($\Delta F/F_{min}$) (n = 60 cardiomyocytes from 7 PVs from 7 rats, $P<0.01$) (Figure 3.21A and C). The propagation velocity of the spontaneous Ca^{2+} transients that occurred as waves was 104.2 ± 5.72 μm/s under control conditions and this was not significantly different at 100.4 ± 5 μm/s after increasing the external Ca^{2+} concentration and adding isoprenaline (n = 22 cardiomyocytes from 8 PVs from 8 rats, n.s.)

The mean amplitude of the electrically evoked Ca^{2+} transients was 0.31 ± 0.06 ($\Delta F/F_{min}$) under control conditions and was unaffected at 0.30 ± 0.06 ($\Delta F/F_{min}$) in presence of isoprenaline and high external Ca^{2+} (n = 7 PVs from 7 rats, n.s.) (Figure 3.22A and C). In 43% of preparations there was evidence of a global increase in the fluorescence signal in the FOV, occurring between the electrically evoked Ca^{2+} transients (Figure 3.22B). ROI analysis determined the frequency of spontaneous Ca^{2+} transients between those that were evoked was increased from 0.14 ± 0.07 Hz in the control recordings to 0.68 ± 0.07 Hz in the presence of isoprenaline and high external Ca^{2+} (n = 18 cardiomyocytes from 5 PVs from 5 rats, $P<0.001$) (Figure 3.22D and E).

3.3.10. Effect of electrical stimulation on the subsequent spontaneous Ca^{2+} transients in the presence of isoprenaline and high external Ca^{2+}

Immediately after a period of electrical stimulation at 1 Hz or greater, there was an increase in the frequency of the spontaneous Ca^{2+} transients compared the control recordings, which were obtained in the absence of any prior stimulation. This is similar to the results obtained in the presence of isoprenaline alone (Figure 3.23A). The mean frequency of the spontaneous Ca^{2+} transients was 0.45 ± 0.05 Hz in the presence of isoprenaline and high external Ca^{2+}, and was significantly increased to 0.60 ± 0.05 Hz after a period of electrical stimulation at 1 Hz ($P<0.05$ *vs.* no prior E.S.). There was a further increase to 0.91 ± 0.07 Hz after a period of electrical stimulation at 3 Hz ($P<0.001$ *vs.* no prior E.S.), before the increase in the frequency of spontaneous Ca^{2+} transients plateaued at the higher frequencies of stimulation. The frequency of the spontaneous Ca^{2+} transients was 0.93 ± 0.07 Hz, 0.94 ± 0.09 Hz and 0.95 ± 0.1 Hz after a period of electrical stimulation at 5, 7 and 9 Hz respectively (n = 36 cardiomyocytes from 7 PVs from 7 rats) (Figure 3.23B).

Following a period of electrical stimulation at frequencies of 5 Hz or greater, the amplitude of the subsequent spontaneous Ca^{2+} transients was significantly decreased compared to the control recordings, which obtained with no prior stimulation. The mean amplitude in the control recordings was 0.31 ± 0.03 ($\Delta F/F_{min}$), and was reduced to 0.27 ± 0.02 ($\Delta F/F_{min}$) after a period of electrical stimulation at 5 Hz ($P<0.01$ *vs.* no prior E.S.). The mean amplitude was 0.25 ± 0.02 ($\Delta F/F_{min}$) and 0.24 ± 0.02 ($\Delta F/F_{min}$) after a period of electrical stimulation at 7 Hz and 9 Hz respectively (n = 36 cardiomyocytes from 7 PVs from 7 rats, $P<0.001$ *v vs.* no prior E.S.) (Figure 3.23C).

The propagation velocity of the spontaneous Ca^{2+} waves was 104.2 ± 4.73 µm/s under control conditions and was increased, although not statistically significantly to 123.6 ± 5.78 µm/s after a period of electrical stimulation at 1 Hz. Immediately following a period of electrical stimulation at 3 Hz the wave velocity was 147.2 ± 9.12 µm/s, which was significantly greater than with no prior electrical stimulation ($P<0.05$ *vs. vs.* no

prior E.S.). There was a further increase in the wave velocity to 165.4 ± 10.58 µm/s after electrical stimulation at 5 Hz and when the frequency of stimulation was increased to 7 and 9 Hz, the wave velocity was 158.3 ± 10.71 µm/s and 163.6 ± 12.65 µm/s respectively (n = 30 cardiomyocytes from 7 PVs from 7 rats, P<0.001 *vs.* no prior E.S.) (Figure 3.23D).

The caffeine induced Ca^{2+} transient after a period of electrical stimulation was also investigated in the presence of isoprenaline and a high external Ca^{2+} concentration. This was to examine if the more pronounced increase in the frequency of spontaneous Ca^{2+} transients after a period of electrical stimulation under these conditions was due to an increased SR Ca^{2+} load. The magnitude of the caffeine induced Ca^{2+} transient was 0.15 ± 0.02 ($\Delta F/F_{min}$) after a period of electrical stimulation at 3 Hz, and was unaffected at 0.15 ± 0.03 ($\Delta F/F_{min}$) in the presence of isoprenaline and high external Ca^{2+} (n = 10 PVs from 10 rats, n.s.) (Figure 3.24A and B). There was also no significant change in the rise time, as it was 0.75 ± 0.11 s after stimulation 3 Hz under untreated conditions and 0.92 ± 0.12 s in the presence of isoprenaline and high Ca^{2+} (n = 10 PVs from 10 rats, n.s.) (Figure 3.24A and C). The time to 50% decline was also not significantly different, being 6.44 ± 0.94 s before and 5.61 ± 0.87 s after adding isoprenaline and increasing the external Ca^{2+} concentration (n = 10 PVs from 10 rats, n.s.) (Figure 3.24A and D).

As can be seen in the representative recordings, when the pulmonary vein was treated with isoprenaline and the external Ca^{2+} concentration was increased, a brief period of electrical stimulation at 1 Hz or greater transiently increased the synchronisation of the subsequent spontaneous Ca^{2+} transients (Figure 3.23E). Under control conditions, the mean synchronisation index was 0.13 ± 0.01 in the first and 0.14 ± 0.02 in the last 2 s. Following a period of electrical stimulation at 1 Hz, the mean synchronisation was increased to 0.23 ± 0.03 in the first 2 s, which was significantly greater than in the last 2 s, where it was 0.10 ± 0.02 (P<0.01). In the first 2 s after electrical stimulation at 3 Hz, there was a further increase in synchronisation to 0.31 ± 0.04, which decreased to 0.10 ± 0.01 in the last 2 s of the recordings (P<0.001). The spontaneous Ca^{2+} transients

remained more synchronous in the first compared to the last 2s after a period of electrical stimulation at 5 to 9 Hz. The mean synchronisation was 0.33 ± 0.04, 0.30 ± 0.05 and 0.28 ±0.05 in the first 2s and 0.10 ±0.02, 0.12 ± 0.02 and 0.14 ± 0.03 in the last 2 s after electrical stimulation at 5, 7 and 9 Hz respectively ($P<0.001$, 0.01 and 0.05) (Figure 3.23F).

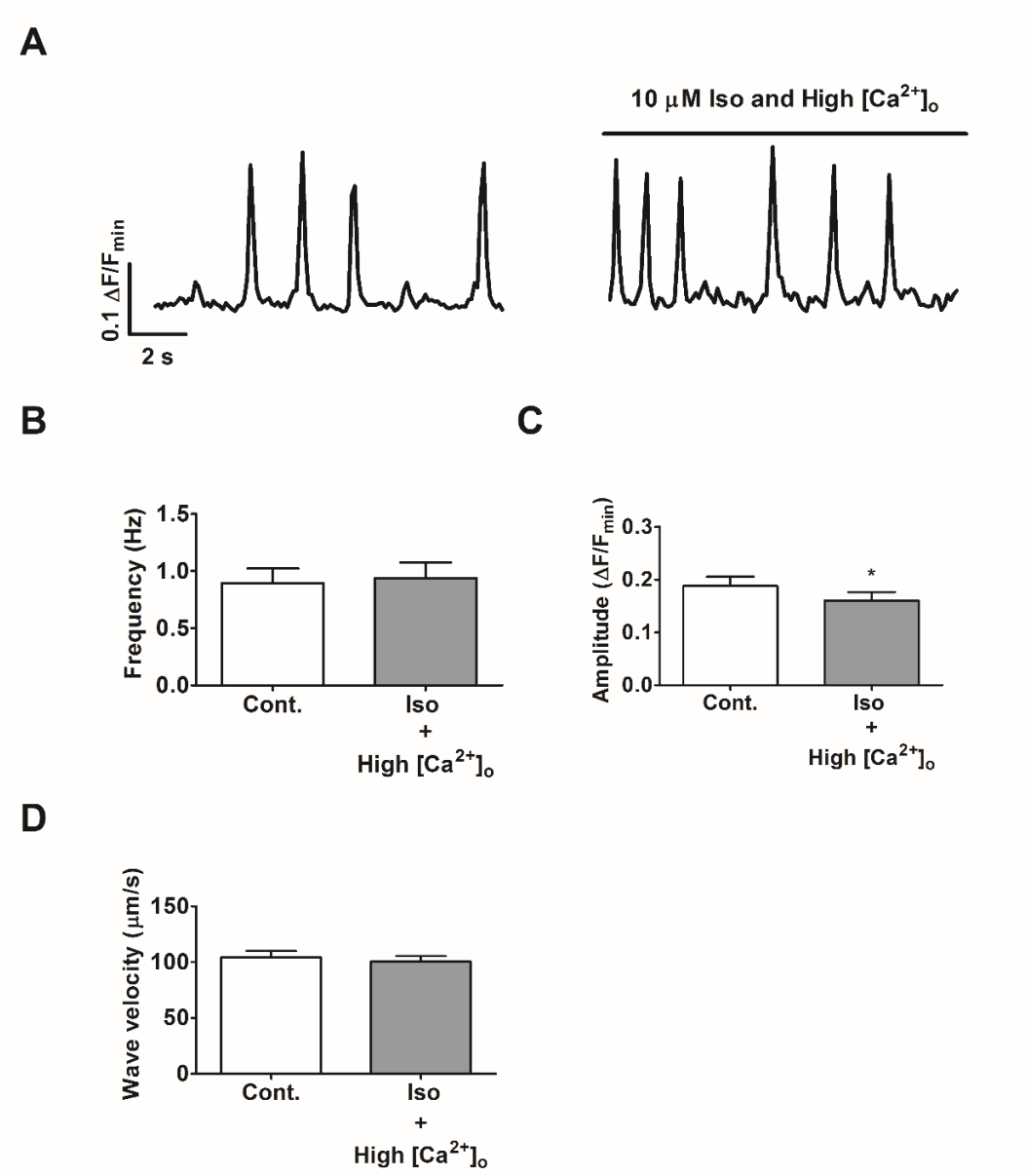

Figure 3.21. The effect of isoprenaline in combination with increasing the external Ca^{2+} concentration on the spontaneous Ca^{2+} transients in pulmonary vein cardiomyocytes. A. Representative recordings of fluo-4 fluorescence in a cardiomyocyte under control conditions, and in the same cell in the presence of isoprenaline (10 μM) and 4.5 mM $[Ca^{2+}]_o$. The mean frequency **(B)** and amplitude **(C)** of the spontaneous Ca^{2+} transients, and Ca^{2+} wave velocity **(D)** under control conditions and in the presence of isoprenaline (10 μM) and high $[Ca^{2+}]_o$. Data represent mean ± s.e.m., $^{**}P<0.01$ and n = 60 cardiomyocytes from 7 PVs from 7 rats for frequency and amplitude and n = 22 cardiomyocytes from 8 PVs from 8 rats for wave velocity.

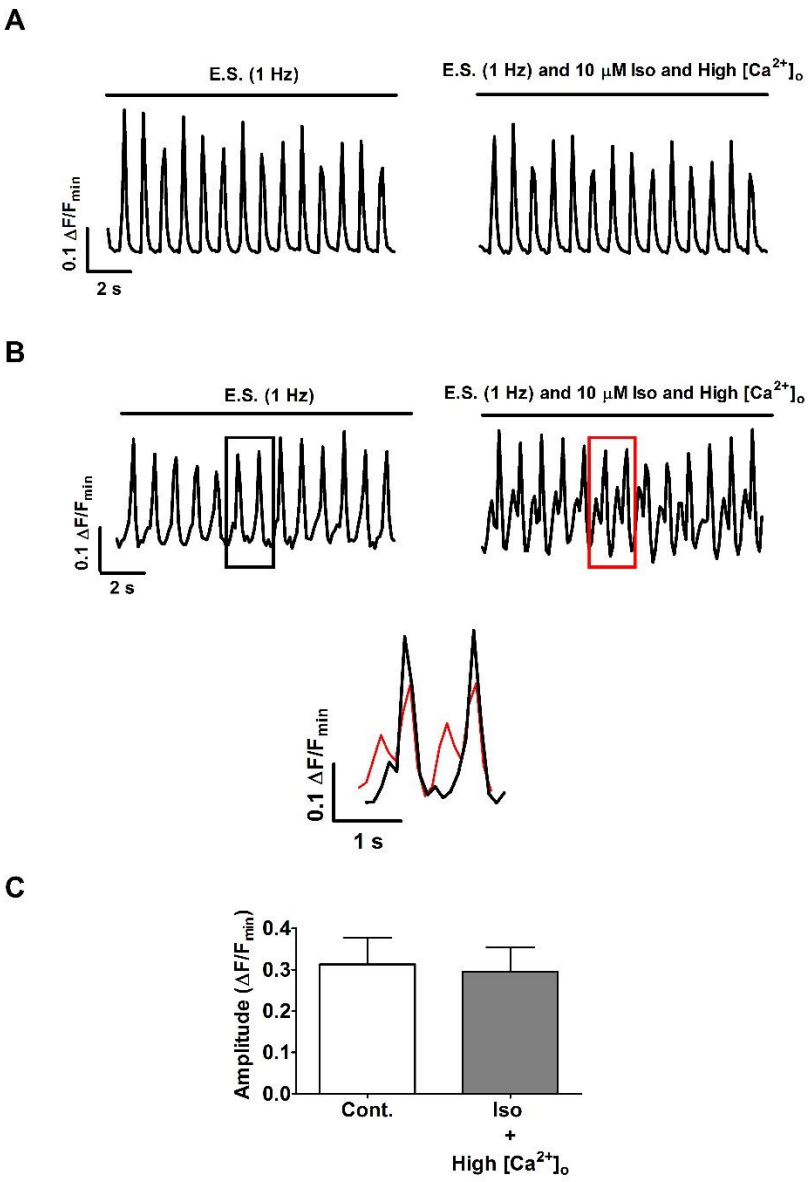

Figure 3.22. The effect of isoprenaline in combination with increasing the external Ca^{2+} concentration on the electrically evoked Ca^{2+} transients in the pulmonary vein. A. Representative recordings of fluo-4 fluorescence in the entire FOV during electrical stimulation at 1 Hz, and in the same region in the presence of isoprenaline (10 μM) and 4.5 mM $[Ca^{2+}]_o$. **B.** Representative recordings from a different preparation. A section from each recording, indicated by the black and red boxes, has been merged and presented over an expanded time scale **C**. The mean amplitude of the electrically evoked Ca^{2+} transients under control conditions and in the presence of isoprenaline (10 μM) and high $[Ca^{2+}]_o$. Data represent mean ± s.e.m. and n = 7 PVs from 7 rats.

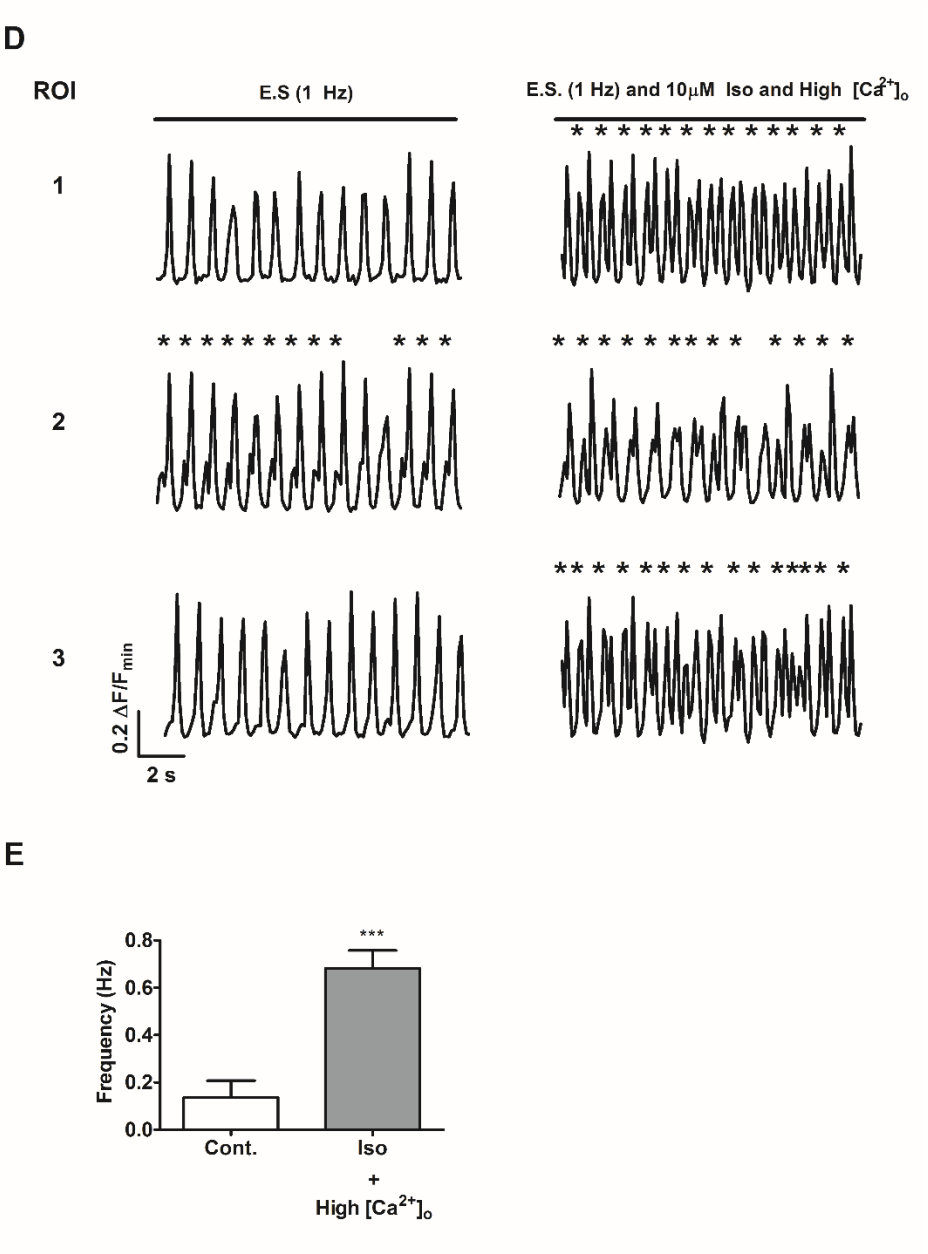

Figure 3.22. (cont.) D. Representative recordings displaying fluo-4 fluorescence in ROIs during electrical stimulation at 1 Hz in a control recording and in the presence of isoprenaline (10 μM) and after the external Ca^{2+} ($[Ca^{2+}]_o$) was increased to 4.5 mM. Spontaneous Ca^{2+} transients are indicated by the asterisks. **E.** Mean frequency of spontaneous Ca^{2+} during electrical stimulation at 1 Hz in the control recordings and after the $[Ca^{2+}]_o$ was increased. Data represent mean ± s.e.m. $^{***}P<0.001$ and n = 18 cardiomyocytes from 5 PVs from 5 rats.

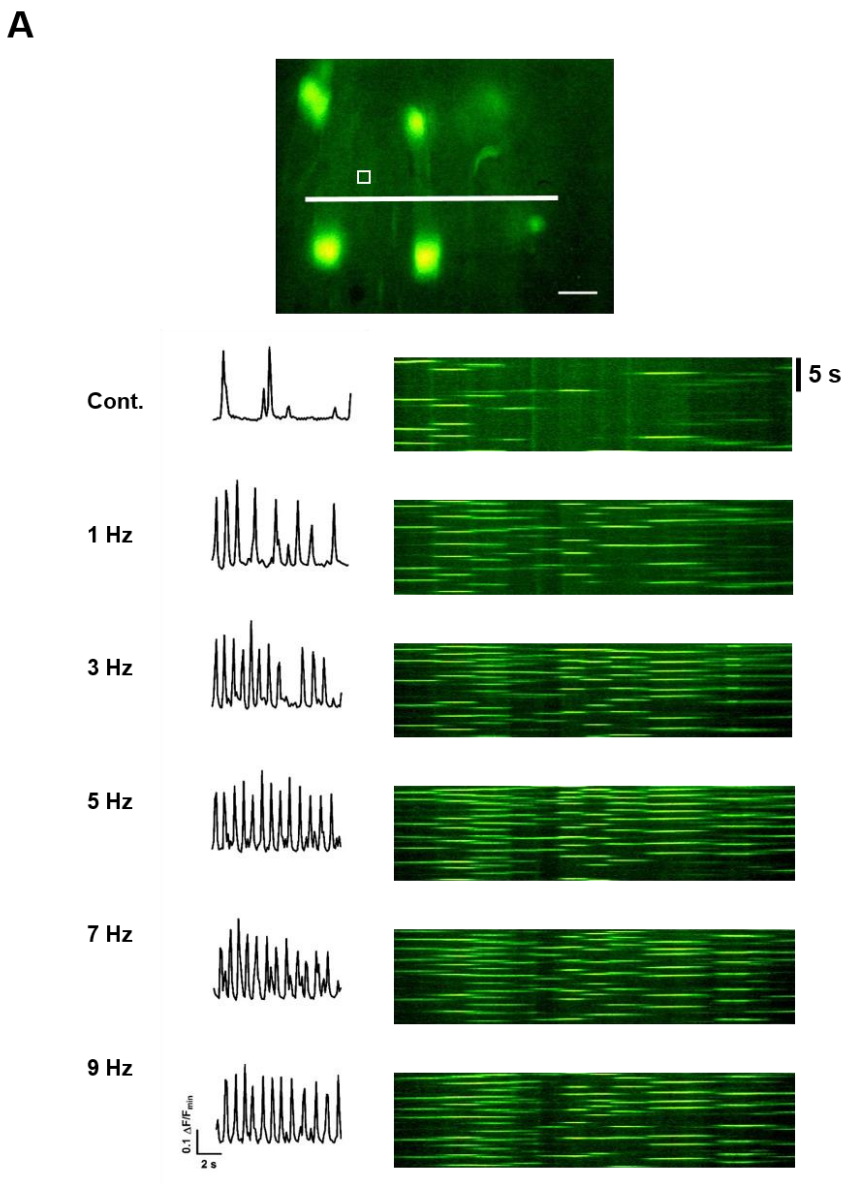

Figure 3.23. The effect isoprenaline in combination with raising the external Ca^{2+} on the subsequent spontaneous Ca^{2+} transients in the pulmonary vein after a period of electrical stimulation. A. Wide field image depicting the region of interest that was used to produce the fluorescence vs. time records and the while line used to generate the pseudo-linescans that are shown below. Images were obtained during a control recording with no prior electrical stimulation, and immediately following termination of a period of electrical stimulation at 1-9 Hz. The external Ca^{2+} concentration was raised from 2.5 mM to 4.5 mM, and the tissue was treated with isoprenaline (10 µM), 2 min prior to commencing the recordings. Scale bar represents 20 µm.

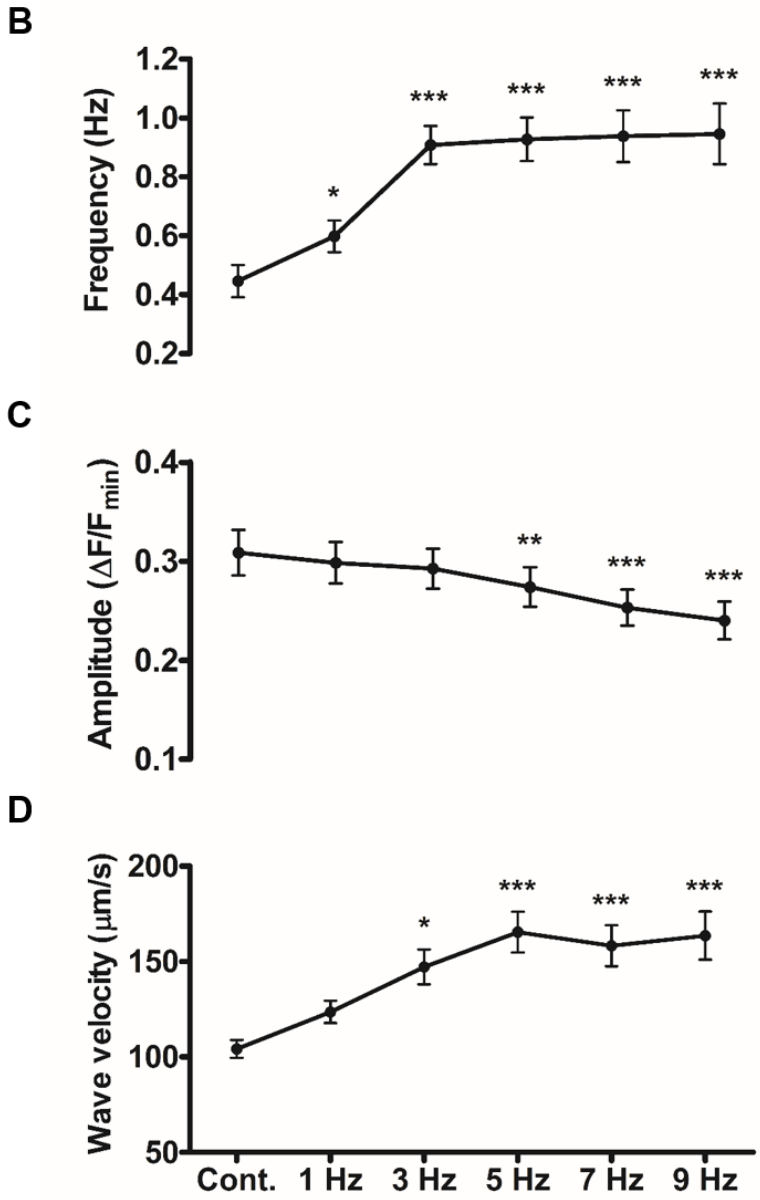

Figure 3.23 (cont.). The mean frequency **(B)** and amplitude **(C) of the spontaneous** Ca^{2+} transients and velocity of Ca^{2+} waves **(D)** in the presence of isoprenaline (10 μM) and high $[Ca^{2+}]_o$ in the control recordings with no prior electrical stimulation, and immediately following a period of electrical stimulation at 1-9 Hz. Data represent mean ± s.e.m., $^{*}P<0.05$, $^{**}P<0.01$., $^{***}P<0.001$ vs. Cont. and n = 36 cardiomyocytes from 7 PVs from 7 rats for frequency and amplitude and 30 cardiomyocytes from 7 PVs from 7 rats for wave velocity.

E

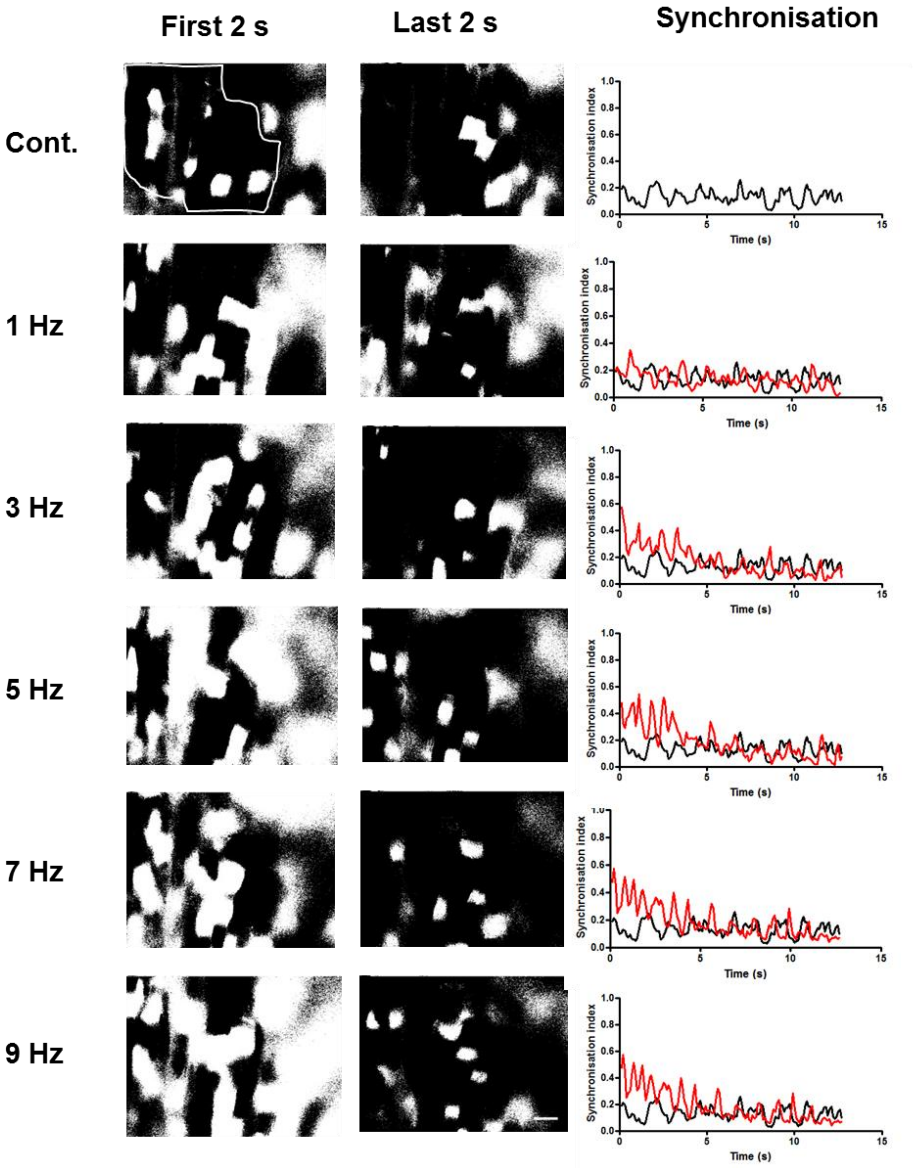

Figure 3.23. (cont.). E. Representative analysis of spontaneous Ca^{2+} transient synchronisation in the presence of isoprenaline and high external Ca^{2+} in a control recording with no prior electrical stimulation, and immediately following termination of a period of electrical stimulation at 1-9 Hz. The wide-field images are threshold images displaying pixels that have a greater intensity than half maximum as white. The mask used for the analysis is shown in white in the top left panel. The recordings on the right represent the synchronisation index for each frame over time in the control recording (black) and after a period of E.S. at 1-9 Hz (red). Scale bar represents 20 μm.

F

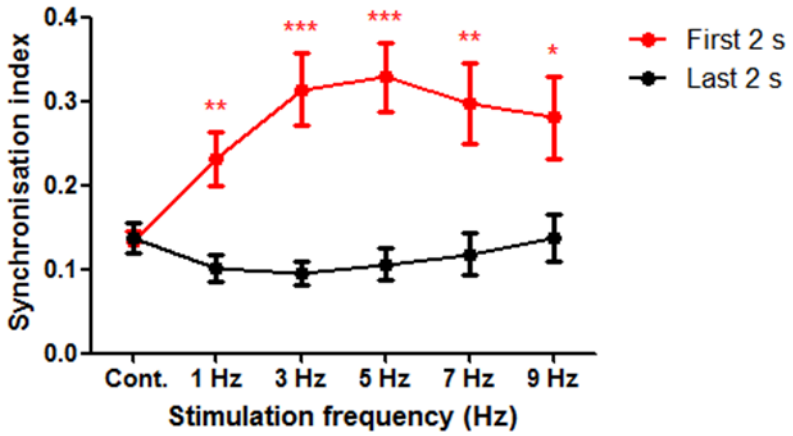

Figure 3.23. (cont.). F. The mean synchronisation during the first 2 s and last 2 s of the recording period in the control recordings with no prior electrical stimulation and immediately following a period of E.S. at 1-9 Hz. Data represent mean ± s.e.m. $^{*}P<0.05$, $^{**}P<0.01$ and $^{***}P<0.001$; first 2 s vs. last 2 s. n = 6 PVs from 6 rats.

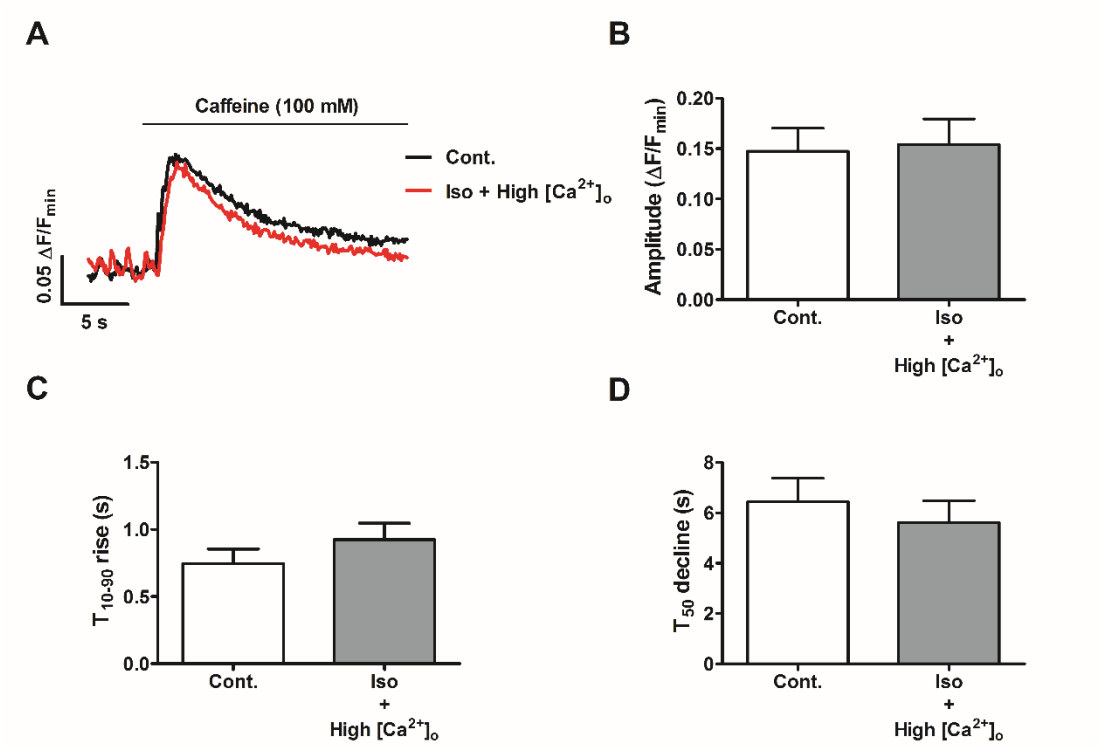

Figure 3.24. The effect of isoprenaline in combination with increasing the external Ca^{2+} concentration on the caffeine induced Ca^{2+} transient. A. Representative recordings of fluo-4 fluorescence in a region of tissue during the application of caffeine (100 mM) under control conditions (black), and in the same region in the presence of isoprenaline (10 µM) and 4.5 mM $[Ca^{2+}]_o$. Recordings were obtained immediately after a period of electrical stimulation at 3 Hz. **B.** The mean amplitude of the caffeine induced Ca^{2+} transient after a period of electrical stimulation at 3 Hz, under control conditions, and then in the presence of isoprenaline and high $[Ca^{2+}]_o$. **C.** The mean rise time (10 to 90%) of the caffeine induced Ca^{2+} transient after electrical stimulation at 3 Hz. **D.** The mean time to 50% decline from the peak of the caffeine induced Ca^{2+} transient after electrical stimulation at 3H and in the presence of isoprenaline and high Ca^{2+}. n = 10 PVs from 10 rats

3.3.11. Effect of noradrenaline on the spontaneous Ca^{2+} transients

In the presence of noradrenaline, synchronous Ca^{2+} transients, like those that were evoked by electrical stimulation, were not observed in any of the preparations. This was surprising since previous studies have shown that noradrenaline induces automaticity in the rat pulmonary vein (Doisne *et al.*, 2009; Maupoil *et al.*, 2007). In order to reconcile the differences between the observations in the present chapter and the literature, the temperature of the physiological salt solution was increased to near 37 °C.

The characteristics of the spontaneous Ca^{2+} transients were compared at room temperature and at 37 °C. The mean frequency of the spontaneous Ca^{2+} transients was significantly higher in the room temperature group, being 1.33 ± 0.08 Hz (n = 31 cardiomyocytes from 7 PVs from 7 rats), compared to 1.01 ± 0.12 Hz at 37 °C (n = 34 cardiomyocytes from 10 PVs from 8 rats, $P<0.05$) (Figure 3.25A). The mean amplitude of the spontaneous Ca^{2+} transients at room temperature was 0.2 ± 0.02 ($\Delta F/F_{min}$) and this was approximately double that at 37 °C, being 0.11 ± 0.01 ($\Delta F/F_{min}$) (n = 34 cardiomyocytes from 10 PVs from 8 rats, $P<0.001$) (Figure 3.25B). In contrast to the frequency and amplitude, the wave velocity was not significantly different between the two groups, where it was 118 ± 5.57 µm/s at room temperature (30 cardiomyocytes from 7 PVs from 7 rats) and 129.4 ± 10.51 µm/s at 37 °C (n = 18 cardiomyocytes from 6 PVs from 4 rats, n.s.) (Figure 3.25C).

As the properties of spontaneous Ca^{2+} transients were different at 37 °C compared to room temperature, time matched control recordings were also obtained. The mean frequency of spontaneous Ca^{2+} transients was 1.01 ± 0.12 Hz and was not significantly different after a 2 min break in the recording, at 0.91 ± 0.11 Hz (n = 34 cardiomyocytes from 10 PVs from 8 rats, n.s.) (Figure 3.26A and B). The mean amplitude was 0.11 ± 0.01 ($\Delta F/F_{min}$), and in this case was significantly changed after 2 min, being 0.09 ± 0.01 ($\Delta F/F_{min}$) (n = 34 cardiomyocytes from 10 PVs from 8 rats, $P<0.01$.) (Figure 3.26A and C). The wave velocity was not significantly different after 2 min, being

129.4 ± 10.51 µm/s in the initial recording and 133.8 ± 9.84 µm/s after 2 min (n = 17 cardiomyocytes from 6 PV from 4 rats, n.s.) (Figure 3.26D).

In the presence of noradrenaline, there was a significant decrease in the amplitude of the spontaneous Ca^{2+} transients from 0.13 ± 0.02 ($\Delta F/F_{min}$) to 0.11 ± 0.02 ($\Delta F/F_{min}$) (n = 24 cardiomyocytes from 7 PVs from 7 rats, $P<0.05$) (Figure 3.27A and B). The frequency of the spontaneous Ca^{2+} transients was increased from 0.76 ± 0.08 Hz under control conditions to 0.96 ± 0.08 Hz in the presence of noradrenaline (n = 24 cardiomyocytes from 7 PVs from 7 rats, $P<0.05$) (Figure 3.27A and C). The mean velocity of the Ca^{2+} waves was 148.4 ± 16.41 µm/s under control conditions and this was not significantly affected at 143.9 ± 10.87 µm/s in the presence of noradrenaline (n = 11 cardiomyocytes from 5 PVs from 4 rats, n.s.) (Figure 3.27D).

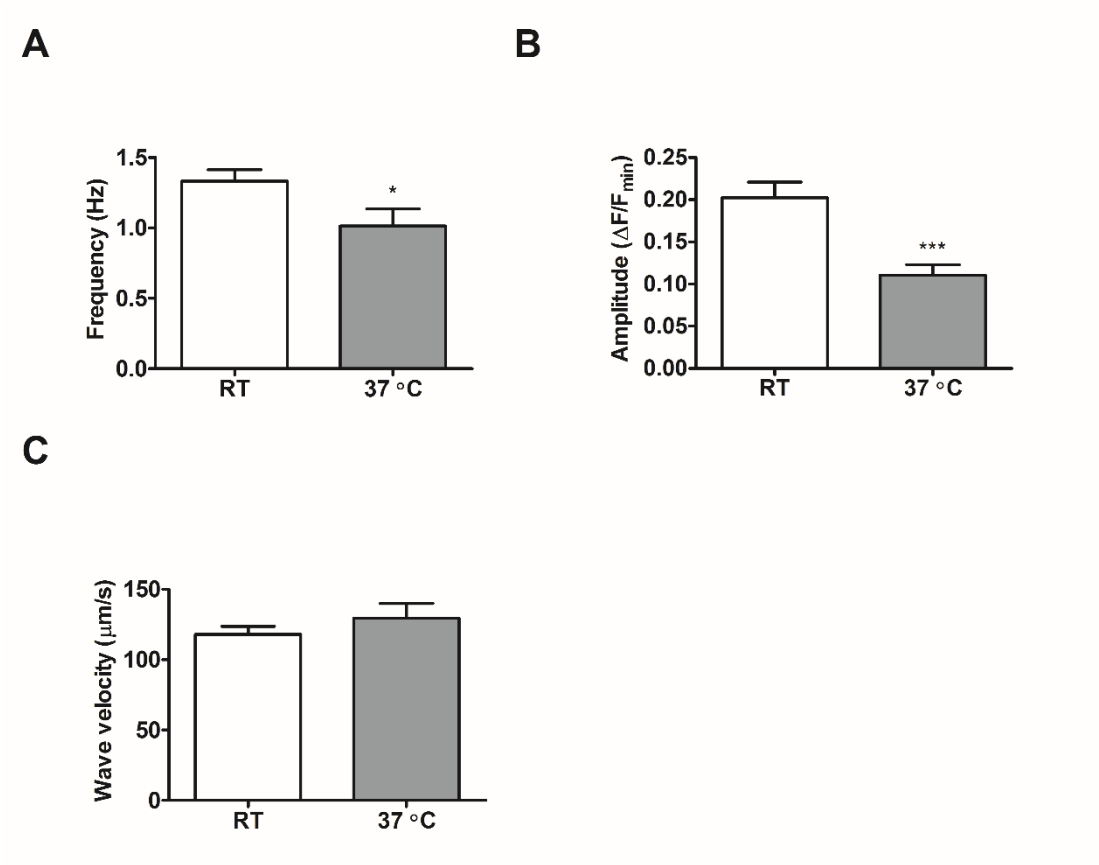

Figure 3.25. Comparison of the spontaneous Ca^{2+} transients at room temperature and at 37 °C. Mean frequency (A), amplitude (B) and velocity (C) of spontaneous Ca^{2+} transients under control conditions at room temperature (RT) and at 37 °C. Data represent mean ± s.e.m. $^{*}P<0.05$, $^{***}P<0.001$. n = 31 cardiomyocytes from 7 PVs from 7 rats for the frequency and amplitude and 30 cardiomyocytes from 7 PVs from 7 rats for the wave velocity at room temperature. For the frequency and amplitude at 37 °C, n = 34 cardiomyocytes from 10 PVs from 8 rats and for the wave velocity at 37 °C, n = 18 cardiomyocytes from 6 PVs from 4 rats.

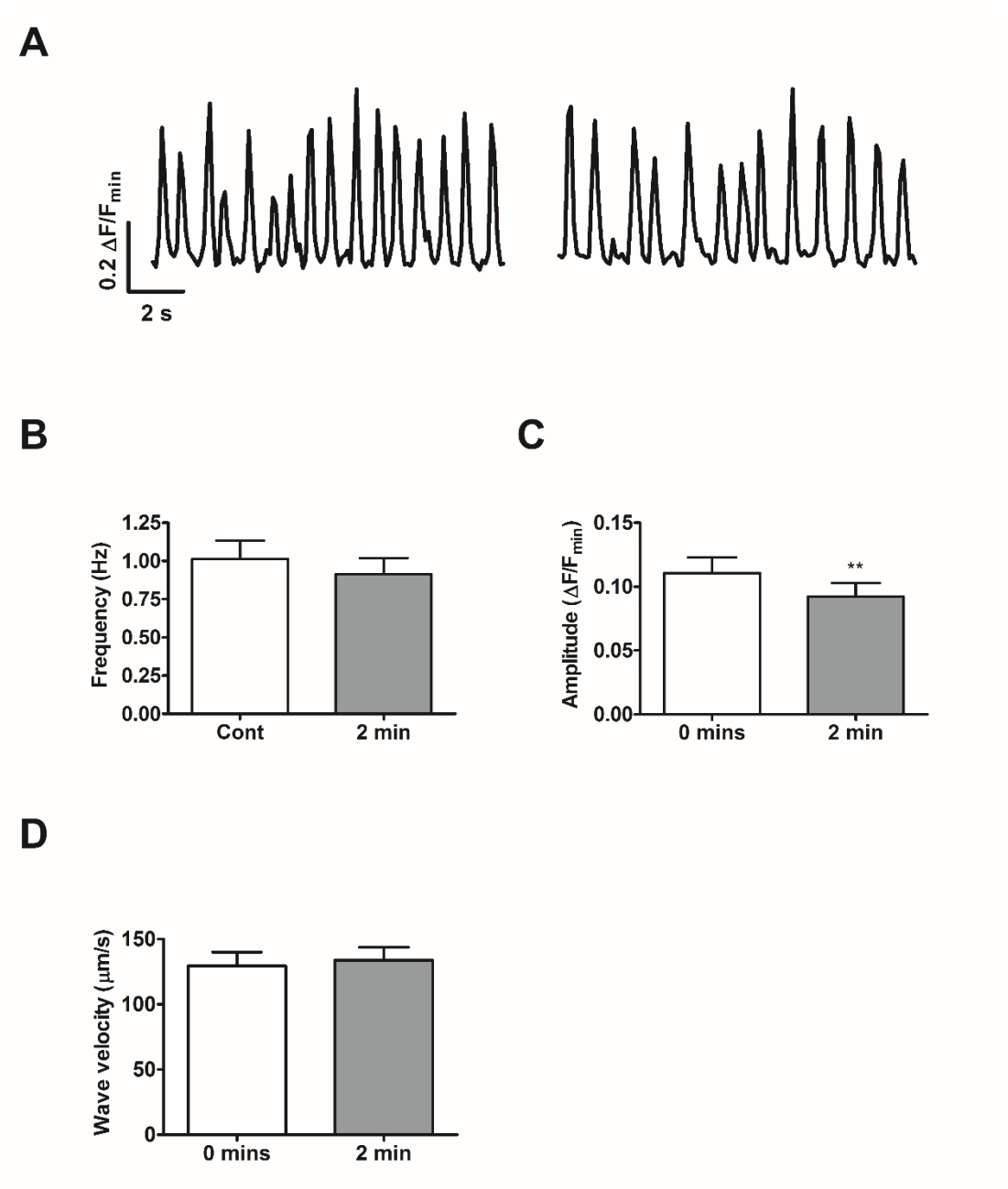

Figure 3.26. Time matched control recordings of spontaneous Ca^{2+} transients in pulmonary vein cardiomyocytes at higher temperature. A. Representative recording of fluo-4 fluorescence in a cardiomyocyte under control conditions and in the same cell after a 2 min break in the recording. The mean frequency **(B)** and amplitude **(C)** of the spontaneous Ca^{2+} transients, and Ca^{2+} wave velocity **(D)**. The temperature of the bath solution was maintained near 37 °C. n = 34 cardiomyocytes from 9 PVs from 7 rats for the frequency and amplitude and n = 17 cardiomyocytes from 6 PV from 4 rats for the wave velocity.

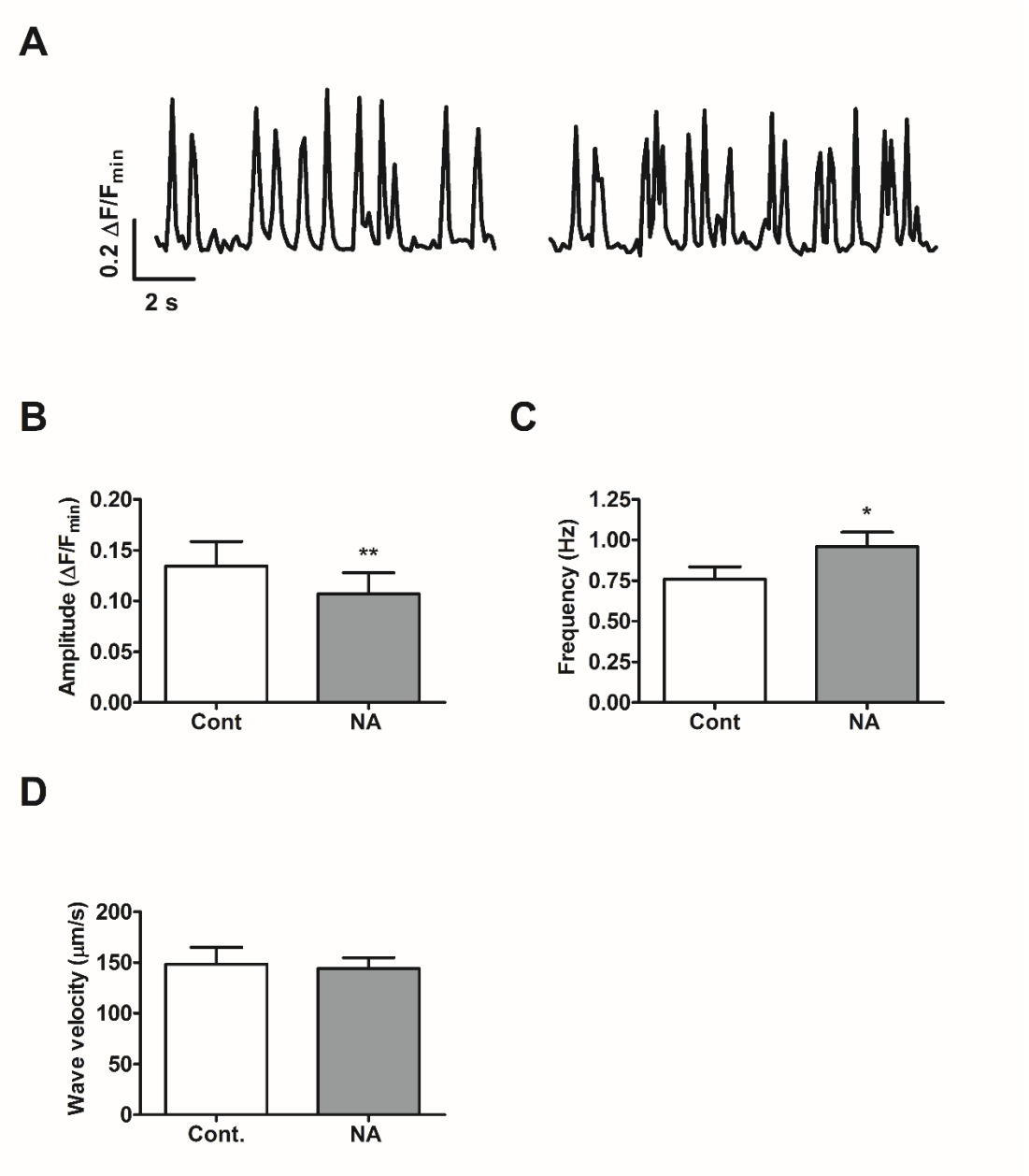

Figure 3.27. The effect of noradrenaline on spontaneous Ca^{2+} transients in pulmonary vein cardiomyocytes. A. Representative recordings of fluo-4 fluorescence in a cardiomyocyte under control conditions, and in the presence of noradrenaline (NA) (10 μM). The mean frequency **(B)** and amplitude **(C)** of the spontaneous Ca^{2+} transients, and Ca^{2+} wave velocity under control conditions, and in the presence of noradrenaline. The temperature of the bath solution was maintained near 37 °C. $^{*}P<0.05$; $^{**}P<0.01$ and n = 24 cardiomyocytes from 7 PVs from 7 rats for frequency and amplitude and n = 11 cardiomyocytes from 5 PVs from 4 rats for wave velocity.

3.4. Discussion

3.4.1. Spontaneous Ca^{2+} transients in the rat pulmonary vein

In the rat pulmonary vein, spontaneous Ca^{2+} transients were present in the absence of any external stimulation, and were usually apparent as waves that propagated along the longitudinal axis of the cell. Spontaneous Ca^{2+} transients could be observed in the extrapulmonary and intrapulmonary sections of the vein, which is consistent with the notion that in the rat, the cardiomyocyte sleeve extends beyond the hilus and into the lung (Hashizume *et al.*, 1998; Mueller-Hoecker *et al.*, 2008). The most notable feature of the spontaneous Ca^{2+} transients was that they were asynchronous, with neighbouring cardiomyocytes displaying spontaneous Ca^{2+} transients at distinct frequencies, and there was no consistent pattern of activity. Asynchronous spontaneous Ca^{2+} transients have previously been observed as waves propagating along the longitudinal axis of the cardiomyocytes in the pulmonary vein of the rat (Logantha *et al.*, 2010; Namekata *et al.*, 2010) and mouse (Rietdorf *et al.*, 2014). Circularly propagating Ca^{2+} waves, similar to those that were observed in the present study, have also been previously reported in the rat pulmonary vein (Namekata *et al.*, 2010). The spontaneous Ca^{2+} transients in the rat pulmonary vein shared similar characteristics to those in the mouse in that they were typically present as waves, and the frequency was highly variable between individual cardiomyocytes (Rietdorf *et al.*, 2014).

The velocity of spontaneous Ca^{2+} waves in the rat pulmonary vein was approximately 100 to 120 µm/s, which is greater than what has been reported in the mouse pulmonary vein, where the velocity was ~70 µm/s (Rietdorf *et al.*, 2014). However, this was similar to the rat ventricle, where the reported wave velocity ranges from 70 to 150 µm/s, usually being ~100 µm/s (Brette *et al.*, 2005; Kaneko *et al.*, 2000; O'Neill *et al.*, 2004; Okada *et al.*, 2005; Takamatsu & Wier, 1990; Wasserstrom *et al.*, 2010). When the external Ca^{2+} concentration was increased, a period of electrical stimulation at 3 Hz or greater induced a much larger increase in the frequency of the spontaneous Ca^{2+} transients than under normal conditions, and this was accompanied by significant

increase in the wave velocity. An increase in Ca^{2+} wave velocity has previously been reported in myocytes in rat ventricular tissue when the external Ca^{2+} concentration was increased, and this correlated with a marked increase in their frequency, suggesting that an increase in Ca^{2+} wave frequency predicts an increase in their velocity (Kaneko *et al.*, 2000; Minamikawa *et al.*, 1997; Wasserstrom *et al.*, 2010). Of particular note, Wasserstrom et al., (2010) reported that the Ca^{2+} wave velocity was approximately 15% greater following rapid pacing, which is similar to what was observed in the pulmonary vein in the present study.

According to the "fire-diffuse-fire" model of Ca^{2+} wave propagation, Ca^{2+} waves travel along the length of a cardiomyocyte due to release of SR Ca^{2+}, which diffuses and activates adjacent clusters of RyRs (Keizer & Smith, 1998; Keizer *et al.*, 1998). However, it is thought that Ca^{2+} wave propagation also depends on a RyR sensitisation wave front that provides local increases in SR Ca^{2+} as the wave travels, priming the RyRs for activation by cytosolic Ca^{2+} (Keller *et al.*, 2007). Thus, propagation of the Ca^{2+} wave is facilitated by SERCA uptake acting in tandem with an increase in cytosolic Ca^{2+} (Maxwell & Blatter, 2012). Inhibition of SERCA has been shown to reduce the Ca^{2+} wave velocity independently of any changes in SR Ca^{2+} load (Keller *et al.*, 2007), and the wave velocity is also slower in in ventricular myocytes from SERCA2 knockout mice (Stokke *et al.*, 2010). Furthermore, in rabbit ventricular myocytes that were permeabilised in order to be able to control intracellular Ca^{2+}, increasing the "external" Ca^{2+} concentration caused an increase in Ca^{2+} wave velocity, which occurred in parallel with increased SERCA activity (MacQuaide *et al.*, 2007). Direct evidence for this comes from the finding that the propagation velocity of Ca^{2+} waves is dependent on the latency period between the rise in intracellular Ca^{2+} at the wave front and the activation of SR Ca^{2+} release at the same location, during which there is a localised increase in SR Ca^{2+} (Maxwell & Blatter, 2012). In summary, these studies demonstrate that the rate of local Ca^{2+} uptake by SERCA is an important determinant of the velocity of Ca^{2+} waves in cardiac myocytes.

The spontaneous Ca^{2+} transients did not cause any notable contraction of the pulmonary vein, which suggests that they did not evoke action potentials. In isolated ventricular myocytes, spontaneous Ca^{2+} waves have been shown to activate a transient inward current (I_{ti}), which has been linked to arrhythmias (Berlin *et al.*, 1989; Cheng *et al.*, 1996). However, in the intact ventricle, spontaneous Ca^{2+} waves are not associated with spontaneous depolarisation, leading to the conclusion that their asynchronous nature means that any depolarisation that is generated dissipates into the surrounding inactive tissue (Fujiwara *et al.*, 2008; Hama *et al.*, 1998; Kaneko *et al.*, 2000; Wasserstrom *et al.*, 2010). Several studies that have monitored the electrical activity in rat pulmonary vein tissue have reported the absence of spontaneous action potentials under control conditions (Doisne *et al.*, 2009; MacLeod & Hunter, 1967; Miyauchi *et al.*, 2005; Paes de Almeida *et al.*, 1975). There is one study where spontaneous action potentials were recorded in the rat pulmonary vein, but the incidence was low at 3.8% (Namekata *et al.*, 2010).

Under control conditions the spontaneous Ca^{2+} transients were present at a lower frequency and amplitude at 37 ˚C, compared to at room temperature. This is similar to earlier studies in mouse and rat ventricular myocytes where Ca^{2+} sparks occurred at a lower frequency at 37 ˚C, compared to at room temperature (Ferrier *et al.*, 2003; Fu *et al.*, 2005). In mouse ventricular myocytes, the Ca^{2+} spark amplitude was reduced as well, while the caffeine induced Ca^{2+} transients were of a lower magnitude at 37 °C, suggesting that changes in SR Ca^{2+} load are responsible (Ferrier *et al.*, 2003). Increasing the temperature has also been shown to reduce the open probability and opening times of single sheep RyRs suspended in lipid bilayers, so it is possible that differences in the function of the Ca^{2+} release channels may also be occurring at different temperatures (Sitsapesan *et al.*, 1991). Despite temperature affecting the frequency of the spontaneous Ca^{2+} transients in rat pulmonary vein cardiomyocytes, it had no significant effect on the propagation velocity of the Ca^{2+} waves.

Spontaneous Ca^{2+} transients have previously been shown to be present under control conditions in the rat pulmonary vein when maintained in physiological salt solution

with a Ca^{2+} concentration of 1.8 mM (Logantha *et al.*, 2010), and also in the mouse pulmonary vein when maintained in Hank's balanced salt solution (HSS) with a Ca^{2+} concentration of 1.3 mM (Rietdorf *et al.*, 2014). In both species, spontaneous Ca^{2+} transients continued for a prolonged period in the absence of extracellular Ca^{2+} (Logantha *et al.*, 2010; Rietdorf *et al.*, 2014). The observations that spontaneous Ca^{2+} transients persist for a significant period in the absence of extracellular Ca^{2+} suggests that there is very little loss of Ca^{2+} from the cell during these spontaneous events and that the SR is very efficient at sequestering any Ca^{2+} that has been released.

3.4.2. Electrically evoked Ca^{2+} transients in the rat pulmonary vein

Electrical field stimulation evoked a synchronous rise in intracellular Ca^{2+} in neighbouring cardiomyocytes, as has previously been shown in the rat (Logantha *et al.*, 2010) and mouse pulmonary vein (Rietdorf *et al.*, 2014). Similar to the report in the mouse, the amplitude of the electrically evoked Ca^{2+} transients was irregular in some of the recordings (Rietdorf *et al.*, 2014). Beat to beat non-uniformity in Ca^{2+} transient amplitude is thought to be caused by differences in L-type Ca^{2+} current density and SR Ca^{2+} load, caused by partial depletion of the SR during spontaneous Ca^{2+} release (Díaz *et al.*, 2004; Llach *et al.*, 2011). However, it has also been suggested that variability in Ca^{2+} transient amplitude is due to the availability of RyRs for activation during each stimulus (Picht *et al.*, 2006). The amplitude of the electrically evoked Ca^{2+} transients was greater than that of the spontaneous ones, being approximately double in magnitude. This most likely reflects the observation that during electrical stimulation there is synchronisation of the Ca^{2+} release events, thereby producing a larger, and global, increase in intracellular Ca^{2+}. Essentially, global Ca^{2+} signals arise via the co-ordinated recruitment of many elementary Ca^{2+} release and entry channels.

Electrically pacing the pulmonary vein interrupted the spontaneous Ca^{2+} transients and there was a brief latency period after cessation of stimulation before they re-emerged, which is in agreement with the reports in the ventricle (Fujiwara *et al.*, 2008; Kaneko

et al., 2000; Wasserstrom *et al.*, 2010). However, spontaneous Ca^{2+} transients were occasionally present between the electrical stimuli, even when the pulmonary vein was maintained in an external Ca^{2+} concentration of 2.5 mM and paced at 1 Hz. This differs from the ventricle where an external Ca^{2+} concentration of 6 mM was required for spontaneous Ca^{2+} transients to be observed between electrical stimuli (Kaneko *et al.*, 2000).

Not every cardiomyocyte in the rat pulmonary vein responded to electrical stimulation. Instead, the electrically evoked Ca^{2+} transients tended to occur in discrete regions of the tissue. It is unclear why this was the case; however, cardiomyocytes that did not respond to electrical stimulation could still display spontaneous Ca^{2+} transients suggesting that these cells were loaded with fluo-4, and that SR Ca^{2+} release was functional.

3.4.3. The effect of β-adrenergic stimulation on the spontaneous and electrically evoked Ca^{2+} transients

In the presence of isoprenaline there was a small decrease in the frequency of the spontaneous Ca^{2+} transients, which was somewhat unexpected since isoprenaline has previously been shown to increase the frequency of spontaneous Ca^{2+} transients in ventricular myocytes (Bovo *et al.*, 2012; Curran *et al.*, 2010; Ullrich *et al.*, 2012). It has been suggested that this is due to phosphorylation of the RyRs resulting in an increased open probability (Bovo *et al.*, 2012; Curran *et al.*, 2007). However, it has also been proposed that isoprenaline increases the SR Ca^{2+} load through its effect on phospholamban phosphorylation (Lindemann *et al.*, 1983), which increases the likelihood for spontaneous Ca^{2+} transients to occur (Domeier *et al.*, 2012).

There are studies that suggest that isoprenaline could have a bimodal effect on cardiomyocytes depending on its concentration. In contractile studies on the rat pulmonary vein, automatic contractions could be induced with isoprenaline when

applied at nanomolar concentrations, in combination with the α-adrenoceptor agonist phenylephrine. However, such activity ceased when the concentration of isoprenaline was raised to 1 μM (Maupoil *et al.*, 2007). This also supports the notion that isoprenaline has a negative effect at higher concentrations in the rat pulmonary vein. A similar phenomenon has been observed in isolated ventricular myocytes, where scattered light fluctuations were used an index for spontaneous SR Ca^{2+} release, and it was found that increasing the concentration of isoprenaline beyond 1 μM reduced their occurrence under resting conditions (Kort & Lakatta, 1988).

The amplitude of the electrically evoked Ca^{2+} transients was slightly reduced in the presence of isoprenaline. This differs from the studies conducted on isolated pulmonary vein cardiomyocytes from the canine (Coutu *et al.*, 2006) and rabbit (Chang *et al.*, 2008), where isoprenaline significantly increased the amplitude, although a comparative study demonstrated that this effect was more prominent in left atrial myocytes (Chang *et al.*, 2008). A possible explanation is that the experiments in the present chapter were conducted at room temperature, whereas those on the rabbit and canine were carried out at approximately 37 °C (Chang *et al.*, 2008; Coutu *et al.*, 2006). Support for this comes from the observation that isoprenaline increases the amplitude of electrically evoked Ca^{2+} transients in atrioventricular node cells at 37 °C (Hancox *et al.*, 1994), but not at room temperature (Ridley *et al.*, 2008). It is noteworthy that pulmonary vein cardiomyocytes have been suggested to have a similar embryonic development to AV node cells, as they have been shown to express the human natural killer-1 (HNK-1) antigen Leu-7. Immunohistochemistry for HNK-1 is typically used to study developing atrioventricular node cells (Blom *et al.*, 1999), and should the embryonic development be reflected in the characteristics of the cells, this could mean that pulmonary vein cardiomyocytes share similar properties. On the other hand, the effect of isoprenaline on atrial and ventricular myocytes does not appear to be temperature dependent, as isoprenaline has been shown to increase the amplitude of electrically evoked Ca^{2+} transients at room temperature and at 37 °C in rat atrial (Jahnel *et al.*, 1992; Mackenzie *et al.*, 2002) and ventricular myocytes (Domeier *et al.*, 2012; Hussain & Orchard, 1997). Therefore, while it is certainly possible that temperature

has an influence on the effect of isoprenaline on the electrically evoked Ca^{2+} transients, further investigation will be required to explain the present findings.

The aforementioned studies conducted on ventricular myocytes also reported that isoprenaline increased the SR Ca^{2+} load (Domeier *et al.*, 2012; Hussain & Orchard, 1997). In the present study, as there was no increase in the amplitude of the electrically evoked Ca^{2+} transients, or increase in the frequency of the spontaneous Ca^{2+} transients, this would suggest that the SR Ca^{2+} load was not increased. The opening of RyRs is known to be modulated by the SR Ca^{2+} concentration (Bassani *et al.*, 1995; Fabiato, 1992; Lukyanenko *et al.*, 1999). Furthermore, it has been established that spontaneous Ca^{2+} release occurs when the concentration in the SR is above a critical threshold level (Jiang *et al.*, 2004; Overend *et al.*, 1997; Xiao *et al.*, 2007). Therefore it is possible that the reason why rat pulmonary vein cardiomyocytes have a tendency to display spontaneous Ca^{2+} transients under control conditions is because they already have a relatively high SR Ca^{2+} load, which would limit the capacity for it to be increased by experimental manipulations (Díaz *et al.*, 1997a).

It is important, however, to consider other reasons why pulmonary vein cardiomyocytes have a high propensity to display spontaneous Ca^{2+} transients under control conditions. For example, IP_3 receptors have been implicated in spontaneous Ca^{2+} signalling in cardiomyocytes from the rat pulmonary vein (Okamoto *et al.*, 2012) and atria (Mackenzie *et al.*, 2002). Furthermore, inhibition of IP_3 receptors by 2-APB has been shown to mostly inhibit spontaneous Ca^{2+} transients in the rat pulmonary vein (Logantha *et al.*, 2010). In isolated rat atrial myocytes, treatment with endothelin-1 induced arrhythmogenic Ca^{2+} transients with a similar incidence as a membrane permeable form of IP_3, and this arrhythmogenic activity was inhibited by 2-APB (Mackenzie et al., 2002).

Another potential reason why pulmonary vein cardiomyocytes have a tendency to display spontaneous Ca^{2+} transients under control conditions is that their threshold for

SR Ca^{2+} release is relatively low. If the threshold for spontaneous Ca^{2+} release is low then there is a greater probability of spontaneous Ca^{2+} transients occurring at a given SR Ca^{2+} content compared to in cardiomyocytes with a higher threshold for spontaneous SR Ca^{2+} release (Eisner *et al.*, 2013 for review). A classic example of this is in heart failure, where enhanced NCX expression and function (Hasenfuss & Pieske, 2002; Litwin & Zhang, 2002), in addition to reduced SERCA activity (Piacentino *et al.*, 2003), leads to a reduced SR Ca^{2+} content due to greater removal and less sequestering of intracellular Ca^{2+} (Piacentino *et al.*, 2003). However, spontaneous SR Ca^{2+} release is reported as being increased in heart failure (Ai *et al.*, 2005; Curran *et al.*, 2007; Shannon *et al.*, 2003), suggesting that there is a re-setting of the steady state to allow more Ca^{2+} to be released at a lower SR content than in the non-failing heart. Consequently, cardiomyocytes from the failing heart are more prone to triggered arrhythmias arising from β-adrenergic stimulation (Pogwizd *et al.*, 2001).

3.4.4. The effect of increasing the external Ca^{2+} concentration on the spontaneous and electrically evoked Ca^{2+} transients

The frequency of spontaneous Ca^{2+} transients in the pulmonary vein was slightly reduced when the external Ca^{2+} concentration was increased. This is in contrast to studies on the rat ventricle and isolated myocytes, where the frequency of spontaneous Ca^{2+} waves was shown to continue to increase as the external Ca^{2+} concentration was raised as high as 5 to 6 mM (Díaz *et al.*, 1997a; Kaneko *et al.*, 2000). As alluded to earlier, an external Ca^{2+} concentration of 6 mM was required for spontaneous Ca^{2+} transients to be present between repetitive electrical stimuli in the ventricle (Kaneko *et al.*, 2000), whereas in the pulmonary vein, this phenomenon was evident when the external Ca^{2+} concentration was 2.5 mM. This suggests that there a greater degree of SR Ca^{2+} loading in the pulmonary vein cardiomyocytes at a lower external Ca^{2+} concentration compared to ventricular myocytes.

The amplitude of the electrically evoked Ca^{2+} transients was unaffected by increasing the external Ca^{2+} concentration, which could possibly be due to the cardiomyocytes

having large SR Ca^{2+} loads to begin with. In support of this hypothesis, rabbit pulmonary vein cardiomyocytes that display spontaneous Ca^{2+} transients have been shown to respond to electrical stimulation with Ca^{2+} transients that were larger in magnitude than those evoked in cardiomyocytes that did not display spontaneous Ca^{2+} transients. Furthermore, the rabbit pulmonary vein cardiomyocytes that displayed spontaneous Ca^{2+} transients had larger SR Ca^{2+} loads than those without spontaneous activity (Chang *et al.*, 2008). This suggests that the amplitude of the electrically evoked Ca^{2+} transients is dependent on the SR Ca^{2+} load and cardiomyocytes that display spontaneous Ca^{2+} activity have a more replete SR. An alternative explanation is that Ca^{2+} dependent inactivation of the LTCCs may be occurring. Ca^{2+} dependent inactivation is caused by an elevated intracellular Ca^{2+} concentration (Haack & Rosenberg, 1994), and is thought to be mediated by calmodulin, which is bound to the carboxy terminal of the channel (Bers, 2008 for review; Peterson *et al.*, 2000; Zühlke *et al.*, 1999). This could be acting as a protective negative feedback mechanism, limiting the amount of Ca^{2+} influx.

In some preparations, when the pulmonary vein was maintained in solution containing a high external Ca^{2+} concentration, there was evidence of a rise in the fluorescence signal in the entire field of view preceding the electrically evoked response. The frequency of spontaneous Ca^{2+} transients occurring between those that were electrically evoked was considerably increased, suggesting that this was indeed caused by spontaneous Ca^{2+} transients occurring in multiple cardiomyocytes in the field of view at the same time. It has been shown in ventricular myocytes that spontaneous Ca^{2+} waves cause a measurable depletion of SR Ca^{2+} (Díaz *et al.*, 1997b; MacQuaide *et al.*, 2009). Therefore, it is not unreasonable to assume that if the frequency of spontaneous Ca^{2+} transients was increased, this would equate to an increased rate of depletion between the electrically evoked Ca^{2+} transients, thereby reducing the available Ca^{2+} for release during each electrical stimulus.

3.4.5. The effect of a period electrical stimulation on the subsequent spontaneous Ca^{2+} transients

In order to characterise the relationship between the electrically evoked and spontaneous Ca^{2+} transients, the frequency of the spontaneous Ca^{2+} transients was examined immediately after periods of electrical stimulation at increasing frequencies. It was found that following a period of electrical stimulation at 3 Hz or greater, there was an increase in the frequency of the subsequent spontaneous Ca^{2+} transients, compared to the control solution with no prior stimulation. The frequency of spontaneous Ca^{2+} transients was increased further following electrical stimulation at higher frequencies (5 to 7 Hz). Similar findings have been reported in the rat ventricle, where the frequency of spontaneous Ca^{2+} transients was increased after a period of electrical stimulation at 1 Hz, and then continued to increase when the rate of prior electrical stimulation was increased to 2 and 3 Hz (Kaneko *et al.*, 2000), In another study, the frequency of spontaneous Ca^{2+} transients was found to be greater following a period of stimulation at 5 Hz compared to 2 Hz (Wasserstrom *et al.*, 2010).

In the presence of isoprenaline, the increase in the frequency of spontaneous Ca^{2+} transients that was observed after a period of electrical stimulation, was more pronounced, and reached significance after stimulation at a lower frequency of 1 Hz. Isoprenaline has been shown in ventricular papillary muscle to increase fluctuations in scattered light after termination of electrical stimulation, which infers that there was increased SR Ca^{2+} release. However, isoprenaline, when applied to the papillary muscle in the absence of any prior electrical stimulation, caused a slight reduction in the scattered light fluctuations (Kort & Lakatta, 1988). This dual effect of isoprenaline could explain why, in the pulmonary vein, isoprenaline only influenced the characteristics of the spontaneous Ca^{2+} transients after a period of electrical stimulation. It has been shown more recently in the ventricle that, following a period of electrical stimulation at 2 Hz or greater in the presence of isoprenaline, the spontaneous Ca^{2+} transients re-emerged at an increased frequency. Unlike when the ventricle was maintained in control solution, this was accompanied by oscillatory

depolarisations and triggered action potentials, suggesting that this mechanism could be arrhythmogenic (Fujiwara *et al.*, 2008).

In the pulmonary vein, raising the external Ca^{2+} concentration increased the frequency of spontaneous Ca^{2+} transients after electrical stimulation to a greater extent than in the control solution, or in the presence of isoprenaline. Similar findings have been made in the rat ventricle, where ECG recordings demonstrated extra-systoles following a period of electrical stimulation at 5 Hz, when the external Ca^{2+} concentration was 6 mM (Wasserstrom *et al.*, 2010). Of particular note, when an extra-systole occurred, spontaneous Ca^{2+} transients were present in all of the cardiomyocytes in the field of view (Wasserstrom *et al.*, 2010).

Based on the observations in the present chapter, it is evident that spontaneous SR Ca^{2+} release in rat pulmonary vein cardiomyocytes is not maximal under control conditions and can occur at an increased frequency. The maximum frequency of spontaneous Ca^{2+} transients that was recorded in a cardiomyocyte under control conditions during the entire series of experiments was 3.17 Hz at room temperature and 2.84 Hz at 37 °C. Given that the resting heart rate of the rat is 330-480 b.p.m., under resting conditions, the activity in the pulmonary vein is likely to be suppressed by the normal sinus rhythm. The contractile studies reported herein show that the frequency of automaticity reached a maximum of approximately 5-6 Hz in the presence of noradrenaline, which suggests that under the experimental conditions used in the Ca^{2+} imaging studies in the present chapter, the spontaneous Ca^{2+} transients would be unlikely to produce automaticity, at least in the manner observed in the contractile studies, which will be covered in the next chapter.

It was apparent in the representative recordings that, in the presence of isoprenaline or a high external Ca^{2+} concentration, the initial spontaneous Ca^{2+} transients after a period of electrical stimulation at 5 Hz were simultaneously present in most or all of the cardiomyocytes in the field of view. Further analysis showed that there was a transient

increase in Ca^{2+} transient synchronisation lasting for a few seconds before returning to normal levels. Of particular importance, the synchronisation could reach as high as 0.8 to 0.9 at the point in which spontaneous Ca^{2+} transients re-emerged after the period of electrical stimulation. This means that 80-90% of the pixels within the region of tissue shows an increase in intracellular Ca^{2+} at the same time. This is similar to the studies in the ventricle (Fujiwara *et al.*, 2008; Wasserstrom *et al.*, 2010), the former of which used mathematical modelling of the latency period between spontaneous Ca^{2+} transients to show that they occurred synchronously after a period of electrical stimulation and that the spontaneous Ca^{2+} transient synchronicity correlated with the size of delayed after depolarisations (Wasserstrom *et al.*, 2010).

It is unclear why increasing the external Ca^{2+} concentration had the greatest effect on the frequency of spontaneous Ca^{2+} transients after a period of electrical stimulation, despite there being a slight decrease under unstimulated conditions. In the rat pulmonary vein, spontaneous Ca^{2+} transients have been shown to be largely abolished by the application of ryanodine (Logantha *et al.*, 2010); therefore, it is likely that the increase in frequency, which was observed after a period of electrical stimulation, was due to modification of SR Ca^{2+} release.

Spontaneous Ca^{2+} release from the SR is not only regulated by the cytosolic Ca^{2+} levels (Rousseau *et al.*, 1986), but also by the SR Ca^{2+} concentration, through a luminal sensing mechanism located on the RyR (Bassani *et al.*, 1995; Chen *et al.*, 2014; Fabiato, 1992; Györke & Terentyev, 2008; Keller *et al.*, 2007; Lukyanenko *et al.*, 2001). In the rat ventricle, it has been shown that the frequency of spontaneous Ca^{2+} waves was higher in myocytes that had a greater SR Ca^{2+} load (Kaneko *et al.*, 2000; Miura *et al.*, 1999). This suggests that the SR Ca^{2+} load determines the frequency of spontaneous Ca^{2+} transients and, should this be the case in the rat pulmonary vein cardiomyocytes, then manipulations that increase the frequency of spontaneous Ca^{2+} transients would also be expected to have increased the SR Ca^{2+} load.

Caffeine was used to examine if the increased frequency of spontaneous Ca^{2+} transients was due an increased SR Ca^{2+} content. Caffeine was used to examine if the increased frequency of spontaneous Ca^{2+} transients was due an increased SR Ca^{2+} content. A brief period of electrical stimulation at 5 Hz had no effect on the magnitude, rise time or decline of the caffeine induced Ca^{2+} transient. Similarly, after a period of electrical stimulation when the external Ca^{2+} concentration was increased and the pulmonary vein was treated with isoprenaline, there was no significant effect on any of the parameters of the caffeine induced Ca^{2+} transient. Most of the studies that have estimated the SR Ca^{2+} content using caffeine have been conducted on isolated cells, whereas the experiments in the present chapter were performed using intact tissue. Due to the ability to gain a closer proximity when applying caffeine to isolated cells, the upstroke velocity of the caffeine induced Ca^{2+} transient appears to be faster in the studies that used isolated ventricular myocytes (Chang *et al.*, 2008; Coutu *et al.*, 2006; Díaz *et al.*, 1997a; Varro *et al.*, 1993), or isolated pulmonary vein cardiomyocytes (Dr Stuart Cruikshank, Robert Gordon University; *personal communication*). Therefore, it is possible that the slower application of caffeine to the multicellular preparation means that Ca^{2+} efflux was already occurring before the SR was depleted, which would limit the magnitude of the caffeine induced Ca^{2+} transient (Bassani *et al.*, 1992; Bers, 2000a; Terracciano *et al.*, 1995).

Another factor to be taken into consideration is the timing of the application of caffeine. Similar to the studies in the ventricle (Fujiwara *et al.*, 2008; Minamikawa *et al.*, 1997), there was a transient latency period between cessation of electrical stimulation to the re-emergence of the spontaneous Ca^{2+} transients. However, due to the technical limitations of using the puffer ejection pipette, caffeine was not applied until up to 3 s after a period of electrical stimulation. It therefore cannot be ruled out that there was an initial increase in the SR Ca^{2+} load which, because of the increased frequency of spontaneous Ca^{2+} transients, resulted in a more rapid depletion of Ca^{2+} from the SR. It has been shown in ventricular myocytes that, increasing the frequency of spontaneous Ca^{2+} transients by applying a low concentration of caffeine causes a reduction in the SR Ca^{2+} load (Domeier *et al.*, 2010; Venetucci *et al.*, 2007).

While it is clear that there are limitations to the approach used to estimate the SR Ca^{2+} content in the present studies, it is unclear what impact they would have had on the results. Therefore, the conclusion that a period of electrical stimulation did not have any effect on the SR Ca^{2+} load should be approached with caution. In future, it would be useful to use an approach that provides higher temporal resolution when assessing the SR Ca^{2+} content and Ca^{2+} buffering processes, as well as conducting these studies on isolated cells. It has been shown in voltage-clamped rat and ferret ventricular myocytes that the application of caffeine results in an increase in intracellular Ca^{2+} and an inward electrogenic NCX exchange current as Ca^{2+} is extruded from the cell. The integral of the Ca^{2+} transient and NCX current could be used to quantify the total Ca^{2+} released from the SR and extruded via the NCX (Trafford *et al.*, 1999; Varro *et al.*, 1993). Therefore, such an approach in the pulmonary vein cardiomyocytes could provide a more accurate technique to assess the SR Ca^{2+} content.

If Ca^{2+} waves occur in cardiac myocytes when the SR Ca^{2+} concentration is above a critical threshold level (Jiang *et al.*, 2004; Overend *et al.*, 1997; Venetucci *et al.*, 2008 for review), then the SR Ca^{2+} load in the pulmonary vein cardiomyocytes appears to already be above this threshold, given the presence of spontaneous Ca^{2+} transients and Ca^{2+} waves under control conditions. The relationship between spontaneous SR Ca^{2+} release and SR content has been shown to be highly non-linear in ventricular myocytes, being exponential in the range in which spontaneous Ca^{2+} waves are present. Due to this steep function, increasing cellular Ca^{2+} loading will increase the frequency of spontaneous Ca^{2+} transients in the absence of any marked changes in SR Ca^{2+} content (Díaz *et al.*, 1997a for review; Shannon *et al.*, 2002; Venetucci *et al.*, 2008). It is therefore possible that the SR Ca^{2+} load in pulmonary vein cardiomyocytes is in this range under control conditions in the rat pulmonary vein.

It is already known that Ca^{2+} handling in rat cardiac myocytes differs from that of larger mammals such as the rabbit. In the rat, SERCA accounts for approximately 90% of cytosolic Ca^{2+} removal during diastole, compared to 70% in the rabbit (Bassani *et al.*, 1994; Negretti *et al.*, 1993). It has been shown in rabbit ventricular myocytes that,

in the first 20 s after termination of electrical stimulation, the frequency of Ca^{2+} sparks is initially higher and then decreases along with the SR Ca^{2+} load. In rat ventricular myocytes, the frequency of Ca^{2+} sparks gradually increases over 10 to 20 s after electrical stimulation; however, this is not accompanied by an increase in the SR Ca^{2+} load and was instead suggested to be due to recovery of Ca^{2+} release channels from inactivation (Satoh *et al.*, 1997). Furthermore, in the rabbit, the SR Ca^{2+} load has been shown to be increased when the frequency of electrical stimulation is increased from 3 to 5 Hz, whereas it was unchanged in the rat (Maier *et al.*, 2000). All of these observations suggest that an intrinsic property of rat cardiac myocytes is that they have relatively high SR Ca^{2+} loads.

High-frequency electrical stimulation activates Ca^{2+}/calmodulin dependent protein kinase II (CaMKII) (Huke & Bers, 2007), which is known to phosphorylate RyRs, increasing their sensitivity to Ca^{2+}, and the open probability of the channel (Currie *et al.*, 2004; Guo *et al.*, 2006; Hain *et al.*, 1995; Wehrens *et al.*, 2004). Furthermore, it is thought that the activity of CaMKII is modulated by the frequency encoded, rather than the total amplitude, of the Ca^{2+} signal (De Koninck & Schulman, 1998). In isolated cardiomyocytes from the pig left ventricle, the frequency of Ca^{2+} sparks was shown to be increased by a period of high-frequency electrical stimulation, and this effect was prevented by inhibiting CaMKII with autocamtide-2-related inhibitory peptide (AIP) or KN-93 (Dries *et al.*, 2013). It is therefore possible that, in the pulmonary vein, increasing the frequency of electrical stimulation increased SR Ca^{2+} release due to CaMKII mediated phosphorylation of the RyRs.

CaMKII also phosphorylates phospholamban, to increase SERCA uptake (Kranias *et al.*, 1988). In permeabilised rabbit ventricular myocytes, increasing the external Ca^{2+} concentration increased SERCA activity, as well as the frequency and velocity of spontaneous Ca^{2+} waves. This was prevented by AIP, which suggests that CaMKII mediates the Ca^{2+} dependent modulation of SERCA activity. (MacQuaide *et al.*, 2007). Should this be the case in pulmonary vein cardiomyocytes, then according to the modified "fire-diffuse-fire" mechanism of Ca^{2+} wave propagation, which accounts for

the importance of dynamic SR Ca^{2+} re-uptake (Keller *et al.*, 2007), high-frequency electrical stimulation, in combination with raising external Ca^{2+}, could be increasing cellular Ca^{2+} loading, leading to enhanced SERCA activity and an increased rate of rise of SR Ca^{2+} at the cytosolic wave front (MacQuaide *et al.*, 2009; Maxwell & Blatter, 2012). The threshold for spontaneous Ca^{2+} release would therefore be reached more quickly, which would result in an increase in the frequency and velocity of the spontaneous Ca^{2+} transients, independently from changes in SR Ca^{2+} content (Eisner *et al.*, 2013 for review). Thus, while the explanation for the increase in frequency after electrical stimulation is unclear at the present time, two possibilities that warrant further investigation are an enhanced SR Ca^{2+} release or enhanced SERCA uptake of Ca^{2+}.

3.4.6. The effect of noradrenaline on the spontaneous Ca^{2+} transients

In the presence of noradrenaline there was a significant increase in the frequency of the spontaneous Ca^{2+} transients, and this was accompanied by a decrease in their amplitude. There was, however, no change in the propagation velocity. Noradrenaline has previously been shown to induce Ca^{2+} transients in rat pulmonary vein tissue; however, this was in cardiomyocytes that did not previously display any spontaneous activity (Namekata *et al.*, 2010). The findings with noradrenaline contrast to the earlier observations with isoprenaline, where there was a slight decrease in the frequency of the spontaneous Ca^{2+} transients. It has previously been shown in the rat pulmonary vein that automaticity in the form of contractions (Maupoil *et al.*, 2007) and action potentials (Doisne *et al.*, 2009) could only be induced by the co-activation of α and β-adrenoreceptors, and not by the sole application of isoprenaline. This could explain why in the present study only noradrenaline caused an increase in the frequency of the spontaneous Ca^{2+} transients. An alternative explanation for the different observations is that the experiments with noradrenaline were performed at higher temperature.

In the present chapter, due to the experiments being carried out at higher temperature, the effect of noradrenaline was assessed after 2 min. However, noradrenaline induced

automaticity in the rat pulmonary vein has been shown to occur up to 17 min following its application (Doisne *et al.*, 2009; Maupoil *et al.*, 2007). Therefore, the possibility that the frequency of spontaneous Ca^{2+} transients might be increased further if recordings were obtained over a longer time period cannot be excluded. Unfortunately, a limitation when performing Ca^{2+} imaging experiments at over 30 ºC is that the extrusion of fluorescent dyes from cells is accelerated (Di Virgilio *et al.*, 1990). This had a major impact when recording, as the quality of the images deteriorated rapidly at higher temperature, and often the fluorescence levels were too low for the images to be analysed. In future, better fluorescent indicators that are more resistant to higher temperatures will need to be examined. Alternatively, a different experimental approach will be required to resolve the issues associated with investigating the effect of noradrenaline over an extended period of time.

3.4.7. Summary

The main finding in the present chapter was that in the rat pulmonary vein, a period of electrical stimulation increased the frequency of the subsequent spontaneous Ca^{2+} transients. Furthermore, this effect was more pronounced in the presence of isoprenaline or if the extracellular Ca^{2+} concentration was increased. However, neither of these interventions increased the frequency of the spontaneous Ca^{2+} transients when no prior electrical stimulation was applied. When the SR Ca^{2+} content was estimated using caffeine, it was demonstrated that the there was no change following a period of electrical stimulation. However, due to the limitations of using caffeine in a multicellular preparation, these findings need to be regarded with caution. Although unlikely to be due to one single mechanism, a more detailed investigation will be required in order to explain these observations. Nevertheless, the interventions used in the present chapter caused the spontaneous Ca^{2+} transients to appear more frequently, which means that there could be greater chance of spontaneous Ca^{2+} transients appearing in the neighbouring cardiomyocytes at the same time (Wasserstrom *et al.*, 2010). Of particular note, there was sometimes an increase in Ca^{2+} in the entire field of view between electrically evoked Ca^{2+} transients. This is important because

mechanisms that increase the frequency and synchronicity of spontaneous SR Ca^{2+} release potentially underlie arrhythmogenic activity in the pulmonary vein.

Chapter 4

The effect of noradrenaline on the contractility of the rat pulmonary vein and the potential for automaticity

4.1. Introduction

The pulmonary vein myocardium is continuous with and electrically coupled to the left atrium (Challice *et al.*, 1974; Cheung, 1981a; Paes de Almeida *et al.*, 1975; Tasaki, 1969), which suggests that *in situ* the pulmonary veins contract according with the sinus rhythm. Magnetic resonance imaging (MRI) of the human heart and surrounding vasculature has since confirmed that the pulmonary veins display maximal contraction during atrial systole (Bowman & Kovács, 2005; Lickfett *et al.*, 2005), and the degree of contraction was reduced after the pulmonary veins were electrically isolated from the left atrium by ablation at the ostia (Atwater *et al.*, 2011).

4.1.1. Electrically evoked contractions of the pulmonary vein

In vitro studies on isolated segments from the rat pulmonary vein have observed rapid transient contractions in response to electrical field stimulation (MacLeod & Hunter, 1967; Maupoil *et al.*, 2007; Sweeney *et al.*, 1999). It was shown that the vein contracted according to the rate of electrical stimulation up to frequencies as high as 10 Hz, and as the stimulation frequency was increased, the resultant contractions became smaller in amplitude (MacLeod & Hunter, 1967). This phenomenon is known as a negative force-frequency relationship (FFR), and has also been reported in the mouse (Heubach *et al.*, 1999; Kirchhefer *et al.*, 2002) and rat atrium (Landmark & Refsum, 1977; Stemmer & Akera, 1986), as well as in rat ventricular tissue (Hoffman & Kelly, 1959; Maier *et al.*, 2000; Schouten & ter Keurs, 1986).

4.1.2. Pulmonary vein contractility is modulated by stimulation of β adrenoreceptors

In the rat pulmonary vein, activation of α and β adrenoreceptors with noradrenaline, or activation of β adrenoreceptors with isoprenaline, has been shown to have a positive inotropic effect, increasing the amplitude of the electrically evoked contractions (MacLeod & Hunter, 1967; Sweeney *et al.*, 1999). The positive inotropic effect of noradrenaline was completely attenuated by the β adrenoreceptor blocker propranolol

(MacLeod & Hunter, 1967), and mostly attenuated by β_1 blockade with atenolol (Sweeney *et al.*, 1999). This suggests that the β adrenoreceptor subtype is responsible for the regulation of the contractile force of the pulmonary vein.

Activation of muscarinic receptors with acetylcholine had a negative inotropic effect, decreasing the amplitude of the electrically evoked contractions, and this was prevented with the muscarinic antagonist atropine (MacLeod & Hunter, 1967; Sweeney *et al.*, 1999). From the studies described above, it can be argued that the contractility of the pulmonary vein myocardial sleeve is regulated by input from the neurotransmitters of the autonomic nervous system. Further support for this hypothesis comes from the reports that the human and canine pulmonary veins are highly innervated by autonomic nerves (Arora *et al.*, 2008; Chevalier *et al.*, 2005; Tan *et al.*, 2006).

4.1.3. Noradrenaline induced automaticity in the rat pulmonary vein

In the rat pulmonary vein, treatment with noradrenaline has been shown to induce automatic bursts of contractions that occurred independently of electrical stimulation (Maupoil *et al.*, 2007). Noradrenaline induced automaticity was inhibited by either the α_1 adrenoreceptor antagonist prazosin or the β_1 adrenoreceptor antagonist atenolol. Automaticity was not observed when the α and β agonists phenylephrine and isoprenaline were applied separately, but was with a combination of the agonists. Thus, it was concluded that noradrenaline induced automaticity occurs through the co-activation of α and β adrenoreceptors (Maupoil *et al.*, 2007). Subsequent electrophysiological studies showed that noradrenaline induces action potentials in rat pulmonary vein tissue (Doisne *et al.*, 2009; Namekata *et al.*, 2010), and in isolated pulmonary vein cardiomyocytes (Okamoto *et al.*, 2012). However, the cellular mechanisms underlying noradrenaline induced automaticity are currently unknown.

4.1.4. Possible mechanisms underlying noradrenaline induced automaticity in the pulmonary vein

4.1.4.1. Increase in intracellular cyclic AMP

The plant alkaloid forskolin directly activates adenylate cyclase, thereby increasing the cellular concentration of cyclic adenosine monophosphate (cAMP), which in turn activates protein kinase A (PKA) (Seamon *et al.*, 1981). In the isolated rat heart, treatment with forskolin has been shown to increase the myocardial cAMP levels and this was accompanied by premature atrial contractions and atrial fibrillation. This effect was prevented by pre-treatment with the L-type Ca^{2+} channel (LTCC) blocker nifedipine, suggesting that the cause was increased Ca^{2+} influx (Huang & Wong, 1989). In a recent study on human atrial trabeculae, forskolin and noradrenaline were reported to induce automatic contractions with a similar incidence (17% and 14% respectively). It was also shown using the whole-cell patch clamp technique, that the L-type Ca^{2+}current (I_{CaL}) was increased in the presence of forskolin, further supporting the role of intracellular Ca^{2+} in automaticity (Christ *et al.*, 2014).

4.1.4.2. Calcium/calmodulin dependent protein kinase II

The contribution of Ca^{2+}/calmodulin dependent protein kinase II (CaMKII) towards cardiac arrhythmias has recently become a focus of research due to its effect on several of the key proteins involved in Ca^{2+} signalling in cardiac myocytes. This includes the LTCCs (Dzhura *et al.*, 2000), ryanodine receptors (RyRs) (Hain *et al.*, 1995) and phospholamban, the regulatory protein of SERCA (Kranias *et al.*, 1988). Cardiac RyRs are phosphorylated by CaMKII at a distinct site (serine^{2845}), increasing their sensitivity to Ca^{2+} and the open probability of the channel, which can lead to increased spontaneous Ca^{2+} release from the SR (Wehrens *et al.*, 2004).

In isolated atrial myocytes from an experimental mouse model of atrial fibrillation, western blotting revealed that CaMKII mediated phosphorylation of the RyRs and PLN was increased (Chelu *et al.*, 2009). Phosphorylation of RyRs by CaMKII was

also found to be greater in atrial myocytes that were isolated from human patients with chronic atrial fibrillation, compared to patients in sinus rhythm. Furthermore, the levels of auto-phosphorylated CaMKII, which is a good indicator of CaMKII activity, were also reported to be higher in patients with chronic atrial fibrillation (Chelu *et al.*, 2009).

Inhibition of CaMKII with KN-93 has been shown to reduce the occurrence of spontaneous contractions in isolated ventricular myocytes from transgenic mice overexpressing CaMKIIδ (Sag *et al.*, 2009), which is the main cardiac isoform (Hoch *et al.*, 1999). Furthermore, isoprenaline induced arrhythmias were inhibited by KN-93 in the same transgenic mouse model *in vivo* (Sag *et al.*, 2009). Biochemical assays have indicated that CaMKII activity is activated after β adrenergic stimulation in ventricular myocytes, through a signalling pathway that is independent of increased cAMP (Wang *et al.*, 2004). Overall, this data suggests that CaMKII might play a role in aberrant Ca^{2+} handling and the generation of automaticity in cardiac myocytes. However, very little is known about the role of CaMKII in the pulmonary vein.

Another cAMP independent mechanism of β-adrenergic stimulation that could be potentially arrhythmogenic is stimulation of nicotinic acid adenine dinucleotide phosphate (NAADP) production. NAADP causes Ca^{2+} to be released from acidic vesicles, such as microsomes (Bak *et al.*, 2001), and its inhibition has been shown to reduce the incidence of isoprenaline induced spontaneous Ca^{2+} transients in mouse ventricular myocytes. Furthermore, NAADP inhibition has also been shown to prevent isoprenaline induced tachycardias *in vivo* (Nebel *et al.*, 2013). Two pore channels (TPRs), which are Ca^{2+} permeable lysosomal proteins, are thought to mediate NAADP evoked Ca^{2+} release, as mice lacking the TPR protein were less prone to ventricular arrhythmias induced by rapid pacing in the presence of isoprenaline. In isolated ventricular myocytes obtained from TPR knockout mice, NAADP failed to increase the amplitude of electrically evoked Ca^{2+} transients, unlike in myocytes obtained from wild type mice. Isoprenaline also increased the Ca^{2+} transient amplitude and this effect was reduced in TPR knockout mice. Inhibition of CaMKII supressed the NAADP

induced increase in Ca^{2+} transient amplitude in ventricular myocytes from wild type mice, suggesting that the effects of NAADP on Ca^{2+} handling in cardiac myocytes are mediated by CaMKII (Capel *et al.*, 2015).

4.1.4.3. Gap junction conductance

Gap junctions allow for the movement of ions and small molecules of less than 1.5 nm in diameter between neighbouring cells (Loewenstein, 1981; Saffitz *et al.*, 1994), and it is well established that gap junctions have a vital role in the conduction of electrical signals through cardiac tissue to produce co-ordinated contractions (Severs *et al.*, 2004; Spray & Burt, 1990). It has been shown in the ventricle that a small proportion of Ca^{2+} waves were able to propagate into adjacent myocytes (Kaneko *et al.*, 2000; Lamont *et al.*, 1998). Previous work in the laboratory has shown that, in the rat pulmonary vein, Ca^{2+} waves could propagate intercellularly (Logantha *et al.*, 2010). Therefore, it is possible that synchronisation of spontaneous Ca^{2+} transients in neighbouring cardiomyocytes could occur due to increased Ca^{2+} diffusion between neighbouring cardiomyocytes through gap junctions (Kimura *et al.*, 1995; Zhang *et al.*, 1996). Electrically uncoupling gap junctions has been implicated in the treatment of ventricular arrhythmias where, in canines that were subjected to brief occlusion of the left anterior descending coronary artery, the gap junction inhibitor carbenoxolone reduced the occurrence of ventricular premature beats and tachycardia (Papp *et al.*, 2007).

4.1.4.4. The Na^+/Ca^{2+} exchanger

In cardiac myocytes, the Na^+/Ca^{2+} exchanger (NCX) is activated by an increase in cytosolic Ca^{2+}, resulting in depolarisation due to Na^+ entry during the removal of Ca^{2+} (Egdell & MacLeod, 2000; Schlotthauer & Bers, 2000). This can result in afterdepolarisations, which, if above the threshold for eliciting action potentials, can trigger automaticity, as has been shown in the canine pulmonary vein (Patterson *et al.*, 2006).

The NCX inhibitor KB-R7943 has been shown to reduce the rate of spontaneous contractions and action potentials in the rabbit pulmonary vein in a concentration dependent manner. However, at concentrations exceeding 10 μM, there was also a reduction in the contraction amplitude, which suggests that the inhibitor may not be specific for the NCX (Wongcharoen *et al.*, 2006). Spontaneous action potentials in the guinea pig pulmonary vein were abolished by another NCX inhibitor, SEA0400 (Namekata *et al.*, 2009), which was also shown to supress noradrenaline induced action potentials in isolated pulmonary vein cardiomyocytes from the rat (Okamoto *et al.*, 2012). However, there have been studies that have raised some doubt as to the specificity of these inhibitors in cardiac myocytes. The I_{CaL} has been shown to be reduced by KB-R7943 (Tanaka *et al.*, 2002) and SEA0400, when applied at micromolar concentrations (Birinyi *et al.*, 2005). Recently, the novel inhibitor, ORM-10103, has been shown to have no significant effect on I_{CaL}, the maximum rate of depolarisation, or the main K^+ currents, even at relatively high concentrations (10 μM) (Jost *et al.*, 2013). Given the number of studies that have proposed a role for the NCX in pulmonary vein automaticity (Chang *et al.*, 2011; Honjo *et al.*, 2003a; Namekata *et al.*, 2009; Patterson *et al.*, 2006; Wongcharoen *et al.*, 2006), it is worth using ORM1010 to investigate its role in noradrenaline induced automaticity in the rat pulmonary vein.

4.1.5. Aims

In the present chapter, the pulmonary veins were isolated from the rat and the contractile response of isolated segments was investigated *in vitro*. The effect of noradrenaline on the amplitude of the electrically evoked contractions was then examined during electrical stimulation at increasing frequencies, to determine if adrenergic stimulation altered the force-frequency relationship. Following on from this, noradrenaline and forskolin were used to examine the role of adrenergic stimulation and the cAMP signalling pathway in the contractility of the pulmonary vein, as well as to try and develop an experimental model of automaticity. To this end, the potential role of CaMKII, gap junctions and the NCX in noradrenaline induced automaticity could then be investigated using various pharmacological inhibitors.

4.2. Materials and Methods

4.2.1. Recording the contractions of the rat pulmonary vein

The main pulmonary veins were isolated from adult male Sprague-Dawley rats (8-10 weeks) as described in section 2.2.1 and were individually mounted in a 10 ml organ bath containing physiological salt solution of the following composition (in mM); 119 NaCl, 25 $NaHCO_3$, 4.7 KCl, 1.17 $MgSO_4$, 1.18 KH_2PO_3, 2.5 $CaCl_2$ and 5.5 glucose. The solution was continually aerated with 95% O_2 and 5% CO_2 to maintain the pH, and the experiments were carried out at 37 °C unless stated otherwise. Each pulmonary vein was mounted vertically, inserted through two platinum ring electrodes, and contractions were evoked by electrical field stimulation. A Grass SD9 stimulator provided 2 ms rectangular pulses at supramaximal voltage (80-100 V), at an initial stimulation frequency of 0.1 Hz. Isometric contractions were measured with a force-displacement transducer (FT03, Grass Instruments Co., Quincy, MA, USA), and sampled at a rate of 1 kHz with a PowerLab® data acquisition device, connected to a PC running LabChart® (ADInstruments Pty Ltd, Bella Vista, Australia). The baseline tension was adjusted to approximately 0.5 g so the contraction amplitude was around 90% of the maximum response, and was allowed 30 to 60 min to stabilise before commencing any experimental protocol (Figure 4.1).

4.2.2. Experimental protocols

4.2.2.1. Effect of increasing the frequency of electrical stimulation on the amplitude of the electrically evoked contractions

The effect of increasing the stimulation frequency on the amplitude of the electrically evoked contractions was determined using the following protocol. The pulmonary vein was stimulated at a control frequency of 0.1 Hz for 60 s. The stimulation frequency was then increased to 0.5, 1, 2, 3, 4, 5, 7 and 9 Hz for 60 s at each frequency. Electrical stimulation was returned to 0.1 Hz for 60 s to allow the contraction amplitude to re-stabilise between each subsequent increase in the stimulation frequency.

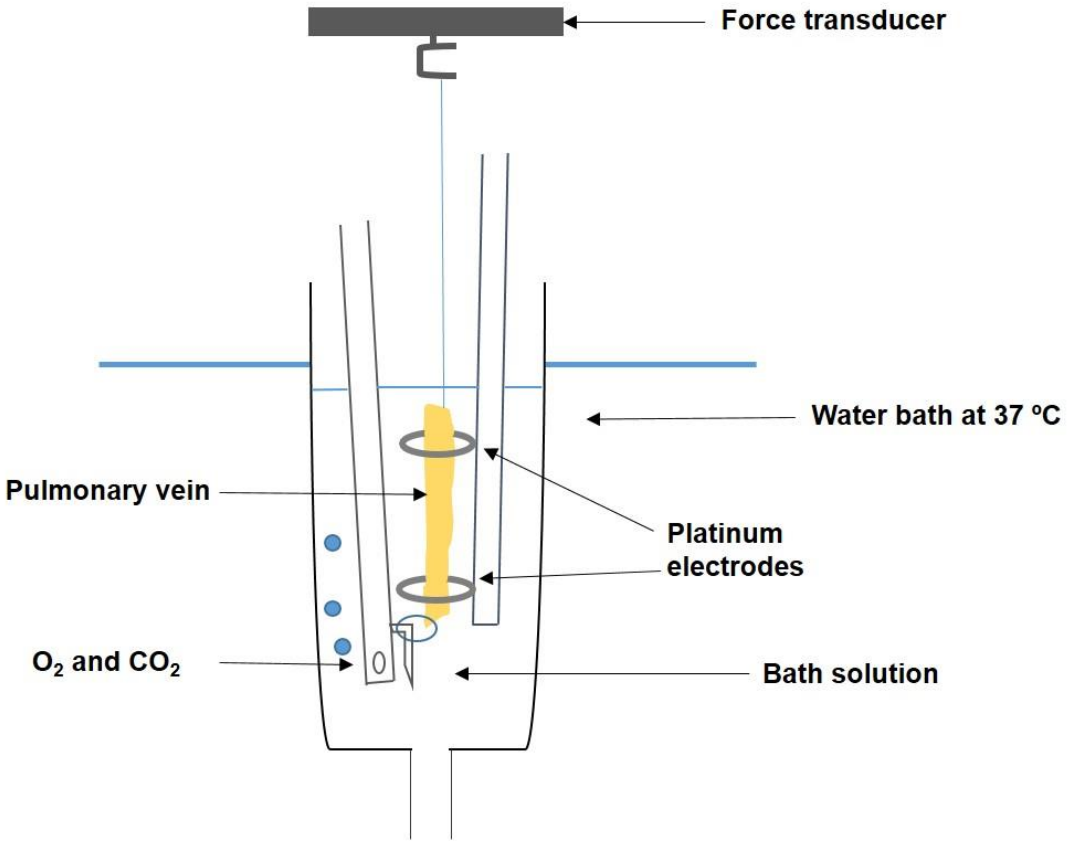

Figure 4.1. Experimental set up for recording contractions of the pulmonary vein. Schematic diagram illustrating the organ bath set up for recording isometric contractions of the pulmonary vein. Fresh solution was perfused through the underside of the organ bath to washout any drugs or reagents. The solution in the bath was continually bubbled with 95 % O_2 and 5 % CO_2 and maintained at 37 ºC with an external water bath.

To investigate the effect of noradrenaline on the contraction amplitude at increasing stimulation frequencies, the entire protocol was repeated 10 min after the application of 10 µM noradrenaline. The tissue was then washed in fresh physiological salt solution and allowed 30 min for recovery, before the experiment was repeated using 100 µM noradrenaline.

4.2.2.2. Induction of automaticity in the pulmonary vein with noradrenaline

The pulmonary vein was continually paced at 0.1 Hz to provide reference contractions, and treated with noradrenaline (100 µM) to induce automaticity. In order to examine if electrical stimulation was required for the induction of automatic contractions, the procedure was repeated in the absence of electrical stimulation. The effect of lowering the temperature was also studied, as the previous experiments examining the intracellular Ca^{2+} signalling in the pulmonary vein were conducted at room temperature. Once automaticity was induced, the temperature of the water bath was lowered to room temperature (21-24 °C) for approximately 15 min, before it was raised back to 37 °C.

4.2.2.3. The effect of forskolin on the contractility of the pulmonary vein

To examine if forskolin was capable of inducing automaticity, the tissue was treated with forskolin (10 µM) and allowed up to 1 hr for the detection of automaticity. During this period the pulmonary vein was electrically paced at 0.1 Hz.

4.2.2.4. The effect of pharmacological inhibitors on noradrenaline induced automaticity

A standard protocol was used to investigate the effect of the different inhibitors on noradrenaline induced automaticity. The pulmonary vein was continuously stimulated

at 0.1 Hz and treated with noradrenaline. Once automaticity was induced, a 10-20 min period was allowed before the inhibitor was added, and its effect was analysed after a suitable equilibration period for the inhibitor to take effect. In some of the experiments, the concentration of the inhibitor was increased after further 10-20 min recording period.

4.2.2.4.1. Time matched control

Time matched control recordings were obtained where the pulmonary vein was treated with noradrenaline (100 µM) and electrically stimulated at 0.1 Hz. Once automaticity was induced, the contractions were recorded for 100 min with no further treatment.

4.2.2.4.2. The effect of inhibiting Ca^{2+}/calmodulin dependent protein kinase II on noradrenaline induced automaticity

The potential role of CaMKII in noradrenaline induced automaticity was investigated using the inhibitors KN-93 (1 µM and then 5 µM) and autocamtide-2-related inhibitory peptide (AIP) (10 µM) (Ishida *et al.*, 1995). A 15 min equilibration period was allowed before analysing the effect of either inhibitor.

4.2.2.4.3. The effect of gap junction uncoupling on noradrenaline induced automaticity

The effect of electrically uncoupling neighbouring cardiomyocytes was studied using the gap junction inhibitor carbenoxolone (100 µM) (de Groot *et al.*, 2003). A 15 min equilibration period was allowed before analysing the effect of carbenoxolone.

4.2.2.4.4. The effect of inhibiting the Na^+/Ca^{2+} exchanger on noradrenaline induced automaticity

The influence of the NCX on noradrenaline induced automaticity was examined by inhibiting the exchanger with ORM-10103 (Jost *et al.*, 2013). An initial concentration of 10 µM was used before it was increased to 20 µM. A 20 min equilibration period was allowed before analysing the effect of ORM-10103.

4.2.3. Analysis of data

4.2.3.1. Determining the contraction amplitude

Data were analysed in LabChart 5.5.6. (ADInstruments Pty Ltd, Bella Vista, Australia). Contractions of the pulmonary vein were detected as periodic (cyclic) events based on a minimum contraction amplitude that was pre-set so that all of the contractions were detected. The contraction amplitude was then calculated from the maximum tension during a cyclic event and the minimum tension before the contraction (Figure 4.2).

4.2.3.2. Determining the force-frequency relationship

For each preparation, the mean contraction amplitude was calculated from the control periods at 0.1 Hz. This included when the stimulation frequency was returned to 0.1 Hz between the incremental increases in frequency to allow for a sufficient sample size for statistical analysis. When the frequency of stimulation was increased the contraction amplitude was expressed as a percentage of the control value. The contraction amplitude in the presence of noradrenaline (10 µM and then 100 µM) was also calculated as a percentage of the mean contraction amplitude at 0.1 Hz in the control recordings.

In order to quantify the initial fast decline in the contractile response that occurred as the stimulation frequency was increased the following analysis was carried out. The difference in amplitude between the 1st contraction and the steady state was calculated and defined as 100%. Thereafter, the time taken for the contraction amplitude to decline by 50% of this value was then determined ($t_{1/2}$ to steady state). When establishing the force-frequency relationship, a 30 s period was allowed for the contraction amplitude to reach a steady state. Then all of the contractions during the following 30 s were used to calculate the mean contraction amplitude at each stimulation frequency.

4.2.3.3. Determining the effect of inhibitors on noradrenaline induced automaticity

The number of contractions per min was taken as an indicator of the level of noradrenaline induced automaticity. This was initially analysed during a 2 min control period before the addition of noradrenaline, and during a 10-20 min period beginning at the onset of automaticity. To investigate the effect of an inhibitor, the number of contractions per min was calculated again from a 10-20 min period following incubation with the inhibitor

It is important to note that the number of contractions per min is the total number and this also includes the electrically evoked contractions. However, as electrical stimulation was maintained at the same frequency during each recording, this should have no impact on the interpretation of the results.

The amplitude of the electrically evoked (0.1 Hz) contractions was also analysed to examine if the inhibitors had any effect on the paced contractile response of the pulmonary vein in the presence of noradrenaline (100 μM). This was calculated during 2 min periods before the addition of noradrenaline (100 μM), immediately after the onset of automaticity, and again after incubation with the inhibitor.

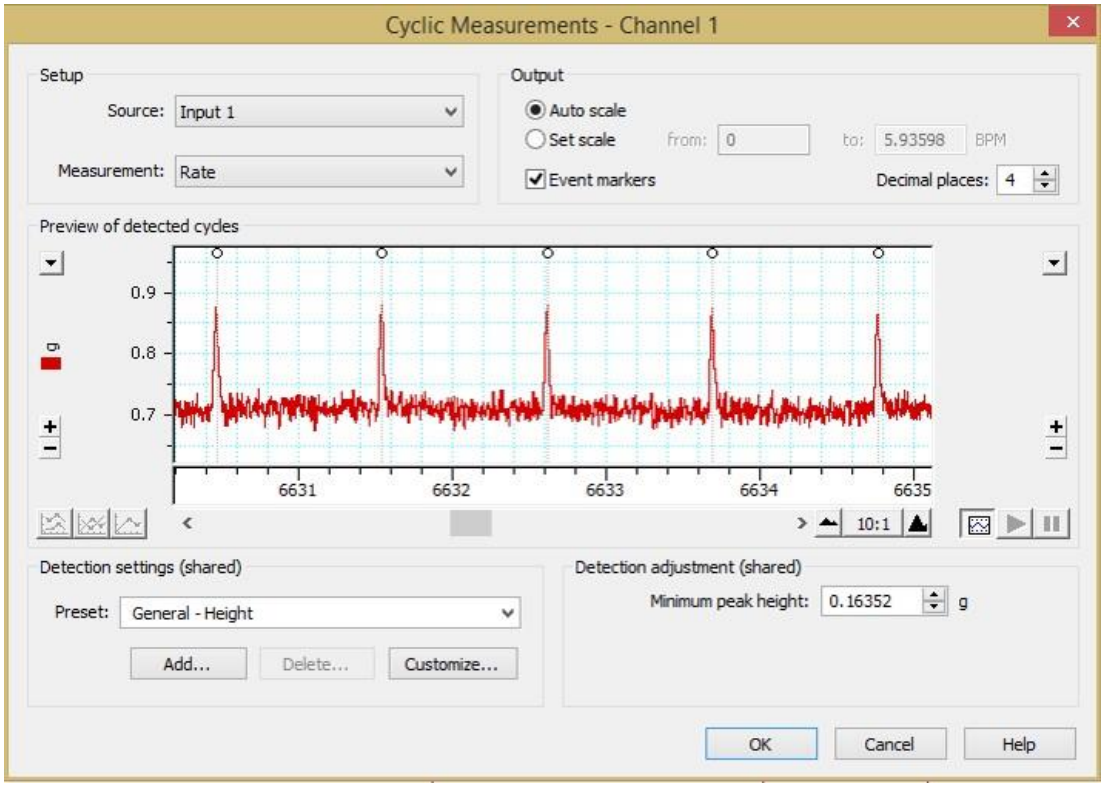

Figure 4.2. Analysis of pulmonary vein contraction amplitude. Screenshot obtained from Chart 5.5.6., which displays the detection of electrically evoked contractions (1 Hz) using a minimum amplitude preset ("minimum peak height"). The peak of each contraction is indicated by a circle. Contractile tension was measured in g.

4.2.3.4. Presentation of data and statistical analysis

Calculated data was exported into Prism (GraphPad Software, Inc., La Jolla, CA, USA) for statistical analysis and presentation of representative recordings. When presenting original records, a median filter of 21 points was applied and the data was resampled at 100 Hz to reduce noise.

Data are expressed as mean ± s.e.m. Up to two pulmonary veins from each rat were used during each experimental day and therefore the sample size (n) for each experiment represents *p* PVs from *q* rats. The force-frequency relationship was compared using a one-way ANOVA with Bonferroni's correction. This was so the contraction amplitude could be compared after each successive increase in the stimulation frequency. To compare the contractile amplitude at a given frequency in the untreated pulmonary vein (control) to the tissue after exposure to noradrenaline (10 μM and 100 μM), a one-way ANOVA with Dunnett's multiple comparison post-test was performed. Comparisons between two groups of data e.g. the effect of noradrenaline (100 μM) or forskolin (10 μM) on the amplitude of the electrically evoked contractions, was performed using Student's paired *t*-test. In order to analyse the effect of an inhibitor (KN-93, AIP, CBX or ORM-10103) on noradrenaline (100 μM) induced automaticity, statistical analysis was performed using Student's paired *t*-test, where there were 2 sample groups and a one-way ANOVA with Bonferroni's correction where there were 3 sample groups. $P<0.05$ was considered as statistically significant.

4.2.4. Chemicals and drugs

Noradrenaline, forskolin and carbenoxolone were prepared at stock concentrations of 100 mM in physiological salt solution on the day of experimentation. AIP and KN-93 were prepared at stock concentrations of 20 mM in sterile water and DMSO respectively, before being stored at -20 ºC prior to use. ORM-10103 was stored at room temperature in DMSO at 20 mM. All the drugs and reagents above were obtained

from Sigma Aldrich (Gillingham, Dorset, UK). All other reagents (NaCl, KCl, glucose, $MgCl_2$, $CaCl_2$, NaOH, MgSO4, $NaHCO_3$ and KH_2PO_4) were obtained from BDH Laboratories (VWR International, Radnor, PA, USA), and the physiological salt solution was prepared on the morning of the experiments.

4.3. Results

Contractions of the pulmonary vein were evoked by electrical field stimulation. Figure 4.3 shows a representative recording of the contraction of the pulmonary vein during electrical stimulation at 0.1 Hz, where there were transient increases in tension in response to the stimulus. The expanded-time scale image (inset) shows a single electrically evoked contraction, which can be observed as a transient cyclic event of approximately 50 to 80 ms, where the contractile tension of the pulmonary vein rises rapidly to a peak before relaxing back to the baseline level. When the electrical stimulus was terminated the pulmonary vein was quiescent (Figure 4.3).

4.3.1. Effect of increasing the stimulation frequency on the contraction of the pulmonary vein

The effect of varying the frequency of electrical stimulation on the contractility of the pulmonary vein was studied, where it was observed that the rat pulmonary vein displayed a negative force-frequency relationship (Figure. 4.4). When the stimulation frequency was increased from 0.1 to 0.5 Hz there was a small decrease in the contractile amplitude, by 4.5 ± 1%. However, when the frequency was increased to 1 Hz there was a significant decrease of 21 ± 1%, compared to that at 0.1 Hz ($P<0.001$, 0.1 Hz *vs*. 1 Hz). Increasing the stimulation frequency to 2 Hz resulted in a further reduction by 38.6 ± 1% ($P<0.001$, 1 Hz *vs*. 2 Hz), and when the stimulation frequency was increased to 3 Hz, there was a small but significant reduction by 4.8% ($P<0.001$, 2 Hz *vs*. 3 Hz). The steady state contraction amplitude no longer decreased with increasing stimulation frequency at 4 and 5 Hz, where the contraction amplitude was 58.5 ± 1% and 58.7 ± 1% respectively, compared to that at 0.1 Hz. During electrical stimulation at 7 Hz, the contraction amplitude was 55.86 ± 1% less than at 0.1 Hz, which was significantly lower than it was at 3 Hz ($P<0.001$, 3 Hz *vs*. 7 Hz). During electrical stimulation at 9 Hz there was a statistically significant reduction in the contraction amplitude at 49.4 ± 1%, compared to at 0.1 Hz ($P<0.001$, 7 Hz *vs*. 9 Hz) (n = 5 PVs from 4 rats) (Figure 4.5).

As can be seen in the representative recordings in Figure 4.4, when the frequency of electrical stimulation was increased from 0.1 Hz, the contraction amplitude declined towards a steady state. The mean amplitude over time under control conditions is summarised in Figure 4.6A, where it is also being compared with the amplitude in the presence of noradrenaline. It is apparent that the decline in contraction amplitude towards steady occurred more rapidly with increasing stimulation frequency. The time taken for the contraction amplitude at a given stimulation frequency to decline by 50% was therefore quantified ($t_{1/2}$ to steady state). After increasing the frequency of electrical stimulation to 1 Hz, the $t_{1/2}$ was 3.77 ± 0.18 s, and this time was significantly reduced to 1.25 ± 0.16 s, when the frequency of electrical stimulation was increased to 3 Hz ($P<0.001$, 1 Hz *vs*. 3 Hz). Increasing the stimulation frequency to 5 Hz further reduced the $t_{1/2}$ to 0.63 ± 0.11 s ($P<0.01$, 3 Hz *vs*. 5 Hz). During electrical stimulation at 7 Hz, the $t_{1/2}$ was 0.28 ± 0.04 s and it was 0.1 ± 0.02 s during stimulation 9 Hz, which was significantly lower than at 5 Hz ($P<0.01$, 5 Hz *vs*. 9 Hz) (n = 6 PVs from 5 rats) (Figure 4.6B).

The force-frequency relationship was also established in the presence of noradrenaline. As can be seen in the representative recordings in Figure 4.4, in the presence of noradrenaline (10 μM) there was an increased contractile amplitude, particularly at the lower frequencies of stimulation. During electrical stimulation at 0.1 Hz, the contraction amplitude was 22.6 ± 2% greater in the presence of noradrenaline and, was 90.5 ± 1% and 59.3 ± 1% greater at 3 and 5 Hz respectively. However, the amplitude of the steady state contractions was only 15.5% greater in the presence of noradrenaline during electrical stimulation at 9 Hz (n = 5 PVs from 4 rats, $P<0.001$ *vs.* control) (Figure 4.7).

Noradrenaline (10 μM) also changed the response of the pulmonary vein to increases in stimulation frequency. Increasing the stimulation frequency from 0.1 Hz to between 0.5 and 3 Hz did not reduce the contraction amplitude, unlike what was observed in the absence of noradrenaline. During electrical stimulation at 3 Hz the amplitude of steady state contractions was only 8.5 ± 2% lower than that at 0.1 Hz. However, there

was a significant decline in amplitude at the higher frequencies of stimulation. At 5 Hz, the steady state contraction amplitude was decreased by 23.8 ± 2% compared to that at 0.1 Hz ($P<0.001$, 0.1 Hz *vs*. 5 Hz) and at 7 and 9 Hz there was a 37.7 ± 2% ($P<0.001$, 5 Hz *vs*. 7 Hz) and 52.3 ± 1% ($P<0.001$, 7 Hz *vs*. 9 Hz) reduction respectively (n = 5 PVs from 4 rats (Figure 4.7).

The response of the pulmonary vein to electrical stimulation was similar when the concentration of noradrenaline was increased to 100 μM, in that the steady state contraction amplitude was only significantly lower than it was at 0.1 Hz during electrical stimulation between 5 and 9 Hz. However in these studies, there was also an increase in contraction amplitude between 0.1 and 1 Hz by 23.5 ± 1 % ($P<0.01$, 0.1 Hz *vs*. 1 Hz). It should be noted that automaticity was observed in 2 pulmonary veins from 2 rats, when noradrenaline was applied at 100 μM, and therefore the results from these preparations were excluded from the analysis of the force-frequency relationship (n = 5 PVs from 4 rat) (Figure 4.7).

At the lower frequencies of stimulation, noradrenaline prevented the initial decline in contraction amplitude after increasing the frequency of electrical stimulation. The $t_{1/2}$ to steady state decreased from 13.47 ± 2.57 s at 5 Hz, to 7.89 ± 1.05 s at 9 Hz. However, this reduction was not statistically significant (n = 6 PVs from 5 rats, n.s.). When the concentration of noradrenaline was increased to 100 μM, the $t_{1/2}$ during electrical stimulation at 5 Hz was 16.2 ± 1.22 s, and this was significantly reduced to 9.67 ± 0.16 s during stimulation at 9 Hz (n = 5 PVs from 4 rats, $P<0.001$, 5 Hz vs. 9 Hz). Overall, the $t_{1/2}$ was considerably greater in the presence of noradrenaline compared to untreated (control) conditions ($P<0.001$ *vs*. Control) (Figure 4.6C).

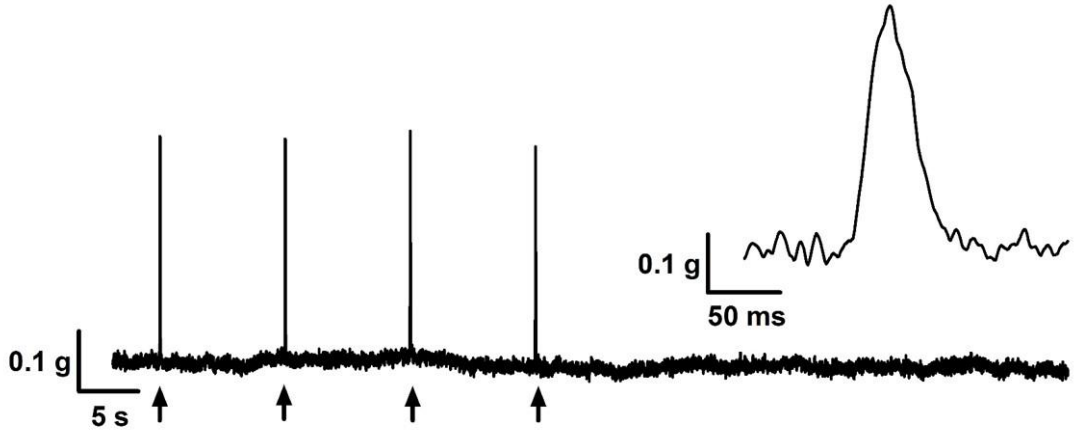

Figure 4.3. Contraction of the rat pulmonary vein in response to electrical field stimulation. Representative recording of isometric contraction of the pulmonary vein in response to electrical stimulation at 0.1 Hz (supramaximal V, 2 ms duration). The arrows indicate the electrical stimulus. Inset is a single electrically evoked contraction of the pulmonary vein displayed over an expanded time scale.

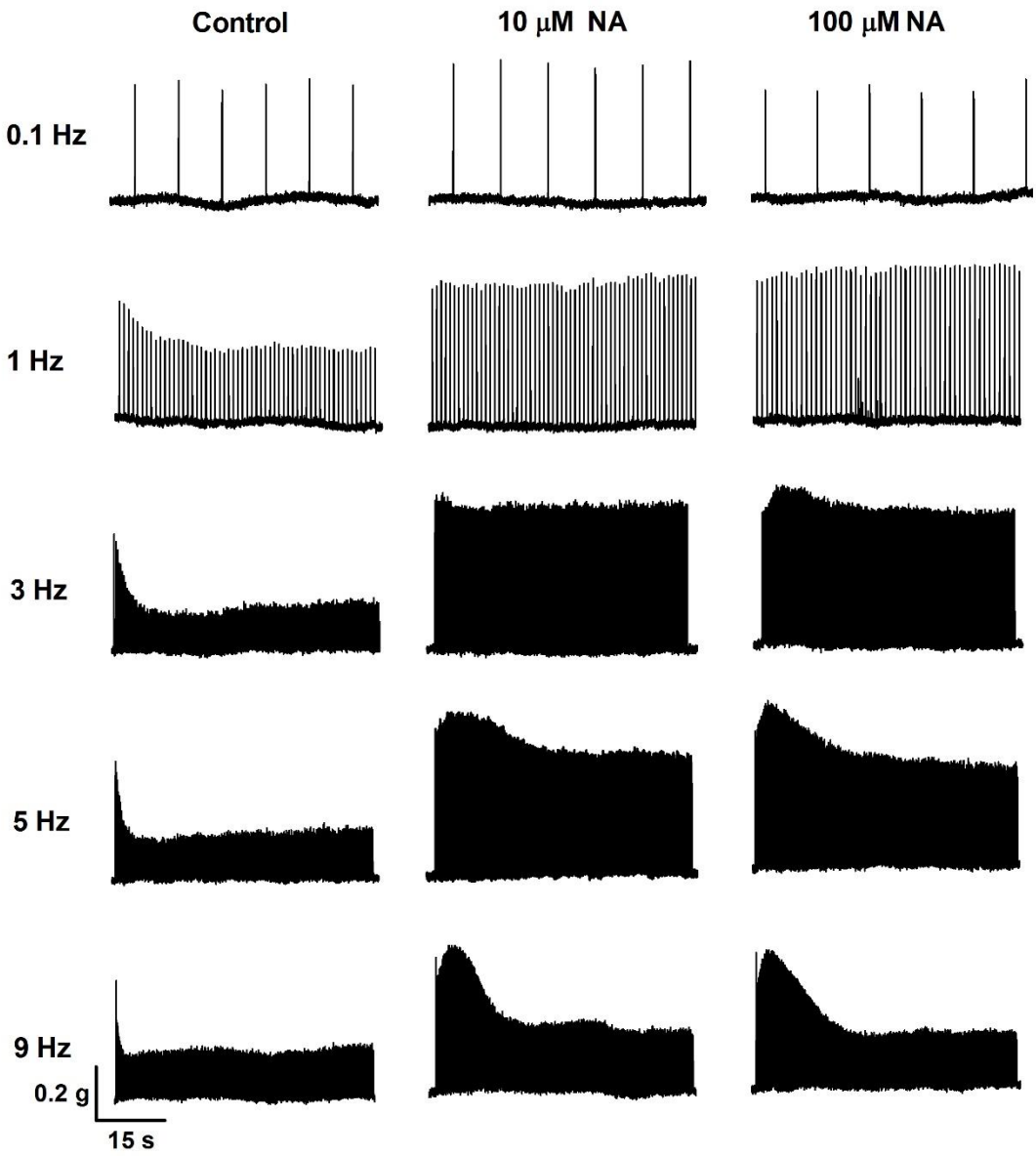

Figure 4.4. The effect of stimulation frequency on contractions of the pulmonary vein. Representative 60 s recordings of contractions of the pulmonary vein during electrical stimulation at increasing frequencies during control recordings, and in the same tissue following 10 min treatment with 10 μM and then 100 μM noradrenaline (NA). Steady state contractions were defined as occurring after 30 s, once any change in the amplitude had stabilised.

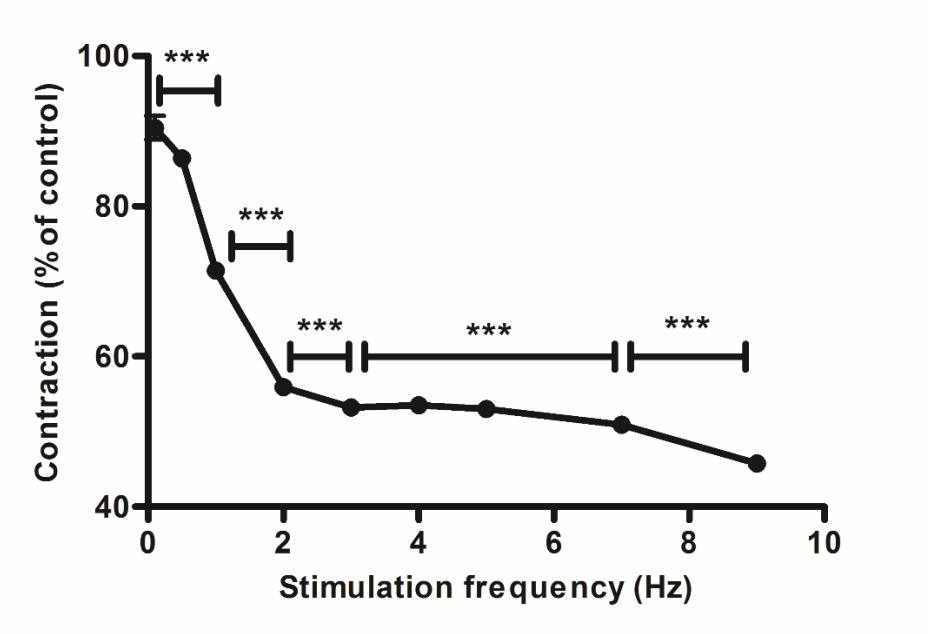

Figure 4.5. Force-frequency relationship in the rat pulmonary vein. The mean amplitude of the steady state contractions during electrical stimulation at increasing frequencies from 0.1 Hz to 9 Hz. Data represent mean ± s.e.m. and is expressed as a percentage of the control contraction amplitude when the vein was stimulated at 0.1 Hz. The absence of visible error bars for 0.5 to 9 Hz is due to the error bars being smaller than the symbols. $^{***}P<0.001$. n = 5 PVs from 4 rats.

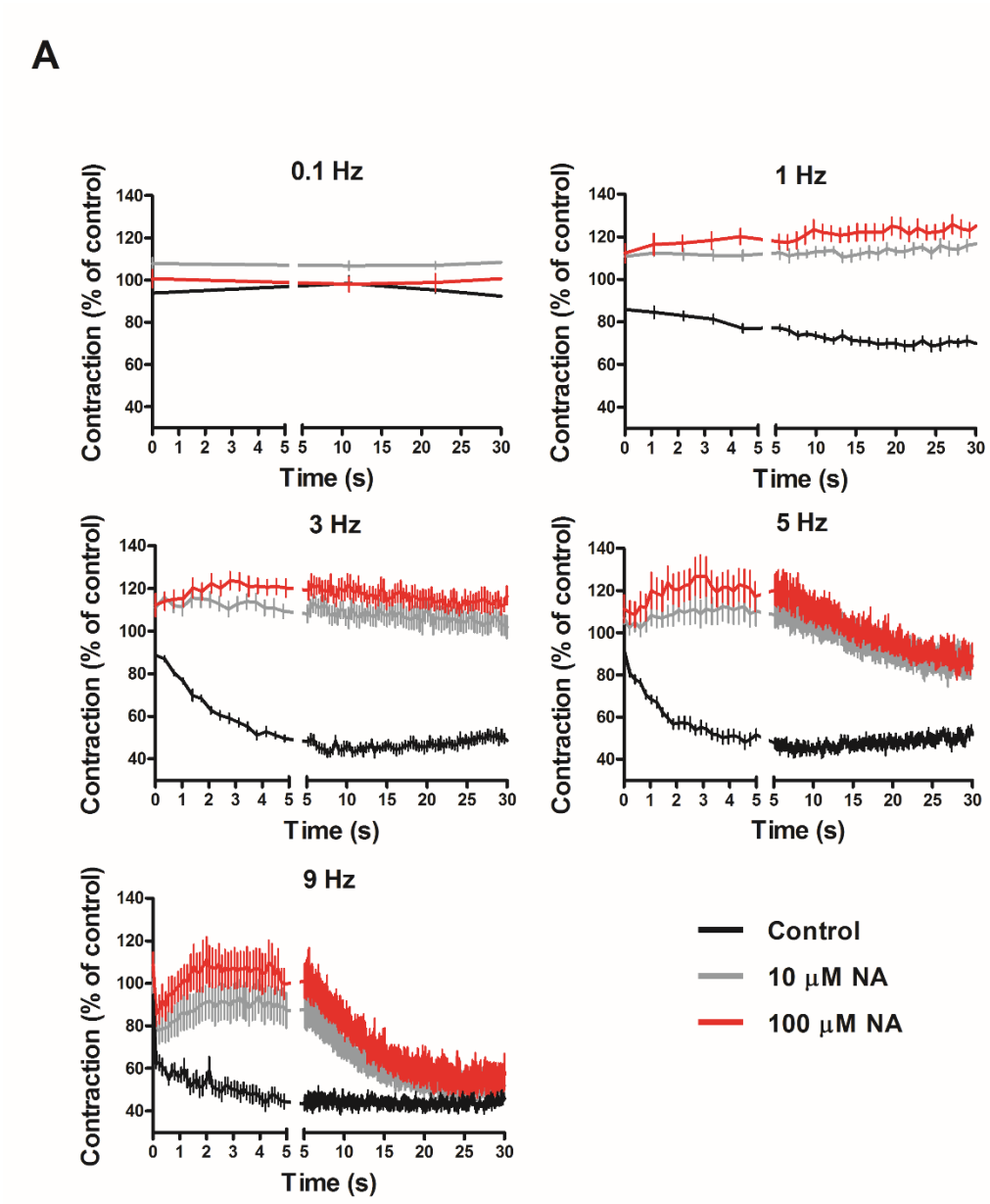

Figure 4.6. The effect of noradrenaline on the force-frequency relationship in the pulmonary vein. A. The mean amplitude of each electrically evoked contraction (% of control at 0.1 Hz) over time in control recordings, and later in the presence of 10 µM and then 100 µM noradrenaline (NA). The first 5 s have been expanded to demonstrate the change in contractile amplitude that occurred immediately following the increase in stimulation frequency from 0.1 Hz. The contraction amplitude during electrical stimulation at 0.1, 1, 3, 5 and 9 Hz are shown. Data represent mean ± s.e.m. n = 7 PVs from 6 rats for control and 10 µM NA and 5 PVs from 4 rats for 100 µM NA

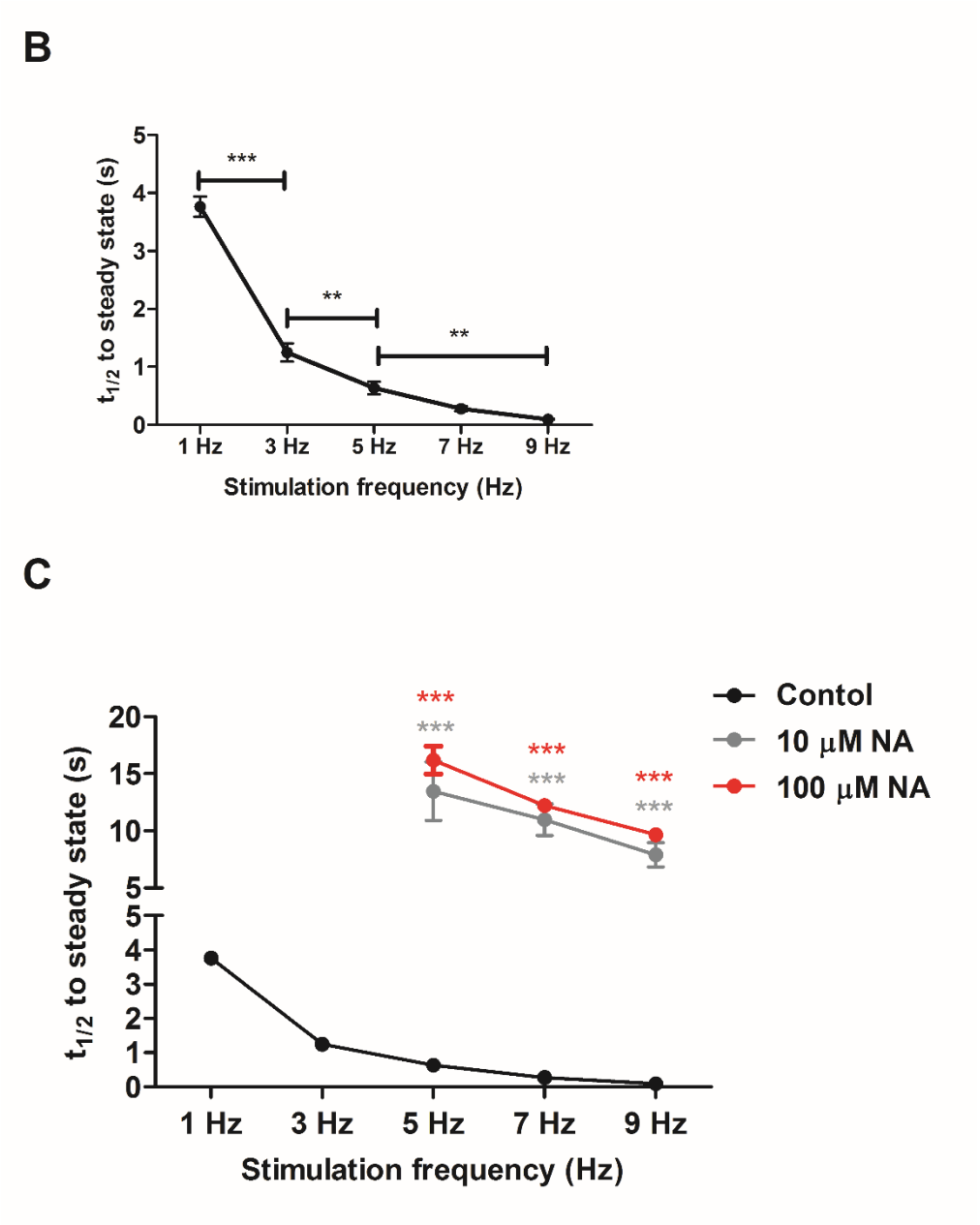

Figure 4.6. (Cont.). B. The time taken for the contraction amplitude to decline by 50% towards the steady state ($t_{1/2}$) after the frequency of electrical stimulation was increased from 0.1 Hz in the untreated tissue. Data represent mean ± s.e.m. $^{***}P<0.001$, $^{**}P<0.01$ and n = 6 PVs from 5 rats. **C.** The $t_{1/2}$ in the presence of 10 µM and 100 µM NA. $^{***}P<0.001$ *vs*. Cont. and n = 5 PVs from 4 rats.

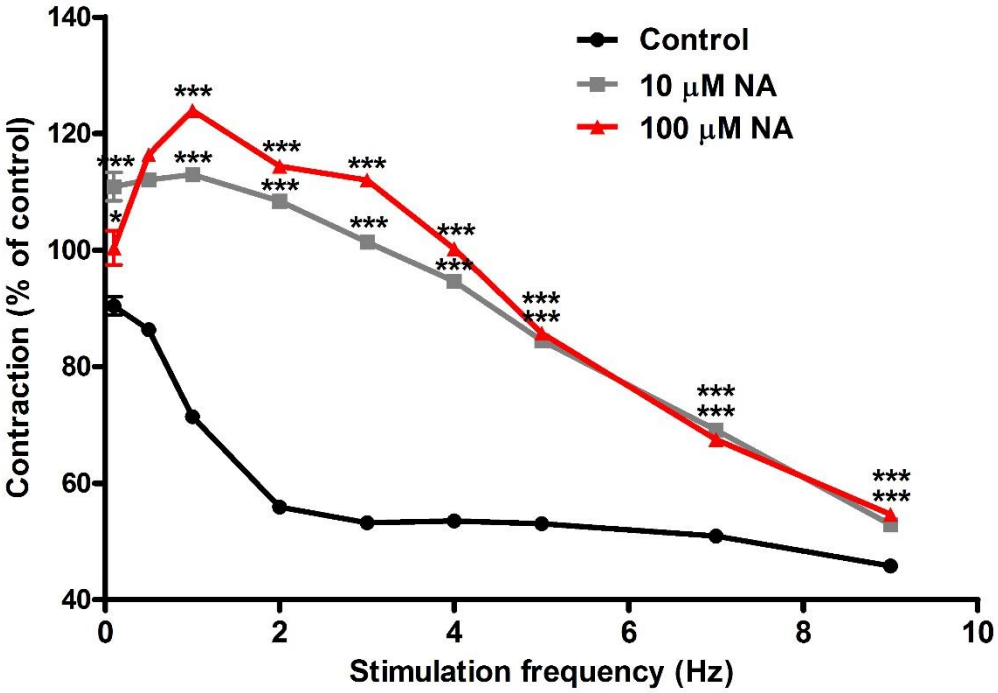

Figure 4.7. Force-frequency relationship in the rat pulmonary vein in the presence of noradrenaline. The mean amplitude of the steady state contractions during electrical stimulation at increasing frequencies from 0.1 to 9 Hz in the presence of 10 μM and then 100 μM NA. The graphs have also been merged with FFR under untreated (Control) conditions. Data represent mean ± s.e.m. and is expressed as a percentage of the control contraction amplitude when the vein was stimulated at 0.1 Hz. $^{*}P<0.05$ *vs*. control and $^{***}P<0.001$ *vs.* control. n = 5 PVs from 4 rats.

4.3.2. Noradrenaline induced automaticity in the pulmonary vein

Noradrenaline (100 µM) induced automaticity was observed in 86% of the preparations (n = 50 PVs from 29 rats). As can be seen in the representative recording in Figure 4.8A, after noradrenaline was applied there was a mean latency period of 9.78 ± 0.58 min before automaticity was observed in the form of short, high frequency bursts of automatic contractions (Figure 4.8B and C). Automaticity was otherwise not observed in the absence of noradrenaline. The duration of each burst and the period of time between bursts varied between different preparations. Noradrenaline induced automaticity ranged from a single contraction to a burst of contractions lasting 32.8 s, and the mean duration of an individual burst was 14.5 ± 1.1 s. The period between bursts ranged from 15.0 s to 359.3 s, with a mean of 104.8 ± 8.9 s (n = 50 PVs from 29 rats).

As well as a large variation in the duration of each burst, the frequency and amplitude of automatic contractions was not uniform throughout. This is highlighted in Figure 4.9, which shows representative recordings of 3 automatic bursts of contractions from the pulmonary veins of 3 different rats. The amplitude tended to be highest at the start of the burst before decreasing to a steady state. However, sometimes the amplitude would increase towards the end, or towards the middle of the burst. The frequency of automatic contractions tended to increase to a maximum in the middle of the burst before decreasing again towards the end (Figure 4.9). This wide variation made it difficult to compare the effect of an inhibitor on noradrenaline induced automaticity, which is why comparing the number of contractions per min was employed.

Electrical stimulation was not a requirement for the induction of automaticity with noradrenaline (100 µM), as automatic contractions were still present in unstimulated conditions (Figure 4.10) (n = 3 PVs from 2 rats). However, when the temperature of the bath was decreased from 37 °C to room temperature (21-24 °C) there was a cessation of automatic contractions, which resumed when the temperature was returned back to 37 °C (Figure 4.11) (n = 3 PVs from 2 rats).

The amplitude of the electrically evoked contractions was compared between pulmonary veins where automaticity was observed in the presence of noradrenaline (100 μM), and pulmonary veins where automaticity was not induced in order to see if noradrenaline still had an effect on the contractions. In pulmonary veins where automaticity was induced, noradrenaline significantly increased the amplitude of the electrically evoked contractions (0.1 Hz) from 0.31 ± 0.01 g to 0.38 ± 0.01 g (n = 7 PVs from 7 rats, $P<0.001$). In pulmonary veins where noradrenaline did not induce automaticity, the contractile amplitude was also significantly increased, this time from 0.19 g to 0.22 ± 0.01 g (n = 5 PVs from 3 rats, $P<0.001$) (Figure 4.12).

4.3.3. Effect of forskolin on the contraction of the pulmonary vein

Forskolin was applied to the pulmonary veins to examine if activation of adenylate cyclase, which causes an increase in intracellular cAMP (Seamon *et al.*, 1981), is capable of inducing automaticity in the rat pulmonary vein. To begin with, noradrenaline (100 μM) was used to determine if automaticity could be induced in the pulmonary vein. If it was, the tissue was then washed in fresh physiological salt solution and allowed 30 min for recovery. Forskolin (10 μM) significantly increased the contraction amplitude from 0.34 ± 0.02 g to 0.46 ± 0.01 g (n = 3 PVs from 2 rats, $P<0.001$). However, automaticity was not induced within 60 min after treatment with forskolin in any of the preparations studied (n = 3 PVs from 2 rats) (Figure 4.13).

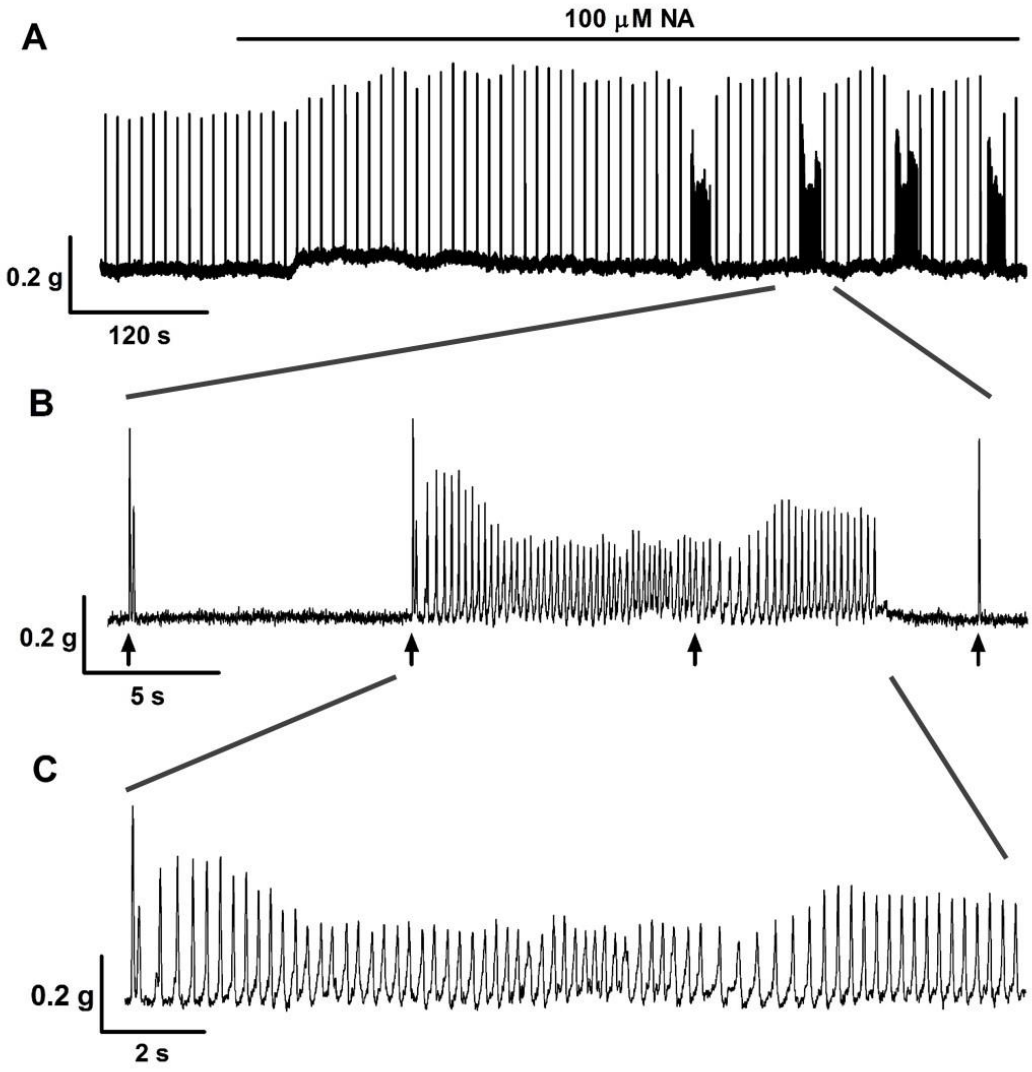

Figure 4.8. Noradrenaline induced automaticity in the rat pulmonary vein. A. Representative recording of contractions of the pulmonary vein during electrical stimulation at 0.1 Hz upon the addition of noradrenaline (NA) (100 μM) **B.** Expanded time-scale of a section of **A.** The arrows indicate the electrical stimulus. **C.** Expanded time-scale of a section of **B.** displaying a single burst of automatic contractions.

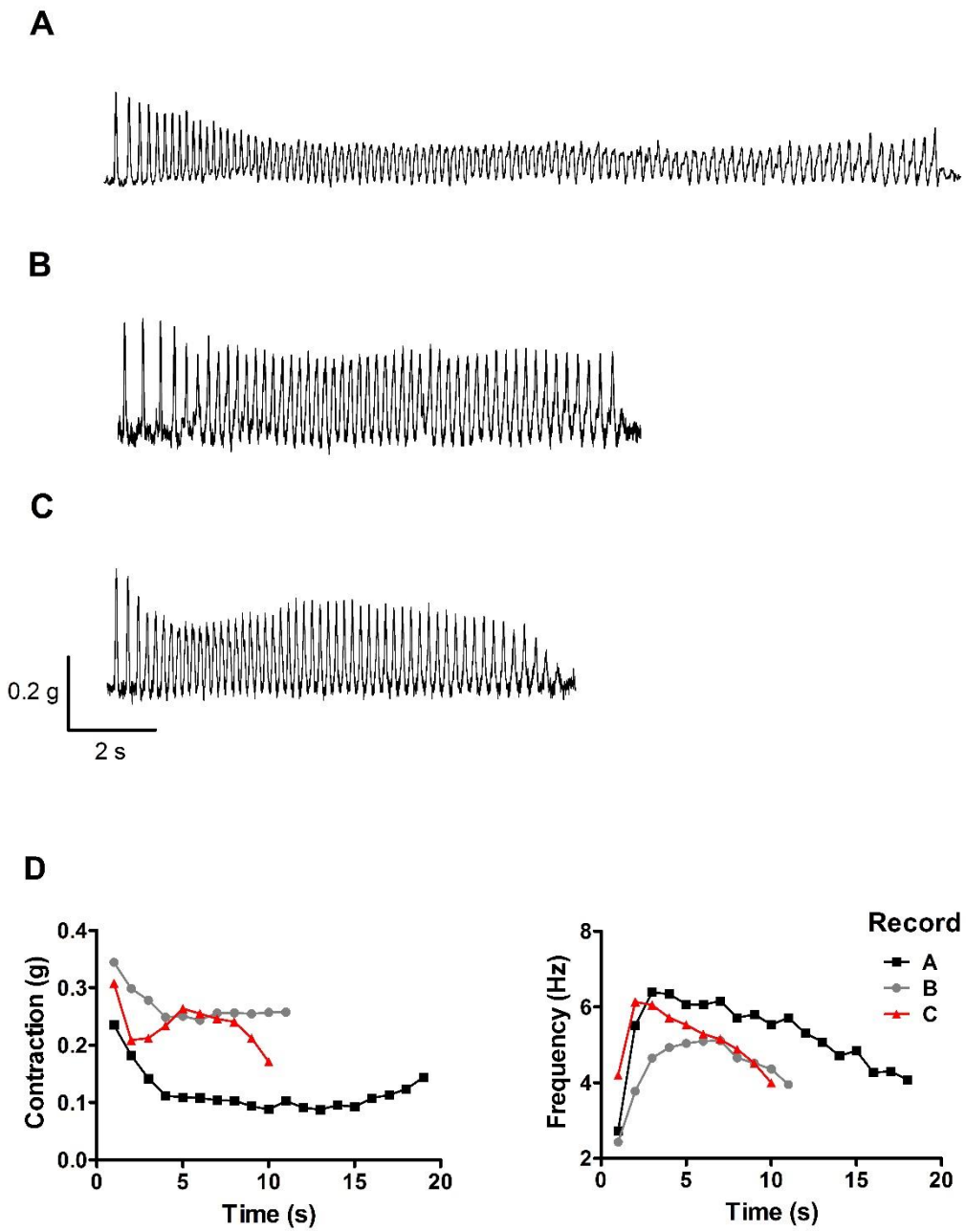

Figure 4.9. Automatic bursts of contractions in the pulmonary vein in the presence of noradrenaline. A. B. and C. Representative recordings of 3 individual bursts of automatic contractions, which were induced by noradrenaline (100 µM) in the pulmonary veins of 3 different rats **D.** The mean amplitude and frequency of contractions during the course of 1 s periods throughout each burst over time.

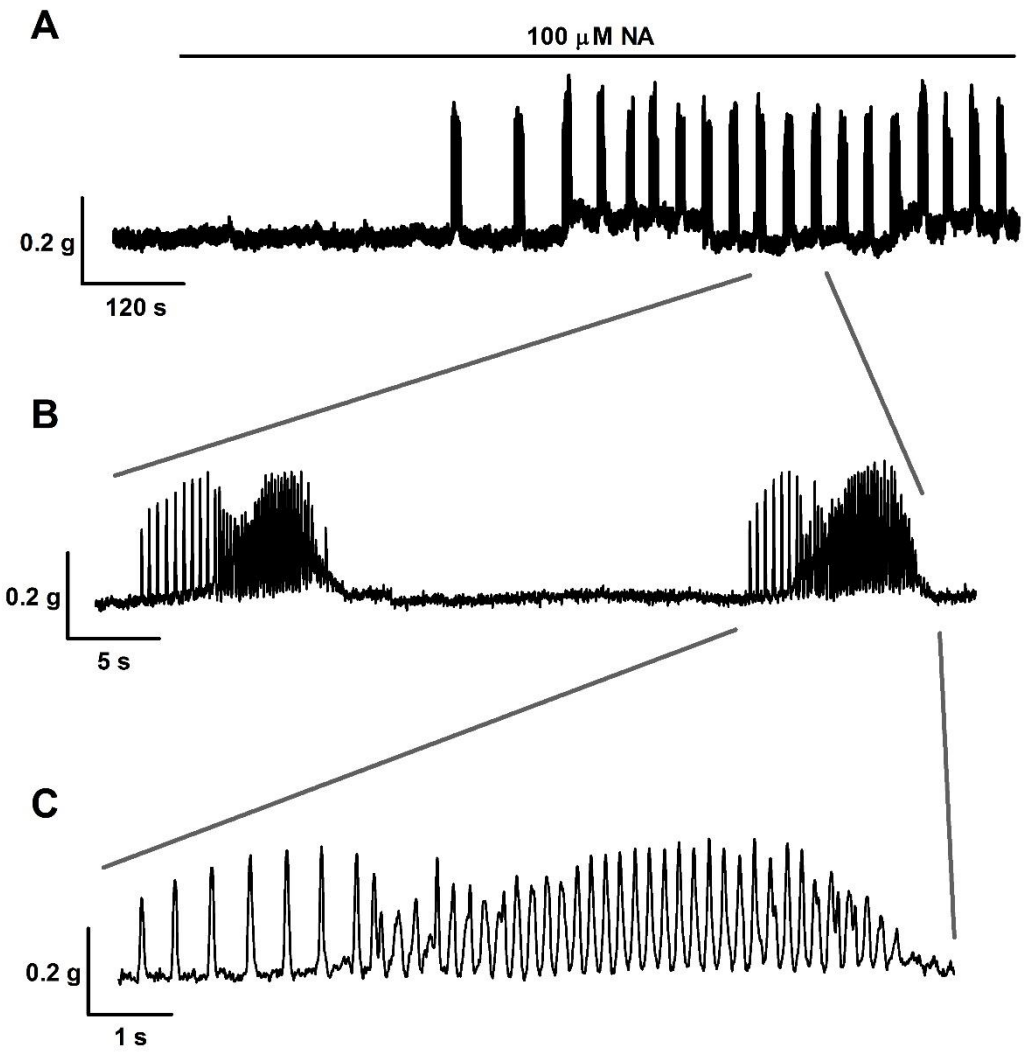

Figure 4.10. Noradrenaline induced automaticity in the pulmonary vein in the absence of electrical field stimulation. A. Representative recording of contractions of the pulmonary vein upon the application of noradrenaline (NA) (100 μM). **B.** Expanded time-scale of a section of **A. C.** Expanded time-scale of a section from **B.** displaying a single burst of automatic contractions.

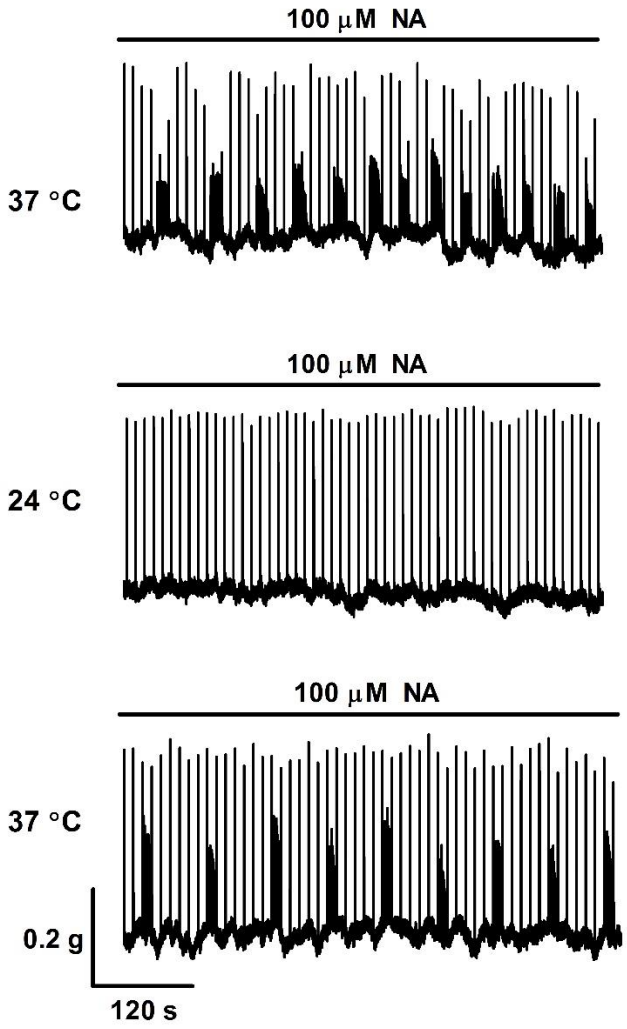

Figure 4.11. The effect of lowering the temperature of the bath solution on noradrenaline induced automaticity in the pulmonary vein. Consecutive recordings of contractions of the same pulmonary vein in the presence of noradrenaline (NA) (100 μM) at 37 °C, when the temperature was lowered to 24 °C, and then when the temperature was raised back to 37 °C. Electrical stimulation was maintained at 0.1 Hz throughout the recording.

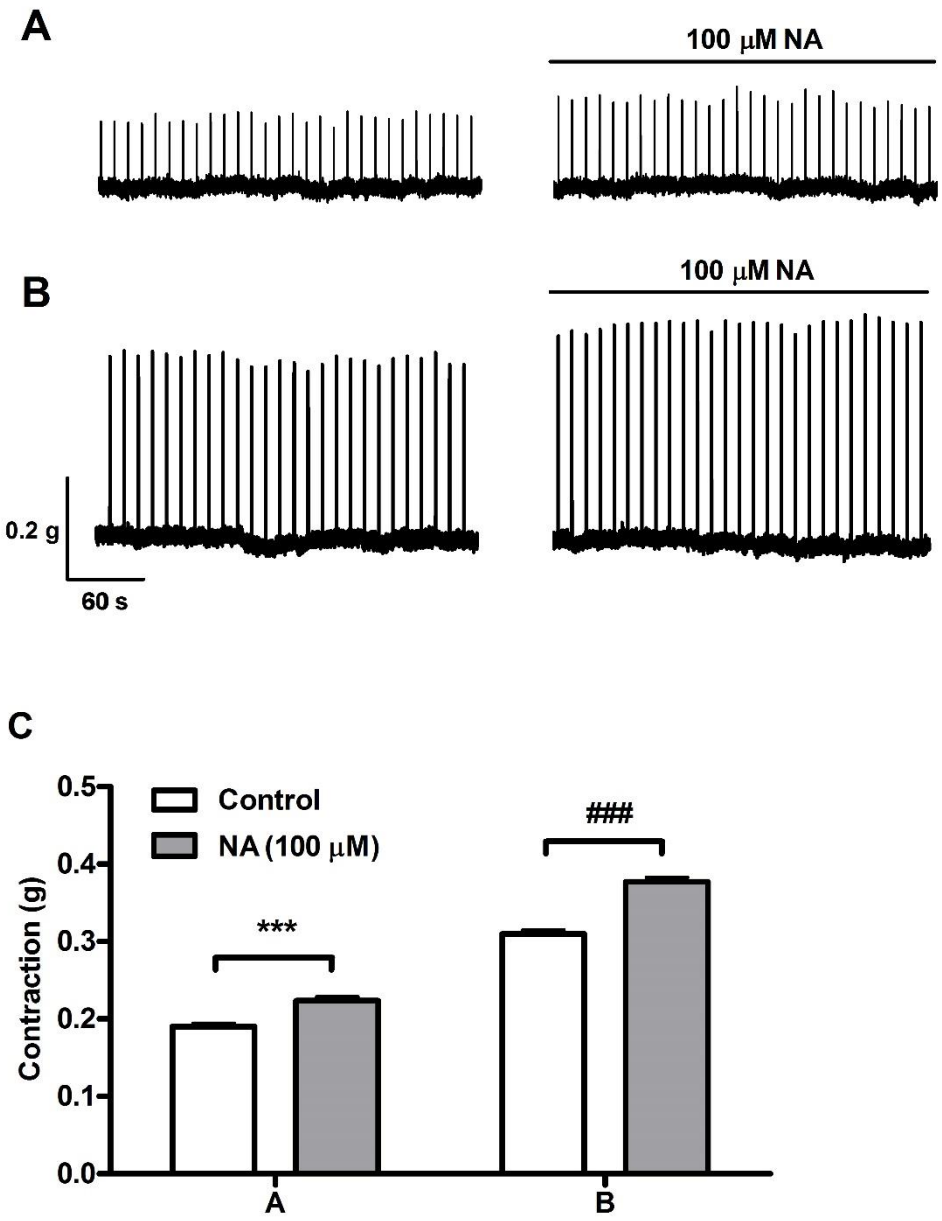

Figure 4.12. The effect of noradrenaline on the amplitude of the electrically evoked contractions of the pulmonary vein. Representative recordings of contractions of the pulmonary vein during electrical stimulation at 0.1 Hz before, and 2 min after, the addition of noradrenaline (NA) (100 μM). Recordings were obtained from a tissue where automaticity could not be induced by NA (100 μM) **(A)** and in another preparation where automaticity could be induced **(B).** The graph displays the mean contraction amplitude before and after exposure to NA (100 μM) for both groups (**A** and **B**). ***P<0.001 *vs.* control and $^{###}$P<0.001 *vs.* control. n = 7 PVs from 7 rats for **A** and 5 PVs from 3 rats for **B**.

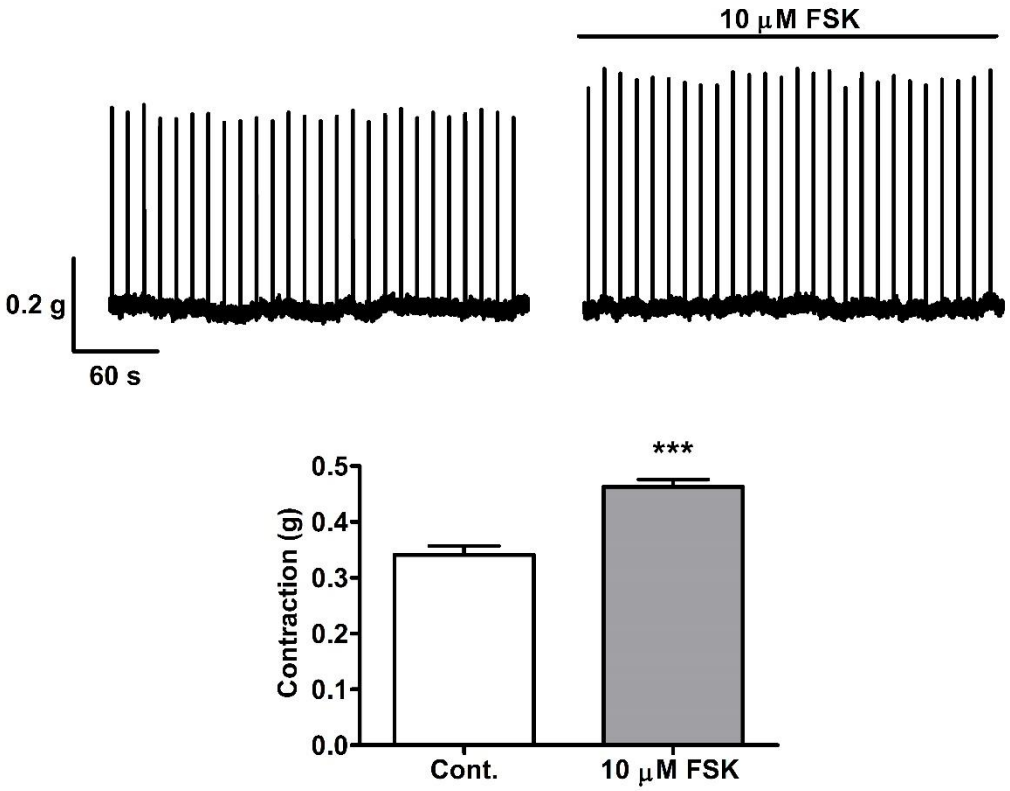

Figure 4.13. The effect of forskolin on the electrically evoked contractions of the pulmonary vein. A. Representative recording of electrically evoked (0.1 Hz) contractions in the pulmonary vein before, and then after 5 min in the presence of forskolin (FSK) (10 μM). **B.** The mean amplitude of the electrically evoked contractions under control conditions and in the presence of FSK (10 μM). Data represent mean ± s.e.m. $^{***}P<0.001$ *vs.* Cont. and n = 3 PVs from 2 rats.

4.3.4. Time matched control

In the control recordings, after a 40 min period following the onset of noradrenaline induced automaticity, the number of contractions decreased slightly, but not significantly, from 67 ± 4 per min to 51 ± 6 per min. From this data it was considered that any statistically significant reduction in the number of contractions per min, within this time frame, was an effect of the inhibitor and did not occur as a result of time. However, 80 min after the onset of automaticity, the number of contractions was significantly reduced to 40 ± 6 per min (n = 6 PVs from 5 rats, $P<0.05$ *vs.* 100 µM NA) (Figure 4.14A and B).

The amplitude of the electrically evoked contractions did not significantly change over time, being 0.51 ± 0.02 g at the onset of automaticity (n = 6 PVs from 5 rats, $P<0.001$ *vs.* control) and 0.49 ± 0.02 g after 40 min. The amplitude was still unchanged at 0.50 ± 0.03 g after 80 min from the onset of noradrenaline induced automaticity (n = 6 PVs from 5 rats, n.s.) (Figure 4.14A and C).

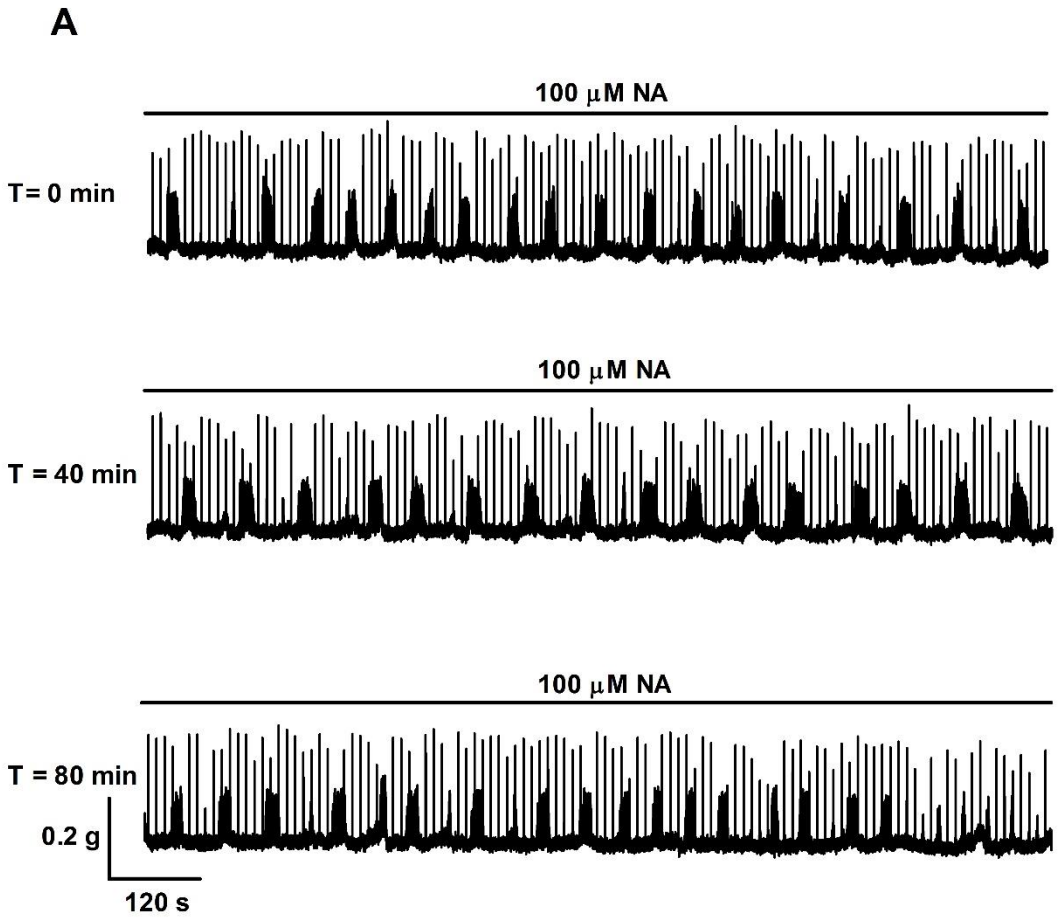

Figure 4.14. Time matched control. A. Contractions of the pulmonary vein in the presence of noradrenaline (NA) (100 μM), beginning at the onset of automaticity (T = 0 min), over a 100 min period. Electrical stimulation was applied at 0.1 Hz throughout the recording.

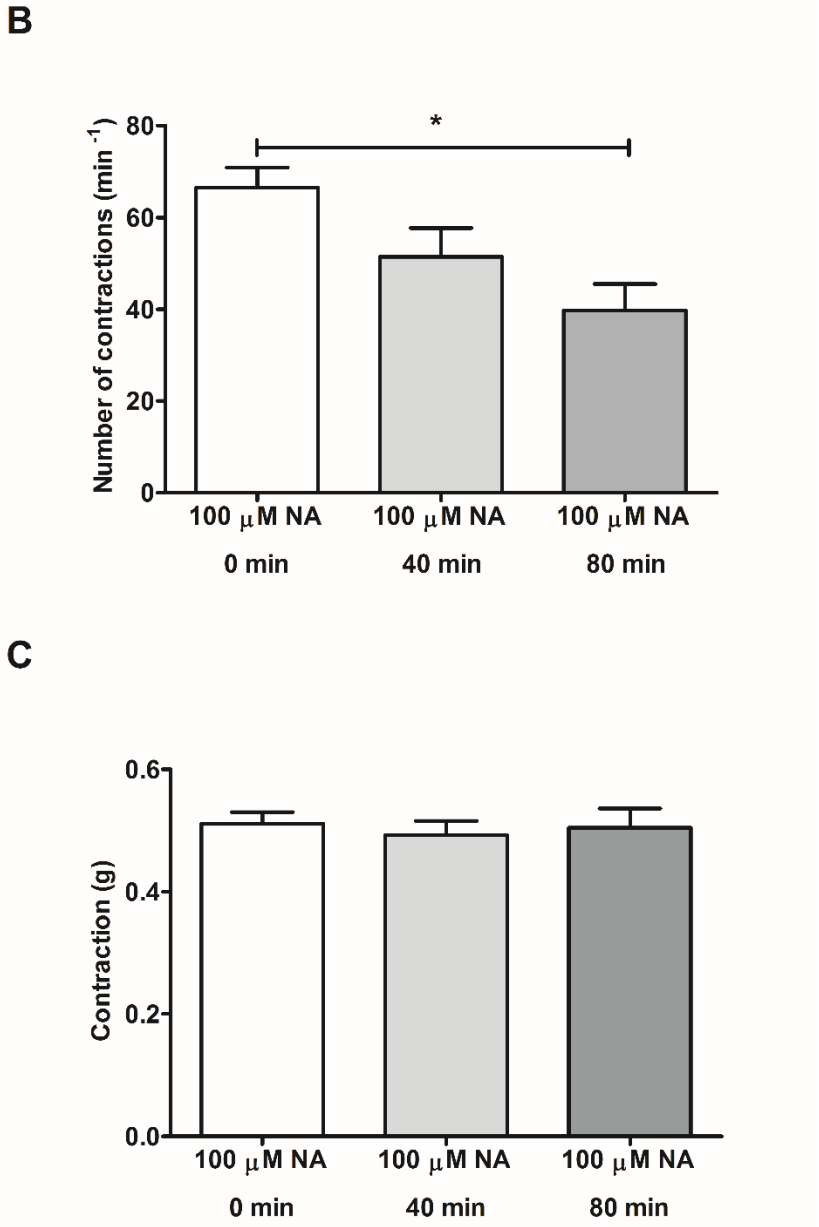

Figure 4.14 (cont.). B. The number of contractions per min at the onset of noradrenaline (NA) induced automaticity, then 40 and 80 min after later. **C.** The mean amplitude of electrically evoked contractions of the pulmonary vein during automaticity in the presence of NA (100 μM), and then 40 and 80 min after the onset of automaticity. $^{*}P<0.025$. n = 6 PVs from 5 rats.

4.3.5. Effect of inhibiting calcium/calmodulin dependent protein kinase II on noradrenaline induced automaticity in the pulmonary vein

The inhibitors KN-93 and AIP were used to investigate if CaMKII is involved in noradrenaline induced automaticity. KN-93 (1 μM) reduced the number of contractions in the presence of noradrenaline (100 μM) from 46 ± 7 per min to 27 ± 5 per min; however, this decrease was not statistically significant. Increasing the concentration of KN-93 to 5 μM, slightly reduced the number of contractions further to 9.6 ± 4.95 per min, which was significantly lower than in the presence of noradrenaline (n = 4 PVs from 4 rats, $P<0.025$) (Figure 4.15A and B).

The amplitude of the electrically evoked contractions was 0.38 ± 0.01 g in the presence of noradrenaline (100 μM), and was not significantly changed, being 0.38 ± 0.01 g in the additional presence of KN-93. However, when the concentration of KN-93 was increased to 5 μM, the amplitude of the electrically evoked contraction was significantly reduced to 0.33 ± 0.01 μM (n = 4 PVs from 4 rats, $P<0.05$ *vs*. 100 μM NA) (Figure 4.15A and C).

The subsequent addition of AIP (10 μM) reduced the number of contractions in the presence of noradrenaline (100 μM) from 34 ± 5 per min to 26 ± 5 per min, but this decrease was not statistically significant (n = 5 PVs from 5 rats, n.s.) (Figure 4.16A and B). Unlike KN93 (5 μM), the presence of AIP (10 μM) had no effect on the mean amplitude of the electrically evoked contractions. The mean amplitude was 0.43 ± 0.01 g in the presence of noradrenaline, and was 0.42 ± 0.01 g after subsequent treatment with AIP (n = 5 PVs from 5 rats) (Figure 4.16A and C). It was also investigated whether inhibiting CaMKII prior to treatment with noradrenaline could prevent noradrenaline induced automaticity. As can be seen in the representative recording in Figure 4.17, pre-incubation with AIP did not prevent automaticity from occurring in the presence of noradrenaline.

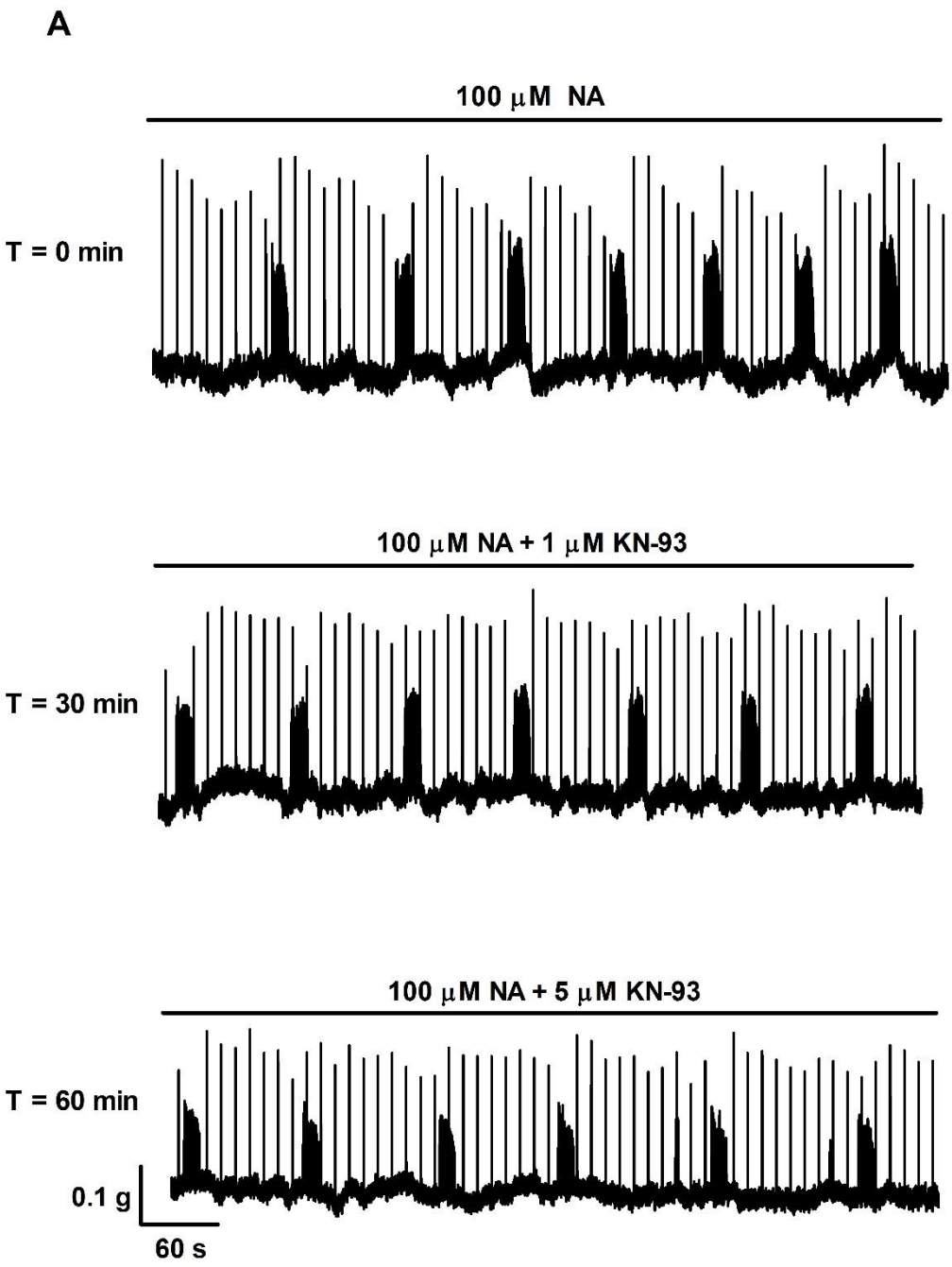

Figure 4.15. The effect of KN-93 on noradrenaline induced automaticity in the pulmonary vein. A. Representative recording displaying contractions of the pulmonary vein during automaticity in the presence of noradrenaline (NA) (100 μM), and following the additional application of KN-93 (1 and then 5 μM. Electrical stimulation was applied at 0.1 Hz throughout the recording.

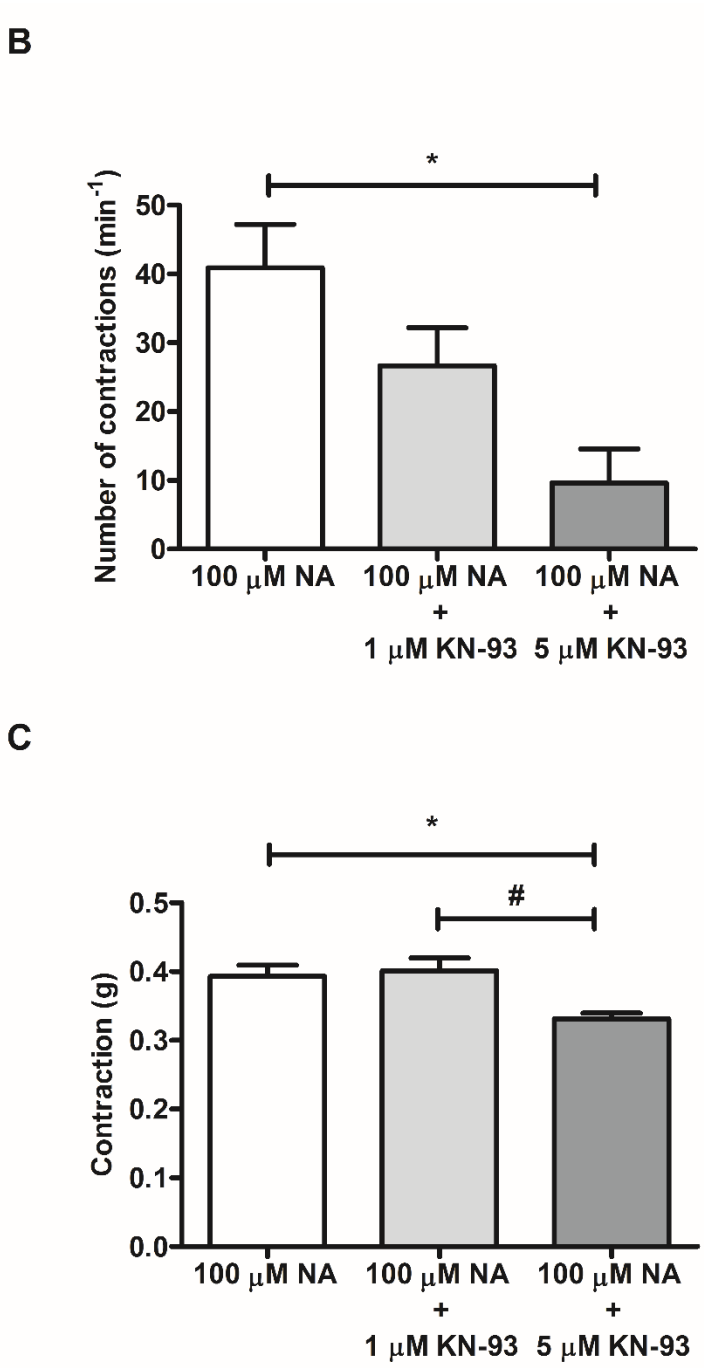

Figure 4.15. B. The mean number of contractions per min during automaticity in the presence of noradrenaline (NA) (100 μM), and after subsequent addition of KN-93 (1 and then 5 μM) **C.** The mean amplitude of the electrically evoked contractions (stimulation at 0.1 Hz), during automaticity, and after the subsequent addition of KN-93 (1 and 5 μM). Data represent mean ± s.e.m. $^{*}P<0.05$ *vs.* 100 μM NA. $^{\#}P<0.05$ vs. 100 μM NA and 5 μM KN-93. n = 4 PVs from 4 rats.

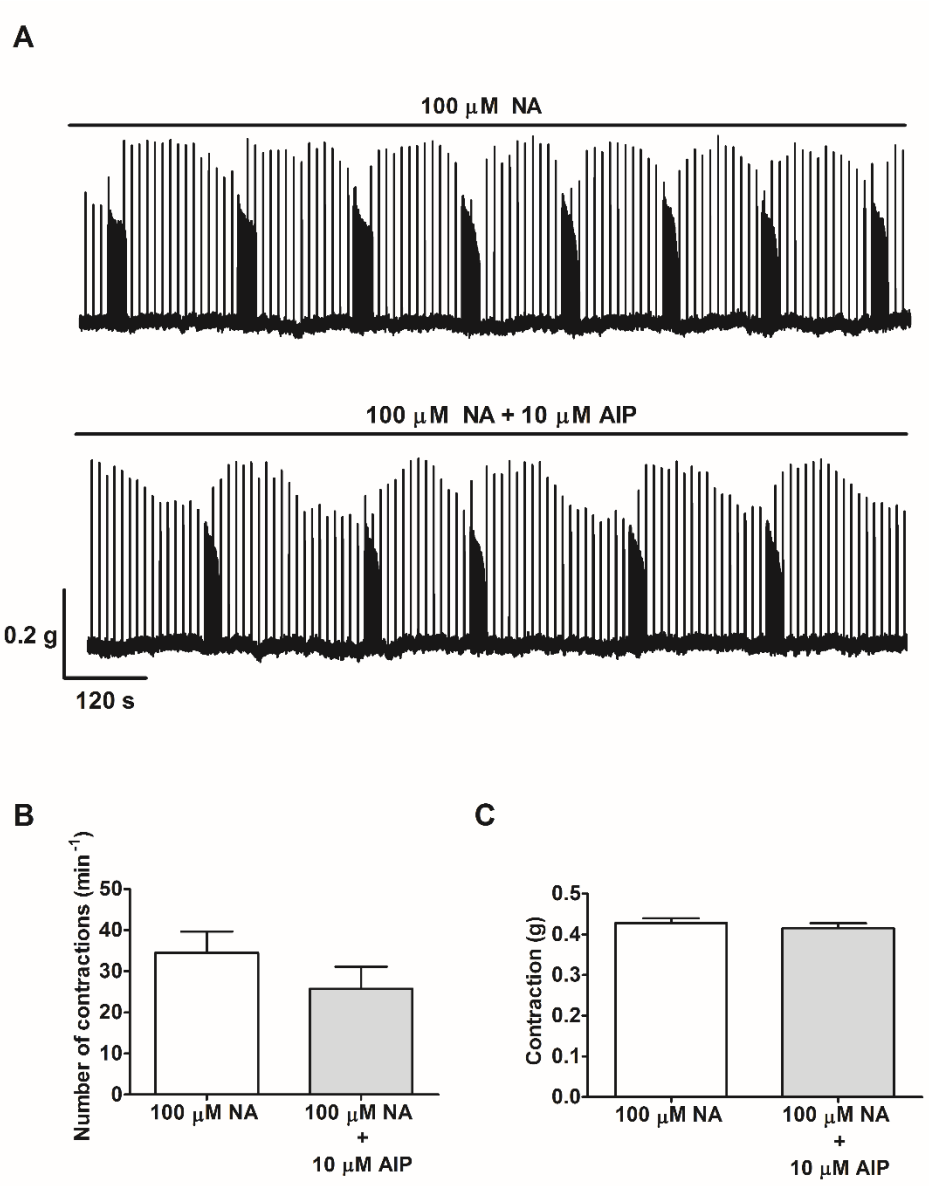

Figure 4.16. The effect of AIP on noradrenaline induced automaticity in the pulmonary vein. A. Representative recording displaying contractions of the pulmonary vein during automaticity in the presence of noradrenaline (NA) (10 μM), and following application of AIP (10 μM). Electrical stimulation was applied at 0.1 Hz throughout the recording. **B.** The mean number of contractions per min during automaticity in the presence of noradrenaline (NA) (100 μM), and after subsequent incubation with AIP (10 μM). **C.** The mean amplitude of the electrically evoked contractions (0.1 Hz) during automaticity, and after the subsequent addition of AIP (10 μM). Data represent mean ± s.e.m. * n = 5 PVs from 5 rats.

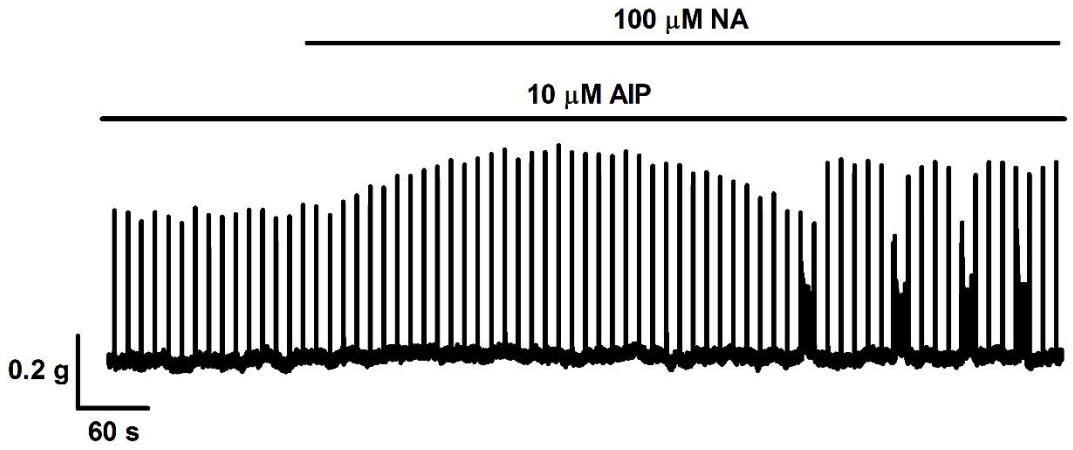

Figure 4.17. The effect of inhibiting CaMKII prior to treatment with noradrenaline. Representative recording of contractions of the pulmonary vein during the induction of automaticity with noradrenaline (NA) (100 μM). The tissue was pre-incubated with AIP (10 μM) 20 min prior to the application of noradrenaline. Electrical stimulation was applied at 0.1 Hz throughout the recording.

4.3.6. Effect of inhibiting gap junctions on noradrenaline induced automaticity of the pulmonary vein

Carbenoxolone (CBX) (100 μM) was used to assess the role of electrical coupling through gap junctions in noradrenaline induced automaticity. In the presence of carbenoxolone (100 μM) the number of contractions was reduced from 38 ± 5 to 16 ± 2 per min (n = 2 PVs from 2 rats) (Figure 4.18A and B). However, the sample size was too small to perform any statistical analysis.

When the pulmonary vein was treated with CBX (100 μM), the mean amplitude of the electrically evoked contractions was decreased from 0.43 ± 0.01 g to 0.32 ± 0.01 g (n = 2 PVs from 2 rats) (Figure 4.18A and C).

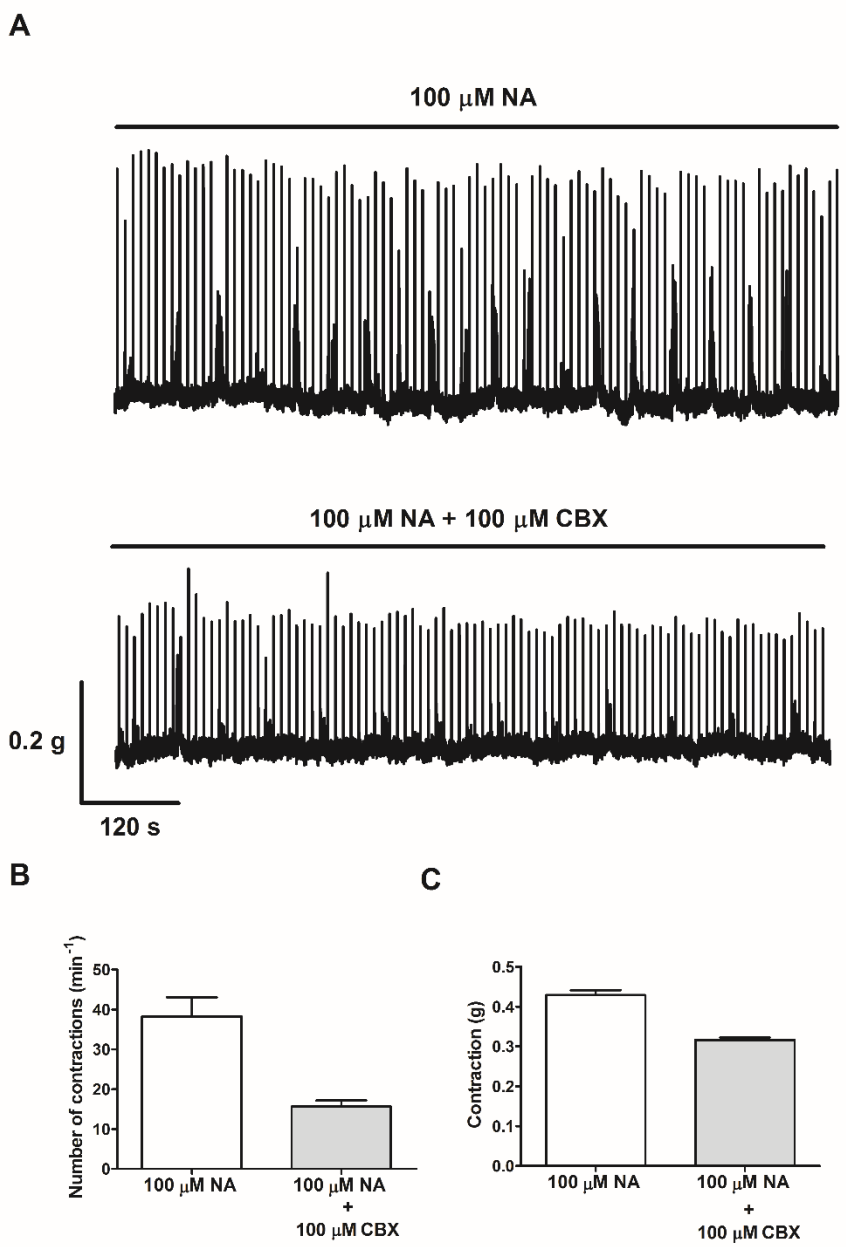

Figure 4.18. The effect of carbenoxolone on noradrenaline induced automaticity in the pulmonary veins. A. Representative recordings displaying contractions of the pulmonary vein during automaticity in the presence of noradrenaline (NA) (100 μM), and following the application of carbenoxolone (CBX) (100 μM). Electrical stimulation was maintained at 0.1 Hz throughout the recording. **B.** The number of contractions per min during automaticity in the presence of NA (100 μM) and after subsequent incubation with CBX (100 μM). **C.** The mean amplitude of electrically evoked (0.1 Hz) contractions during automaticity and after the subsequent addition of CBX (100 μM). Data represent mean. n = 2 PVs from 2 rats.

4.3.7. Effect of inhibiting the Na^+/Ca^{2+} exchanger on noradrenaline induced automaticity of the pulmonary vein

To investigate whether the NCX is involved in the generation of noradrenaline induced automaticity in the pulmonary vein, the tissue was treated with ORM-10103 after the induction of automaticity. After the addition of ORM-10103 (10 μM) the number of contractions in the presence of noradrenaline was significantly reduced from 60 ± 7 per min to 26 ± 2 per min (n = 11 PVs from 8 rats, P<0.001 *vs*. 100 μM NA). When the concentration of ORM-10103 was increased to 20 μM, there was a further reduction in the number of contractions to 14 ± 3 per min (n = 11 PVs from 8 rats, P<0.001 vs. 100 μM NA) (Figure 4.19A and B).

The amplitude of the electrically evoked contractions was 0.46 ± 0.02 g in the presence of noradrenaline (100 μM) and was only slightly reduced to 0.44 ± 0.01 g following treatment with ORM10103. However, when the concentration of the inhibitor was increased to 20 μM, the amplitude of electrically evoked contractions was significantly reduced to 0.39 ± 0.02 g (n = 11 PVs from 8 rats, P<0.01) (Figure 4.19A and C).

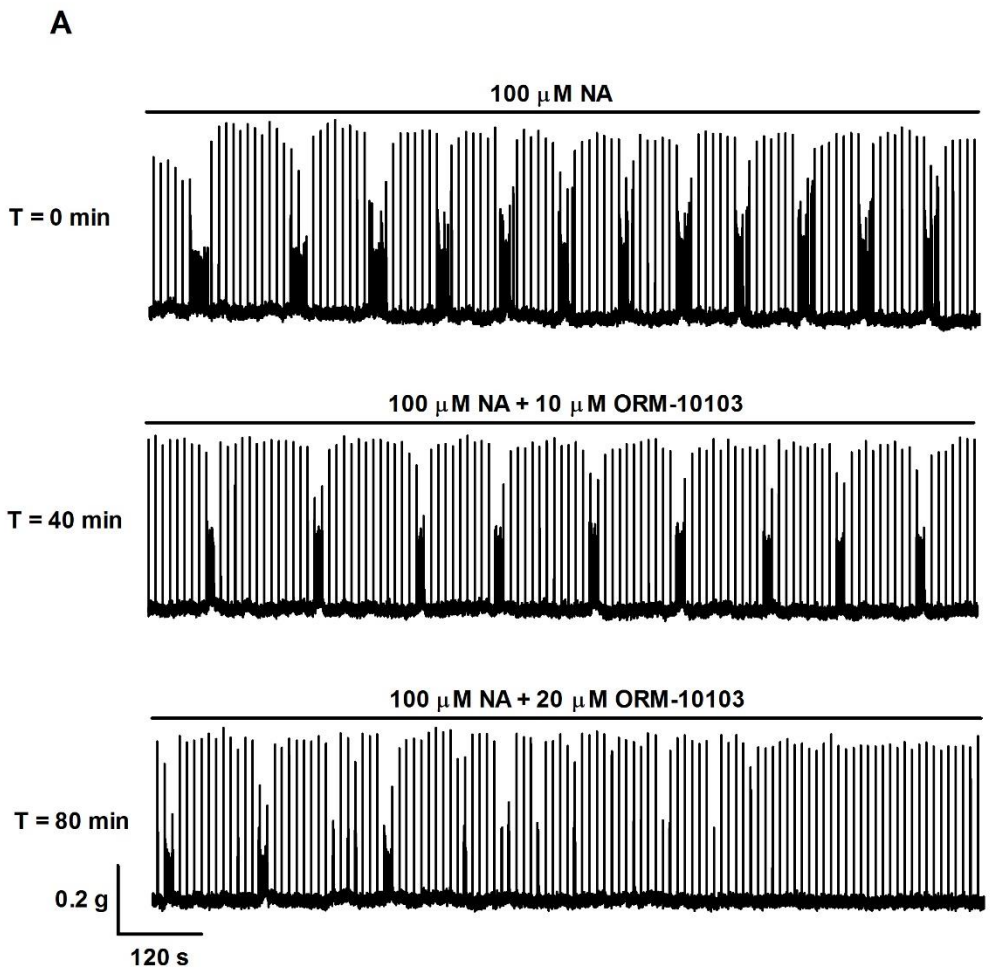

Figure 4.19. The effect of ORM-10103 on noradrenaline induced automaticity in the pulmonary vein. A. Representative recording displaying contractions of the pulmonary vein during automaticity in the presence of noradrenaline (NA) (10 μM), and following the subsequent application of ORM-10103 (10 μM and then 20 μM). Electrical stimulation was applied at 0.1 Hz throughout the recording.

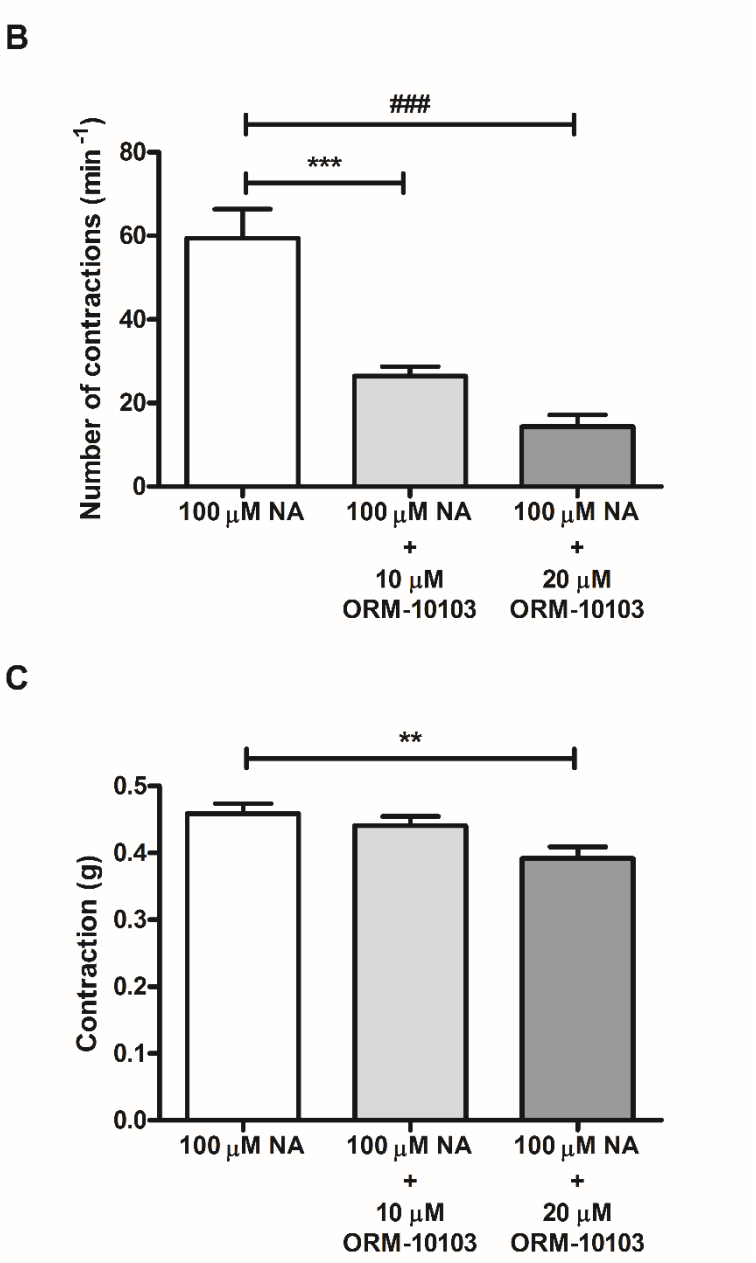

Figure 4.19 (cont.). B. The mean amplitude of electrically evoked (0.1 Hz) contractions during automaticity in the presence of noradrenaline (100 μM), and after the subsequent addition of ORM-10103 (10 μM and then 20 μM). **C.** The number of contractions per min during automaticity in the presence of noradrenaline (NA) (100 μM) and after subsequent incubation with ORM-10103 (10 and then 20 μM). Data represent mean ± s.e.m. $^{***}P<0.001$. n = 11 PVs from 8 rats.

4.4. Discussion

4.4.1. Electrically evoked contractions of the pulmonary vein

In the absence of electrical stimulation, the rat pulmonary vein did not display any spontaneous contractions. When electrical field stimulation was applied, the tissue responded with contractions that were comparable in time-course (<80 ms) to those previously recorded in tissue from the pulmonary vein, as well as the atria and ventricle (Maier *et al.*, 2000; Maupoil *et al.*, 2007; Stemmer & Akera, 1986). Thus, it is highly likely that these contractions arose from the cardiomyocytes as opposed to smooth muscle cells, because the electrically evoked contraction of smooth muscle requires repeated stimuli and occurs over a much longer time course (Jackson *et al.*, 2002; Vanhoutte, 1974). This is further supported by the fact that the pulmonary vein was mounted vertically, and the cardiomyocytes are orientated longitudinally and obliquely, whereas smooth muscle cells have been shown to be arranged circumferentially in the vein (Hashizume *et al.*, 1998).

4.4.2. Force-frequency relationship

The rat pulmonary vein displayed a negative force-frequency relationship, whereby the amplitude of the electrically evoked contractions was decreased when the stimulation frequency was increased. This was most evident between 0.1 and 3 Hz. Increasing the stimulation frequency between 4 and 9 Hz resulted in no further decline in the contraction amplitude.

A negative force-frequency relationship has previously been observed in the rat pulmonary vein (MacLeod & Hunter, 1967), atria (Landmark & Refsum, 1977; Stemmer & Akera, 1986) and ventricle (Bouchard & Bose, 1989; Maier *et al.*, 2000). This appears to be a characteristic of rodent myocardium, since the same tissue obtained from larger mammals, such as the guinea pig and rabbit, has been shown to display a positive force-frequency relationship (Bouchard & Bose, 1989; de Borda *et al.*, 1974; Kurihara & Sakai, 1985; Luk *et al.*, 2008; Maier *et al.*, 2000; Stemmer &

Akera, 1986). The reason for these differences are still unclear; however, it has been suggested that the positive force-frequency relationship observed in larger mammals is due to an increase in the SR Ca^{2+} load and Ca^{2+} transient amplitude (Hattori *et al.*, 1991; Maier *et al.*, 2000). This has been proposed to be due to the accumulation of intracellular Na^{+} occurring at increasing stimulation frequencies, which results in enhanced reuptake of Ca^{2+} into the sarcoplasmic reticulum (SR), and depressed extrusion of Ca^{2+} through the NCX (Kurihara & Sakai, 1985; Maier *et al.*, 2000).

A possible explanation for the negative force-frequency relationship that was observed in the present study is that there was insufficient time for the SR to refill at the higher stimulation frequencies, resulting in a reduced SR Ca^{2+} load and contractile force. However, the experiments in chapter 3 where fluo-4 was used to the monitor Ca^{2+} signalling in the pulmonary vein suggest otherwise. The caffeine induced Ca^{2+} transient was found to be unchanged from unstimulated conditions after a period of electrical stimulation at 5 Hz. (Figure 3.14). Moreover, studies using rat ventricular trabeculae, have shown that the negative force-frequency relationship was not accompanied by significant changes in SR Ca^{2+} load; as estimated by rapid cooling contractures (Banijamali *et al.*, 1991; Bouchard & Bose, 1989; Maier *et al.*, 2000). This evidence suggests that decreased SR loading does not occur with increasing stimulation frequency, and there therefore must be different frequency-dependent mechanism that determines the contractile force in rat cardiac tissue.

Rat cardiac myocytes have been shown to have relatively high basal intracellular Na^{+} levels compared to other species, which limits the removal of Ca^{2+} though the NCX (Shattock & Bers, 1989). It has been estimated in rat ventricular myocytes that SERCA accounts for approximately 90% of the total removal of Ca^{2+} from the cytosol during relaxation, compared to 70% in the rabbit (Bassani *et al.*, 1994; Negretti *et al.*, 1993). The relative contribution of SR Ca^{2+} uptake and the NCX for the removal of cytosolic Ca^{2+} was estimated in rat ventricular trabeculae by comparing the magnitude of two sequential cooling contractures. It was found that the ratio of the two cytosolic Ca^{2+} removal mechanisms was unchanged by increasing the frequency of electrical

stimulation. However, compared to the rabbit trabeculae, the SR was more dominant than the NCX for the removal of Ca^{2+} at all of the stimulation frequencies examined (Maier *et al.*, 2000). Therefore, it is possible in rat cardiac tissue at low stimulation frequencies, the sarcoplasmic reticulum Ca^{2+} ATPase (SERCA) is already so dominant that there is minimal capacity for the myocyte to increase the SR Ca^{2+} load at the higher frequencies of stimulation.

Some rat ventricular myocytes when isolated, have been shown to display a positive force-frequency relationship, and these cells had a reduced SR Ca^{2+} load compared to myocytes in the population that displayed a negative force-frequency relationship. Furthermore, in the myocytes that displayed a positive force-frequency relationship, the intracellular Na^{+} concentration and SR Ca^{2+} load increased in accordance with increasing stimulation frequency (Frampton *et al.*, 1991). This is not inconsistent with the hypothesis that in rat cardiac tissue that displays a negative force-frequency relationship, the myocytes already have a high degree of SR loading to begin with.

If the SR Ca^{2+} load is unaltered by increasing the frequency of electrical stimulation, then the dominant factor for determining contractile force in the rat pulmonary vein would therefore be the fraction of Ca^{2+} released from the SR during each contraction. It was suggested by Maier *et al.*, (2000) that the negative force-frequency relationship observed in rat cardiac tissue is due to there being less time for the RyRs to recover from an inactive state. According to this hypothesis, the magnitude of Ca^{2+} released from the SR during each contraction is not determined by the quantity of available Ca^{2+}, but instead by the refractoriness of the Ca^{2+} release channels (Györke & Fill, 1993; Satoh *et al.*, 1997; Schiefer *et al.*, 1995).

An alternative explanation for the negative force-frequency relationship observed in the rat model is intracellular acidosis, occurring at the higher frequencies of stimulation. In the Langendorff perfused rat heart, increasing the frequency of electrical stimulation from 3 to 5 Hz has been shown to result in a reduction in the left

ventricular pressure, which is indicative of decreased contractile force. The amplitude of Ca^{2+} transients that were evoked by electrical stimulation was not significantly changed during electrical stimulation at 5 Hz; however, there was a reduction in the intracellular pH. On the other hand, in the guinea pig heart, where a positive force-frequency relationship was observed, the intracellular pH was unchanged by increasing the stimulation frequency (Morii *et al.*, 1996). Acidosis has been shown in isolated ventricular myocytes to desensitise the response of the myofilaments to Ca^{2+}, which resulted in a reduction in the contractile amplitude (Fabiato & Fabiato, 1978).

4.4.3. The effect of noradrenaline on the force-frequency relationship

When the pulmonary vein was treated with noradrenaline there was a potentiation of the contractile response, as well as a blunting of the negative force-frequency relationship. The application of forskolin also increased the contractile amplitude, suggesting that the positive inotropic effect of noradrenaline was due to activation of adenylate cyclase, and the subsequent elevation of intracellular cAMP (Seamon *et al.*, 1981). Similar findings that noradrenaline blunts the negative force-frequency relationship have also been made in the atria of the rat (Stemmer & Akera, 1986) and mouse (Heubach *et al.*, 1999).

Protein kinase A, which is activated by cAMP, phosphorylates LTCCs, increasing Ca^{2+} influx upon depolarisation (Brum *et al.*, 1984; Hulme *et al.*, 2003; Yatani & Brown, 1989). This would result in increased gain for Ca^{2+} -induced Ca^{2+} release, allowing for a greater fractional release during each Ca^{2+} transient (Valdivia *et al.*, 1995; Viatchenko-Karpinski & Györke, 2001; Zhou *et al.*, 1999). There could also be a direct effect on the RyR, as protein kinase A is known to increase the open probability of the channel (Yoshida *et al.*, 1992). The latter point is particularly relevant if the restitution of the RyRs is responsible for the negative force-frequency relationship in the rat pulmonary vein. Protein kinase A also phosphorylates phospholamban, removing its inhibitory effect on SERCA, which would increase the rate of SR Ca^{2+} refilling (Lindemann *et al.*, 1983; Patel *et al.*, 1995).

Another factor to be taken into consideration is the possible effect of noradrenaline, downstream of intracellular Ca^{2+} signalling, on the contractile machinery of the cardiomyocytes. In rat ventricular myocytes that were chemically skinned to allow the intracellular Ca^{2+} concentration to be controlled, stimulation of α-adrenoreceptors has been shown to increase the sensitivity of the myofilament to Ca^{2+} (Endoh & Blinks, 1988; Puceat *et al.*, 1990). Phosphorylation of myosin light chain kinase, which directly phosphorylates myosin light chain II to allow binding to actin, has been implicated as the underlying mechanism (Andersen *et al.*, 2002; Clement *et al.*, 1992; Endou *et al.*, 1991; Venema *et al.*, 1993). Therefore, it is possible that noradrenaline increased the sensitivity of the myofilament to Ca^{2+}, which would increase the contractility of the pulmonary vein.

4.4.4. Noradrenaline induced automaticity in the rat pulmonary vein

In the presence of noradrenaline, the pulmonary vein displayed automaticity, and this occurred even in the absence of electrical stimulation. Following the application of noradrenaline, there was a latency period of approximately 10 min before the pulmonary vein responded with periodic bursts of contractions, where the amplitude and frequency of contractions within each burst was highly variable. It was also clear that the amplitude of the automatic contractions was lower than those that were electrically evoked at 0.1 Hz. This is likely to have been due to the higher frequency during the burst (~4 to 6 Hz), and probably occurred via the same mechanism as the negative force-frequency relationship. The duration of each burst and the cycle period between bursts also varied considerably between different preparations. The characteristics of noradrenaline induced automaticity, vis-à-vis the periodic nature as well as the amplitude and frequency, are in agreement with the earlier study in the rat pulmonary vein by Maupoil *et al.*, (2007).

Forskolin increased the amplitude of the electrically evoked contractions in the pulmonary vein; however, automaticity was never observed, which suggests that

increased intracellular cAMP is not the sole mechanism. This is consistent the previous report by Maupoil *et al*., (2007) that the generation of automaticity requires the co-activation of α and β-adrenoreceptors. Similar findings have been made in the rat atria, where automatic contractions were not observed in the presence of forskolin or isoprenaline (Wolkowicz *et al.*, 2007). Sporadic automatic contractions could be induced, however, by treatment with 2-APB which, while typically used as an inhibitor of IP_3 receptors, can potentiate SR Ca^{2+} release when applied at high concentrations (Bootman *et al.*, 2002). Interestingly, when 2-APB was applied to the rat atria, in combination with forskolin or isoprenaline, high frequency (~4 Hz) automatic contractions were observed (Wolkowicz *et al.*, 2007). This again suggests that multiple cellular mechanisms are likely to underlie automaticity in cardiac tissue and this could translate to the pulmonary vein myocardial sleeve.

Automaticity has also been shown to be induced by noradrenaline in isolated cardiomyocytes from the rat pulmonary vein, although in this case automaticity was characterised by the sustained firing of action potentials, rather than repetitive bursts of activity (Okamoto *et al.*, 2012). The study on isolated cells was in agreement though, with the previous reports in the intact tissue, that automaticity requires the co-activation of α and β-adrenoreceptors (Doisne *et al.*, 2009; Maupoil *et al.*, 2007). This suggests that the classical α-adrenoreceptor signalling pathway, where the G-protein mediated activation of phospholipase C results in the increased production of IP_3, may be involved (Poggioli *et al.*, 1986; Scholz *et al.*, 1992). It is plausible that, during the period between bursts, the increased intracellular concentration of IP_3, combined with the increased open probability of RyRs associated with β-adrenoreceptor stimulation (Yoshida *et al.*, 1992), provided the necessary increase in cytosolic Ca^{2+} to activate depolarising inward currents, and generate automatic action potentials and contractions (Patterson *et al.*, 2006; Schlotthauer & Bers, 2000). ATP and endothelin-1, which are agonists for the G-protein-coupled receptor that mediates IP_3 production, have been shown to increase the forward mode NCX current in human ventricular myocytes (Signore *et al.*, 2013). Automaticity, which was induced in the rat atria using 2-APB, has also been shown to be supressed by inhibiting the forward mode NCX with Ni^{2+} (Huo *et al.*, 2010). Direct support for this hypothesis are the findings that

noradrenaline induced automaticity could be supressed in isolated cardiomyocytes by pharmacological inhibition of phospholipase C or IP_3 receptors (Okamoto *et al.*, 2012).

Stimulation of α-adrenoreceptors has also been shown to reduce background K^+ currents in atrial myocytes (Braun *et al.*, 1992; Jahnel *et al.*, 1991). As the inward rectifier K^+ current (I_{K1}) is known to be involved in maintaining the resting membrane potential of cardiac myocytes (Hutter & Noble, 1960; Koumi *et al.*, 1995; Noble & Tsien, 1968), a reduction in this current could lead to electrical instability and depolarisation. It is possible that this is relevant to the pulmonary vein, as canine pulmonary vein cardiomyocytes that display spontaneous action potentials have been shown to have smaller I_{K1} than those that were quiescent (Chen *et al.*, 2001; Chen *et al.*, 2002b).

4.4.5. Possible mechanisms underlying noradrenaline induced automaticity

4.4.5.1. Ca^{2+}/calmodulin-dependent protein kinase II

There was a significant reduction in the occurrence of noradrenaline induced contractions in the presence of the CaMKII inhibitor KN-93, but not AIP. However, with AIP being a peptide, it would have limited membrane permeability, which could explain the difference in results. In future, a myristoylated form of AIP could be used, which has greater membrane permeability and has been shown to have an effect on intracellular Ca^{2+} signalling in cardiac myocytes (Guo & Duff, 2006; MacQuaide *et al.*, 2007; Vinogradova *et al.*, 2000). Alternatively, AIP with an Antennapedia transport peptide attached could be used, as this would also allow for greater membrane permeability (Thorén *et al.*, 2000).

One other study has investigated the role of CaMKII on automaticity in the pulmonary vein. This was conducted in the rabbit, where spontaneous action potentials and contractions were present in 49% of the preparations. After treatment with

phenylephrine or isoprenaline, the rate of spontaneous action potentials and contractions was increased. The subsequent addition of KN-93 had no effect; however, pre-treatment with the inhibitor reduced the extent to which the agonists increased the frequency of spontaneous activity. This suggests that inhibitors of CaMKII may prevent, but not supress, automaticity (Lo *et al.*, 2007). Although in the current investigation, automaticity could still be induced with noradrenaline when the pulmonary vein was pre-treated with AIP; however, given the concerns above regarding the membrane permeability of AIP, this would have to be tested with KN-93. It is important however to consider that the experiments by Lo *et al.*, (2007) were performed on a different species where, unlike the rat, spontaneous contractions were observed under control conditions. Therefore, while it would seem that CaMKII has some involvement in noradrenaline induced automaticity, it is difficult at this stage to draw conclusions as to its exact role.

4.4.5.2. Gap junction conductance

The gap junction inhibitor carbenoxolone appeared to reduce the occurrence of automatic contractions in the presence of noradrenaline. Electrophysiological studies on the rat pulmonary vein have not determined if noradrenaline induced automaticity initiates at ectopic foci before conducting throughout the myocardial sleeve, or whether there is a simultaneous depolarisation across the tissue (Doisne *et al.*, 2009; Namekata *et al.*, 2010). Triggered activity in the canine pulmonary vein, which was induced by stimulation of the stellate ganglion following sinus node crushing, has been shown to occur at ectopic foci that were rich in sympathetic nerves. Moreover, the transcardiac noradrenaline levels were increased by the aforementioned *in vivo* intervention suggesting that the ectopic electrical activity may have been caused by activation of adrenoreceptors (Tan *et al.*, 2008). The gap junction inhibitor heptanol has also been shown to prevent triggered propagated contractions in ventricular trabeculae, which were induced by pacing at 2 Hz for brief intervals, interspersed with periods of rest (Zhang *et al.*, 1996). A possible mechanism would therefore be that inhibiting gap junctions, increases the intercellular resistance, preventing the interaction between neighbouring cardiomyocytes, and the propagation of electrical

signals (Krishnan *et al.*, 2005). The exact mechanisms behind the inhibition of noradrenaline induced automaticity in the pulmonary vein by carbenoxolone cannot be elaborated on in the present study, although the preliminary data certainly proposes a role for intercellular signalling through gap junctions.

4.4.5.3. The Na^+/Ca^{2+} exchanger

Inhibiting the NCX with ORM-10103 partially supressed noradrenaline induced automaticity in a concentration dependent manner. However, when the concentration of ORM-10103 was raised from 10 to 20 µM, the amplitude of the electrically evoked contractions was reduced. As the contractile amplitude was shown to be unchanged during the time matched control experiments, this is likely to have been an effect of the inhibitor. A potential candidate is the I_{CaL}, which has been shown to slightly, but not significantly, reduced in the presence of 10 µM ORM-10103 (Jost *et al.*, 2013).

Inhibition of the NCX with SEA0400 has previously been shown to supress noradrenaline induced automaticity in isolated pulmonary vein cardiomyocytes from the rat. Simultaneous measurements of the Ca^{2+} and electrical activity were made using the fluorescent dye indo-1 and the whole-cell patch clamp method. In the presence of noradrenaline there were transient increases in intracellular Ca^{2+}, which occurred simultaneously with an oscillatory inward current. This suggested that an increase in cytosolic Ca^{2+} concentration resulted in activation of the NCX, which generated depolarisation and elicited action potentials (Okamoto *et al.*, 2012). The role of intracellular Ca^{2+} in the generation of action potentials via the NCX has also been demonstrated in the rabbit pulmonary vein, where triggered action potentials, which were induced by rapid pacing and treatment with a low concentration of ryanodine, were prevented by inhibiting the forward mode of the NCX with Ni^{2+} (Honjo *et al.*, 2003a).

.4.4.5. Summary

The rat pulmonary vein displayed a negative force-frequency relationship, suggesting that the pulmonary vein has similar contractile properties as the rat atria and ventricle. Noradrenaline blunted the negative force-frequency relationship and also induced automaticity. While it is likely that multiple signalling pathways are involved in the generation of automaticity in the presence of noradrenaline, the present investigation provides evidence to support the role of the NCX. The exact cellular mechanisms behind noradrenaline induced automaticity, as well as the application of these findings to human tissue still merits future investigation.

Chapter 5

General Discussion

5.1. Noradrenaline induced automaticity in the rat pulmonary vein

This study has shown that noradrenaline induces automaticity in the pulmonary vein in the form of periodic bursts of contractions that occur independently of electrical stimulation. Similar observations have previously been made in the rat pulmonary vein, where it was shown that automaticity relied on the co-activation of α and β adrenoreceptors (Maupoil *et al.*, 2007). In the present study, automaticity was not induced by direct activation of adenylate cyclase with forskolin, which supports the findings that β adrenergic stimulation alone does not cause automaticity (Maupoil *et al.*, 2007)

The role of the Na^+/Ca^{2+} exchanger (NCX) in noradrenaline induced automaticity was investigated, as it is known to be activated by an increase in intracellular Ca^{2+} to generate a depolarising inward current (Kass *et al.*, 1978; Schlotthauer & Bers, 2000). It was found that the novel NCX inhibitor ORM10103 reduced the incidence of automaticity in a concentration dependent manner. This is consistent with studies that have shown that the NCX is involved in generating automaticity and triggered activity in the pulmonary veins of the canine (Patterson *et al.*, 2006), rabbit (Honjo *et al.*, 2003a) and guinea pig (Namekata *et al.*, 2009), as well as in isolated cardiomyocytes from the rat pulmonary vein (Okamoto *et al.*, 2012).

The localisation of the NCX was examined by immunocytochemistry, where it was shown to be more likely to be distributed as transverse striations in the pulmonary vein, compared to left atrial cardiomyocytes. The NCX was not densely expressed at the intercalated disc region, like it was in ventricular myocytes; however, it is unknown whether the different expression of the NCX serves a physiological function or reflects extensive infolding of the sarcolemma (Kieval *et al.*, 1992; Page, 1978). When Di-4 ANEPPS was used to compare the atrial and pulmonary vein cardiomyocytes, it was found that the dye predominately stained the periphery of the atrial myocytes suggesting that they possessed few or no T-tubules. On the other hand, the vast majority of pulmonary vein cardiomyocytes had more substantial T-tubule system. This could be related to the propensity of the pulmonary vein towards automaticity, as

previous investigations have found that noradrenaline does not induce automaticity in the rat atria (Doisne *et al.*, 2009; Maupoil *et al.*, 2007). It is possible that in pulmonary vein cardiomyocytes, when spontaneous Ca^{2+} transients occur, by virtue of their proximity, the NCX would have preferential access to locally released Ca^{2+}. Consequently, cardiomyocytes with a more extensive T-tubule system would be expected to be more prone to automaticity generated by Ca^{2+} removal via the NCX (Trafford *et al.*, 2013).

The presence of T-tubules could also have an influence on the spatial characteristics of spontaneous SR Ca^{2+} release. In rat atrial myocytes lacking T-tubules, spontaneous Ca^{2+} sparks have been shown to only occur at the periphery of the cells, whereas in atrial myocytes with T-tubules, spontaneous Ca^{2+} sparks were observed in the cell interior. This suggests that spontaneous SR Ca^{2+} release occurs where the ryanodine receptors (RyRs) are in apposition with the sarcolemma (Kirk *et al.*, 2003). Studies in human atrial myocytes have also shown a tendency towards Ca^{2+} sparks occurring in the cell interior (Gassanov *et al.*, 2006; Hove-Madsen *et al.*, 2006). As pulmonary vein cardiomyocytes had a more substantial T-tubule network, it is therefore possible that there is a greater localisation of RyRs in the proximity of the sarcolemma. Should this be the case, then the implications for spontaneous SR Ca^{2+} release, and the ability for the cardiomyocytes to generate Ca^{2+} waves requires further investigation using an imaging set up with a higher acquisition rate.

It has also been suggested that the so called “eager sites” for spontaneous SR Ca^{2+} release are located where there is coupling of ryanodine and IP_3 receptors, the latter of which have been shown to be localised at the cell periphery in atrial myocytes (Lipp *et al.*, 2000; Mackenzie *et al.*, 2002). Given this information, it is noteworthy that studies in isolated rat pulmonary vein cardiomyocytes have shown that IP_3 receptors are distributed at the T-tubules in the cell interior, and noradrenaline induced automaticity was supressed by their inhibition (Okamoto *et al.*, 2012). Furthermore, spontaneous Ca^{2+} transients in the intact pulmonary vein have been shown to be inhibited by 2-APB (Logantha *et al.*, 2010). In contrast, spontaneous Ca^{2+} transients in

mouse lung slices have been shown to be unaffected by 2-APB (Rietdorf *et al.*, 2014), and therefore the role of IP_3 receptors in pulmonary vein automaticity merits further investigation.

The present study demonstrates an important role for the NCX in noradrenaline induced automaticity. However, there are reports that automaticity can be generated by other mechanisms. Recently, a voltage-dependent Cl^- channel that is activated on hyperpolarisation, has been identified in isolated pulmonary vein cardiomyocytes. The current generated by this channel was suggested to facilitate noradrenaline induced automaticity by accelerating diastolic depolarisation, as automaticity was either reduced in incidence or was abolished altogether by Cl^- channel blockers (Okamoto *et al.*, 2014). It was also recently shown that rat pulmonary vein cardiomyocytes have a basal tetrodotoxin (TTX)-sensitive Na^+ permeability. Blockade with TTX reduced the incidence of noradrenaline induced automaticity by slowing diastolic depolarisation and increasing the cycle period between the automatic bursts of action potentials. This suggests that the Na^+ current contributes to the slow diastolic depolarisation between the bursts of automaticity (Malécot *et al.*, 2015). These studies highlight the complexity of physiological systems and the difficulties associated with identifying individual mechanisms. Nevertheless, the present study proposes a role for the NCX, and therefore this could be a useful target for research into selective pharmacological intervention.

5.2. Spontaneous Ca^{2+} transients in the pulmonary vein and the effect of noradrenaline

When the intracellular Ca^{2+} concentration was monitored with fluo-4, spontaneous Ca^{2+} transients that were asynchronous in neighbouring cardiomyocytes were observed under control conditions. The frequency of spontaneous Ca^{2+} transients was increased by the presence of noradrenaline; however, synchronous Ca^{2+} transients, like those that were observed during electrical stimulation, were not observed. The contractile studies showed that noradrenaline was only able to induce automaticity at 37 °C, but not at room temperature, and that there was a latency period of

approximately 10 min before automaticity was observed. Due to the difficulties associated with using Ca^{2+} sensitive fluorescent indicators at higher temperatures, images could not be obtained over longer time course, and therefore whether noradrenaline induced automaticity occurs by entraining the spontaneous Ca^{2+} transients to become synchronous cannot be elucidated at this time.

Different experimental approaches were employed at room temperature to determine if the spontaneous Ca^{2+} transients could be induced to occur more frequently, thus becoming more synchronous (Brunello *et al.*, 2013; Stern *et al.*, 1983). In some preparations, when the external Ca^{2+} concentration was increased and the pulmonary vein was electrically stimulated at 1 Hz, there was evidence of a premature increase in fluo-4 fluorescence in the field of view, between the electrically evoked Ca^{2+} transients. Further analysis using ROIs determined that this was caused by an increase in the frequency of spontaneous Ca^{2+} transients occurring between those that were electrically evoked, suggesting that they were simultaneously present in multiple neighbouring cardiomyocytes. Following termination of a period of electrical stimulation, particularly at the higher rates (>5 Hz), the frequency of spontaneous Ca^{2+} transients was greater than that without prior stimulation. Furthermore, this effect was markedly enhanced in the presence of isoprenaline, or when the external Ca^{2+} concentration was increased. Under these conditions, the spontaneous Ca^{2+} transients that occurred after the cessation of electrical stimulation appeared in the pseudo-linescan images to be present in multiple cardiomyocytes at the same time. To determine if the spontaneous Ca^{2+} transients were occurring more synchronously, the percentage of pixels displaying a rise in fluorescence was used to provide an index of the Ca^{2+} transient synchronisation over time. It was found that immediately after a period of electrical stimulation, there was a transient increase in the synchronisation of the spontaneous Ca^{2+} transients, which lasted for a few seconds before returning to control levels by the end of the recording period.

The mechanisms underlying the increase in the frequency of spontaneous Ca^{2+} transients are unclear at the present time. However, estimation of the SR Ca^{2+} load

using caffeine suggests that it was not caused by increased SR loading. An alternative explanation is that there was sensitisation of the RyRs (Venetucci *et al.*, 2008) or increased SERCA activity (Maxwell & Blatter, 2012). For instance, CaMKII, which is known to phosphorylate RyRs and increase SR Ca^{2+} release (Hain *et al.*, 1995; Wehrens *et al.*, 2004), has been shown to be activated by high frequency electrical stimulation in ventricular myocytes (Dries *et al.*, 2013; Huke & Bers, 2007). CaMKII has also been shown to modulate the frequency and velocity of Ca^{2+} waves through its effects of SERCA activity (MacQuaide *et al.*, 2007). This would increase the rate in which the local SR Ca^{2+} content reaches the threshold for spontaneous release as the wave travels along the cardiomyocyte (Maxwell & Blatter, 2012)

In the contractile studies, inhibition of CaMKII with KN-93 reduced the occurrence of noradrenaline induced automaticity, and this decrease was statistically significant in the presence of 5 μM KN-93. However, there was a reduction in the number of contractions per min within this time frame in the time matched control experiments, albeit not to the same extent. There was also a significant reduction in the amplitude of the electrically evoked contractions in the presence of 5 μM KN-93, suggesting that it attenuated the increase that was observed with noradrenaline. There is continued debate over the involvement of CaMKII on the positive inotropic effect of β-adrenergic stimulation, with some studies suggesting the lack on an acute effect of CaMKII inhibition on cardiac myocyte contractility (Wang *et al.*, 2004; Zhang *et al.*, 2005). It is therefore difficult at this stage to conclude whether CaMKII plays a role in the positive inotropic effect of noradrenaline in the pulmonary vein. Similarly, further investigation is required to elucidate role of CaMKII on noradrenaline induced automaticity and the increase in the frequency of spontaneous Ca^{2+} transients.

The investigations described herein indicate that the spontaneous Ca^{2+} transients in the pulmonary vein are not maximal under control conditions, and can occur at a greater frequency. It has been shown in the rat ventricle that following a period of high frequency electrical stimulation, the emergence of spontaneous Ca^{2+} transients at a higher frequency produced triggered electrical activity. This demonstrated a direct link

between spontaneous Ca^{2+} transients and depolarisation (Fujiwara *et al.*, 2008; Wasserstrom *et al.*, 2010). It is tempting to speculate that a similar phenomenon might exist in the rat pulmonary vein, especially since, after a period of high-frequency electrical stimulation in the presence of isoprenaline or high external Ca^{2+}, the initial synchronisation was often as high as 0.8 to 0.9. Simultaneous measurement of the electrical activity and Ca^{2+} signalling would be required to verify this proposition and confirm that increasing the frequency of spontaneous Ca^{2+} transients causes arrhythmogenic activity.

5.3. Electrically evoked Ca^{2+} transients

When the pulmonary vein was electrically stimulated, synchronous Ca^{2+} transients were evoked in neighbouring cardiomyocytes. The electrically evoked Ca^{2+} transients occurred in discrete regions of tissue, surrounded by cardiomyocytes that did not respond to stimulation. Although the electrically evoked Ca^{2+} transients appeared to be homogenous in the individual cardiomyocytes; imaging using a system with a higher temporal resolution will be required to determine the spatiotemporal characteristics of the intracellular Ca^{2+} transient in pulmonary vein cardiomyocytes. It is thought that the spatial properties of electrically evoked Ca^{2+} transients in cardiac myocytes is determined by the extent of the T-tubule network. Thus, ventricular myocytes have been shown to display spatially homogenous Ca^{2+} transients (Brette *et al.*, 2004; Cannell *et al.*, 1995; Shacklock *et al.*, 1995), whereas in atrial myocytes the Ca^{2+} transient tends to begin at the periphery of the cells, before propagating inward (Kockskämper *et al.*, 2001; Mackenzie *et al.*, 2001; Mackenzie *et al.*, 2004; Woo *et al.*, 2002). The observation that the pulmonary vein cardiomyocytes had a more extensive T-tubule network compared to atrial myocytes could therefore have possible consequences for the properties of the electrically evoked Ca^{2+} transients.

The distribution of RyRs was similar in pulmonary vein and left atrial cells, and the present study shows the novel finding that junctional RyRs are also present along the periphery of pulmonary vein cardiomyocytes. Immunolabelling for the LTCCs showed that they were more likely to be organised in striated manner in pulmonary

vein, compared to left atrial, cardiomyocytes. It has previously been shown that 10% of rat atrial myocytes have a more extensive T-tubule network, and these cells have larger I_{CaL} and a greater membrane capacitance, which is indicative of a greater cellular surface area (Frisk *et al.*, 2014). This suggests that the density of the LTCCs might be related to the presence of T-tubules, and therefore the function of the T-tubules in the pulmonary vein cardiomyocytes could be to enable a more spatially homogenous increase in intracellular Ca^{2+} upon depolarisation.

5.4. The rat pulmonary vein displays a negative force-frequency relationship

The contractile properties in response to electrical stimulation were also investigated, and it was shown that the rat pulmonary vein displayed a negative force-frequency relationship. Based on studies on the rat ventricle, it has been suggested that the negative force-frequency relationship is due to the SR being relatively full at the lower stimulation frequencies, limiting the capacity to increase its Ca^{2+} load (Maier *et al.*, 2000). It is believed that in cardiac tissue that displays a negative force-frequency relationship, the dominant frequency-dependent effect on the magnitude of Ca^{2+} release is not the SR Ca^{2+} load (Maier *et al.*, 2000), and therefore must be another factor such as the refractoriness of the RyRs (Györke & Fill, 1993; Niggli, 2011 for review; Satoh *et al.*, 1997; Schiefer *et al.*, 1995).

The observations that the rat pulmonary vein displayed a negative force-frequency relationship, and spontaneous Ca^{2+} transients were present under unstimulated conditions, suggests that the cardiomyocytes already have a high degree of SR Ca^{2+} loading under control conditions. Therefore, the SR in the rat pulmonary vein cardiomyocytes could be fully replete, limiting the ability to accumulate more Ca^{2+}. This could explain why isoprenaline or increasing the external Ca^{2+} concentration did not increase the amplitude of the electrically evoked Ca^{2+} transients. Furthermore, it would explain why a period of electrical stimulation did not increase the magnitude of the caffeine induced Ca^{2+} transient. The finding that the frequency of spontaneous Ca^{2+} transients was reduced after increasing the external Ca^{2+} concentration was

unexpected. The reason for this is unknown; however, though statistically significant, this was a small reduction and it is unclear whether this would be biologically significant. In future, it would be useful to confirm if lowering the external Ca^{2+} back to the control concentration would cause the frequency of spontaneous Ca^{2+} transients to increase again.

Further support for the hypothesis that the SR is relatively full under control conditions is the observation that spontaneous Ca^{2+} transients were often present between repetitive stimuli at 1 Hz, when the external Ca^{2+} concentration was 2.5 mM. In the rat ventricle, such activity was not observed at similar external Ca^{2+} concentrations (Kaneko *et al.*, 2000). Furthermore, in the absence of prior electrical stimulation, the frequency of spontaneous Ca^{2+} transients in the pulmonary vein was slightly reduced upon raising the external Ca^{2+} concentration, whereas in ventricular myocytes the frequency of spontaneous Ca^{2+} transients was increased when the external Ca^{2+} concentrations was raised as high as 5 to 6 mM (Díaz *et al.*, 1997a; Kaneko *et al.*, 2000).

The observation that there was no increase in the frequency of spontaneous Ca^{2+} transients in the presence of isoprenaline could also be explained by the replete SR paradigm. However, other factors that could modulate the effect of isoprenaline on the pulmonary vein cardiomyocytes cannot be ignored. There have been some studies suggesting that isoprenaline might have a dual effect in cardiac myocytes. In a previous study, automaticity that was induced in the rat pulmonary vein with a combination of isoprenaline and phenylephrine, ceased when the concentration of isoprenaline was raised beyond 1 μM (Maupoil *et al.*, 2007). In ventricular papillary muscle, spontaneous fluctuations in scattered light, which were used as an index for contractions, were slightly reduced by isoprenaline. As contractile activity is caused by changes in intracellular Ca^{2+}, this infers that there was reduced SR Ca^{2+} release. However, following a period of electrical stimulation, there was in the increase scattered light fluctuations in the presence of isoprenaline (Kort & Lakatta, 1988). This suggests that isoprenaline could have a stimulatory or inhibitory effect depending on

the experimental conditions, and could explain why isoprenaline only had an effect on the characteristics of the spontaneous Ca^{2+} transients after a period of electrical stimulation. An alternative explanation is that the experiments with isoprenaline were performed at room temperature. Noradrenaline only induced automaticity in the rat pulmonary vein at 37 °C, suggesting that the effect of adrenergic stimulation on the pulmonary vein is temperature dependent.

5.5. Future experiments

It is not yet known whether automaticity induced by noradrenaline initiates at ectopic foci before propagating throughout the tissue. From the present studies it appears that uncoupling gap junctions with carbenoxolone had an inhibitory effect on noradrenaline induced automaticity suggesting that intercellular signalling is a factor. To resolve this matter, an extracellular electrode array could be used to map the conduction of electrical activity in the individual regions of the pulmonary vein (Hocini *et al.*, 2002; Honjo *et al.*, 2003a). Mapping the electrical activity in the pulmonary vein would also examine if the regions of tissue that did not respond to electrical stimulation with Ca^{2+} transients still responded with electrical activity. This would determine if the cardiomyocytes were not depolarising or whether there is a regional heterogeneity in intracellular Ca^{2+} signalling in the pulmonary vein myocardial sleeve.

The present study demonstrates the novel finding that the mitochondria in pulmonary vein cardiomyocytes spontaneously flicker, suggesting that they spontaneously depolarise (Duchen *et al.*, 1998). It is thought that influx of Ca^{2+} into the mitochondrial matrix is important for depolarisation (Duchen *et al.*, 1998; Lu *et al.*, 2016), therefore this finding merits further investigation. It would be necessary to image the tissue of a much longer time period in order to provide quantitative data on the kinetics of mitochondrial depolarisations, and it would also be useful to determine if there are any changes following the experimental manipulations that induced an increase in spontaneous Ca^{2+} transient frequency.

Finally, the experiments in the present thesis were conducted in healthy rats. It would be interesting to examine the cellular structure and intracellular Ca^{2+} signalling in pulmonary vein cardiomyocytes in different disease models. For instance, automaticity has recently been shown to be present without any *in vitro* intervention in pulmonary veins from rats that underwent surgery to create a fistula between the abdominal aorta and inferior vena cava (Hamaguchi *et al.*, 2015). This surgical model induces chronic volume overload in the heart, leading to cardiac hypertrophy (Garcia & Diebold, 1990), which was also reported in the pulmonary vein. Interestingly, automaticity was not only observed as the sustained firing of action potentials, but could also occur as repetitive bursts (Hamaguchi *et al.*, 2015), similar to what has been observed in the presence of noradrenaline in healthy rats (Doisne *et al.*, 2009; Namekata *et al.*, 2010). It is therefore conceivable that the intracellular Ca^{2+} signalling in the pulmonary vein, and susceptibility towards automaticity, will be altered in other *in vivo* disease models that are associated with atrial fibrillation, such as rapid atrial pacing (Sugiyama *et al.*, 2005). Nevertheless, a better understanding of the properties of the pulmonary vein cardiomyocytes in tissue obtained from healthy animals is important for understanding the physiological changes that occur due to pathological conditions.

Chapter 6

References

Ai, X., Curran, J.W., Shannon, T.R., Bers, D.M., and Pogwizd, S.M. (2005). Ca^{2+}/ calmodulin-dependent protein kinase modulates cardiac ryanodine receptor phosphorylation and sarcoplasmic reticulum Ca^{2+} leak in heart failure . Circulation Research *97(12)*, 1314-1322.

Al-Khatib, S.M., Allen LaPointe, N.M., Chatterjee, R., Crowley, M.J., Dupre, M.E., Kong, D.F., Lopes, R.D., Povsic, T.J., Raju, S.S., Shah, B., *et al.* (2014). Rate- and rhythm-control therapies in patients with atrial fibrillation: a systematic review. Annals of Internal Medicine *160(11)*, 760-773.

Allen, D.G., and Blinks, J.R. (1978). Calcium transients in aequorin-injected frog cardiac muscle. Nature *273(5663)*, 509-513.

Allessie, M.A., Bonke, F.I., and Schopman, F.J. (1976). Circus movement in rabbit atrial muscle as a mechanism of tachycardia. II. The role of nonuniform recovery of excitability in the occurrence of unidirectional block, as studied with multiple microelectrodes. Circulation Research *39(2)*, 168-177.

Allessie, M.A., Boyden, P.A., Camm, A.J., Kléber, A.G., Lab, M.J., Legato, M.J., Rosen, M.R., Schwartz, P.J., Spooner, P.M., Van Wagoner, D.R., *et al.* (2001). Pathophysiology and prevention of atrial fibrillation. Circulation *103(5)*, 769-777.

Andersen, G.Ø., Qvigstad, E., Schiander, I., Aass, H., Osnes, J.B., and Skomedal, T. (2002). Alpha(1)-AR-induced positive inotropic response in heart is dependent on myosin light chain phosphorylation. American Journal of Physiology: Heart and Circulatory Physiology *283(4)*, 1472-1480.

Arora, R., Ulphani, J.S., Villuendas, R., Ng, J., Harvey, L., Thordson, S., Inderyas, F., Lu, Y., Gordon, D., Denes, P., *et al.* (2008). Neural substrate for atrial fibrillation: implications for targeted parasympathetic blockade in the posterior left atrium. American Journal of Physiology: Heart and Circulatory Physiology *294(1)*, 134-144.

Arora, R., Verheule, S., Scott, L., Navarrete, A., Katari, V., Wilson, E., Vaz, D., and Olgin, J.E. (2003). Arrhythmogenic Substrate of the Pulmonary Veins Assessed by High-Resolution Optical Mapping. Circulation *107*, 1816-1821.

Asghari, P., Schulson, M., Scriven, D.R., Martens, G., and Moore, E.D. (2009). Axial tubules of rat ventricular myocytes form multiple junctions with the sarcoplasmic reticulum. Biophysical Journal *96(11)*, 4651-4660.

Atwater, B.D., Wallace, T.W., Kim, H.W., Hranitzky, P.M., Bahnson, T.D., Hegland, D.D., and Daubert, J.P. (2011). Pulmonary vein contraction before and after radiofrequency ablation for atrial fibrillation. Journal of Cardiovascular Electrophysiology *22(2)*, 169-174.

Ayettey, A.S., and Navaratnam, V. (1978). The T-tubule system in the specialized and general myocardium of the rat. Journal of Anatomy *127(1)*, 125-140.

Bagwe, S., Berenfeld, O., Vaidya, D., Morley, G.E., and Jalife, J. (2005). Altered right atrial excitation and propagation in connexin40 knockout mice. Circulation *112(15)*, 2245-2253.

Bak, J., Billington, R.A., Timar, G., Dutton, A.C., and Genazzani, A.A. (2001). NAADP receptors are present and functional in the heart. Current Biology: CB *11(12)*, 987-990.

Banijamali, H.S., Gao, W.D., MacIntosh, B.R., and ter Keurs, H.E. (1991). Force-interval relations of twitches and cold contractures in rat cardiac trabeculae. Effect of ryanodine. Cardiovascular Research *69(4)*, 937-948.

Barr, L., Dewey, M.M., and Berger, W. (1965). Propagation of action potentials and the structure of the nexus in cardiac muscle. The Journal of General Physiology *48*, 797-823.

Bassani, J.W., Bassani, R.A., and Bers, D.M. (1994). Relaxation in rabbit and rat cardiac cells: species-dependent differences in cellular mechanisms. The Journal of Physiology *476(2)*, 279-293.

Bassani, J.W., Yuan, W., and Bers, D.M. (1995). Fractional SR Ca release is regulated by trigger Ca and SR Ca content in cardiac myocytes. The American Journal of Physiology *268(5 pt. 1)*, 1313-1319.

Bassani, R.A., Bassani, J.W., and Bers, D.M. (1992). Mitochondrial and sarcolemmal Ca^{2+} transport reduce $[Ca^{2+}]i$ during caffeine contractures in rabbit cardiac myocytes. The Journal of Physiology *453*, 591-608.

Baughman, J.M., Perocchi, F., Girgis, H.S., Plovanich, M., Belcher-Timme, C., Sancak, Y., Bao, X.R., Strittmatter, L., Goldberger, O., Bogorad, R.L., *et al.* (2011). Integrative genomics identifies MCU as an essential component of the mitochondrial calcium uniporter. Nature *476(7260)*, 341-345.

Bean, B.P. (1985). Two kinds of calcium channels in canine atrial cells. Differences in kinetics, selectivity, and pharmacology. The Journal of General Physiology *86(1)*, 1-30.

Benjamin, E.J., Wolf, P.A., D'Agostino, R.B., Silbershatz, H., Kannel, W.B., and Levy, D. (1998). Impact of Atrial Fibrillation on the Risk of Death : The Framingham Heart Study. Circulation *98*, 946-952.

Bennett, M.A., and Pentecost, B.L. (1970). The pattern of onset and spontaneous cessation of atrial fibrillation in man. Circulation *41(6)*, 981-988.

Berlin, J.R. (1995). Spatiotemporal changes of Ca^{2+} during electrically evoked contractions in atrial and ventricular cells. The American Journal of Physiology *269(3 pt. 2)*, 1165-1170.

Berlin, J.R., Cannell, M.B., and Lederer, W.J. (1989). Cellular origins of the transient inward current in cardiac myocytes. Role of fluctuations and waves of elevated intracellular calcium. Circulation Research *65(1)*, 115-126.

Berridge, M.J., and Irvine, R.F. (1989). Inositol phosphates and cell signalling. Nature *341(6239)*, 197-205.

Bers, D.M. (2000a). Calcium fluxes involved in control of cardiac myocyte contraction. Circulation Research *87(4)*, 275-281.

Bers, D.M. (2000b). Ryanodine and the calcium content of cardiac SR assessed by caffeine and rapid cooling contractures. The American Journal of Physiology *253(3 pt. 1)*, 408-415.

Bers, D.M. (2002). Cardiac excitation-contraction coupling. Nature *415*, 198-205.

Bers, D.M. (2008). Calcium cycling and signaling in cardiac myocytes. Annual Review of Physiology *70*, 23-49.

Bettoni, M., and Zimmermann, M. (2002). Autonomic Tone Variations Before the Onset of Paroxysmal Atrial Fibrillation. Circulation *105*, 2753-2759.

Birinyi, P., Acsai, K., Bányász, T., Tóth, A., Horváth, B., Virág, L., Szentandrássy, N., Magyar, J., Varró, A., Fülöp, F., *et al.* (2005). Effects of SEA0400 and KB-R7943 on Na^+/Ca^{2+} exchange current and L-type Ca^{2+} current in canine ventricular cardiomyocytes. Naunyn-Schmiedeberg's Archives of Pharmacology *372(1)*, 63-70.

Blatter, L.A., Kockskämper, J., Sheehan, K.A., Zima, A.V., Hüser, J., and Lipsius, S.L. (2003). Local calcium gradients during excitation-contraction coupling and alternans in atrial myocytes. The Journal of Physiology *546(1)*, 19-31.

Blom, N.A., Gittenberger-de Groot, A.C., DeRuiter, M.C., Poelmann, R.E., Mentink, M.M., and Ottenkamp, J. (1999). Development of the cardiac conduction tissue in human embryos using HNK-1 antigen expression: possible relevance for understanding of abnormal atrial automaticity. Circulation *99(6)*, 800-806.

Bogdanov, K.Y., Vinogradova, T.M., and Lakatta, E.G. (2001). Sinoatrial nodal cell ryanodine receptor and Na(+)-Ca(2+) exchanger: molecular partners in pacemaker regulation. Circulation Research *88(12)*, 1254-1258.

Bootman, M.D., Collins, T.J., Mackenzie, L., Roderick, H.L., Berridge, M.J., and Peppiatt, C.M. (2002). 2-aminoethoxydiphenyl borate (2-APB) is a reliable blocker of store-operated Ca^{2+} entry but an inconsistent inhibitor of InsP3-induced Ca^{2+} release. FASEB Journal *16(10)*, 1145-1150.

Bootman, M.D., Higazi, D.R., Coombes, S., and Roderick, H.L. (2006). Calcium signalling during excitation-contraction coupling in mammalian atrial myocytes. Journal of Cell Science *119(9)*, 3915-3925.

Bootman, M.D., Lipp, P., and Berridge, M.J. (2001). The organisation and functions of local Ca(2+) signals. Journal of Cell Science *114(12)*, 2213-2222.

Bouchard, R.A., and Bose, D. (1989). Analysis of the interval-force relationship in rat and canine ventricular myocardium. The American Journal of Physiology *257(6 pt. 2)*, 2036-2047.

Bovo, E., Lipsius, S.L., and Zima, A.V. (2012). Reactive oxygen species contribute to the development of arrhythmogenic Ca^{2+} waves during β-adrenergic receptor stimulation in rabbit cardiomyocytes. The Journal of Physiology *590(14)*, 3291-3304.

Bowman, A.W., and Kovács, S.J. (2005). Prediction and assessment of the time-varying effective pulmonary vein area via cardiac MRI and Doppler echocardiography. American Journal of Physiology Heart and Circulatory Physiology *288(1)*, 280-286.

Boyett, M.R., and Dobrzynski, H. (2007). The sinoatrial node is still setting the pace 100 years after its discovery. Circulation Research *100(11)*, 1543-1545.

Brady, N.R., Elmore, S.P., van Beek, J.J., Krab, K., Courtoy, P.J., Hue, L., and Westerhoff, H.V. (2004). Coordinated behavior of mitochondria in both space and time: a reactive oxygen species-activated wave of mitochondrial depolarization. Biophysical Journal *87(3)*, 2022-2034.

Braun, A.P., Fedida, D., and Giles, W.R. (1992). Activation of alpha 1-adrenoceptors modulates the inwardly rectifying potassium currents of mammalian atrial myocytes. Pflügers Archiv - European Journal of Physiology *421(5)*, 431-439.

Brette, F., Despa, S., Bers, D.M., and Orchard, C.H. (2005). Spatiotemporal characteristics of SR Ca(2+) uptake and release in detubulated rat ventricular myocytes. Journal of Molecular and Cellular Cardiology *39(5)*, 804-812.

Brette, F., Komukai, K., and Orchard, C.H. (2002). Validation of formamide as a detubulation agent in isolated rat cardiac cells. American Journal of Physiology - Heart and Circulatory Physiology *283*, 1720-1728.

Brette, F., Sallé, L., and Orchard, C.H. (2004). Differential modulation of L-type Ca^{2+} current by SR Ca^{2+} release at the T-tubules and surface membrane of rat ventricular myocytes. Circulation Research *95(1)*, 1-7.

Brette, F., Sallé, L., and Orchard, C.H. (2006). Quantification of calcium entry at the T-tubules and surface membrane in rat ventricular myocytes. Biophysical Journal *90(1)*, 381-389.

Bronquard, C., Maupoil, V., Arbeille, B., Fetissof, F., Findlay, I., Cosnay, P., and Freslon, J.L. (2007). Contractile and relaxant properties of rat-isolated pulmonary veins related to localization and histology. Fundamental and Clinical Pharmacology *21(1)*, 55-65.

Brown, A.M., Lee, K.S., and Powell, T. (1981). Sodium current in single rat heart muscle cells. The Journal of Physiology *318*, 479-500.

Brum, G., Osterrieder, W., and Trautwein, W. (1984). Beta-adrenergic increase in the calcium conductance of cardiac myocytes studied with the patch clamp. Pflügers Archiv - European Journal of Physiology *401(2)*, 111-118.

Brunello, L., Slabaugh, J.L., Radwanski, P.B., Ho, H.-T., Belevych, A.E., Lou, Q., Chen, H., Napolitano, C., Lodola, F., Priori, S.G., *et al.* (2013). Decreased RyR2 refractoriness determines myocardial synchronization of aberrant Ca^{2+} release in a genetic model of arrhythmia. Proceedings for the National Academy of Sciences of the United States of America *110(25)*, 1032-1037.

Brunton, T.L., and Frayer, J. (1876). Note on independent pulsation of the pulmonary vein and vena cava. Proceedings of the Royal Society of London *25*, 174-176.

Bub, G., Camelliti, P., Bollensdorff, C., Stuckey, D.J., Picton, G., Burton, R.A., Clarke, K., and Kohl, P. (2010). Measurement and analysis of sarcomere length in rat cardiomyocytes in situ and in vitro. American Journal of Physiology Heart and Circulatory Physiology *298(5)*, 1616-1625.

Butler, R.N. (1997). Population aging and health. BMJ (Clinical Research Editorial) *315(7115)*, 1082-1084.

Cannell, M.B., Cheng, H., and Lederer, W.J. (1994). Spatial non-uniformities in $[Ca^{2+}]i$ during excitation-contraction coupling in cardiac myocytes. Biophysical Journal *67(5)*, 1942-1956.

Cannell, M.B., Cheng, H., and Lederer, W.J. (1995). The control of calcium release in heart muscle. Science (New York, NY) *268(5213)*, 1045-1049.

Capel, R.A., Bolton, E.L., Lin, W.K., Aston, D., Wang, Y., Liu, W., Wang, X., Burton, R.A., Bloor-Young, D., Shade, K.T., *et al.* (2015). Two-pore Channels (TPC2s) and Nicotinic Acid Adenine Dinucleotide Phosphate (NAADP) at Lysosomal-Sarcoplasmic Reticular Junctions Contribute to Acute and Chronic β-Adrenoceptor Signaling in the Heart. The Journal of Biological Chemistry *290(50)*, 30087-30098.

Capogrossi, M.C., Houser, S.R., Bahinski, A., and Lakatta, E.G. (1987). Synchronous occurrence of spontaneous localized calcium release from the sarcoplasmic reticulum generates action potentials in rat cardiac ventricular myocytes at normal resting membrane potential. Circulation Research *61*, 498-503.

Capogrossi, M.C., and Lakatta, E.G. (1985). Frequency modulation and synchronization of spontaneous oscillations in cardiac cells. American Journal of Physiology *248(3 pt. 2)*, 412-418.

Cappato, R., Calkins, H., Chen, S.-A., Davies, W., Iesaka, Y., Kalman, J., Kim, Y.-H., Klein, G., Packer, D., and Skanes, A. (2005). Worldwide Survey on the Methods, Efficacy, and Safety of Catheter Ablation for Human Atrial Fibrillation. Circulation *111*, 1100-1105.

Carafoli, E. (1991). Calcium pump of the plasma membrane. Physiological Reviews *71(1)*, 129-153.

Carl, S.L., Felix, K., Caswell, A.H., Brandt, N.R., Ball, W.J.J., Vaghy, P.L., Meissner, G., and D.G., F. (1995). Immunolocalization of sarcolemmal dihydropyridine receptor and sarcoplasmic reticular triadin and ryanodine receptor in rabbit ventricle and atrium. The Journal of Cell Biology *129(3)*, 673-682.

Catterall, W.A., Perez-Reyes, E., Snutch, T., and Striessnig, J. (2005). International Union of Pharmacology. XLVIII. Nomenclature and structure-function relationships of voltage-gated calcium channels. Pharmacological Reviews *57(4)*, 411-425.

Chaldoupi, S.M., Loh, P., Hauer, R.N., de Bakker, J.M., and van Rijen, H.V. (2009). The role of connexin40 in atrial fibrillation. Cardiovascular Research *84(1)*, 15-23.

Challice, C.E., Wilkens, J.L., and Chohan, K.S. (1974). Electrical impulse conduction in pulmonary veins. Biophysical Journal *14(11)*, 901-904.

Chang, S.-H., Chen, Y.-C., Chiang, S.-J., Higa, S., Cheng, C.-C., Chen, Y.-J., and S-A., C. (2008). Increased Ca(2+) sparks and sarcoplasmic reticulum Ca(2+) stores potentially determine the spontaneous activity of pulmonary vein cardiomyocytes. Life Sciences *83*, 284-292.

Chang, S.-L., Chen, Y.-C., Chen, Y.-J., Wangcharoen, W., Lee, S.-H., Lin, C.-I., and Chen, S.-A. (2007). Mechanoelectrical feedback regulates the arrhythmogenic activity of pulmonary veins. Heart (British Cardiac Society) *93(1)*, 82-88.

Chang, S.-L., Chen, Y.-C., Yeh, Y.-H., Lin, Y.-K., Wu, T.-J., Lin, C.-I., Chen, S.-A., and Chen, Y.-J. (2011). Heart Failure Enhanced Pulmonary Vein Arrhythmogenesis and Dysregulated Sodium and Calcium Homeostasis with Increased Calcium Sparks. Journal Cardiovascular Electrophysiology *22*, 1378-1386.

Chard, M., and Tabrizchi, R. (2009). The role of pulmonary veins in atrial fibrillation: A complex yet simple story. Pharmacology & Therapeutics *124*, 207-218.

Chelu, M.G., Sarma, S., Sood, S., Wang, S., van Oort, R.J., Skapura, D.G., Li, N., Santonastasi, M., Müller, F.U., Schmitz, W., *et al.* (2009). Calmodulin kinase II-mediated sarcoplasmic reticulum Ca^{2+} leak promotes atrial fibrillation in mice. The Journal of Clinical Investigation *119(7)*, 1940-1951.

Chen, S.-A., Hsieh, M.-H., Tai, C.-T., Tsai, C.-F., Prakash, V.S., Yu, W.-C., Hsu, T.-L., Ding, Y.-A., and Chang, M.-S. (1999a). Initiation of atrial fibrillation by ectopic beats originating from the pulmonary veins: electrophysiological characteristics, pharmacological responses, and effects of radiofrequency ablation. Circulation *100(18)*, 1879-1886.

Chen, S.-A., Tai, C.-T., Yu, W.-C., Chen, Y.-J., Tsai, C.-F., Hsieh, M.-H., Chen, C.-C., Prakash, V.S., Ding, Y.-A., and Chang, M. (1999b). Right atrial focal atrial fibrillation: electrophysiologic characteristics and radiofrequency catheter ablation. Journal of Cardiovascular Electrophysiology *10*, 328-335.

Chen, W., Wang, R., Chen, B., Zhong, X., Kong, H., Bai, Y., Zhou, Q., Xie, C., Zhang, J., Guo, A., *et al.* (2014). The ryanodine receptor store-sensing gate controls Ca^{2+} waves and Ca^{2+}-triggered arrhythmias. 20(2), 184-192.

Chen, Y.-C., Chen, S.-A., Chen, Y.-J., Chang, M.-S., Chan, P., and Lin, C.-I. (2002a). Effects of thyroid hormone on the arrhythmogenic activity of pulmonary vein cardiomyocytes. Journal of the American College of Cardiology *39(2)*, 366-372.

Chen, Y.-J., Chen, S.-A., Chang, M.-S., and Lin, C.-I. (2000). Arrhythmogenic activity of cardiac muscle in pulmonary veins of the dog: implication for the genesis of atrial fibrillation. Cardiovascular Research *48*, 265-273.

Chen, Y.-J., Chen, S.-A., Chen, Y.-C., Yeh, H.-I., Chan, P., Chang, M.-S., and Lin, C.-I. (2001). Effects of Rapid Atrial Pacing on the Arrhythmogenic Activity of Single Cardiomyocytes From Pulmonary Veins. Circulation *104*, 2849-2854.

Chen, Y.-J., Chen, S.-A., Chen, Y.-C., Yeh, H.-I., Chang, M.-S., and Lin, C.-I. (2002b). Electrophysiology of single cardiomyocytes isolated from rabbit pulmonary veins: implication in initiation of focal atrial fibrillation. Basic Research Cardiology *97*, 26-34.

Cheng, H., Lederer, M.R., Lederer, W.J., and Cannell, M.B. (1996). Calcium sparks and $[Ca^{2+}]i$ waves in cardiac myocytes. The American Journal of Physiology *270(1 pt. 1)*, 148-159.

Cheng, H., Lederer, W.J., and Cannell, M.B. (1993). Calcium sparks: elementary events underlying excitation-contraction coupling in heart muscle. Science *262*, 740-744.

Cheung, D.W. (1981a). Electrical activity of the pulmonary vein and its interaction with the right atrium in the guinea-pig. The Journal of Physiology *314*, 445-456.

Cheung, D.W. (1981b). Pulmonary vein as an ectopic focus in digitalis-induced arrhythmia. Nature *294*, 582-584.

Chevalier, P., Tabib, A., Meyronnet, D., Chalabreysse, L., Restier, L., Ludman, V., Aliès, A., Adeleine, P., Thivolet, F., Burri, H., *et al.* (2005). Quantitative study of nerves of the human left atrium. Heart Rhythm *2(5)*, 518-522.

Chou, C.-C., Nihei, M., Zhou, S., Tan, A., Kawase, A., Macias, E.S., Fishbein, M.C., Lin, S.-F., and Chen, P.-S. (2005). Intracellular Calcium Dynamics and Anisotropic Reentry in Isolated Canine Pulmonary Veins and Left Atrium. Circulation *111*, 2889-2897.

Christ, T., Rozmaritsa, N., Engel, A., Berk, E., Knaut, M., Metzner, K., Canteras, M., Ravens, U., and Kaumann, A. (2014). Arrhythmias, elicited by catecholamines and serotonin, vanish in human chronic atrial fibrillation. Proceedings of the National Academy of Sciences of the United States of America *111(30)*, 11193-11198.

Clement, O., Puceat, M., Walsh, M.P., and Vassort, G. (1992). Protein kinase C enhances myosin light-chain kinase effects on force development and ATPase activity in rat single skinned cardiac cells. The Biochemical Journal *258(1)*, 311-317.

Coutu, P., Chartier, D., and Nattel, S. (2006). Comparison of Ca^{2+}-handling properties of canine pulmonary vein and left atrial cardiomyocytes. American Journal of Physiology - Heart and Circulatory Physiology *291*, H2290-H2300.

Cruickshank, S.F., and Drummond, R.M. (2003). The effects of hypoxia on $[Ca^{2+}]i$ signalling in phenotypically distinct myocytes from the rat pulmonary vein. Journal of Physiology *548P*, P56.

Curran, J., Brown, K.H., Santiago, D.J., Pogwizd, S., Bers, D.M., and Shannon, T.R. (2010). Spontaneous Ca waves in ventricular myocytes from failing hearts depend on Ca(2+)-calmodulin-dependent protein kinase II. Journal of Molecular and Cellular Cardiology *49(1)*, 25-32.

Curran, J., Hinton, M.J., Ríos, E., Bers, D.M., and Shannon, T.R. (2007). Beta-adrenergic enhancement of sarcoplasmic reticulum calcium leak in cardiac myocytes is mediated by calcium/calmodulin-dependent protein kinase. Circulation Research *100(3)*, 391-398.

Curran, J., Musa, H., Kline, C.F., Makara, M.A., Little, S.C., Higgins, J.D., Hund, T.J., Band, H., and Mohler, P.J. (2015). Eps15 Homology Domain-containing Protein 3 Regulates Cardiac T-type Ca^{2+} Channel Targeting and Function in the Atria. The Journal of Biological Chemistry *290(19)*, 12210-12221.

Currie, S., Loughrey, C.M., Craig, M.A., and Smith, G.L. (2004). Calcium/calmodulin-dependent protein kinase IIdelta associates with the ryanodine receptor complex and regulates channel function in rabbit heart. The Biochemical Journal *377(2)*, 357-366.

Davis, L.M., Kanter, H.L., Beyer, E.C., and Saffitz, J.E. (1994). Distinct gap junction protein phenotypes in cardiac tissues with disparate conduction properties. Journal of the American College of Cardiology *24(4)*, 1124-1132.

Davis, L.M., Rodefeld, M.E., Green, K., Beyer, E.C., and Saffitz, J.E. (1995). Gap junction protein phenotypes of the human heart and conduction system. Journal of Cardiovascular Electrophysiology *6 (10 pt. 1)*, 813-822.

de Borda, L.S., Gimeno, A.L., and Gimeno, M.F. (1974). Frequency-force relationship on isolated rat and guinea pig atria. Effects of cholinergic and adrenergic receptor antagonists. Proceedings for the Society of Experimental Biology and Medicine *145(4)*, 1151-1157.

de Groot, J.R., Veenstra, T., Verkerk, A.O., Wilders, R., Smits, J.P., Wilms-Schopman, F.J., Wiegerinck, R.F., Bourier, J., Belterman, C.N., Coronel, R., *et al.* (2003). Conduction slowing by the gap junctional uncoupler carbenoxolone. Cardiovascular Research *60(2)*, 288-297.

De Koninck, P., and Schulman, H. (1998). Sensitivity of CaM kinase II to the frequency of Ca^{2+} oscillations. Science *279(5348)*, 227-230.

De Stefani, D., Raffaello, A., Teardo, E., Szabò, I., and Rizzuto, R. (2011). A forty-kilodalton protein of the inner membrane is the mitochondrial calcium uniporter. Nature *476(7360)*, 336-340.

Dedkova, E.N., and Blatter, L.A. (2013). Calcium signaling in cardiac mitochondria. Journal of Molecular and Cellular Cardiology *58*, 125-133.

Delcamp, T.J., Dales, C., Ralenkotter, L., Cole, P.S., and Hadley, R.W. (1988). Intramitochondrial [Ca^{2+}] and membrane potential in ventricular myocytes exposed to anoxia-reoxygenation. The American Journal of Physiology *275(2 pt. 2)*, 484-494.

Di Virgilio, F., Steinberg, T.H., and Silverstein, S.C. (1990). Inhibition of Fura-2 sequestration and secretion with organic anion transport blockers. Cell Calcium *11*, 57-62.

Díaz, M.E., O'Neill, S.C., and Eisner, D.A. (2004). Sarcoplasmic reticulum calcium content fluctuation is the key to cardiac alternans. Circulation Research *94(5)*, 650-656.

Díaz, M.E., Trafford, A.W., O'Neill, S.C., and Eisner, D.A. (1997b). A measurable reduction of s.r. Ca content follows spontaneous Ca release in rat ventricular myocytes. Pflügers Archiv: European Journal of Physiology *434(6)*, 852-854.

Díaz, M.E., Trafford, A.W., O'Neill, S.C., and Eisner, D.A. (1997a). Measurment of sarcoplasmic reticulum Ca^{2+} content and sarcolemmal Ca^{2+} fluxes in isolated rat ventricular myocytes during spontaneous Ca^{2+} release. Journal of Pysiology *501*, 3-16.

Dibb, K.M., Clarke, J.D., Horn, M.A., Richards, M.A., Graham, H.K., Eisner, D.A., and Trafford, A.W. (2009). Characterization of an extensive transverse tubular network in sheep atrial myocytes and its depletion in heart failure. Circulation Heart Failure *2(5)*, 482(489).

DiFrancesco, D. (1991). The contribution of the 'pacemaker' current (if) to generation of spontaneous activity in rabbit sino-atrial node myocytes. The Journal of Physiology *434*, 23-40.

Doisne, N., Maupoil, V., Cosnay, P., and Findlay, I. (2009). Catecholaminergic automatic activity in the rat pulmonary vein: electrophysiological differences between cardiac muscle in the left atrium and pulmonary vein. American Journal of Physiology - Heart and Circulatory Physiology *297*, H102-H108.

Domeier, T.L., Blatter, L.A., and Zima, A.V. (2010). Changes in intra-luminal calcium during spontaneous calcium waves following sensitization of ryanodine receptor channels. Channels (Austin, Texas) *4(2)*, 87-92.

Domeier, T.L., Maxwel, J.T., and Blatter, L.A. (2012). β-Adrenergic stimulation increases the intra-sarcoplasmic reticulum Ca^{2+} threshold for Ca^{2+} wave generation. Journal of Physiology *590*, 6093-6103.

Doshi, R.-N., Wu, T.-J., Yashima, M., Kim, Y.-H., Ong, J.-J., Cao, J.-M., Hwang, C., Yashar, P., Fishbein, M.C., Karagueuzian, H.S., *et al.* (1999). Relation between ligament of Marshall and adrenergic atrial tachyarrhythmia. Circulation *100(8)*, 876-883.

Dries, E., Bito, V., Lenaerts, I., Antoons, G., Sipido, K.R., and Macquaide, N. (2013). Selective modulation of coupled ryanodine receptors during microdomain activation of calcium/calmodulin-dependent kinase II in the dyadic cleft. Circulation Research *113(11)*, 1242-1252.

Duchen, M.R. (1999). Contributions of mitochondria to animal physiology: from homeostatic sensor to calcium signalling and cell death. The Journal of Physiology *516(1)*, 1-17.

Duchen, M.R., Leyssens, A., and Crompton, M. (1998). Transient mitochondrial depolarizations reflect focal sarcoplasmic reticular calcium release in single rat cardiomyocytes. The Journal of Cell Biology *142(4)*, 975-988.

Dzhura, I., Wu, Y., Colbran, R.J., Balser, J.R., and Anderson, M.E. (2000). Calmodulin kinase determines calcium-dependent facilitation of L-type calcium channels. Nature Cell Biology *2(3)*, 173-177.

Ebashi, F., and Ebashi, S. (1962). Removal of calcium and relaxation in actomyosin systems. Nature *194*, 378-379.

Ebashi, S., Ebashi, F., and Kodama, A. (1967). Troponin as the Ca++-receptive protein in the contractile system. Journal of Biochemistry *62(1)*, 137-138.

Egdell, R.M., and MacLeod, K.T. (2000). Calcium Extrusion During Aftercontractions in Cardiac Myocytes: The Role of the Sodium-calcium Exchanger in the Generation of the Transient Inward Current. Journal of Molecular and Cellular Cardiology *32(1)*, 85-93.

Ehara, T., Matsuoka, S., and Noma, A. (1989). Measurement of reversal potential of Na^{+}-Ca^{2+} exchange current in single guinea-pig ventricular cells. The Journal of Physiology *410*, 227-249.

Ehrlich, J.R., Cha, T.-J., Zhang, L., Chartier, D., Melnyk, P., Hohnloser, S.H., and Nattel, S. (2003). Cellular electrophysiology of canine pulmonary vein cardiomyocytes: action potential and ionic current properties. The Journal of Physiology *551*, 801-813.

Eisner, D.A., Bode, E., Venetucci, L., and Trafford, A.W. (2013). Calcium flux balance in the heart. Journal of Molecular and Cellular Cardiology *58*, 110-117.

Endoh, M., and Blinks, J.R. (1988). Actions of sympathomimetic amines on the Ca^{2+} transients and contractions of rabbit myocardium: reciprocal changes in myofibrillar responsiveness to Ca^{2+} mediated through alpha- and beta-adrenoceptors. Circulation Research *62(2)*, 247-265.

Endou, M., Hattori, Y., Tohse, N., and Kanno, M. (1991). Protein kinase C is not involved in alpha 1-adrenoceptor-mediated positive inotropic effect. The American Journal of Physiology *260(1 pt. 2)*, 27-36.

Fabiato, A. (1983). Calcium-induced release of calcium from the cardiac sarcoplasmic reticulum. The American Journal of Physiology *245*, 1-14.

Fabiato, A. (1992). Two kinds of calcium-induced release of calcium from the sarcoplasmic reticulum of skinned cardiac cells. Advantages in Experimental Medicine and Biology *311*, 245-262.

Fabiato, A., and Fabiato, F. (1975). Contractions induced by a calcium-triggered release of calcium from the sarcoplasmic reticulum of single skinned cardiac cells. The Journal of Physiology *249(3)*, 469-495.

Fabiato, A., and Fabiato, F. (1978). Effects of pH on the myofilaments and the sarcoplasmic reticulum of skinned cells from cardiace and skeletal muscles. The Journal of Physiology *276*, 233-255.

Favaro, G. (1910). Contributi all'istologia umana e comparata del vasi polmonari. Monatsschr Anat u Physiol *27*, 375-410.

Ferrier, G.R., Saunders, J.H., and Mendez, C. (1973). A cellular mechanism for the generation of ventricular arrhythmias by acetylstrophanthidin. Circulation Research *32(5)*, 600-609.

Ferrier , G.R., Smith, R.H., and Howlett, S.E. (2003). Calcium sparks in mouse ventricular myocytes at physiological temperature. American Journal of Physiology Heart and Circulatory Physiology *285(4)*, 1495-1505.

Firek, L., and Giles, W.R. (1995). Outward currents underlying repolarization in human atrial myocytes. *30(1)*, 31-38.

Fluhler, E., Burnham, V.G., and Loew, L.M. (1985). Spectra, membrane binding, and potentiometric responses of new charge shift probes. Biochemistry *24(21)*, 5749-5755.

Forbes, M.S., Hawkey, L.A., and Sperelakis, N. (1984). The transverse-axial tubular system (TATS) of mouse myocardium: its morphology in the developing and adult animal. The American Journal of Anatomy *170(2)*, 143-162.

Frampton, J.E., Harrison, S.M., Boyett, M.R., and Orchard, C.H. (1991). Ca^{2+} and Na^{+} in rat myocytes showing different force-frequency relationships. The American Journal of Physiology *261(5 pt. 1)*, 739-750.

Frank, J.S., Mottino, G., Chen, F., Peri, V., Holland, P., and Tuana, B.S. (1994). Subcellular distribution of dystrophin in isolated adult and neonatal cardiac myocytes. The American Journal of Physiology *267(6 pt. 1)*, 1707-1716.

Franzini-Armstrong, C., Protasi, F., and Tijskens, P. (2005). The assembly of calcium release units in cardiac muscle. Annals of the New York Academy of Sciences *1047*, 76-85.

Frisk, M., Koivumäki, J.T., Norseng, P.A., Maleckar, M.M., Sejersted, O.M., and Louch, W.E. (2014). Variable t-tubule organization and Ca^{2+} homeostasis across the atria. American Journal of Physiology Heart and Circulatory Physiology *307(4)*, 609-620.

Fu, Y., Zhang, G.-Q., Hao, X.-M., Wu, C.-H., Chai, Z., and Wang, S.-Q. (2005). Temperature dependence and thermodynamic properties of Ca^{2+} sparks in rat cardiomyocytes. Biophysical Journal *89(4)*, 2533-2541.

Fujioka, Y., Hiroe, K., and Matsuoka, S. (2000). Regulation kinetics of Na^{+}-Ca^{2+} exchange current in guinea-pig ventricular myocytes. The Journal of Physiology *529(3)*, 611-623.

Fujiwara, K., Tanaka, H., Mani, H., Nakagami, T., and Takamatsu, T. (2008). Burst emergence of intracellular Ca^{2+} waves evokes arrhythmogenic oscillatory depolarization via the Na^{+}-Ca^{2+} exchanger: simultaneous confocal recording of membrane potential and intracellular Ca^{2+} in the heart. Circulation Research *103(5)*.

Fuster, V., Rydén, L.E., Cannom, D.S., Crijns, H.J., Curtis, A.B., Ellenbogen, K.A., Halperin, J.L., Le Heuzey, J.-Y., Kay, G.N., Lowe, J.E., *et al.* (2006). ACC/AHA/ESC 2006 Guidelines for the Management of Patients With Atrial Fibrillation. Circulation *114*, 257-354.

Gaborit, N., Le Bouter, S., Szuts, V., Varro, A., Escande, D., Nattel, S., and Demolombe, S. (2007). Regional and tissue specific transcript signatures of ion channel genes in the non-diseased human heart. The Journal of Physiology *582(2)*, 675-693.

Gadsby, D.C. (1980). Activation of electrogenic Na^{+}/K^{+} exchange by extracellular K^{+} in canine cardiac Purkinje fibers. Proceedings of the National Academy of Sciences of the United States of America *77(7)*, 4035-4039.

Garcia, R., and Diebold, S. (1990). Simple, rapid, and effective method of producing aortocaval shunts in the rat. Cardiovascular Research *24(5)*, 430-432.

Garciarena, C.D., Youm, J.B., Swietach, P., and Vaughan-Jones, R.D. (2013). H^+-activated Na^+ influx in the ventricular myocyte couples Ca^{2+}-signalling to intracellular pH. Journal of Molecular and Cellular Cardiology *61*, 51-59.

Gassanov, N., Brandt, M.C., Michels, G., Lindner, M., Er, F., and Hoppe, U.C. (2006). Angiotensin II-induced changes of calcium sparks and ionic currents in human atrial myocytes: potential role for early remodeling in atrial fibrillation. Cell calcium *39(2)*, 175-186.

Gee, K.R., Brown, K.A., Chen, W.-N., Bishop-Stewart, J., Gray, D., and Johnson, I. (2000). Chemical and physiological characterization of fluo-4 Ca(2+)-indicator dyes. Cell Calcium *27(2)*, 97-106.

Ginsburg, K.S., and Bers, D.M. (2004). Modulation of excitation-contraction coupling by isoproterenol in cardiomyocytes with controlled SR Ca^{2+} load and Ca^{2+} current trigger. The Journal of Physiology *556(2)*, 463-480.

Go, A.-S., Hylek, E.M., Phillips, K.A., Chang, Y.-C., Henault, L.E., Selby, J.V., and Singer, D.E. (2001). Prevalence of Diagnosed Atrial Fibrillation in Adults. JAMA: The Journal of the American Medical Association *285*, 2370-2375.

Goldman, M.E., Pearce, L.A., Hart, R.G., Zabalgoitia, M., Asinger, R.W., Safford, R., and Halperin, J.L. (1999). Pathophysiologic correlates of thromboembolism in nonvalvular atrial fibrillation: I. Reduced flow velocity in the left atrial appendage (The Stroke Prevention in Atrial Fibrillation [SPAF-III] study). Journal of the American Society of Echocardiography *12(12)*, 1080-1087.

Gorza, L., Schiaffino, S., and Volpe, P. (1993). Inositol 1,4,5-trisphosphate receptor in heart: evidence for its concentration in Purkinje myocytes of the conduction system. The Journal of Cell Biology *212(2)*, 345-353.

Guerra, P.G., Thibault, B., Dubuc, M., Talajic, M., Roy, D., Crépeau, J., Nattel, S., and Tardif, J.C. (2003). Identification of atrial tissue in pulmonary veins using intravascular ultrasound. Journal of the American Society of Echocardiography *16(9)*, 982-987.

Guo, J., and Duff, H.J. (2006). Calmodulin kinase II accelerates L-type Ca^{2+} current recovery from inactivation and compensates for the direct inhibitory effect of $[Ca^{2+}]i$ in rat ventricular myocytes . The Journal of Physiology *574(2)*, 509-518.

Guo, T., Zhang, T., Mestril, R., and Bers, D.M. (2006). Ca^{2+}/Calmodulin-dependent protein kinase II phosphorylation of ryanodine receptor does affect calcium sparks in mouse ventricular myocytes. Circulation Research *99(4)*, 398-406.

Györke, S., and Fill, M. (1993). Ryanodine receptor adaptation: control mechanism of Ca(2+)-induced Ca^{2+} release in heart. Science *260(5109)*, 807-809.

Györke, S., Lukyanenko, V., and Györke, I. (1997). Dual effects of tetracaine on spontaneous calcium release in rat ventricular myocytes. The Journal of Physiology *500(2)*, 297-309.

Györke, S., and Terentyev, D. (2008). Modulation of ryanodine receptor by luminal calcium and accessory proteins in health and cardiac disease. Cardiovascular Research *77(2)*, 245-255.

Haack, J.A., and Rosenberg, R.L. (1994). Calcium-dependent inactivation of L-type calcium channels in planar lipid bilayers. Biophysical Journal *66(4)*, 1051-1060.

Hain, J., Onoue, H., Mayrleitner, M., Fleischer, S., and Schindler, H. (1995). Phosphorylation modulates the function of the calcium release channel of sarcoplasmic reticulum from cardiac muscle. The Journal of Biological Chemistry *270(5)*, 2074-2081.

Haïssaguerre, M., Jaïs, P., Shah, D.C., Garrigue, S., Takahashi, A., Lavergne, T., Hocini, M., Peng, J.T., Roudaut, R., and Clémenty, J. (2000a). Electrophysiological end point for catheter ablation of atrial fibrillation initiated from multiple pulmonary venous foci. Circulation *101(12)*, 1409-1417.

Haïssaguerre, M., Pierre, J., Shah, D.C., Takahashi, A., Hocini, M., Quiniou, G., Garrigue, S., Le Mouroux, A., Le Métayer, P., and Clémenty, J. (1998). Spontaneous Initiation of Atrial Fibrillation by Ectopic Beats Originating in the Pulmonary Veins. The New England Journal of Medicine *339*, 659-666.

Haïssaguerre, M., Shah, D.C., Jaïs, P., Hocini, M., Yamane, T., Deisenhofer, I., Chauvin, M., Garrigue, S., and Clémenty, J. (2000b). Electrophysiological Breakthroughs From the Left Atrium to the Pulmonary Veins. Circulation *102*, 2463-2465.

Hama, T., Takahashi, A., Ichihara, A., and Takamatsu, T. (1998). Real time in situ confocal imaging of calcium wave in the perfused whole heart of the rat. Cellular Signalling *10(5)*, 331-337.

Hamaguchi, S., Hikita, K., Tanaka, Y., Tsuneoka, Y., Namekata, I., and Tanaka, H. (2016). Enhancement of Automaticity by Mechanical Stretch of the Isolated Guinea Pig Pulmonary Vein Myocardium. Biological and Pharmaceutical Bulletin *39(7)*, 1216-1219.

Hamaguchi, S., Tsuneoka, Y., Tanaka, A., Irie, M., Tsuruta, M., Nakayama, T., Namekata, I., Nada, M., Aimoto, M., Takahara, A., *et al.* (2015). Manifestation of automaticity in the pulmonary-vein myocardium of rats with abdominal aorto-venocaval shunt. Journal of Pharmacological Sciences *128(4)*, 212-215.

Han, W., Bao, W., Wang, Z., and Nattel, S. (2002). Comparison of ion-channel subunit expression in canine cardiac Purkinje fibers and ventricular muscle. Circulation Research *91(9)*, 790-797.

Hancox, J.C., Levi, A.J., and Brooksby, P. (1994). Intracellular calcium transients recorded with Fura-2 in spontaneously active myocytes isolated from the atrioventricular node of the rabbit heart. Proceedings Biological Sciences/ The Royal Society *255(1343)*, 99-105.

Hasenfuss , G., and Pieske, B. (2002). Calcium cycling in congestive heart failure . Journal of Molecular and Cellular Cardiology *34(8)*, 951-969.

Hashizume, H., Tango, M., and Ushiki, T. (1998). Three-dimensional cytoarchitecture of rat pulmonary venous walls: a light and scanning electron microscopic study. Anatomy and Embryology *198*, 473-480.

Hassink, R.J., Aretz, H.T., Ruskin, J., and Keane, D. (2003). Morphology of atrial myocardium in human pulmonary veins: a postmortem analysis in patients with and without atrial fibrillation. Journal of the American College of Cardiology *42*, 1108-1114.

Hatem, S.N., Bénardeau, A., Rücker-Martin, C., Marty, I., de Chamisso, P., Villaz, M., and Mercadier, J.J. (1997). Different compartments of sarcoplasmic reticulum participate in the excitation-contraction coupling process in human atrial myocytes. Circulation Research *80(3)*, 345-353.

Hattori, Y., Toyama, J., and Kodama, I. (1991). Cytosolic calcium staircase in ventricular myocytes isolated from guinea pigs and rats. Cardiovascular Research *25(8)*, 622-629.

He, X.-Z., Wang, H.-Y., Shen, Y., Zhong, Q.-H., Fang, S.-X., Peng, W.-J., and Xue, J.-F. (2012). Cardiomyocyte progenitors in a canine pulmonary vein model of persistent atrial fibrillation. Journal of Cardiology *60(3)*, 242-247.

Heilbrunn, L.V., and Wiercinski, F.J. (1947). The action of various cations on muscle protoplasm. Journal of Cellular Physiology *29(1)*, 15-32.

Heubach, J., Trebess, I., Wettwer, E., Himmel, H.M., Michel, M.C., Kaumann, A.J., Koch, W.J., Harding, S.E., and Ravens, U. (1999). L-type calcium current and contractility in ventricular myocytes from mice overexpressing the cardiac beta 2-adrenoceptor. Cardiovascular Research *42(1)*, 173-182.

Hirose, M., and Laurita, K.R. (2007). Calcium-mediated triggered activity is an underlying cellular mechanism of ectopy originating from the pulmonary vein in dogs. American Journal of Physiology - Heart and Circulatory Physiology *292*, H1861-H1867.

Ho, S.-Y., Cabrera, J.A., Tran, V.H., Farré, J., Anderson, R.H., and Sánchez-Quintana, D. (2001). Architecture of the pulmonary veins: relevance to radiofrequency ablation. Heart *86*, 265-270.

Hoch, B., Meyer, R., Hetzer, R., Krause, E.G., and P., K. (1999). Identification and expression of delta-isoforms of the multifunctional Ca^{2+}/calmodulin-dependent protein kinase in failing and nonfailing human myocardium. Circulation Research *84(6)*, 713-721.

Hocini, M., Ho, S.Y., Kawara, T., Linnenbank, A.C., Potse, M., Shah, D., Jaïs, P., Janse, M.J., Haïssaguerre, M., and de Bakker, J.M.T. (2002). Electrical Conduction in Canine Pulmonary Veins. Circulation *105*, 2442-2448.

Hoffman, B.F., and Kelly, J.J.J. (1959). Effects of rate and rhythm on contraction of rat papillary muscle. The American Journal of Physiology *197*, 1199-1204.

Hollander, J.M., Thapa, D., and Shepherd, D.L. (2014). Physiological and structural differences in spatially distinct subpopulations of cardiac mitochondria: influence of cardiac pathologies. American Journal of Physiology Heart and Circulatory Physiology *307(1)*, 1-14.

Honjo, H., Boyett, M.R., Niwa, R., Inada, S., Yamamoto, M., Mitsui, K., Horiuchi, T., Shibata, N., Kamiya, K., and Kodama, I. (2003a). Pacing-Induced Spontaneous Activity in Myocardial Sleeves of Pulmonary Veins After Treatment With Ryanodine. Circulation *107*, 1937-1943.

Honjo, H., Inada, S., Lancaster, M.K., Yamamoto, M., Niwa, R., Jones, S.A., Shibata, N., Mitsui, K., Horiuchi, T., Kamiya, K., *et al.* (2003b). Sarcoplasmic reticulum Ca^{2+} release is not a dominating factor in sinoatrial node pacemaker activity. Circulation Research *92(3)*, 41-44.

Houser, S.R. (2000). When does spontaneous sarcoplasmic reticulum CA(2+) release cause a triggered arrythmia? Cellular versus tissue requirements. Circulation Research *87(9)*, 725-727.

Hove-Madsen, L., Prat-Vidal, C., Llach, A., Ciruela, F., Casadó, V., Lluis, C., Bayes-Genis, A., Cinca, J., and Franco, R. (2006). Adenosine A2A receptors are expressed in human atrial myocytes and modulate spontaneous sarcoplasmic reticulum calcium release. Cardiovascular Research *72(2)*, 292-302.

Hsieh, M.-H., Chen, S.-A., Tai, C.-T., Tsai, C.-F., Prakash, V.S., Yu, W.-C., Liu, C.-C., Ding, Y.-A., and Chang, M.-S. (1999). Double multielectrode mapping catheters facilitate radiofrequency catheter ablation of focal atrial fibrillation originating from pulmonary veins. Journal of Cardiovascular Electrophysiology *10(2)*, 136-144.

Huang, X.-D., and Wong, T.-M. (1989). Arrhythmogenic effect of forskolin in the isolated perfused rat heart: influence of nifedipine or reduction of external calcium. Clinical and Experimental Pharmacology and Physiology *16(10)*, 751-757.

Huke, S., and Bers, D.M. (2007). Temporal dissociation of frequency-dependent acceleration of relaxation and protein phosphorylation by CaMKII. Journal of Molecular and Cellular Cardiology *42(3)*, 590-599.

Hulme, J.T., Lin, T.W.C., Westenbroek, R.E., Scheuer, T., and Catterall, W.A. (2003). β-Adrenergic regulation requires direct anchoring of PKA to cardiac CaV1.2 channels via a leucine zipper interaction with A kinase-anchoring protein 15. Proceedings of the National Academy of Sciences *100*, 13093-13098.

Huo, R., Li, Z., Lu, C., Xie, Y., Wang, B., Tu, Y.-J., Hu, J.-T., Xu, C.-Q., Yang, B.-F., and Dong, D.-L. (2010). Inhibition of 2-aminoethoxydiphenyl borate-induced rat atrial ectopic activity by anti-arrhythmic drugs. Cellular Physiology and Biochemistry: International Journal of Experimental Cellular Physiology, Biochemistry and Pharmacology *25(4-5)*, 425-432.

Hüser, J., Lipsius, S.L., and Blatter, L.A. (1996). Calcium gradients during excitation-contraction coupling in cat atrial myocytes. The Journal of Physiology *494(3)*, 641-654.

Hussain, M., and Orchard, C.H. (1997). Sarcoplasmic reticulum Ca^{2+} content, L-type Ca^{2+} current and the Ca^{2+} transient in rat myocytes during β-adrenergic stimulation. Journal of Physiology *505*, 385-402.

Hutter, O.F., and Noble, D. (1960). Rectifying properties of heart muscle. Nature *188*, 495.

Huxley, H.E. (1961). The contractile structure of cardiac and skeletal muscle. Circulation *24*, 328-335.

Ishida, A., Kameshita, I., Okuno, S., Kitani, T., and Fujisawa, H. (1995). A novel highly specific and potent inhibitor of calmodulin-dependent protein kinase II. Biochemical and Biophysical Research Communications *212(3)*, 806-812.

Jackson, V.M., Trout, S.J., and Cunnane, T.C. (2002). Regional variation in electrically-evoked contractions of rabbit isolated pulmonary artery. British Journal of Pharmacology *137(4)*, 488-496.

Jahnel, U., Nawrath, H., Carmeliet, E., and Vereecke, J. (1991). Depolarization-induced influx of sodium in response to phenylephrine in rat atrial heart muscle. The Journal of Physiology *432*, 621-637.

Jahnel, U., Nawrath, H., Shieh, R.C., Sharma, V.K., Williford, D.J., and Sheu, S.S. (1992). Modulation of cytosolic free calcium concentration by alpha 1-adrenoceptors in rat atrial cells. Naunyn-Schmiedeberg's Archives of Physiology *346(1)*, 88-93.

Jaïs, P., Hocini, M., Macle, L., Choi, K.-J., Deisenhofer, I., Weerasooriya, R., Shah, D.C., Garrigue, S., Raybaud, F., Scavee, C., *et al.* (2002). Distinctive electrophysiological properties of pulmonary veins in patients with atrial fibrillation. Circulation *106(19)*, 2479-2485.

Jalife, J., Berenfeld, O., and Mansour, M. (2002). Mother rotors and fibrillatory conduction: a mechanism of atrial fibrillation. Cardiovascular Research *54*, 204-216.

James, P., Inui, M., Tada, M., Chiesi, M., and Carafoli, E. (1990). Nature and site of phospholamban regulation of the Ca^{2+} pump of sarcoplasmic reticulum. Nature *342(6245)*, 90-92.

Jang, Y., Wang, H., Xi, J., Mueller, R.A., Norfleet, E.A., and Xu, Z. (2007). NO mobilizes intracellular Zn^{2+} via cGMP/PKG signaling pathway and prevents mitochondrial oxidant damage in cardiomyocytes. Cardiovascular Research *75(2)*, 426-433.

Jayasinghe, I.D., Cannell, M.B., and Soeller, C. (2009). Organization of ryanodine receptors, transverse tubules, and sodium-calcium exchanger in rat myocytes. Biophysical Journal *97(10)*, 2664-2672.

Jiang, D., Xiao, B., Yang, D., Wang, R., Choi, P., Zhang, L., Cheng, H., and Chen, S.-R. (2004). RyR2 mutations linked to ventricular tachycardia and sudden death reduce the threshold for store-overload-induced Ca^{2+} release (SOICR). Proceedings of the National Academy of Sciences of the United States of America *101(35)*, 13062-13067.

Jóhannsson, E., Nagelhus, E.A., McCullagh, K.J., Sejersted, O.M., Blackstad, T.W., Bonen, A., and Ottersen, O.P. (1997). Cellular and subcellular expression of the monocarboxylate transporter MCT1 in rat heart. A high-resolution immunogold analysis. Circulation Research *80(3)*, 400-407.

Jones, S.A., Yamamoto, M., Tellez, J.O., Billeter, R., Boyett, M.R., Honjo, H., and Lancaster, M.K. (2008). Distinguishing properties of cells from the myocardial sleeves of the pulmonary veins: a comparison of normal and abnormal pacemakers. Circulation Arrhythmia and Electrophysiology *1(1)*, 39-48.

Jones, W.K., Sánchez, A., and Robbins, J. (1994). Murine pulmonary myocardium: developmental analysis of cardiac gene expression. Developmental Dynamics: An Official Publication of the American Association of Anatomists *200(2)*, 117-128.

Jost, N., Nagy, N., Corici, C., Kohajda, Z., Horváth, A., Acsai, K., Biliczki, P., Levijoki, J., Pollesello, P., Koskelainen, T., *et al.* (2013). ORM-10103, a novel specific inhibitor of the Na^+/Ca^{2+} exchanger, decreases early and delayed afterdepolarizations in the canine heart. British Journal of Pharmacology *170(4)*, 768-778.

Kaneko, T., Tanaka, H., Oyamada, M., Kawata, S., and Takamatsu, T. (2000). Three distinct types of Ca(2+) waves in Langendorff-perfused rat heart revealed by real-time confocal microscopy. Circulation Research *86(10)*, 1093-1099.

Kang, T.M., and Hilgemann, D.W. (2004). Multiple transport modes of the cardiac Na^+/Ca^{2+} exchanger. Nature *427(6974)*, 544-548.

Kannel, W.B., and Benjamin, E.J. (2009). Current perceptions of the epidemiology of atrial fibrillation. Cardiology Clinics *27(1)*.

Kannel, W.B., Wolf, P.A., Benjamin, E.J., and Levy, D. (1998). Prevalence, incidence, prognosis, and predisposing conditions for atrial fibrillation: population-based estimates. The American Journal of Cardiology *82(8A)*, 2-9.

Kanter, H.L., Saffitz, J.E., and E.C, B. (1992). Cardiac myocytes express multiple gap junction proteins. Circulation Research *70(2)*, 438-444.

Kapoor, N., Tran, A., Kang, J., Zhang, R., Philipson, K.D., and Goldhaber, J.I. (2015). Regulation of Calcium Clock-Mediated Pacemaking by Inositol-1,4,5-Trisphosphate Receptors in Mouse Sinoatrial Nodal Cells. The Journal of Physiology, doi: 10.1113/JP270082.

Karrer, H.E. (1959). The striated musculature of blood vessels. I. General cell morphology. The Journal of Biophysical and Biochemical Cytology *6*, 383-392.

Karrer, H.E. (1960). The striated musculature of blood vessels. II. Cell interconnections and cell surface. The Journal of Biophysical and Biochemical Cytology *8*, 135-150.

Kass, R.S., Lederer, W.J., Tsien, R.W., and Weingart, R. (1978). Role of calcium ions in transient inward currents and aftercontractions induced by strophanthidin in cardiac Purkinje fibres. The Journal of Physiology *281*, 187-208.

Kassianos, G., Arden, C., Hogan, S., Baldock, L., and Fuat, A. (2014). The non-anticoagulation costs of atrial fibrillation management: findings from an observational study in NHS Primary Care. Drugs in Context *doi: 10.7573/dic.212254*.

Katritsis, D., Ioannidis, J.P., Anagnostopoulos, C.E., Sarris, G.E., Giazitzoglou, E., Korovesis, S., and Camm, A.J. (2001). Identification and catheter ablation of extracardiac and intracardiac components of ligament of Marshall tissue for treatment of paroxysmal atrial fibrillation. Journal of Cardiovascular Electrophysiology *12*, 750-758.

Kawai, M., Hussain, M., and Orchard, C.H. (2009). Excitation-contraction coupling in rat ventricular myocytes after formamide-induced detubulation. The American Journal of Physiology *277(2 pt. 2)*, 603-609.

Keizer, J., and Smith, G.D. (1998). Spark-to-wave transition: saltatory transmission of calcium waves in cardiac myocytes. Biophhysical Chemistry *72(1-2)*, 87-100.

Keizer, J., Smith, G.D., Ponce-Dawson, S., and Pearson, J.E. (1998). Saltatory propagation of Ca^{2+} waves by Ca^{2+} sparks. Biophysical Journal *75(2)*, 595-600.

Keller, M., Kao, J.P., Egger, M., and Niggli, E. (2007). Calcium waves driven by "sensitization" wave-fronts. Cardiovascular Research *74(1)*, 39-45.

Kettlewell, S., Burton, F.L., Smith, G.L., and Workman, A.J. (2013). Chronic myocardial infarction promotes atrial action potential alternans, afterdepolarizations, and fibrillation. Cardiovascular Research *99(1)*, 215-224.

Khan, R. (2004). Identifying and understanding the role of pulmonary vein activity in atrial fibrillation. Cardiovascular Research *64*, 387-394.

Kholová, I., and Kautzner, J. (2003). Anatomic characteristics of extensions of atrial myocardium into the pulmonary veins in subjects with and without atrial fibrillation. Pacing & Clinical Electrophysiolgy - PACE *26*, 1348-1355.

Kieval, R.S., R.J, B., Lindenmayer, G.E., Ambesi, A., and Lederer, W.J. (1992). Immunofluorescence localization of the Na-Ca exchanger in heart cells. The American Journal of Physiology *263(2 pt. 1)*, 545-550.

Kimura, H., Oyamada, Y., Ohshika, H., Mori, M., and Oyamada, M. (1995). Reversible inhibition of gap junctional intercellular communication, synchronous contraction, and synchronism of intracellular Ca^{2+} fluctuation in cultured neonatal rat cardiac myocytes by heptanol. Experimental Cell Research *220(2)*, 348-356.

Kimura, J., Miyamae, S., and Noma, A. (1987). Identification of sodium-calcium exchange current in single ventricular cells of guinea-pig. The Journal of Physiology *384*, 199-222.

Kirchhefer, U., Baba, H.A., Kobayashi, Y.M., Jones, L.R., Schmitz, W., and Neumann, J. (2002). Altered function in atrium of transgenic mice overexpressing triadin 1. American Journal of Physiology Heart and Circulatory Physiology *283(4)*, 1334-1343.

Kirchhoff, S., Nelles, E., Hagendorff, A., Krüger, O., Traub, O., and K, W. (1998). Reduced cardiac conduction velocity and predisposition to arrhythmias in connexin40-deficient mice. Current Biology: Cell Biology *8(5)*, 299-302.

Kirk, M.M., Izu, L.T., Chen-Izu, Y., McCulle, S.L., Wier, W.G., Balke, C.W., and Shorofsky, S.R. (2003). Role of the transverse-axial tubule system in generating calcium sparks and calcium transients in rat atrial myocytes. The Journal of Physiology *547(2)*, 441-451.

Klavins, J.V. (1963). Demonstration of striated muscle in the pulmonary veins of the rat. Journal of Anatomy, London *97*, 239-241.

Klietsch, R., Ervasti, J.M., Arnold, W., Campbell, K.P., and Jorgensen, A.O. (1993). Dystrophin-glycoprotein complex and laminin colocalize to the sarcolemma and transverse tubules of cardiac muscle. Circulation Research *72(2)*, 349-360.

Kockskämper, J., Sheehan, K.A., Bare, D.J., Lipsius, S.L., Mignery, G.A., and Blatter, L.A. (2001). Activation and propagation of Ca(2+) release during excitation-contraction coupling in atrial myocytes. Biophysical journal *81*, 2590-2605.

Kodama, I., Kamiya, K., and Toyama, J. (1997). Cellular electropharmacology of amiodarone. Cardiovascular research *35(1)*, 13-29.

Kong, H., Jones, P.P., Koop, A., Zhang, L., Duff, H.J., and Chen, S.R. (2008). Caffeine induces Ca^{2+} release by reducing the threshold for luminal Ca^{2+} activation of the ryanodine receptor. Biophysical Journal *414(3)*, 441-452.

Kort, A.A., and Lakatta, E.G. (1984). Calcium-dependent mechanical oscillations occur spontaneously in unstimulated mammalian cardiac tissues. Circulation Research *54*, 396-404.

Kort, A.A., and Lakatta, E.G. (1988). Bimodal effect of stimulation on light fluctuation transients

monitoring spontaneous sarcoplasmic reticulum calcium release in rat

cardiac muscle. Circulation Research *63(5)*, 960-968.

Koss, K.L., and Kranias, E.G. (1996). Phospholamban: a prominent regulator of myocardial contractility. Circulation Research *79(6)*, 1059-1063.

Kostin, S., Scholz, D., Shimada, T., Maeno, Y., Mollnau, H., Hein, S., and Schaper, J. (1998). The internal and external protein scaffold of the T-tubular system in cardiomyocytes. Cell and Tissue Research *294(3)*, 449-460.

Koumi, S., Backer, C.L., and Arentzen, C.E. (1995). Characterization of inwardly rectifying K^+ channel in human cardiac myocytes. Alterations in channel behavior in myocytes isolated from patients with idiopathic dilated cardiomyopathy. Circulation *92(2)*, 164-174.

Koyama-Honda, I., Ritchie, K., Fujiwara, T., Iino, R., Murakoshi, H., Kasai, R.S., and Kusumi, A. (2005). Fluorescence imaging for monitoring the colocalization of two single molecules in living cells. Biophysical Journal *88(3)*, 2126-2136.

Kracklauer, M.P., Feng, H.Z., Jiang, W., Lin, J.L., Lin, J.J., and Jin, J.P. (2013). Discontinuous thoracic venous cardiomyocytes and heart exhibit synchronized developmental switch of troponin isoforms. The FEBS Journal *280(3)*, 880-891.

Kramer, A.W., and Marks , L.S. (1965). The occurence of cardiac muscle in the pulmonary veins of Rodentia. Journal of Morphology *117*, 139-149.

Kranias, E.G., Gupta, R.C., Jakab, G., Kim, H.W., Steenaart, N.A., and Rapundalo, S.T. (1988). The role of protein kinases and protein phosphatases in the regulation of cardiac sarcoplasmic reticulum function. Molecular and Cellular Biochemistry *82(1-2)*, 37-44.

Kress, M., Huxley, H.E., Faruqi, A.R., and Hendrix, J. (1986). Structural changes during activation of frog muscle studied by time-resolved X-ray diffraction. Journal of Molecular Biology *188(3)*, 325-342.

Krishnan, J., Chakravarthy, V.S., Radhakrishnan, S., and Victor, S. (2005). Neural influence is essential for synchronizing cardiac oscillators: A computational model. Indian Journal of Thoracic and Cardiovascular Surgery *24(4)*, 262-268.

Kurihara, S., and Sakai, T. (1985). Effects of rapid cooling on mechanical and electrical responses in ventricular muscle of guinea-pig. The Journal of Physiology *361*, 361-378.

Kurz, F.T., Aon, M.A., O'Rourke, B., and Armoundas, A.A. (2010). Wavelet analysis reveals heterogeneous time-dependent oscillations of individual mitochondria. American Journal of Physiology Heart and Circulatory Physiology *299(5)*, 1736-1740.

Kuz'min, V.S., and Rozenshtraukh, L.V. (2012). Changes in the excitability of the rat pulmonary vein myocardium induced by adrenergic stimulation. Doklady Biological Sciences *443*, 71-74.

Lakatta, E.G., and DiFrancesco, D. (2009). What keeps us ticking: a funny current, a calcium clock, or both? Journal of Molecular and Cellular Cardiology *47(2)*, 157-170.

Lakatta, E.G., and Lappé, D.L. (1981). Diastolic scattered light fluctuation, resting force and twitch force in mammalian cardiac muscle. The Journal of Physiology *315*, 369-394.

Lakatta, E.G., Maltsev, V.A., Bogdanov, K.Y., Stern, M.D., and Vinogradova, T.M. (2003). Cyclic variation of intracellular calcium: a critical factor for cardiac pacemaker cell dominance. Circulation Research *92(3)*, 45-50.

Lamont, C., Luther, P.W., Balke, C.W., and Wier, W.G. (1998). Intercellular Ca^{2+} waves in rat heart muscle. The Journal of Physiology *512(3)*, 669-676.

Landmark, K., and Refsum, H. (1977). The Effect of Calcium and Beat Interval on the Contractile Force and Refractoriness of the Isolated Rat Atrium in the Absence and Presence of Nifedipine: A Possible Mechanism for the Negative Staircase Phenomenon. Acta Pharmacologica et Toxicologica (Copenhagen) *40(4)*, 505-516.

Lehman, W., Rosol, M., Tobacman, L.S., and Craig, R. (2001). Troponin organization on relaxed and activated thin filaments revealed by electron microscopy and three-dimensional reconstruction. Journal of Molecular Biology *307(3)*, 739-744.

Levi, A.J., Boyett, M.R., and Lee, C.O. (1994). The cellular actions of digitalis glycosides on the heart. Progess in Biophysics and Molecular Physiology *62(1)*, 1-54.

Lévy, S., Camm, A., Saksena, S., Aliot, E., Breithardt, G., Crijns, H.J., Davies, D.W., Kay, G.N., Prystowsky, E.N., Sutton, R., *et al.* (2003). International consensus on nomenclature and classification of atrial fibrillation:

A collaborative project of the Working Group on Arrhythmias and the

Working Group of Cardiac Pacing of the European Society of Cardiology

and the North American Society of Pacing and Electrophysiology. Journal of Cardiovascular Electrophysiology *14(4)*, 443-445.

Li, J.-Y., Wang, H.-J., Xu, B., Wang, X.-P., Fu, Y.-C., Chen, M.-Y., Zhang, D.-X., Liu, Y., Xue, Q., and Li, Y. (2012). Hyperpolarization activated cation current (I(f)) in cardiac myocytes from pulmonary vein sleeves in the canine with atrial fibrillation. Journal of Geriatric Cardiology *9(4)*, 366-374.

Li, X., Zima, A.V., Sheikh, F., Blatter, L.A., and Chen, J. (2005). Endothelin-1-induced arrhythmogenic Ca^{2+} signaling is abolished in atrial myocytes of inositol-1,4,5-trisphosphate(IP3)-receptor type 2-deficient mice. Circulation Research *96(12)*, 1274-1281.

Lickfett, L., Dickfeld, T., Kato, R., Tandri, H., Vasamreddy, C.R., Berger, R., Bluemke, D., Lüderitz, B., Halperin, H., and Calkins, H. (2005). Changes of pulmonary vein orifice size and location throughout the cardiac cycle: dynamic analysis using magnetic resonance cine imaging. Journal of Cardiovascular Electrophysiology *16(6)*, 582-588.

Lin, W.-S., Prakash, V.S., Tai, C.-T., Hsieh, M.-H., Tsai, C.-F., Yu, W.-C., Lin, Y.-K., Ding, Y.-A., Chang, M.-S., and Chen, S.-A. (2000). Pulmonary vein morphology in patients with paroxysmal atrial fibrillation initiated by ectopic beats originating from the pulmonary veins: implications for catheter ablation. Circulation *101(11)*, 1274-1281.

Lindemann, J.P., Jones, L.R., Hathaway, D.R., Henry, B.G., and Watanabe, A.M. (1983). beta-Adrenergic stimulation of phospholamban phosphorylation and Ca^{2+}-ATPase activity in guinea pig ventricles. Journal of Biological Chemistry *258*, 464-471.

Lipp, P., Hüser, J., Pott, L., and Niggli, E. (1996). Subcellular properties of triggered Ca^{2+} waves in isolated citrate-loaded guinea-pig atrial myocytes characterized by ratiometric confocal microscopy. The Journal of Physiology *497(3)*, 599-610.

Lipp, P., Laine, M., Tovey, S.C., Burrell, K.M., Berridge, M.J., Li, W., and Bootman, M.D. (2000). Functional InsP3 receptors that may modulate excitation-contraction coupling in the heart. Current Biology *10(15)*, 939-942.

Lipsius, S.L., Hüser, J., and Blatter, L.A. (2001). Intracellular Ca^{2+} release sparks atrial pacemaker activity. News in Physiological Sciences *16*, 101-106.

Litwin, S.E., and Zhang, D. (2002). Enhanced sodium-calcium exchange in the infarcted heart : effects on sarcoplasmic reticulum content and cellular contractility. Annals of the New York Academy of Sciences *976*, 446-453.

Llach, A., Molina, C.E., Fernandes, J., Padró, J., Cinca, J., and Hove-Madsen, L. (2011). Sarcoplasmic reticulum and L-type Ca^{2+} channel activity regulate the beat-to-beat stability of calcium handling in human atrial myocytes. The Journal of Physiology *589(13)*, 3247-3262.

Lo, L.-W., Chen, Y.-C., Chen, Y.-J., Wongcharoen, W., Lin, C.-I., and Chen, S.-A. (2007). Calmodulin kinase II inhibition prevents arrhythmic activity induced by alpha and beta adrenergic agonists in rabbit pulmonary veins. European Journal of Pharmacology *571*, 197-208.

Loew, L.M., Tuft, R.A., Carrington, W., and Fay, F.S. (1993). Imaging in five dimensions: time-dependent membrane potentials in individual mitochondria. Biophysical Journal *65(6)*, 2396-2407.

Loewenstein, W.R. (1981). Junctional intercellular communication: the cell-to-cell membrane channel. Physiological Reviews *61(4)*, 829-913.

Logantha, S.J., Cruickshank, S.F., Rowan, E.G., and Drummond, R.M. (2010). Spontaneous and electrically evoked Ca^{2+} transients in cardiomyocytes of the rat pulmonary vein. Cell Calcium *48*, 150-160.

Louch, W.E., Sheehan, K.A., and Wolska, B.M. (2011). Methods in cardiomyocyte isolation, culture, and gene transfer. Journal of Molecular and Cellular Cardiology *51(3)*, 288-298.

Lu, X., Kwong, J.Q., Molkentin, J.D., and Bers, D.M. (2016). Individual Cardiac Mitochondria Undergo Rare Transient Permeability Transition Pore Openings. Circulation Research *118(5)*, 834-841.

Lu, Z., Scherlag, B.J., Lin, J., Yu, L., Guo, J.-H., Niu, G., Jackman, W.M., Lazzara, R., Jiang, H., and Po, S.S. (2009). Autonomic mechanism for initiation of rapid firing from atria and pulmonary veins: evidence by ablation of ganglionated plexi. Cardiovascular Research *84(2)*, 245-252.

Ludatscher, R. (1968). Fine structure of the muscular wall of rat pulmonary veins. Journal of anatomy *103*, 345-357.

Ludwig, A., Zong, X., Stieber, J., Hullin, R., Hofmann, F., and Biel, M. (1999). Two pacemaker channels from human heart with profoundly different activation kinetics. The EMBO Journal *18(9)*, 2323-2329.

Luk, H.-N., Lo, C.-P., Tien, H.-C., Lee, D., Chen, Z.-L., Wang, F., Hsin, S.-T., and Day, Y.-J. (2008). Mechanical characterization of rabbit pulmonary vein sleeves in in vitro intact ring preparation. Journal of Chinese Medical Association *71(12)*, 610-618.

Lukyanenko, V., Chikando, A., and Lederer, W.J. (2009). Mitochondria in cardiomyocyte Ca^{2+} signaling. The International Journal of Biochemistry and Cell Biology *41(10)*, 1957-1971.

Lukyanenko, V., Subramanian, S., Györke, I., Wiesner, T.F., and Györke, S. (1999). The role of luminal Ca^{2+} in the generation of Ca^{2+} waves in rat ventricular myocytes. The Journal of Physiology *518(1)*, 173-186.

Lukyanenko, V., Viatchenko-Karpinski, S., Smirnov, A., Wiesner, T.F., and Györke, S. (2001). Dynamic regulation of sarcoplasmic reticulum Ca(2+) content and

release by luminal Ca(2+)-sensitive leak in rat ventricular myocytes. Biophysical Journal *81(2)*, 785-798.

Luongo, T.S., Lambert, J.P., Yuan, A., Zhang, X., Gross, P., Song, J., Shanmughapriya, S., Gao, E., Jain, M., Houser, S.R., *et al.* (2015). The Mitochondrial Calcium Uniporter Matches Energetic Supply with Cardiac Workload during Stress and Modulates Permeability Transition. Cell Reports *12(1)*, 23-34.

Mackenzie, L., Bootman, M.D., Berridge, M.J., and Lipp, P. (2001). Predetermined recruitment of calcium release sites underlies excitation-contraction coupling in rat atrial myocytes. The Journal of Physiology *530(3)*, 417-429.

Mackenzie, L., Bootman, M.D., Laine, M., Berridge, M.J., Thuring, J., Holmes, A., Li, W.H., and Lipp, P. (2002). The role of inositol 1,4,5-trisphosphate receptors in Ca(2+) signalling and the generation of arrhythmias in rat atrial myocytes. The Journal of Physiology *541(2)*, 395-409.

Mackenzie, L., Roderick, H.L., Berridge, M.J., Conway, S.J., and Bootman, M.D. (2004). The spatial pattern of atrial cardiomyocyte calcium signalling modulates contraction. Journal of Cell Science *117(26)*, 6327-6337.

MacLeod, D.P., and Hunter, E.G. (1967). The pharmacology of the cardiac muscle of the great veins in the rat. Canadian Journal of Physiology and Pharmacology *45*, 463-473.

MacQuaide, N., Dempster, J., and Smith, G.L. (2007). Measurement and modeling of Ca^{2+} waves in isolated rabbit ventricular cardiomyocytes. Biophysical Journal *93(7)*, 2581-2595.

MacQuaide, N., Dempster, J., and Smith, G.L. (2009). Assessment of sarcoplasmic reticulum Ca^{2+} depletion during spontaneous Ca^{2+} waves in isolated permeabilized rabbit ventricular cardiomyocytes. Biophysical Journal *96(7)*, 2744-2754.

Maier, L.S., Bers, D.M., and Pieske, B. (2000). Differences in Ca(2+)-handling and sarcoplasmic reticulum Ca(2+)-content in isolated rat and rabbit myocardium. Journal of Cellular and Molecular Cardiology *32(12)*, 2249-2258.

Malécot, C.O., Bredeloux, P., Findlay, I., and Maupoil, V. (2015). A TTX-sensitive resting Na^{+} permeability contributes to the catecholaminergic automatic activity in rat pulmonary vein. Journal of Cardiovascular Electrophysiology *26(3)*, 311-319.

Masani, F. (1986). Node-like cells in the myocardial layer of the pulmonary vein of rats: an ultrastructural study. Journal of Anatomy *145*, 133-142.

Maupoil, V., Bronquard, C., Freslon, J.L., Cosnay, P., and Findlay, I. (2007). Ectopic activity in the rat pulmonary vein can arise from simultaneous activation of alpha1- and beta1-adrenoceptors. British Journal of Pharmacology *150*, 899-905.

Maxwell , J.T., and Blatter, L.A. (2012). Facilitation of cytosolic calcium wave propagation by local calcium uptake into the sarcoplasmic reticulum in cardiac myocytes. The Journal of Physiology *590(23)*, 6037-6045.

Mechmann, S., and Pott, L. (1986). Identification of Na-Ca exchange current in single cardiac myocytes. Nature *319(6054)*, 597-599.

Melnyk, P., Ehrlich, J.R., Pourrier, M., Villeneuve, L., Cha, T.-J., and Nattel, S. (2005). Comparison of ion channel distribution and expression in cardiomyocytes of canine pulmonary veins versus left atrium. Cardiovascular Research *65(1)*, 104-116.

Metzger, J.M., and Westfall, M.V. (2004). Covalent and noncovalent modification of thin filament action: the essential role of troponin in cardiac muscle regulation. 94(2), 146-158.

Michaels, D.C., Matyas, E.P., and Jalife, J. (1987). Mechanisms of sinoatrial pacemaker synchronization: a new hypothesis. Circulation Research *61(5)*, 704-714.

Millino, C., Sarinella, F., Tiveron, C., Villa, A., Sartore, S., and Ausoni, S. (2000). Cardiac and smooth muscle cell contribution to the formation of the murine pulmonary veins. Developmental Dynamics: An Official Publication of the American Association of Anatomists.

Minamikawa, T., Cody, S.H., and Williams, D.A. (1997). In situ visualization of spontaneous calcium waves within perfused whole rat heart by confocal imaging. The American Journal of Physiology *272(1 pt. 2)*, 236-243.

Miura, M., Boyden, P.A., and ter Keurs, H.E. (1999). Ca^{2+} waves during triggered propagated contractions in intact trabeculae. Determinants of the velocity of propagation. Circulation Research *84(12)*, 1459-1468.

Miyata, H., Silverman, H.S., Sollott, S.J., Lakatta, E.G., Stern, M.D., and Hansford, R.G. (1991). Measurement of mitochondrial free Ca^{2+} concentration in living single rat cardiac myocytes. The American Journal of Physiology *261(4 pt. 2)*, 1123-1134.

Miyauchi, Y., Hayashi, H., Miyauchi, M., Okuyama, Y., Mandel, W.J., Chen, P.-S., and Karagueuzian, H.S. (2005). Heterogeneous pulmonary vein myocardial cell repolarization implications for reentry and triggered activity. Heart Rhythm *2*, 1339-1345.

Mommersteeg, M.T., Brown, N.A., Prall, O.W., de Gier-de Vries, C., Harvey, R.P., Moorman, A.F., and Christoffels, V.M. (2007). Pitx2c and Nkx2-5 are required for the formation and identity of the pulmonary myocardium. Circulation Research *101(9)*, 902-909.

Morel, E., Meyronet, D., Thivolet-Bejuy, F., and Chevalier, P. (2008). Identification and distribution of interstitial Cajal cells in human pulmonary veins. Heart Rhythm *5(7)*, 1063-1067.

Morii, I., Kihara, Y., Konishi, T., Inubushi, T., and Sasayama, S. (1996). Mechanism of the negative force-frequency relationship in physiologically intact rat ventricular myocardium--studies by intracellular Ca^{2+} monitor with indo-1 and by 31P-nuclear magnetic resonance spectroscopy. Japanese Circulation Journal *60(8)*, 593-603.

Moschella, M.C., and Marks, A.R. (1993). Inositol 1,4,5-trisphosphate receptor expression in cardiac myocytes. The Journal of Cell Biology *120(5)*, 1137-1146.

Mueller-Hoecker, J., Beitinger, F., Fernandez, B., Bahlmann, O., Assmann, G., Troidl, C., Dimomeletis, I., Kääb, S., and E, D. (2008). Of rodents and humans: a light microscopic and ultrastructural study on cardiomyocytes in pulmonary veins. International Journal of Medical Sciences *5*, 152-158.

Mundiña de Weilenmann, C., Vittone, L., de Cingolani, G., and Mattiazzi, A. (1987). Dissociation between contraction and relaxation: the possible role of phospholamban phosphorylation. Basic Research in Pharmacology *82(6)*, 507-516.

Murphy, N.F., Simpson, C.R., Jhund, P.S., Stewart, S., Kirkpatrick, M., Chalmers, J., MacIntyre, K., and McMurray, J.J. (2007). A national survey of the prevalence, incidence, primary care burden and treatment of atrial fibrillation in Scotland. Heart (British Cardiac Society) *93(5)*, 606-612.

Namekata, I., Tsuneoka, Y., Akiba, A., Nakamura, H., Shimada, H., Takahara, A., and Tanaka, H. (2010). Intracellular calcium and membrane potential oscillations in the guinea pig and rat pulmonary vein myocardium. Bioimages *18*, 11-22.

Namekata, I., Tsuneoka, Y., Takahara, A., Shimada, H., Sugimoto, T., Takeda, K., Nagaharu, M., Shigenobu, K., Kawanishi, T., and Tanaka, H. (2009). Involvement of the Na^{+}/Ca^{2+} Exchanger in the Automaticity of Guinea-Pig Pulmonary Vein Myocardium as Revealed by SEA0400. Journal of Pharmacological Sciences *110*, 111-116.

Nao, T., Ohkusa, T., Hisamatsu, Y., Inoue, N., Matsumoto, T., Yamada, J., Shimizu, A., Yoshiga, Y., Yamagata, T., Kobayashi, S., *et al.* (2003). Comparison of expression of connexin in right atrial myocardium in patients with chronic atrial fibrillation versus those in sinus rhythm. The American Journal of Cardiology *91(6)*, 678-683.

Nathan, H., and Eliakim, M. (1966). The junction between the left atrium and the pulmonary veins. An anatomic study of human hearts. Circulation *34(3)*, 412-422.

Nathan, H., and Gloobe, H. (1970). Myocardial atrio-venous junctions and extensions (sleeves) over the pulmonary and caval veins. Anatomical observations in various mammals. Thorax *25(3)*, 317-324.

Nattel, S. (1998). Experimental evidence for proarrhythmic mechanisms of antiarrhythmic drugs. Cardiovascular Research *37*, 567-577.

Nattel, S. (2002). New ideas about atrial fibrillation 50 years on. Nature *415*, 219-226.

Nattel, S., Maguy, A., Le Bouter, S., and Yeh, Y.-H. (2007). Arrhythmogenic ion-channel remodeling in the heart: heart failure, myocardial infarction, and atrial fibrillation. Physiological Reviews *87(2)*, 425-256.

Nault, I., Miyazaki, S., Forclaz, A., Wright, M., Jadidi, A., Jaïs, P., Hocini, M., and Haïssaguerre, M. (2010). Drugs vs. ablation for the treatment of atrial fibrillation: the evidence supporting catheter ablation. European Heart Journal *31*, 1046-1054.

Nebel, M., Schwoerer, A.P., Warszta, D., Siebrands, C.C., Limbrock, A.C., Swarbrick, J.M., Fliegert, R., Weber, K., Bruhn, S., Hohenegger, M., *et al.* (2013). Nicotinic acid adenine dinucleotide phosphate (NAADP)-mediated calcium signaling and arrhythmias in the heart evoked by β-adrenergic stimulation. The Journal of Biological Chemistry *288(22)*, 16017-16030.

Negretti, N., O'Neil, S.C., and Eisner, D.A. (1993). The relative contributions of different intracellular and sarcolemmal systems to relaxation in rat ventricular myocytes. Cardiovascular Research *27(10)*, 1826-1830.

Nguyen, B.-L., Fishbein, M.C., Chen, L.-S., Chen, P.-S., and Masroor, S. (2009). Histopathological substrate for chronic atrial fibrillation in humans. Heart Rhythm *6(4)*, 454-460.

Niggli, E. (2011). Ryanodine receptors: waking up from refractoriness. Cardiovascular Research *91(4)*, 563-564.

Noble, D., and Tsien, R.-W. (1968). The kinetics and rectifier properties of the slow potassium current in cardiac Purkinje fibres. The Journal of Physiology *195(1)*, 185-214.

O'Neill, S.C., Miller, L., Hinch, R., and Eisner, D.A. (2004). Interplay between SERCA and sarcolemmal Ca^{2+} efflux pathways controls spontaneous release of Ca^{2+} from the sarcoplasmic reticulum in rat ventricular myocytes. The Journal of Physiology *559(1)*, 121-128.

O'Rourke, B., Reibel, D.K., and Thomas, A.P. (1990). High-speed digital imaging of cytosolic Ca^{2+} and contraction in single cardiomyocytes. The American Journal of Physiology *259(1 pt. 2)*, 230-242.

Okada , J., Sugiura, S., Nishimura, S., and Hisada, T. (2005). Three-dimensional simulation of calcium waves and contraction in cardiomyocytes using the finite element method. American Journal of Physiology Cell Physiology *288(3)*, 510-522.

Okamoto, Y., Kawamura, K., Nakamura, Y., and Ono, K. (2014). Pathological impact of hyperpolarization-activated chloride current peculiar to rat pulmonary vein cardiomyocytes. *Journal of Molecular and Cellular Cardiology*, 53-62.

Okamoto, Y., Takano, M., Takayoshi, O., and Ono, K. (2012). Arrhythmogenic coupling between the Na^{+} -Ca^{2+} exchanger and inositol 1,4,5-triphosphate receptor in rat pulmonary vein cardiomyocytes. Journal of Molecular and Cellular Cardiology *52(5)*, 988-997.

Orchard, C.H., Eisner, D.A., and Allen, D.G. (1983). Oscillations of intracellular Ca^{2+} in mammalian cardiac muscle. Nature *304(5928)*, 735-358.

Orchard, C.M., and Brette, F. (2008). T-Tubules and sarcoplasmic reticulum function in cardiac ventricular myocytes. Cardiovascular Research *77(2)*, 237-244.

Otsu, K., Willard, H.F., Khanna, V.K., Zorzato, F., Green, N.M., and MacLennan, D.H. (1990). Molecular cloning of cDNA encoding the Ca^{2+} release channel (ryanodine receptor) of rabbit cardiac muscle sarcoplasmic reticulum. The Journal of Biological Chemistry *265(23)*, 13462-13483.

Overend, C.L., Eisner, D.A., and O'Neill, S.C. (1997). The effect of tetracaine on spontaneous Ca^{2+} release and sarcoplasmic reticulum calcium content in rat ventricular myocytes. The Journal of Physiology *502(3)*, 471-479.

Paes de Almeida, O., Bohm, C.M., de Paula Carvalho, M., and Paes de Carvalho, A. (1975). The cardiac muscle in the pulmonary vein of the rat: a morphological and electrophysiological study. Journal of Morphololgy *145*, 409-433.

Page, E. (1978). Quantitative ultrastructural analysis in cardiac membrane physiology. *235(5)*, 147-158.

Papp, R., Gönczi, M., Kovács, M., Seprényi, G., and Végh, A. (2007). Gap junctional uncoupling plays a trigger role in the antiarrhythmic effect of ischaemic preconditioning. Cardiovascular Research *74(3)*, 396-405.

Pappone, C., Oreto, G., Rosanio, S., Vicedomini, G., Tocchi, M., Gugliotta, F., Salvati, A., Dicandia, C., Calabrò, M.P., Mazzone, P., *et al.* (2001). Atrial electroanatomic remodeling after circumferential radiofrequency pulmonary vein ablation: efficacy of an anatomic approach in a large cohort of patients with atrial fibrillation. Circulation *104(21)*, 2539-2544.

Pappone, C., Rosanio, S., Oreto, G., Tocchi, M., Gugliotta, F., Vicedomini, G., Salvati, A., Dicandia, C., Mazzone, P., Santinelli, V., *et al.* (2000). Circumferential Radiofrequency Ablation of Pulmonary Vein Ostia : A New Anatomic Approach for Curing Atrial Fibrillation. Circulation *102*, 2619-2628.

Pappone, C., Santinelli, V., Manguso, F., Vicedomini, G., Gugliotta, F., Augello, G., Mazzone, P., Tortoriello, V., Landoni, G., Zangrillo, A., *et al.* (2004). Pulmonary vein denervation enhances long-term benefit after circumferential ablation for paroxysmal atrial fibrillation. Circulation *109(3)*, 327-334.

Parmacek, M.S., and Solaro, R.J. (2004). Biology of the troponin complex in cardiac myocytes. Progress in Cardiovascular Diseases *47(3)*, 159-176.

Patel, J.R., Coronado, R., and Moss, R.L. (1995). Cardiac sarcoplasmic reticulum phosphorylation increases Ca^{2+} release induced by flash photolysis of nitr-5. Circulation Research *77(5)*, 943-949.

Patterson, E., Lazzara, R., Szabo, B., Liu, H., Tang, D., Li, Y.-H., Scherlag, B.J., and Po, S.S. (2006). Sodium-calcium exchange initiated by the Ca^{2+} transient: an arrhythmia trigger within pulmonary veins. Journal of the American College of Cardiology *47(6)*, 1196-1206.

Patterson, E., Po, S.S., Scherlag, B.J., and Lazzara, R. (2005). Triggered firing in pulmonary veins initiated by in vitro autonomic nerve stimulation. Heart Rhythm *2*, 624-631.

Peaslee, E.R. (1857). Human histology in its relations to descriptive anatomy, physiology and pathology. (Philadelphia: Blanchard and Lea).

Perez-Lugones, A., McMahon, J.T., Ratliff, N.B., Saliba, W.I., Schweikert, R.A., Marrouche, N.F., Saad, E.B., Navia, J.L., McCarthy, P.M., Tchou, P., *et al.* (2003). Evidence of specialized conduction cells in human pulmonary veins of patients with atrial fibrillation. Journal of Cardiovascular Electrophysiology *14(8)*, 803-809.

Peterson, B.Z., Lee, J.-S., Mulle, J.G., Wang, Y., de, L.M., and Yue, D.-T. (2000). Critical determinants of Ca(2+)-dependent inactivation within an EF-hand motif of L-type Ca(2+) channels. Biophysical Journal *78(4)*, 1906-1920.

Philipson, K.D., Longoni, S., and Ward, R. (1988). Purification of the cardiac Na^+-Ca^{2+} exchange protein. Biochimica et Biophyica Acta *945(2)*, 298-306.

Piacentino, V.r., Weber, C.R., Chen, X., Weisser-Thomas, J., Margulies, K.B., Bers, D.M., and Houser, S.R. (2003). Cellular basis of abnormal calcium transients of failing human ventricular myocytes . Circulation Research *92(6)*, 651-658.

Picht, E., DeSantiago, J., Blatter, L.A., and Bers, D.M. (2006). Cardiac alternans do not rely on diastolic sarcoplasmic reticulum calcium content fluctuations. Circulation Research *99(7)*, 740(748).

Po, S.S., Li, Y., Tang, D., Liu, H., Geng, N., Jackman, W.M., Scherlag, B., Lazzara, R., and Patterson, E. (2005). Rapid and stable re-entry within the pulmonary vein as a mechanism initiating paroxysmal atrial fibrillation. Journal of the American College of Cardiology *45(11)*, 1871-1877.

Po, S.S., Scherlag, B.J., Yamanashi, W.S., Edwards, J., Zhou, J., Wu, R., Geng, N., Lazzara, R., and Jackman, W.M. (2006). Experimental model for paroxysmal atrial fibrillation arising at the pulmonary vein-atrial junctions. Heart Rhythm *3(2)*, 201-208.

Poggioli, J., Sulpice, J.C., and Vassort, G. (1986). Inositol phosphate production following alpha 1-adrenergic, muscarinic or electrical stimulation in isolated rat heart. FEBS letters *206(2)*, 292-298.

Pogwizd, S.M., Schlotthauer, K., Li, L., Yuan, W., and Bers, D.M. (2001). Arrhythmogenesis and contractile dysfunction in heart failure : Roles of sodium-calcium exchange , inward rectifier potassium current , and residual beta-adrenergic responsiveness. Circulation Research *88(11)*, 1159-1167.

Polain de Waroux, J.-B., Talajic, M., Khairy, P., Guerra, P.G., Roy, D., Thibault, B., Dubuc, M., and Macle, L. (2009). Pulmonary vein isolation for the treatment of atrial fibrillation: past, present and future. Future Cardiology *6*, 51-66.

Polontchouk, L., Haefliger, J.A., Ebelt, B., Schaefer, T., Stuhlmann, D., Mehlhorn, U., Kuhn-Regnier, F., De Vivie, E.R., and Dhein, S. (2001). Effects of chronic atrial fibrillation on gap junction distribution in human and rat atria. Journal of the American College of Cardiology *38(3)*, 883-891.

Puceat, M., Clement, O., Lechene, P., Pelosin, J.M., Ventura-Clapier, R., and Vassort, G. (1990). Neurohormonal control of calcium sensitivity of myofilaments in rat single heart cells. Circulation Research *67(2)*, 517-524.

Quednau, B.D., Nicoll, D.A., and Philipson, K.D. (1997). Tissue specificity and alternative splicing of the Na^+/Ca^{2+} exchanger isoforms NCX1, NCX2, and NCX3 in rat. American Journal of Physiology *272(4 pt. 1)*, 1250-1261.

Rakowski, R.F., Gadsby, D., and De Weer, P. (1989). Stoichiometry and voltage dependence of the sodium pump in voltage-clamped, internally dialyzed squid giant axon. 93(5), 903-941.

Ramos-Franco, J., Fill, M., and Mignery, G.A. (1998). Isoform-specific function of single inositol 1,4,5-trisphosphate receptor channels. Biophysical Journal *75(2)*, 834-839.

Reeves, J.P., and Hale, C.C. (1984). The stoichiometry of the cardiac sodium-calcium exchange system. The Journal of Biological Chemistry *259(12)*, 7733-7739.

Reuter, H. (1974). Exchange of calcium ions in the mammalian myocardium. Mechanisms and physiological significance. Circulation Research *34(5)*, 599-605.

Richards, M.A., Clarke, J.D., Saravanan, P., Voigt, N., Dobrev, D., Eisner, D.A., Trafford, A.W., and Dibb, K.M. (2011). Transverse tubules are a common feature in large mammalian atrial myocytes including human. American Journal of Physiology - Heart and Circulatory Physiology *301*, 1996-2005.

Ridley, J., Cheng, H., Harrison, O., Jones, S., Smith, G., Hancox, J., and Orchard, C. (2008). Spontaneous frequency of rabbit atrioventricular node myocytes depends on SR function. Cell Calcium *44(6)*, 580-591.

Rietdorf, K., Bootman, M.D., and Sanderson, M.J. (2014). Spontaneous, pro-arrhythmic calcium signals disrupt electrical pacing in mouse pulmonary vein sleeve cells. PLoS One *9(2)*, e88649.

Rietdorf, K., Masoud, S., McDonald, F., Sanderson, M.J., and Bootman, M.D. (2015). Pulmonary vein sleeve cell excitation-contraction-coupling becomes dysynchronized by spontaneous calcium transients. Biochemical Society Transactions *43(3)*, 410-416.

Rigg, L., and Terrar, D.A. (1996). Possible role of calcium release from the sarcoplasmic reticulum in pacemaking in guinea-pig sino-atrial node. Experimental Physiology *81(5)*, 877-880.

Ringer, S. (1883). A further Contribution regarding the influence of the different Constituents of the Blood on the Contraction of the Heart. The Journal of Physiology *4(1)*, 29-42.

Robbins, I.M., Colvin, E.V., Doyle, T.P., Kemp, W.E., Loyd, J.E., McMahon, W.S., and Kay, G.N. (1998). Pulmonary vein stenosis after catheter ablation of atrial fibrillation. Circulation *98(17)*, 1769-1775.

Rousseau, E., Ladine, J., Liu, Q.-Y., and Meissner, G. (1988). Activation of the Ca^{2+} release channel of skeletal muscle sarcoplasmic reticulum by caffeine and related compounds. Archives of Biochemistry and Biophysics *267(1)*, 75-86.

Rousseau, E., and Meissner, G. (1989). Single cardiac sarcoplasmic reticulum Ca^{2+}-release channel: activation by caffeine. The American Journal of Physiology *256(2 pt. 2)*, 328-333.

Rousseau, E., Smith, J.S., Henderson, J.S., and Meissner, G. (1986). Single channel and 45Ca^{2+} flux measurements of the cardiac sarcoplasmic reticulum calcium channel. Biophysical Journal *50(5)*, 1009-1014.

Rousseau, E., Smith, J.S., and Meissner, G. (1987). Ryanodine modifies conductance and gating behavior of single Ca^{2+} release channel. American Journal of Physiology - Cell Physiology *253*, C364-C368.

Roy, D., Talajic, M., Dorian, P., Connolly, S., Eisenberg, M.J., Green, M., Kus, T., Lambert, J., Dubuc, M., Gagné, P., *et al.* (2000). Amiodarone to Prevent Recurrence of Atrial Fibrillation. New England Journal of Medicine *342*, 913-920.

Saad, E.B., Marrouche, N.F., Saad, C.P., Ha, E., Bash, D., White, R.D., Rhodes, J., Prieto, L., Martin, D.O., Saliba, W.I., *et al.* (2003). Pulmonary Vein Stenosis after Catheter Ablation of Atrial Fibrillation: Emergence of a New Clinical Syndrome. Annals of Internal Medicine *138*, 634-638.

Saffitz, J.E., Kanter, H.L., Green, K.G., Tolley, T.K., and Beyer, E.C. (1994). Tissue-specific determinants of anisotropic conduction velocity in canine atrial and ventricular myocardium. Circulation Research *74*, 1065-1070.

Sag, C.M., Wadsack, D.P., Khabbazzadeh, S., Abesser, M., Grefe, C., Neumann, K., Opiela, M.K., Backs, J., Olson, E.N., Brown, J.H., *et al.* (2009). Calcium/calmodulin-dependent protein kinase II contributes to cardiac arrhythmogenesis in heart failure. Circulation Heart Failure *2(6)*, 664-675.

Saito, T., Waki, K., and Becker, A.E. (2000). Left atrial myocardial extension onto pulmonary veins in humans: anatomic observations relevant for atrial arrhythmias. Journal of Cardiovascular Electrophysiology *11*, 888-894.

Sakakibara, Y., Wasserstrom, J.A., Furukawa, T., Jia, H., Arentzen, C.E., Hartz, R.S., and Singer, D.H. (1992). Characterization of the sodium current in single human atrial myocytes. Circulation Research *71(3)*, 535-546.

Sanders, K.M., and Ward, S.M. (2006). Interstitial cells of Cajal: a new perspective on smooth muscle function. The Journal of Physiology *576(3)*, 721-726.

Sandow, A. (1952). Excitation-contraction coupling in muscular response. The Yale Journal of Biology and Medicine *25(3)*, 176-201.

Sanfilippo, A.J., Abascal, V.M., Sheehan, M., Oertel, L.B., Harrigan, P., Hughes, R.A., and Weyman, A.E. (1990). Atrial enlargement as a consequence of atrial fibrillation. A prospective echocardiographic study. Circulation *82(3)*, 792-797.

Satoh, H., Blatter, L.A., and Bers, D.M. (1997). Effects of $[Ca^{2+}]i$, SR Ca^{2+} load, and rest on Ca^{2+} spark frequency in ventricular myocytes. The American Journal of Physiology *272(2 pt. 2)*, 657-668.

Savelieva, I., and Camm, J. (2008). Anti-arrhythmic drug therapy for atrial fibrillation: current anti-arrhythmic drugs, investigational agents, and innovative approaches. Europace: European Pacing, Arrhythmias and Cardiac Electrophysiology: Journal of the Working Groups on Cardiac Pacing, Arrhythmias and Cardiac Electrophysiology of the European Society of Cardiology *10(6)*, 647-665.

Scaduto, R.C.J., and Grotyohann, L.W. (1999). Measurement of mitochondrial membrane potential using fluorescent rhodamine derivatives. Biophysical *76(1 pt. 1)*, 469-477.

Schatzmann, H.J. (1966). ATP-dependent Ca++-extrusion from human red cells. Experimentia *22(6)*, 364-365.

Schauerte, P., Scherlag, B.J., Patterson, E., Scherlag, M.A., Matsudaria, K., Nakagawa, H., Lazzara, R., and Jackman, W.M. (2001). Focal atrial fibrillation: experimental evidence for a pathophysiologic role of the autonomic nervous system. Journal of Cardiovascular Electrophysiology *12*, 592-599.

Schiefer, A., Meissner, G., and Isenberg, G. (1995). Ca^{2+} activation and Ca^{2+} inactivation of canine reconstituted cardiac sarcoplasmic reticulum Ca(2+)-release channels. The Journal of Physiology *489(pt. 2)*, 337-348.

Schlotthauer, K., and Bers, D.M. (2000). Sarcoplasmic Reticulum Ca^{2+} Release Causes Myocyte Depolarization : Underlying Mechanism and Threshold for Triggered Action Potentials. Circulation Research *87*, 774-780.

Scholz, J., Troll, U., Sandig, P., Schmitz, W., Scholz, H., and Schulte, A.E.J. (1992). Existence and alpha 1-adrenergic stimulation of inositol polyphosphates in mammalian heart. Molecular Pharmacology *42(1)*, 134-140.

Schouten, V.J., and ter Keurs, H.E. (1986). The force-frequency relationship in rat myocardium. The influence of muscle dimensions. Pflügers Archiv: European Journal of Physiology *407(1)*, 14-17.

Schulson, M.N., Scriven, D.R., Fletcher, P., and Moore, E.D. (2011). Couplons in rat atria form distinct subgroups defined by their molecular partners. Journal of Cell Science *24(7)*, 1167-1174.

Scriven, D.R., Asghari, P., Schulson, M.N., and Moore, E.D. (2010). Analysis of Cav1.2 and ryanodine receptor clusters in rat ventricular myocytes. Biophysics Journal *99(12)*, 3923-3929.

Scriven, D.R., Dan, P., and Moore, E.D. (2000). Distribution of proteins implicated in excitation-contraction coupling in rat ventricular myocytes. Biophysical Journal *79(5)*.

Scriven, D.R., and Moore, E.D. (2013). Ca^{2+} channel and Na^{+}/Ca^{2+} exchange localization in cardiac myocytes. Journal of Molecular and Cellular Cardiology *58*, 22-31.

Seamon, K.B., Padgett, W., and Daly, J.W. (1981). Forskolin: unique diterpene activator of adenylate cyclase in membranes and in intact cells. Proceedings of the National Academy of Scientists of the United States of America *78(6)*, 3363-3367.

Seol, C.-A., Kim, J., Kim, W.-T., Ha, J.-M., Choe, H., Jang, Y.-J., Shim, E.-B., Youm, J.-B., Earm, Y.-E., and Leem, C.-H. (2008). Simulation of spontaneous action potentials of cardiomyocytes in pulmonary veins of rabbits. Progress is Biophysics and Molecular Biology *96(1-3)*, 132-151.

Severs, N.J., Coppen, S.R., Dupont, E., Yeh, H.-I., Ko, Y.-S., and Matsushita, T. (2004). Gap junction alterations in human cardiac disease. Cardiovascular Research *62(2)*, 368-377.

Shacklock, P.S., Wier, W.G., and Balke, C.W. (1995). Local Ca^{2+} transients (Ca^{2+} sparks) originate at transverse tubules in rat heart cells. The Journal of Physiology *487(3)*, 601-608.

Shah, D., Haissaguerre, M., Jais, P., and Hocini, M. (2003). Nonpulmonary vein foci: do they exist? Pacing and Clinical Electrophysiology:PACE *26(7 pt. 2)*, 1631-1635.

Shannon, T.R., Ginsburg, K.S., and Bers, D.M. (2002). Quantitative assessment of the SR Ca^{2+} leak-load relationship. Circulation Research *91(7)*, 594-600.

Shannon, T.R., Pogwizd, S.M., and Bers, D.M. (2003). Elevated sarcoplasmic reticulum Ca^{2+} leak in intact ventricular myocytes from rabbits in heart failure. Circulation Research *93(7)*, 592-594.

Shapira, A.R. (2009). Catheter ablation of supraventricular arrhytmias and atrial fibrillation. American Family Physician *80*, 1089-1094.

Shattock, M.J., and Bers, D.M. (1989). Rat vs. rabbit ventricle: Ca flux and intracellular Na assessed by ion-selective microelectrodes. The American Journal of Physiology *256(4 pt. 1)*, 813-822.

Shkryl, V.M., and Blatter, L.A. (2013). Ca(2+) release events in cardiac myocytes up close: insights from fast confocal imaging. PloS One *8(4)*, e61525.

Signore, S., Sorrentino, A., Ferreira-Martins, J., Kannappan, R., Shafaie, M., Del Ben, F., Isobe, K., Arranto, C., Wybieralska, E., Webster, A., *et al.* (2013). Inositol 1,4,5-trisphosphate Receptors and Human Left Ventricular Myocytes. Circulation *128(12)*, 1286-1297.

Singh, B.N., Singh, S.N., Reda, D.J., Tang, X.-C., Lopez, B., Harris, C.L., Fletcher, R.D., Sharma, S.C., Atwood, J.E., Jacobson, A.K., *et al.* (2005). Amiodarone versus sotalol for atrial fibrillation. The New England Journal of Medicine *352(18)*, 1861-1872.

Sitsapesan, R., Montgomery, R.A., MacLeod, K.T., and Williams, A.J. (1991). Sheep cardiac sarcoplasmic reticulum calcium-release channels: modification of conductance and gating by temperature. The Journal of Physiology *434*, 469-488.

Smyrnias, I., Mair, W., Harzheim, D., Walker, S.A., Roderick, H.L., and Bootman, M.D. (2010). Comparison of the T-tubule system in adult rat ventricular and atrial myocytes, and its role in excitation-contraction coupling and inotropic stimulation. Cell calcium *47*, 210-223.

Soeller, C., and Cannell, M.B. (1999). Examination of the transverse tubular system in living cardiac rat myocytes by 2-photon microscopy and digital image-processing techniques. Circulation Research *84(3)*, 266-275.

Solaro, R.J., and Rarick, H.M. (1998). Troponin and tropomyosin: proteins that switch on and tune in the activity of cardiac myofilaments. Circulation Research *83(5)*, 471-480.

Song, L.S., Sobie, E.A., McCulle, S., Lederer, W.J., Balke, C.W., and Cheng, H. (2006). Orphaned ryanodine receptors in the failing heart. Proceedings of the National Academy of Sciences of the United States of America *103(11)*, 4305-4310.

Sorgente, A., Tung, P., Wylie, J., and Josephson, M.E. (2012). Six Year Follow-Up After Catheter Ablation of Atrial Fibrillation: A Palliation More Than a True Cure. American Journal of Cardiology *109(8)*, 1179-1186.

Spach, M.S., Barr, R.C., and Jewett, P.H. (1972). Spread of excitation from the atrium into thoracic veins in human beings and dogs. The American Journal of Cardiology *30(8)*, 844-854.

Spach, M.S., and Boineau, J.P. (1997). Microfibrosis produces electrical load variations due to loss of side-to-side cell connections: a major mechanism of structural heart disease arrhythmias. Pacing and Clinical Electrophysiology: PACE *20(2 pt. 2)*, 397-413.

Spray, D.C., and Burt, J.M. (1990). Structure-activity relations of the cardiac gap junction channel. The American Journal of Physiology *258(2 pt. 1)*, 195-205.

Steiner, I., Hájková, P., Kvasnicka, J., and Kholová, I. (2006). Myocardial sleeves of pulmonary veins and atrial fibrillation: a postmortem histopathological study of 100 subjects. Virchows Archiv: An International Journal of Pathology *449(1)*, 88-95.

Stemmer, P., and Akera, T. (1986). Concealed positive force-frequency relationships in rat and mouse cardiac muscle revealed by ryanodine. The American Journal of Physiology *251(6 pt. 2)*, 1106-1110.

Stern, M.D. (1992). Theory of excitation-contraction coupling in cardiac muscle. Biophysical Journal, 497-517.

Stern, M.D., Kort, A.A., Bhatnagar, G.M., and Lakatta, E.G. (1983). Scattered-light intensity fluctuations in diastolic rat cardiac muscle caused by spontaneous Ca++-dependent cellular mechanical oscillations. The Journal of General Physiology, 119-153.

Stewart, S., Murphy, N.F., Walker, A., McGuire, A., and McMurray, J.J. (2004). Cost of an emerging epidemic: an economic analysis of atrial fibrillation in the UK. Heart *90(3)*, 286-292.

Stokke, M.K., Hougen, K., Sjaastad, I., Louch, W.E., Briston, S.J., Enger, U.H., Andersson, K.B., Christensen, G., Eisner, D.A., Sejersted, O.M., *et al.* (2010). Reduced SERCA2 abundance decreases the propensity for Ca^{2+} wave development in ventricular myocytes. Cardiovascular Research *86(1)*, 63-71.

Sugiyama, A., Takahara, A., Honsho, S., Nakamura, Y., and Hashimoto, K. (2005). A simple in vivo atrial fibrillation model of rat induced by transesophageal atrial burst pacing. Journal of Pharmacological Science *98(3)*, 315-318.

Sun, Q., Tang, M., Pu, J., and Zhang, S. (2008). Pulmonary venous structural remodeling in a canine model of chronic atrial dilation due to mitral regurgitation. The Canadian Journal of Cardiology *24(4)*, 305-308.

Sun, X.-H., Protasi, F., Takahashi, M., Takeshima, H., Ferguson, D.G., and Franzini-Armstrong, C. (1995). Molecular architecture of membranes involved in excitation-contraction coupling of cardiac muscle. The Journal of Cell Biology *129(3)*, 659-671.

Sweeney, C.M., Jones, J.F., and Bund, S.J. (1999). Adrenoceptor and cholinoceptor modulation of rat pulmonary vein cardiac muscle contractility. Vascular Pharmacology *46(3)*, 166-170.

Tada, M., Kirchberger, M.A., Repke, D.I., and Katz, A.M. (1974). The stimulation of calcium transport in cardiac sarcoplasmic reticulum by adenosine 3':5'-monophosphate-dependent protein kinase. The Journal of Biological Chemistry *249(19)*, 6174-6180.

Tagawa, M., Higuchi, K., Chinushi, M., Washizuka, T., Ushiki, T., Ishihara, N., and Aizawa, Y. (2001). Myocardium extending from the left atrium onto the pulmonary veins: a comparison between subjects with and without atrial fibrillation. Pacing & Clinical Electrophysiogy - PACE *24*, 1459-1463.

Takahara, A., Sugimoto, T., Kitamura, T., Takeda, K., Tsuneoka, Y., Namekata, I., and Tanaka, H. (2011). Electrophysiological and pharmacological characteristics of triggered activity elicited in guinea-pig pulmonary vein myocardium. Journal of Pharmacological Sciences *115*, 176-181.

Takahara, A., Takeda, K., Tsuneoka, Y., Hagiwara, M., Namekata, I., and Tanaka, H. (2012). Electrophysiological effects of the class Ic antiarrhythmic drug pilsicainide on the guinea-pig pulmonary vein myocardium. Journal of Pharmacological Sciences *118(4)*, 506-511.

Takahashi, N., Imataka, K., Seki, A., and Fujii, J. (1982). Left atrial enlargement in patients with paroxysmal atrial fibrillation. Japanese Heart Journal *25(5)*, 677-683.

Takamatsu, T., and Wier, W.G. (1990). Calcium waves in mammalian heart: quantification of origin, magnitude, waveform, and velocity. *4(5)*, 1519-1525.

Takase, B., Nagata, M., Matsui, T., Kihara, T., Kameyama, A., Hamabe, A., Noya, K., Satomura, K., Ishihara, M., Kurita, A., *et al.* (2004). Pulmonary vein dimensions and variation of branching pattern in patients with paroxysmal atrial fibrillation using magnetic resonance angiography. Japanese Heart Journal *45(1)*, 81-92.

Takeda, S. (2005). Crystal structure of troponin and the molecular mechanism of muscle regulation. Journal of Electron Microscopy (Tokyo) *54(1)*, 35-41.

Tan, A.-Y., Li, H., Wachsmann-Hogiu, S., Chen, L.-S., Chen, P.-S., and Fishbein, M.C. (2006). Autonomic innervation and segmental muscular disconnections at the human pulmonary vein-atrial junction: implications for catheter ablation of atrial-pulmonary vein junction. Journal of the American College of Pharmacology *48(1)*, 132-143.

Tan, A.-Y., Zhou, S., Jung, B.-C., Ogawa, M., Chen, L.-S., Fishbein, M.C., and Chen, P.-S. (2008). Ectopic atrial arrhythmias arising from canine thoracic veins during in vivo stellate ganglia stimulation. American Journal of Physiology Heart and Circulatory Physiology *295(2)*, 691-698.

Tanaami, T., Ishida, H., Seguchi, H., Hirota, Y., Kadono, T., Genka, C., Nakazawa, H., and Barry, W. (2005). Difference in propagation of Ca^{2+} release in atrial and ventricular myocytes. The Japanese Journal of Physiology *55(2)*, 81-91.

Tanaka, H., Nishimaru, K., Aikawa, T., Hirayama, W., Tanaka, Y., and Shigenobu, K. (2002). Effect of SEA0400, a novel inhibitor of sodium-calcium exchanger, on myocardial ionic currents. British Journal of Pharmacology *135(5)*, 1096-1100.

Tasaki, H. (1969). Electrophysiological study of the striated muscle cells of the extrapulmonary vein of the guinea-pig. Japanese Circulation Journal *33*, 1087-1098.

Taylor, I.M. (1980). Observations on the sinuatrial nodal artery of the rat. Journal of Anatomy, 821-831.ter Keurs, H., and Boyden, P. (2007). Calcium and Arrhythmogenesis. Physiological Reviews *87*, 457-506.

Terasawa, T., Balk, E.M., Chung, M., Garlitski, A.C., Alsheikh-Ali, A.A., Lau, J., and Ip, S. (2009). Systematic review: comparative effectiveness of radiofrequency catheter ablation for atrial fibrillation. Annals of Internal Medicine *151(3)*, 191-202.

Terracciano, C.M., Naqvi, R.U., and MacLeod, K.T. (1995). Effects of rest interval on the release of calcium from the sarcoplasmic reticulum in isolated guinea pig ventricular myocytes. Circulation Research *77(2)*, 354-360.

Thomas, M.J., Sjaastad, I., Andersen, K., Helm, P.J., Wasserstrom, J.A., Sejersted, O.M., and Ottersen, O.P. (2003). Localization and function of the Na^{+}/Ca^{2+}-exchanger in normal and detubulated rat cardiomyocytes. Journal of Molecular and Cellular Cardiology *35(11)*, 1325-1337.

Thorén, P.E., Persson, D., Karlsson, M., and Nordén, B. (2000). The antennapedia peptide penetratin translocates across lipid bilayers - the first direct observation. FEBS letters *482(3)*, 265-268.

Tidball, J.G., Cederdahl, J.E., and Bers, D.M. (1991). Quantitative analysis of regional variability in the distribution of transverse tubules in rabbit myocardium. Cell and Tissue Research *264(2)*, 293-298.

Trafford, A.W., Clarke, J.D., Richards, M.A., Eisner, D.A., and Dibb, K.M. (2013). Calcium signalling microdomains and the t-tubular system in atrial myoytes: potential roles in cardiac disease and arrhythmias. Cardiovascular Research *98(2)*, 192-203.

Trafford, A.W., Díaz, M.E., and Eisner, D.A. (1999). A novel, rapid and reversible method to measure Ca buffering and time-course of total sarcoplasmic reticulum Ca content in cardiac ventricular myocytes. Pflügers Archiv: European Journal of Physiology *437(3)*, 501-503.

Trafford, A.W., Sibbring, G.C., Díaz, M.E., and Eisner, D.A. (2000). The effects of low concentrations of caffeine on spontaneous Ca release in isolated rat ventricular myocytes. Cell Calcium *28(4)*, 269-276.

Trollinger, D.R., Cascio, W.E., and Lemasters, J.J. (1997). Selective loading of Rhod 2 into mitochondria shows mitochondrial Ca^{2+} transients during the contractile cycle in adult rabbit cardiac myocytes.Selective loading of Rhod 2 into mitochondria shows mitochondrial Ca^{2+} transients during the contractile cycle in adult rabbit cardiac myocytes. Biochemical and Biophysical Research Communications *236(3)*, 738-742.

Tsai, C.-F., Tai, C.-T., Hsieh, M.-H., Lin, W.-S., Yu, W.-C., Ueng, K.-C., Ding, Y.-A., Chang, M.-S., and Chen, S.-A. (2000). Initiation of Atrial Fibrillation by Ectopic Beats Originating From the Superior Vena Cava : Electrophysiological Characteristics and Results of Radiofrequency Ablation. Circulation *102*, 67-74.

Tsang, T.-S., Petty, G.W., Barnes, M.E., O'Fallon, W.M., Bailey, K.R., Wiebers, D.O., Sicks, J.D., Christianson, T.J., Seward, J.B., and Gersh, B.J. (2003). The prevalence of atrial fibrillation in incident stroke cases and matched population controls in Rochester, Minnesota: changes over three decades. Journal of the American College of Cardiology *42(1)*, 93-100.

Tsuneoka, Y., Kobayashi, Y., Honda, Y., Namekata, I., and Tanaka, H. (2012). Electrical activity of the mouse pulmonary vein myocardium. Journal of Pharmacological Sciences *119*, 287-292.

Tu, H., Wang, Z., and Bezprozvanny, I. (2005). Modulation of mammalian inositol 1,4,5-trisphosphate receptor isoforms by calcium: a role of calcium sensor region. Biophysical Journal *88(2)*, 1056-1069.

Ullrich, N.D., Valdivia, H.H., and Niggli, E. (2012). PKA phosphorylation of cardiac ryanodine receptor modulates SR luminal Ca^{2+} sensitivity. Journal of Molecular and Cellular Cardiology *53(1)*, 33-42.

Unudurthi, S.D., Wolf, R.M., and Hund, T.J. (2014). Role of sinoatrial node architecture in maintaining a balanced source-sink relationship and synchronous cardiac pacemaking. Frontiers in Physiology *26(5)*, doi: 10.3389/fphys.2014.00446.

Valdivia, H.H., Kaplan, J.H., Ellis-Davies, G.C., and Lederer, W.J. (1995). Rapid adaptation of cardiac ryanodine receptors: modulation by Mg^{2+} and phosphorylation. Science *267(5206)*, 1997-2000.

van den Hoff, M.J., Kruithof, B.P., and Moorman, A.F. (2004). Making more heart muscle. Bioessays: *News and Reviews in Molecular, Cellular and Developmental Biology*.

van der Velden, H.M., van Kempen, M.J., Wijffels, M.C., van Zijverden, M., Groenewegen, W.A., Allessie, M.A., and Jongsma, H.J. (1998). Altered pattern of connexin40 distribution in persistent atrial fibrillation in the goat. 9(6), 596-607.

Vanhoutte, P.M. (1974). Inhibition by acetylcholine of adrenergic neurotransmission in vascular smooth muscle. Circulation Research *33(3)*, 317-323.

Varro, A., Negretti, N., Hester, S.B., and Eisner, D.A. (1993). An estimate of the calcium content of the sarcoplasmic reticulum in rat ventricular myocytes. *Pflügers Archiv*: European Journal of Physiology *432(1-2)*, 158-160.

Venema, R.C., Raynor, R.L., Noland, T.A.J., and Kuo, J.F. (1993). Role of protein kinase C in the phosphorylation of cardiac myosin light chain 2. The Biochemical Journal *294(pt. 2)*, 401-406.

Venetucci, L., Trafford, A.W., and Eisner, D.A. (2007). Increasing ryanodine receptor open probability alone does not produce arrhythmogenic Ca waves: threshold Ca content is required. Circulation Research *100*, 105-111.

Venetucci, L.A., Trafford, A.W., O'Neill, S.C., and Eisner, D.A. (2008). The sarcoplasmic reticulum and arrhythmogenic calcium release. Cardiovascular Research *77(2)*, 285-292.

Verheule, S., van Kempen, M.J., Postma, S., Rook, M.B., and Jongsma, H.J. (2001). Gap junctions in the rabbit sinoatrial node. American Journal of Physiology Heart and Circulatory Physiology *280(5)*, 2103-2115.

Verheule, S., Wilson, E.E., Arora, R., Engle, S.K., Scott, L.R., and Olgin, J.E. (2002). Tissue structure and connexin expression of canine pulmonary veins. Cardiovascular Research *55(4)*, 727-738.

Vervloessem, T., Yule, D.I., Bultynck, G., and Parys, J.B. (2014). The type 2 inositol 1,4,5-trisphosphate receptor, emerging functions for an intriguing Ca^{2+}-release channel. Biochimica et Biophysica Acta *doi: 10.1016/j.bbamcr.2014.12.006*, Epub ahead of print.

Viatchenko-Karpinski, S., and Györke, S. (2001). Modulation of the Ca(2+)-induced Ca(2+) release cascade by beta-adrenergic stimulation in rat ventricular myocytes. The Journal of Physiology *533(3)*, 837-848.

Vinogradova, T.M., Zhou, Y.-Y., Maltsev, V., Lyashkov, A., Stern, M., and Lakatta, E.G. (2004). Rhythmic ryanodine receptor Ca^{2+} releases during diastolic depolarization of sinoatrial pacemaker cells do not require membrane depolarization. *Circulation Research*, 802-809.

Vinogradova, T.M., Zhou, Y.Y., Bogdanov, K.Y., Yang, D., Kuschel, M., Cheng, H., and Xiao, R.P. (2000). Sinoatrial node pacemaker activity requires Ca(2+)/calmodulin-dependent protein kinase II activation. Circulation Research *87(9)*, 760-767.

Wagner, E., Lauterbach, M.A., Kohl, T., Westphal, V., Williams, G.S., Steinbrecher, J.H., Streich, J.H., Korff, B., Tuan, H.T., Hagen, B., *et al.* (2012). Stimulated emission depletion live-cell super-resolution imaging shows proliferative remodeling of T-tubule membrane structures after myocardial infarction. Circulation Research *111(4)*, 402-414.

Wakili, R., Yeh, Y.-H., Yan, Q.-X., Greiser, M., Chartier, D., Nishida, K., Maguy, A., Villeneuve, L.R., Boknik, P., Voigt, N., *et al.* (2010). Multiple potential molecular contributors to atrial hypocontractility caused by atrial tachycardia remodeling in dogs. Circulation Arrhythmia and Electrophysiology *3(5)*, 530-541.

Wang, S.-Q., Song, L.-S., Lakatta, E.G., and Cheng, H. (2001). Ca^{2+} signalling between single L-type Ca^{2+} channels and ryanodine receptors in heart cells. Nature *410(6828)*, 592-596.

Wang, T.-M., Chiang, C.-E., Sheu, J.-R., Tsou, C.-H., Chang, H.-M., and Luk, H.-N. (2003). Homogenous distribution of fast response action potentials in canine pulmonary vein sleeves: a contradictory report. International Journal of Cardiology *89*, 187-195.

Wang, W., Zhu, W., Wang, S., Yang, D., Crow, M.-T., Xiao, R.-P., and H, C. (2004). Sustained beta1-adrenergic stimulation modulates cardiac contractility by Ca^{2+}/calmodulin kinase signaling pathway. Circulation Research *95(8)*, 798-806.

Wang, Z., Fermini, B., and Nattel, S. (1994). Rapid and slow components of delayed rectifier current in human atrial myocytes. Cardiovascular Research *28(10)*, 1540-1546.

Wasserstrom, J.A., and Aistrup, G.L. (2005). Digitalis: new actions for an old drug. American Journal of Physiology - Heart and Circulatory Physiology *289*, H1781-H1793.

Wasserstrom, J.A., Holt, E., Sjaastad, I., Lunde, P.K., Odegaard, A., and Sejersted, O.M. (2000). Altered E-C coupling in rat ventricular myocytes from failing hearts 6 wk after MI. American Journal of Physiology Heart and Circulatory Physiology *279(2)*, 798-807.

Wasserstrom, J.A., Shiferaw, Y., Chen, W., Ramakrishna, S., Patel, H., Kelly, J.E., O'Toole, M.J., Pappas, A., Chirayil, N., Bassi, N., *et al.* (2010). Variability in Timing of Spontaneous Calcium Release in the Intact Rat Heart Is Determined by the Time Course of Sarcoplasmic Reticulum Calcium Load / Novelty and Significance. Circulation Research *107*, 1117-1126.

Wehrens, X.H., Lehnart, S.E., Reiken, S.R., and Marks, A.R. (2004). Ca^{2+}/calmodulin-dependent protein kinase II phosphorylation regulates the cardiac ryanodine receptor. Circulation Research *94(6)*, 61-70.

Wellens, H.J.J. (2000). Pulmonary Vein Ablation in Atrial Fibrillation : Hype or Hope? Circulation *102*, 2562-2564.

Wetzel, U., Boldt, A., Lauschke, J., Weigl, J., Schirdewahn, P., Dorszewski, A., Doll, N., Hindricks, G., Dhein, S., and Kottkamp, H. (2005). Expression of connexins 40 and 43 in human left atrium in atrial fibrillation of different aetiologies. Heart *91(2)*, 166-170.

Wier, W.G., Cannell, M.B., Berlin, J.R., Marban, E., and Lederer, W.J. (1987). Cellular and subcellular heterogeneity of $[Ca^{2+}]i$ in single heart cells revealed by fura-2. Science *235(4786)*, 325-328.

Wier, W.G., ter Keurs, H.E., Marban, E., Gao, W.D., and Balke, C.W. (1997). Ca^{2+} 'sparks' and waves in intact ventricular muscle resolved by confocal imaging. Circulation Research *81(4)*, 462-469.

Wilhelm, M., Kirste, W., Kuly, S., Amann, K., Neuhuber, W., Weyand, M., Daniel, W.G., and Garlichs, C. (2006). Atrial distribution of connexin 40 and 43 in patients with intermittent, persistent, and postoperative atrial fibrillation. Heart, Lung and Circulation *15(1)*, 30-37.

Winslow, R.L., Varghese, A., Noble, D., Adlakha, C., and Hoythya, A. (1993). Generation and propagation of ectopic beats induced by spatially localized Na-K pump inhibition in atrial network models. Proceedings: Biological Sciences/The Royal Society *254(1339)*, 55-61.

Wolf, P.A., Abbott, R.D., and Kannel, W.B. (1991). Atrial fibrillation as an independent risk factor for stroke: the Framingham Study. Stroke *22*, 983-988.

Wolkowicz, P.E., Grenett, H.E., Huang, J., Wu, H.-C., Ku, D.-D., and Urthaler, F. (2007). A pharmacological model for calcium overload-induced tachycardia in isolated rat left atria. European Journal of Pharmacology *576(1-3)*, 122-131.

Wongcharoen, W., Chen, Y.-C., Chen, Y.-J., Chang, C.-M., Yeh, H.-I., Lin, C.-I., and Chen, S.-A. (2006). Effects of a Na^+/Ca^{2+} exchanger inhibitor on pulmonary vein electrical activity and ouabain-induced arrhythmogenicity. Cardiovascular Research *70*, 497-508.

Woo, S.-H., Cleemann, L., and Morad, M. (2002). Ca^{2+} current-gated focal and local Ca^{2+} release in rat atrial myocytes: evidence from rapid 2-D confocal imaging. The Journal of Physiology *543(2)*, 439-453.

Workman, A.J., Smith, G.L., and Rankin, A.C. (2011). Mechanisms of termination and prevention of atrial fibrillation by drug therapy. Pharmacology and Therapeutics *131*, 221-241.

Wyse, D.G., Waldo, A.L., DiMarco, J.P., Domanski, M.J., Rosenberg, Y., Schron, E.B., Kellen, J.C., Greene, H.L., Mickel, M.C., Dalquist, J.E., *et al.* (2002). A comparison of rate control and rhythm control in patients with atrial fibrillation. The New England Journal of Medicine *347(23)*, 1825-1833.

Xiao, B., Tian, X., Xie, W., Jones, P.P., Cai, S., Wang, X., Jiang, D., Kong, H., Zhang, L., Chen, K., *et al.* (2007). Functional consequence of protein kinase A-dependent phosphorylation of the cardiac ryanodine receptor: sensitization of store overload-induced Ca^{2+} release. The Journal of Biological Chemistry *282(41)*, 30256-30264.

Xie, Y., Sato, D., Garfinkel, A., Qu, Z., and Weiss, J.N. (2010). So little source, so much sink: requirements for afterdepolarizations to propagate in tissue. Biophysical Journal *99(5)*, 1408-1415.

Yamamoto, M., Dobrzynski, H., Tellez, J., Niwa, R., Billeter, R., Honjo, H., Kodama, I., and Boyett, M.R. (2006). Extended atrial conduction system characterised by the expression of the HCN4 channel and connexin45. Cardiovascular research *72(2)*, 271-281.

Yang, Z., Pascarel, C., Steele, D.S., Komukai, K., Brette, F., and Orchard, C.H. (2002). Na^{+}-Ca^{2+} exchange activity is localized in the T-tubules of rat ventricular myocytes. Circulation Research *91(4)*, 315-322.

Yatani, A., and Brown, A.M. (1989). Rapid beta-adrenergic modulation of cardiac calcium channel currents by a fast G protein pathway. Sciences (New York, NY) *245(4913)*, 71-74.

Yeager, M. (1998). Structure of cardiac gap junction intercellular channels. Journal of Structural Biology *121(2)*, 231-245.

Yeh, H.-I., Lai, Y.-J., Lee, Y.-N., Chen, Y.-J., Chen, Y.-C., Chen, C.-C., Chen, S.-A., Lin, C.-I., and Tsai, C.-H. (2003). Differential expression of connexin43 gap junctions in cardiomyocytes isolated from canine thoracic veins. The Journal of Histochemistry and Cytochemistry: Offical Journal of the Histochemical Society *51(2)*, 259-266.

Yoshida, A., Takahashi, M., Imagawa, T., Shigekawa, M., Takisawa, H., and Nakamura, T. (1992). Phosphorylation of Ryanodine Receptors in Rat Myocytes during β-Adrenergic Stimulation. Journal of Biochemistry *111*, 186-190.

Yu, W.-C., Hsu, T.-L., Tai, C.-T., Tsai, C.-F., Hsieh, M.-H., Lin, W.-S., Lin, Y.-K., Tsao, H.-M., Ding, Y.-A., Chang, M.-S., *et al.* (2001). Acquired pulmonary vein stenosis after radiofrequency catheter ablation of paroxysmal atrial fibrillation. Journal of Cardiovascular Electrophysiology *12*, 887-892.

Zhang, R., Khoo, M.S., Wu, Y., Yang, Y., Grueter, C.E., Ni, G., Price, E.J., Thiel, W., Guatimosim, S., Song, L.S., *et al.* (2005). Calmodulin kinase II inhibition protects against structural heart disease. Nature Medicine *11(4)*, 409-417.

Zhang, Y.-M., Miura, M., and ter Keurs, H.E. (1996). Triggered propagated contractions in rat cardiac trabeculae. Inhibition by octanol and heptanol. Circulation Research *79(6)*, 1077-1085.

Zhou, Y.-Y., Song, L.-S., Lakatta, E.G., Xiao, R.-P., and Cheng, H. (1999). Constitutive beta2-adrenergic signalling enhances sarcoplasmic reticulum Ca^{2+} cycling to augment contraction in mouse heart. The Journal of Physiology *521(2)*, 351-361.

Zhou, Z., and Lipsius, S.L. (1993). Na(+)-Ca^{2+} exchange current in latent pacemaker cells isolated from cat right atrium. The Journal of Physiology *466*, 263-285.

Zimmermann, M., and Kalusche, D. (2001). Fluctuation in autonomic tone is a major determinant of sustained atrial arrhythmias in patients with focal ectopy originating from the pulmonary veins. J Cardiovasc Electrophysiol *12*, 285-291.

Zorov, D.B., Filburn, C.R., Klotz, L.O., Zweier, J.L., and Sollott, S.J. (2000). Reactive oxygen species (ROS)-induced ROS release: a new phenomenon accompanying induction of the mitochondrial permeability transition in cardiac myocytes. The Journal of Experimental Medicine *192(7)*, 1001-1014.

Zorov, D.B., Juhaszova, M., and Sollott, S.J. (2006). Mitochondrial ROS-induced ROS release: an update and review. Biochimica et Biophysica Acta *1757(5-6)*, 509-517.

Zucchi, R., and Ronca-Testoni, S. (1997). The sarcoplasmic reticulum Ca^{2+} channel/ryanodine receptor: modulation by endogenous effectors, drugs and disease states. Pharmacological Reviews *49(1)*, 1-51.

Zühlke, R.D., Pitt, G.S., Deisseroth, K., Tsien, R.W., and Reuter, H. (1999). Calmodulin supports both inactivation and facilitation of L-type calcium channels. Nature *399(6732)*, 159-162.